NASA TECHNICAL MEMORANDUM

NASA TM X-73630

NASA TM X-73630

INTERHEMISPHERIC SURVEY OF MINOR UPPER ATMOSPHERIC CONSTITUENTS DURING OCTOBER-NOVEMBER 1976

Lewis Research Center
Cleveland, Ohio 44135
March 1977

1. Report No.	2. Government Accession No.	3. Recipient's Catalog No.
NASA TM X-73630		

4. Title and Subtitle	5. Report Date
INTERHEMISPHERIC SURVEY OF MINOR UPPER ATMOSPHERIC CONSTITUENTS DURING OCTOBER-NOVEMBER 1976	March 1977
	6. Performing Organization Code
7. Author(s)	8. Performing Organization Report No. E-9130
	10. Work Unit No.
9. Performing Organization Name and Address Lewis Research Center National Aeronautics and Space Administration Cleveland, Ohio 44135	11. Contract or Grant No.
	13. Type of Report and Period Covered Technical Memorandum
12. Sponsoring Agency Name and Address National Aeronautics and Space Administration Washington, D.C. 20546	14. Sponsoring Agency Code

15. Supplementary Notes

Compiled by Daniel J. Gauntner, NASA Lewis Research Center, Cleveland, Ohio 44135, and Louis C. Haughney, NASA Ames Research Center, Moffett Field, California 94035.

16. Abstract

The NASA CV-990 aircraft conducted a Latitude Survey Mission over the Pacific Ocean from October 26 to November 18, 1976. It flew between 75^{o} N and 61.5^{o} S latitudes to obtain data on the concentrations and distributions of minor constituents and pollutants in the upper atmosphere. The CV-990 aircraft coordinated several flights with a NASA U-2 aircraft, NOAA ground station measurements in Alaska, Hawaii, and American Samoa, and with Australian and New Zealand ground stations, aircraft, and a balloon experiment in the Southern hemisphere. Data were obtained for species including ozone, total ozone, the oxides of nitrogen, the chlorofluoromethanes, water vapor, nitric acid, carbon monoxide, carbon dioxide, hydrogen chloride, Aitken nuclei, ammonia, aerosols, temperatures, and winds. Individual experiment results and selected analyses are presented. The experimental data include total column densities, latitude variations, interhemisphere differences, and vertical profiles.

17. Key Words (Suggested by Author(s))	18. Distribution Statement
Air Quality; Trace Constituent Measurements; Atmospheric Ozone; Water Vapor; Chlorofluoromethanes; Oxides of Nitrogen; Aerosols; Troposphere - Stratosphere; Meteorology	Unclassified - unlimited STAR category 45

19. Security Classif. (of this report)	20. Security Classif. (of this page)	21. No. of Pages	22. Price*
Unclassified	Unclassified		

* For sale by the National Technical Information Service, Springfield, Virginia 22161

FOREWORD

Each report, including data and interpretative analyses, contained herein was prepared by the individual experiment teams.

While some efforts were made to standardize the report format, the experiment teams were not restricted to a specific system of units for reporting their results. The reader is cautioned to understand units, including time and date, before intercomparing results.

The National Aeronautics and Space Administration expresses its gratitude for the willing participation and cooperation it received during the Latitude Survey Mission from all the experiment teams, especially those from Australia, France, and New Zealand.

CONTENTS

NASA U-2 AIRCRAFT MEASUREMENTS

CORRELATED MEASUREMENTS

SUMMARY

The NASA 1976 CV-990 Latitude Survey Mission made fifteen data flights, totaling 81 hours of flight time, from October 26 to November 18. The extreme latitudes reached were $75^{o}N$ and $61.5^{o}S$. The purpose was to study the concentrations of minor constituents and pollutants in the upper atmosphere over the Pacific Ocean. There were eight experiments on board the CV-990 aircraft. Several CV-990 flights were coordinated with flights of a NASA U-2 aircraft, flying a similar mission at 18 and 21 km, to obtain simultaneous measurements. Four experiments were on-board the U-2 aircraft. Other CV-990 flights were coordinated with NOAA ground stations (GMCC) in Alaska, Hawaii, and American Samoa. In the Southern Hemisphere Australian and New Zealand ground, aircraft, and balloon experiments were coordinated with local CV-990 flights.

Data were obtained for concentrations of ozone (surface, in-situ, total column), F-11, F-12, F-113, F-114, methyl chloride, chloroform, methyl chloroform, CH_4, CCl_4, NO, NO_2, N_2O, HNO_3 (total column), HCl, H_2O, CO_2, SF_6, NH_3, Aitken nuclei, aerosols (impactor and lidar), and temperature and winds. A piggyback experiment measuring the neutron flux also obtained data from the CV-990.

This report contains major results and selected analyses from each of the participating experiments.

THE NASA 1976 CV-990 LATITUDE SURVEY MISSION

Louis C. Haughney
Ames Research Center

INTRODUCTION

The NASA 1976 CV-990 Latitude Survey Mission was part of an extensive study of the minor constituents in the atmosphere. The study was conducted in October and November 1976, over the Pacific Ocean from latitudes north of Alaska to latitudes south of Australia and New Zealand. Many research groups in the United States, Australia, and New Zealand made coordinated measurements of such constituents as ozone, water vapor, fluorocarbons, nitrogen-oxygen compounds, and aerosols. The platforms used by these groups included ground stations, aircraft, radiosondes, ozonesondes, and a very high altitude scientific balloon. The groups participating in the study were: in the United States, the NASA Headquarters Offices of Upper Atmospheric Research and of the Airborne Instrumentation Research Program, and the NOAA Office of Geophysical Monitoring and Climatic Change; in Australia, the Commonwealth Scientific and Industrial Research Organization (CSIRO) and the Bureau of Meteorology (Department of Science), and the University of Melbourne; and in New Zealand, the New Zealand Meteorological Service and the University of Canterbury. Office National d'Études et de Recherches Aérospatiales (ONERA), France, also contributed an experiment to the CV-990 payload.

In the Northern Hemisphere, the airborne measurements were made by using the NASA medium-altitude (12 km) CV-990 airplane and the two NASA high-altitude (20 km) U-2 airplanes; the three aircraft are managed by the Airborne Missions and Applications Division of Ames Research Center. The U-2/NASA 709 was based in Fairbanks, Alaska for 11 flights in early October 1976; and the U-2/NASA 708 was based in Honolulu, Hawaii for 11 flights in early November 1976. In the Southern Hemisphere, the airborne measurements were made by the NASA CV-990 and by a CSIRO low-altitude (4.5 km) Piper Commanche airplane. CSIRO also uses other aircraft on a routine basis for atmospheric measurements at low and medium altitudes.

This report deals principally with the NASA CV-990 participation in the overall study.

ORIGIN OF THE NASA 1976 CV-990 LATITUDE SURVEY MISSION

The Latitude Survey Mission came about as part of the NASA Global Air Sampling Program (GASP), which is directed by the NASA Lewis Research Center. GASP is a long-range program to measure several minor atmospheric constituents in the upper tropopause and the lower stratosphere and to use that data to determine the effect of airplane engine exhausts upon the atmosphere. Automated air sampling systems are flying on several 747 passenger airplanes

in routine airline service. The NASA CV-990 airplane is used by GASP to develop the automated instrument packages and to obtain data in areas off regular airline routes, such as on the mission reported here. For the latter investigations, the CV-990 GASP package carries additional manually operated instruments to supplement the automated package.

In order to make the Latitude Survey Mission a much more comprehensive study than could be achieved by the GASP experiment alone, NASA added six more atmospheric experiments to the CV-990 payload. It was thus possible to measure a wide variety of minor atmospheric species with both in situ and remote sensing techniques. Air sampling with some in-flight analyses, microwave limb scanning, infrared radiometry, and infrared absorption spectroscopy of the solar spectrum were among the techniques employed. An eighth experiment, which was carried on a noninterference basis as a piggyback experiment, measured the latitude distribution of neutrons and secondary charged particles produced by cosmic rays. A list of the experiments, the investigating teams, the instruments used, and the species measured is given in table 1.

CV-990 FLIGHT OPERATIONS

Between October 26 and November 18, 1976, the CV-990 NASA 712 airplane, Galileo II, made 15 flights over a latitude range from 75° N (north of Alaska) to 61.5° S (south of New Zealand). Table 2 lists the flights and their significant features. The flight routes are shown in the maps of figure 1. After the initial flight over the western United States, the airplane flew to Fairbanks, Alaska; Honolulu, Hawaii; Pago Pago, American Samoa; Melbourne, Australia; and Christchurch, New Zealand. It then returned to its home base at Moffett Field, California via Pago Pago and Honolulu. Local flights were made at each of those bases, except at Pago Pago, in order to make detailed coordinations with ground stations, other aircraft, and balloons. Also, the local flights out of Fairbanks and Christchurch allowed the airplane to reach its northernmost and southernmost points. The airplane usually flew at 10 to 12 km (33,000 to 40,000 ft) except where altitude profiles were made over cooperating ground stations.

At the high latitudes, the airplane was very often above the tropopause. In the low latitudes, it was always below it. In the mid-latitudes, it sometimes seemed as though the airplane were skimming through the crests of a wave-shaped tropopause (e.g., Flight No. 8).

COORDINATIONS WITH OTHER RESEARCH GROUPS

An important feature of this mission was the widespread coordination along the flight route with other research groups in making simultaneous measurements of the minor atmospheric components. Particularly valuable were the cross calibrations made in Melbourne, Australia. Standard air

samples used by the CSIRO Division of Atmospheric Physics were analyzed by the two CV-990 gas chromatographs belonging to the Washington State University and the Ames Research Center experiments. The measurements of the three teams agreed within 7 percent. The cooperating groups and the persons responsible for carrying out the coordinations are listed below:

- Ames Research Center, NASA

  - Stratospheric Projects Office: Ilia G. Poppoff
  - High Altitude Missions Branch: Susan M. Norman

    U-2/NASA 708 high-altitude airplane (18-21 km)
    Three coordinated flights near Hawaii (Flight Nos. 6, 14, and 15)

- NOAA Environmental Research Laboratories

  - Geophysical Monitoring and Climatic Change (GMCC):
    Kirby J. Hanson and James Watkins

    GMCC ground observatories at Point Barrow, Alaska (Flight No. 3); Mauna Loa, Hawaii (Flight No. 5); and American Samoa (Flight No. 7)

- Australia, Department of Science: The Honorable James J. Webster, Minister of Science

  - Central Office: Lewis F. Wainwright

    Coordination of Australian participation

  - Commonwealth Scientific and Industrial Research Organization (CSIRO)

    Division of Atmospheric Physics: Graeme Pearman and Paul Fraser

    Ground stations at:

    Aspendale (near Melbourne (Flight No. 9))
    Cape Grim, Tasmania, Baseline Station (Flight No. 9)
    Hobart, Tasmania (Flight Nos. 9 and 11)
    Macquarie Island (Flight No. 11)

    Low-altitude Piper Commanche aircraft (4.5 km) over the Bass Strait between Melbourne and Cape Grim (Flight No. 9)

    Division of Cloud Physics: J. L. Gras and University of Melbourne: Jean Laby

    High-altitude (35 km) scientific balloon (Hibal) launched at Mildura, Victoria (Flight No. 10)

  - Bureau of Meteorology: John W. Zillman

    Special radiosonde launches (Flight No. 9)

- New Zealand Meteorological Service: J. F. de Lisle and John S. Hickman; and the University of Canterbury: Grahame J. Fraser

  - Ground stations at:

    Invercargill (Flight Nos. 11, 12, and 13)
    Christchurch (Flight Nos. 11, 12, and 13)
    Wellington (Flight Nos. 11, 12, and 13)

  - Ozonesonde launches at Wellington (Flight Nos. 11, 12, and 13)

  - Radiosonde launches from several stations

MANAGEMENT

The NASA 1976 CV-990 Latitude Survey Mission was managed by the Medium Altitude Missions Branch (formerly the Airborne Science Office) of the Ames Research Center, NASA. Louis C. Haughney of that branch was the Mission Manager. Fred J. Drinkwater III, of the Ames Flight Operations Division, was the Command Pilot. Dr. Edith I. Reed, NASA Headquarters Office of Upper Atmospheric Studies, was the Program Scientist.

TABLE 1.- EXPERIMENTS FOR THE 1976 CV-990 LATITUDE SURVEY MISSION

1.	Title:	Global Air Sampling Program (GASP)
	Experimeters:	Erwin A. Lezberg, Porter J. Perkins, Daniel C. Briehl[a]: Lewis Research Center; Gerald F. Murray,[a] Ulf R. C. Gustafsson,[a] Robert E. Johnson[a]: United Airlines
	Objective:	In situ sampling and analysis
	Measurements:	Automated "747" system — O_3, CO, F-11, F-12, N_2O, and particle size and number Prototype "990" system — H_2O, N_2O, CO_2, particle size and number, and O_3 by both in situ sampling and by remote sensing of near UV solar absorption
2.	Title:	Microwave Limb Sounder
	Experimenters:	Joseph W. Waters,[a] Paul N. Swanson[a]: Jet Propulsion Laboratory; Jack J. Gustincic[a]: Consulting Engineer
	Objective:	Remote sensing of thermal radiation in the microwave region from the atmospheric limb (altitudes of 25 to 80 km)
	Measurements:	H_2O, 183.310 GHz line (1.64 mm wavelength) — all flights O_3, 184.378 GHz line (1.63 mm wavelength) — Flight No. 10 only
3.	Title:	Atmospheric Halocarbon Measurements
	Experimenters:	Edward C. Y. Inn, John C. Arvesen,[a] Bennett J. Tyson[a]: Ames Research Center
	Objective:	In situ sampling and analysis with an automated gas chromatograph (HP model 5840A)
	Measurements:	Freon-11, -12, -113, -114, CCl_4, CH_3CCl_3, $CHCl_3$, N_2O, SF_6

[a]Participated in CV-990 flights.

TABLE 1.- EXPERIMENTS FOR THE 1976 CV-990 LATITUDE SURVEY

MISSION - Continued

4.	Title:	Study of Minor Atmospheric Constituents by Infrared Absorption Spectrometry
	Experimenters:	Andre Girard, Jean Besson,[a] Louis Gramont,[a] Jean Marcault[a]: Office National d'Études et de Recherches Aérospatiales (ONERA), France
	Objective:	Remote sensing by measuring atmospheric absorption of solar radiation in the near infrared (3-9 μm) with an automated grille spectrometer
	Measurements:	NO_2, HNO_3, HCl, NO, CH_4, H_2O, O_3
5.	Title:	Remote Measurements of Atmospheric Pollutants with an Infrared Heterodyne Radiometer
	Experimenters:	James M. Hoell, Jr.[a]: Langley Research Center; Bernard J. Peyton,[a] Ronald Lange,[a] Michael Savage[a]: AIL Division of Cutler-Hammer
	Objective:	Remote sensing with a dual laser heterodyne spectrometer in the near infrared (9-11 μm); both solar absorption spectroscopy of the atmospheric limb and emission spectroscopy from the atmospheric column underneath the airplane
	Measurements:	O_3
6.	Title:	Atmospheric Halocarbon Measurements
	Experimenters:	Rei Rasmussen, Joseph Krasnec[a]: Washington State University
	Objective:	In situ sampling and analysis with an automated gas chromatograph (PE model 3920B)
	Measurements:	Freon-11, -12, -113, CCl_4, CH_3CCl_3, $CHCl_3$, CHCl, CCl_2

[a]Participated in CV-990 flights.

TABLE 1.- EXPERIMENTS FOR THE 1976 CV-990 LATITUDE SURVEY

MISSION - Concluded

7.	Title:	Infrared Measurements of Atmospheric Water Vapor and Temperature
	Experimenters:	Peter M. Kuhn[a]: NOAA Atmospheric Physics and Chemistry Laboratory; Harold Cauthen[a]: Emagram Co.
	Objective:	Remote sensing of stratospheric and upper tropospheric water vapor and of the underlying surface by infrared radiometers and an image scanner
	Measurements:	H_2O — Total column density above airplane Ambient air temperature Underlying surface imagery
8.	Title:	Cosmic Ray Study
	Experimenters:	John E. Hewitt, Clarence A. Syvertson[a]: Ames Research Center; Anne S. Bunker: San Jose State University
	Objective:	To study effect of geomagnetic latitude changes on the atmospheric neutron and charged particle fluxes
	Measurements:	Neutrons, $0.02 < E < 20$ Mev, moderated BF_3 counter Charged particles, ionization chamber (RSS-111)

[a]Participated in CV-990 flights.

TABLE 2.- NASA 1976 CV-990 LATITUDE SURVEY MISSION FLIGHT LOG

Data flt. No.	Route	Date (U.T.)	Time[a] (U.T.)	Flight[b] duration	Latitude range	Flight plan and coordinations
1	Moffett Field - Moffett Field	Oct. 26-27	20:00--2:02	6 hr 20 min	33° 29'N-40° 20'N	1. Altitude profile over NOAA GMCC station at Boulder 37,000 ft — 21:53-22:12 25,000 ft — 22:18-22:30 2. Sunset run 39,000 ft — 00:12-01:17
2	Moffett Field - Fairbanks	Oct. 28-29	21:19-02:12	5 hr 05 min	37° 25'N-66° 47'N	Sunset run 35,000 ft — 23:56-01:58
3	Fairbanks - Fairbanks	Oct. 29-30	19:11-00:58	6 hr 00 min	64° 29'N-75° 20'N	1. Midday sun over southern horizon — two runs 33,000 ft, 75°N — 20:39:42-21:30:38 37,000 ft, 71.5°N — 22:03:40-22:38:01 2. Altitude profile over NOAA GMCC station at Point Barrow 37,000 ft — 22:12:10-22:46:20

[a]Times listed are for takeoff to landing.
[b]"Flight duration" includes taxiing time to and from parked positions.

TABLE 2.- NASA 1976 CV-990 LATITUDE SURVEY MISSION FLIGHT LOG - Continued

Data flt. No.	Route	Date (U.T.)	Time[a] (U.T.)	Flight[b] duration	Latitude range	Flight plan and coordinations
						21,000 ft — 22:52:29-23:07:01 3500 ft — 23:15:39-23:31:00 1100 ft — 23:34:44-23:47:00
4	Fairbanks - Honolulu/Hickam	Oct. 30	16:34-22:46	6 hr 30 min	64° 29'N-21° 20'N	Sunrise run 33,000 ft — 17:04:13-18:22:15
5	Honolulu/Hickam - Honolulu/Hickam	Nov. 1	15:36-20:12	4 hr 45 min	21° 20'N-14° 52'N	1. Sunrise run 33,000-36,000 ft — 16:12:08-17:22:05 2. Altitude profile over NOAA GMCC station on Mauna Loa, Hawaii 35,000 ft — 18:06:50-18:12:06 21,000 ft — 18:20:52-18:34:10 15,000 ft — 18:37:57-18:53:00 11,000 ft — 18:55:30-19:11:00

[a]Times listed are for takeoff to landing.
[b]"Flight duration" includes taxiing time to and from parked positions.

TABLE 2.- NASA 1976 CV-990 LATITUDE SURVEY MISSION FLIGHT LOG - Continued

Data flt. No.	Route	Date (U.T.)	Time[a] (U.T.)	Flight[b] duration	Latitude range	Flight plan and coordinations
						3. Kilauea Crater 6200 ft — 19:22:30 4. IR imagery, north shore of Island of Hawaii 1500 ft — 19:30:00-19:41:25
6	Honolulu/Hickam - Honolulu/Hickam	Nov. 3	20:03-23:10	3 hr 30 min	21° 20'N-14° 20'N	1. Coordination with NASA 708/U-2 high-altitude airplane 2. Scheduled transit flight to Pago Pago, Samoa; flight aborted after 1-1/2 hr due to oil leak in engine No. 2.
Nov. 4, 5, 6 — delay at Honolulu/Hickam for change of engine No. 2.						
7	Honolulu/Hickam - Pago Pago	Nov. 7-8	20:43-02:13	5 hr 35 min	21° 20'N-14° 20'S	1. Altitude profile over NOAA GMCC station on American Samoa 11,000 ft — 01:38:10-01:50:45 3200 ft — 01:56:00-02:07:00

[a]Times listed are for takeoff to landing.
[b]"Flight duration" includes taxiing time to and from parked positions.

TABLE 2.- NASA 1976 CV-990 LATITUDE SURVEY MISSION FLIGHT LOG - Continued

Data flt. No.	Route	Date (U.T.)	Time[a] (U.T.)	Flight[b] duration	Latitude range	Flight plan and coordinations
8	Pago Pago - Sydney - Melbourne	Nov. 8-9	21:16-03:18 04:44-05:53	6 hr 15 min 1 hr 20 min	14° 20'S- 37° 40'S	Landed at Sydney for refueling
9	Melbourne - Melbourne	Nov. 10-11	18:21-00:19	6 hr 10 min		1. Sunrise run 35,000 and 37,000 ft — 19:15:08-20:05:18 2. Altitude profile over Bass Strait and CSIRO Baseline Station at Cape Grim, Tasmania 37,000 ft — 21:16:50-21:34:25 21,000 ft — 21:43:02-21:58:48 10,100 ft — 22:02:41-22:18:17 3. Coordinate with CSIRO low-altitude (1000-15,000 ft) airplane over Bass Strait and Cape Grim — 21:16:50-22:18:17

[a]Times listed are for takeoff to landing.
[b]"Flight duration" includes taxiing time to and from parked positions.

TABLE 2.- NASA 1976 CV-990 LATITUDE SURVEY MISSION FLIGHT LOG - Continued

Data flt. No.	Route	Date (U.T.)	Time[a] (U.T.)	Flight[b] duration	Latitude range	Flight plan and coordinations
						4. Overflight of Hobart O_3 station 38,300 ft — 22:35 5. Altitude profile over CSIRO laboratory at Aspendale (Melbourne) 39,000 ft — 22:47:55-23:20:26 25,000 ft — 23:22:26-23:41:35 10,000 ft — 23:46:28-00:02:18 6. Ozonesonde launch at Aspendale
10	Melbourne - Melbourne	Nov. 11	19:40-22:44	3 hr 15 min	37° 40'S-34° 00'S	1. CSIRO "HIBAL" balloon launch at Mildura: altitude profile 36,000 ft — 20:18:49-20:27:19 31,000 ft — 21:15:46-21:38:47 25,000 ft — 21:43:53-21:49:09 15,000 ft — 22:02:20-22:21:44

[a] Times listed are for takeoff to landing.
[b] "Flight duration" includes taxiing time to and from parked positions.

TABLE 2.- NASA 1976 CV-990 LATITUDE SURVEY MISSION FLIGHT LOG - Continued

Data flt No.	Route	Date (U.T.)	Time[a] (U.T.)	Flight[b] duration	Latitude range	Flight plan and coordinations
						2. Sun run 36,000 ft — 20:53:20-21:12:06
11	Melbourne - Christchurch	Nov. 12- 13	23:14- 04:04	5 hr 05 min	37° 40'S- 54° 30'S- 43° 29'S	1. Overflights of CSIRO ground stations Hobart - O_3 35,000 ft — 00:03 Macquarie Island - O_3 35,000 ft — 01:49 2. Overflights of New Zealand ground stations Campbell Island - radiosonde 37,000 ft —02:37 Invercargill - O_3 37,000 ft — 03:20
12	Christchurch - Christchurch	Nov. 14	02:48- 08:10	5 hr 30 min	43° 29'S- 61° 46'S	1. Overflights of New Zealand ground stations Invercargill - O_3 33,000 ft — 03:20 Campbell Island - radiosonde 33,000 ft — 04:13

[a]Times listed are for takeoff to landing.
[b]"Flight duration" includes taxiing time to and from parked positions.

TABLE 2.- NASA 1976 CV-990 LATITUDE SURVEY MISSION FLIGHT LOG - Continued

Data flt. No.	Route	Date (U.T.)	Time[a] (U.T.)	Flight[b] duration	Latitude range	Flight plan and coordinations
						2. Reached southernmost point of mission: 61° 46'S, 170° 39'E at 37,000 ft, 05:24 3. Sunset run 37,000/39,000 ft — 06:45-07:44
13	Christchurch - Pago Pago	Nov. 16	00:51-06:02	5 hr 20 min	43° 29'S-14° 20'S	1. Overflights of New Zealand ground stations Wellington - ozonesonde 33,000 ft — 01:16 Raoul Island - radiosonde 35,000 ft — 02:54 2. Sunset run 37,000/39,000 ft — 04:10-05:38
14	Pago Pago - Honolulu/Hickam	Nov. 17-18	22:19-04:111	6 hr 00 min	14° 20'S-21° 20'N	1. Sunset run 39,000 ft — 02:42-03:45 2. Coordination with NASA 708/U-2 on sunset run

[a]Times listed are for takeoff to landing.
[b]"Flight duration" includes taxiing time to and from parked positions.

TABLE 2.- NASA 1976 CV-990 LATITUDE SURVEY MISSION FLIGHT LOG - Concluded

Data flt. No.	Route	Date (U.T.)	Time[a] (U.T.)	Flight[b] duration	Latitude range	Flight plan and coordinations
15	Honolulu/Hickam - Moffett Field	Nov. 18	18:46-23:17	4 hr 40 min	21° 20'N-37° 25'N	Coordination with NASA 708/U2 on entire route
Total time - data flights				81 hr 20 min		
Non-data Flights						
--	Moffett Field - Moffett Field	Oct. 22	17:06-20:51	4 hr 00 min	--	Maintenance check and pilot proficiency
--	Honolulu/Hickam - Honolulu/Hickam	Nov. 7	04:20-04:52	0 hr 40 min	--	Maintenance check of replacement engine No. 2
Total time - non-data flights				4 hr 40 min		
Total time - all flights				86 hr 00 min		

[a] Times listed are for takeoff to landing.
[b] "Flight duration" includes taxiing time to and from parked positions.

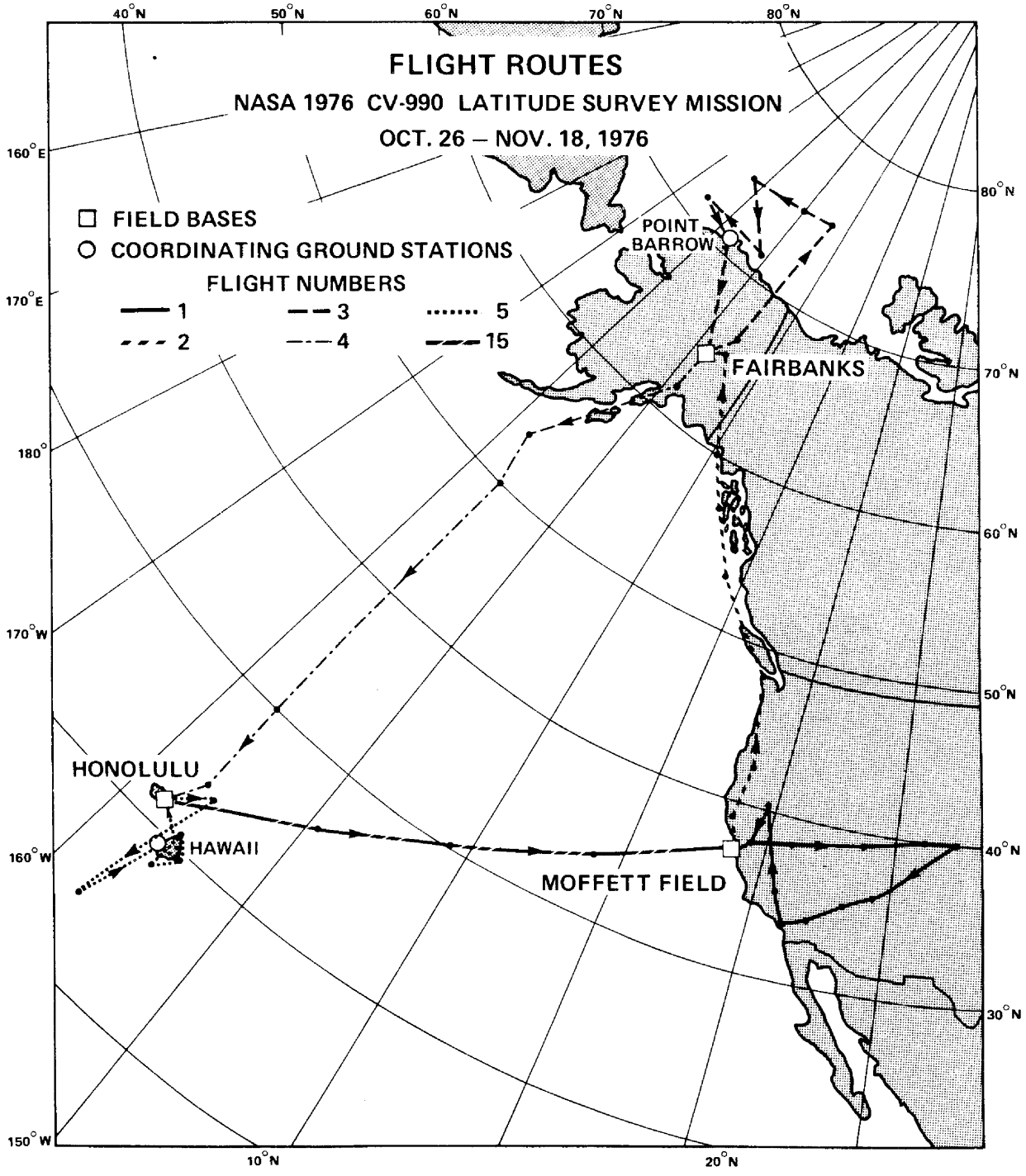

(a) Northern latitudes.

Figure 1.- CV-990 latitude survey routes.

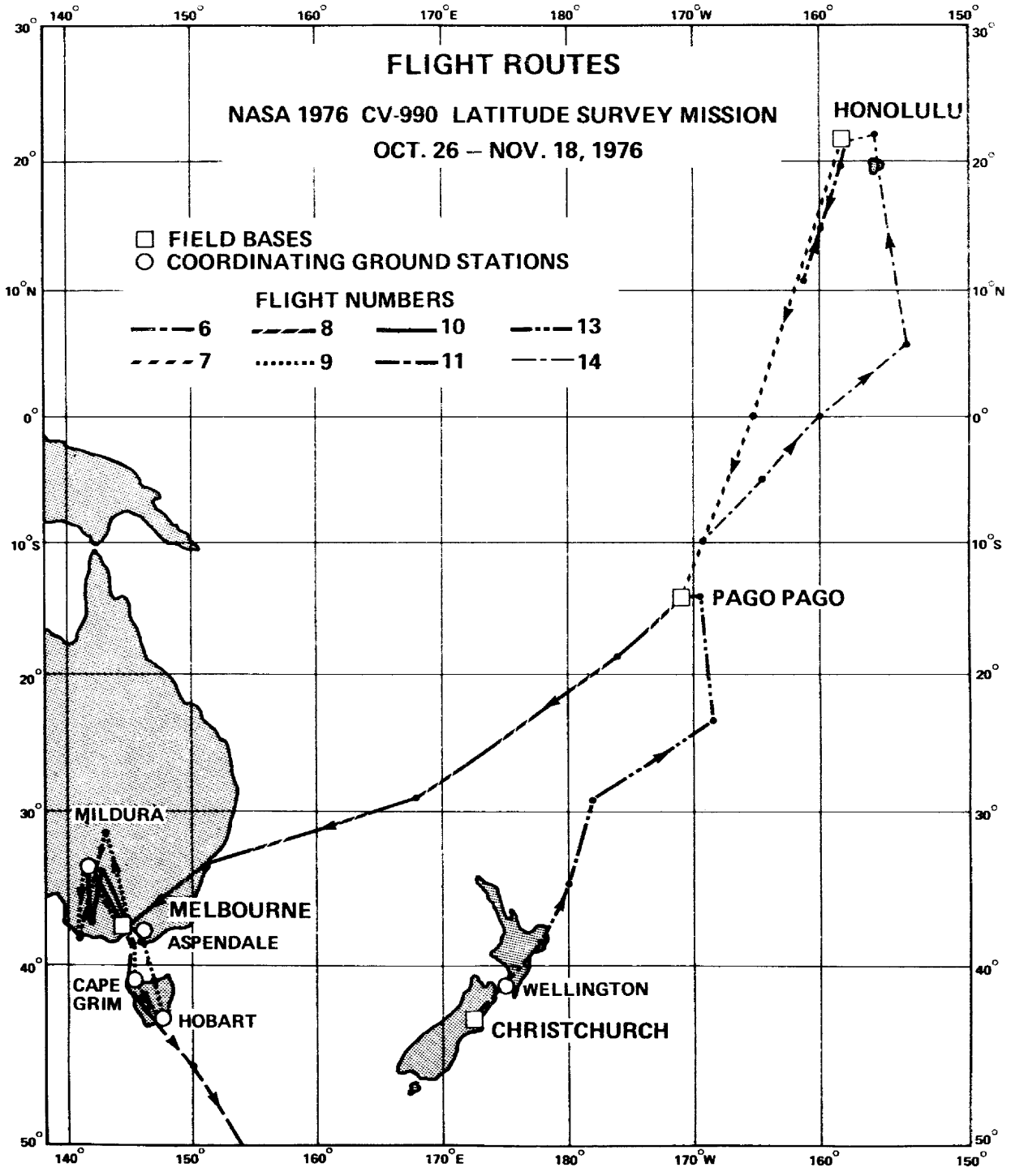

(b) Equatorial and southern latitudes.

Figure 1.- Continued.

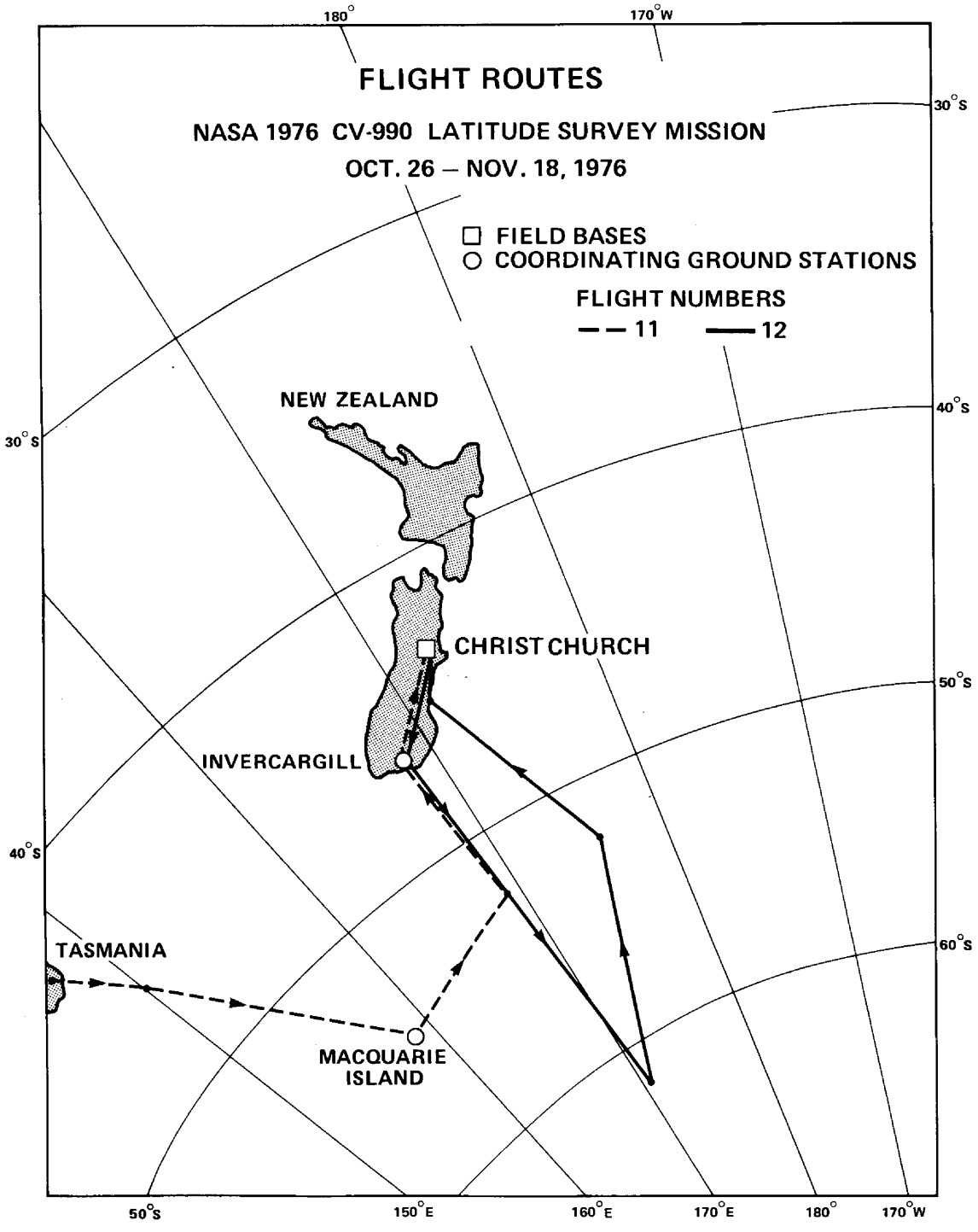

(c) Southern latitudes.

Figure 1.- Concluded.

GLOBAL ATMOSPHERIC SAMPLING PROGRAM ATOMSPHERIC CONSTITUENT MEASUREMENTS DURING THE CV-990 LATITUDE SURVEY MISSION

Daniel Briehl and Daniel J. Gauntner

NASA Lewis Research Center

Cleveland, Ohio 44135

INTRODUCTION

The latitudinal distributions of various atmospheric constituents were measured over the Pacific Ocean as part of the NASA Global Atmospheric Sampling Program (GASP). In addition to these measurements with flight instruments, other measurements were made with prototype instruments undergoing flight evaluations.

The GASP program currently operates automated constituent measurement systems on four B-747 aircraft flying in the commercial air corridors. The NASA CV-990 research aircraft is also equipped with an automated system. It is used for special flights to obtain information not obtainable from the 747 flights because of (1) area flown, or (2) tests of prototype instrumentation, which can be flown and monitored by onboard observers.

The objectives of the GASP Latitude Survey Mission on the CV-990 were threefold: to collect atmospheric constituent data synoptically over a north-south range of latitudes; to evaluate prototype sampling instruments in flight for possible inclusion in the automated B-747 systems; and also to compare GASP constituent data obtained during the mission with data obtained by other experiments using different techniques.

Flight instruments to measure ozone, water vapor, particles, condensation nuclei, and F-11 distributions were flown on the CV-990. Prototype instruments for measuring nitrous oxide, carbon dioxide, and total ozone were included in the aircraft system.

DESCRIPTION OF EXPERIMENT

Experimental System - The experimental system consisted of five in situ instruments for measuring trace constituents, and an ultra-violet spectrophotometer (UVS) for measuring ozone overburden above the flight level of the aircraft. The in situ instruments included: (1) an ultra-violet absorption ozone monitor; (2) an infrared absorption carbon dioxide monitor; (3) an infrared absorption nitrous oxide monitor; (4) a light scattering particle counter; and (5) a cooled-mirror water vapor monitor.

Sample air for the ozone, carbon dioxide, nitrous oxide monitors and the light scattering particle counter entered from a sample probe mounted in the forward part of the aircraft, was directed to the instruments, and was then exhausted through a static discharge probe. Sample air for the ozone, carbon

dioxide and nitrous oxide instruments was pressurized and maintained at one atmosphere by a single stage diaphragm pump and a system of pressure regulators. (Ref. 1) The advantages of operating these instruments at higher than cabin pressure were a gain in instrument sensitivity and an elimination of the possibility of leaks into the sample system from the cabin. Sample air for the light scattering particle counter was not pressurized to avoid particle losses and contamination by a pump. A heat transfer mass flowmeter located downstream of the instrument was used to measure sample flow-rate.

The in situ ozone monitor was a self-contained ultraviolet absorption photometer. The operation of this instrument was based on the measurement of the absorption by ozone at 39417 cm^{-1} (253.7 nm) in an absorption chamber 71 centimeters long. Measurements were updated every 20 seconds upon the completion of two half-cycle periods. During the first half cycle, the sample flow was passed through a catalytic scrubber which removed the ozone and produced a reference integrated light intensity measurment. During the second half cycle the ozone was not scrubbed and the light intensity was integrated over the same time period as the reference measurement. The difference between the two measurements was related to the ozone concentration. Both the carbon dioxide and the nitrous oxide monitors measured the absorption of infrared radiation. Each instrument contained a source of infrared radiation and two narrow band pass optical filters, one to isolate a waveband where the test gas does not absorb, and another to isolate a waveband where it absorbs strongly. A single beam of radiation was modulated by alternately passing the reference and sample filters through the beam. Any difference signal obtained when the cell contained no test gas was nulled. The absorbance measured when the cell contained test gas was proportional to the partial pressure of the absorbing gas. The reference and sample wavebands transmitted by the CO_2 filters were centered at about 2500 cm^{-1} (4000 nm) and 2350 cm^{-1} (4253 nm) respectively. Sample cell path length was one meter. Carbon dioxide free sample air was obtained by drawing air through a lithium hydroxide scrubber to remove carbon dioxide.

The nitrous oxide monitor used a reference wavelength of 2380 cm^{-1} (4202 nm) and a sample wavelength of 2200 cm^{-1} (4545 nm). Sample cell path length was 20 meters. Instrument zero was obtained by evacuating the cell to 0.27 newtons per square centimeter.

The particle counter used a near forward light scattering technique to measure the number of airborne particles larger than 0.3 micrometers in diameter. As the air sample passed through the sensor it was illuminated by a light beam, and light scattered by the particles was detected by a photomultiplier tube. Under normal operating conditions each particle caused a pulse in the photomultiplier output. The particle concentration was determined by counting the number of output pulses during a one minute period and then dividing that number by the corresponding sample flowrate. Particle counter flowrate was 7,000 cubic centimeters per minute.

The cooled mirror hygrometer consisted of a sensing unit and an electronics package. The sensing unit consisted of a mirror mounted on a two-stage thermoelectric cooler. The sample flow was directed across the face of the mirror. The mirror is illuminated and two photodetectors are located so as to monitor the direct and diffuse components of the reflected light. The photodetectors are arranged in a bridge circuit. The mirror is cooled until a thin condensate layer is maintained on the mirror surface and the

output of the optical bridge is balanced. This point is the dew-frost point temperature and was measured by a platinum resistance thermometer. The sensor unit was mounted below a modified total temperature air scoop which supplied the sample flow.

The UVS is used to determine total ozone overburden from measurements of downward ultraviolet radiation from 25000 to 50000 cm^{-1} (400 to 200 nm). UV flux is measured omni-directionally up to 75 degrees from the vertical by a diffuser, a movable wheel containing bandpass filters and a photodiode.

Automated System - The automated system is operated by a pre-programmed data management and control unit. The system (Ref. 2) records on magnetic tape all system status, constituent data, and related meteorological parameters. The typical GASP data are processed at NASA-Lewis and then archived at the National Climatic Center (NCC), Asheville, North Carolina (Ref. 3). All valid constituent and meteorological data obtained from the survey mission will be archived at the NCC.

The GASP automated system contained in situ instruments for the measurement of ozone, carbon monoxide, condensation nuclei, and light scattering particles. The system was also equipped with a package containing 4 sample bottles which could be filled at the discretion of the field experimenter or the CV-990 Flight Director. A total of eight packages were filled during the mission. These bottles are being analyzed in the laboratory for F-11 (for technique, see Ref. 3) and will be analyzed for F-12, N_2O, and CCl_4.

The automated system acquired sample air through a 2.54 cm probe permanently fixed outside the boundary layer to the underbody of the CV-990 fuselage. The sample air for the ozone and carbon monoxide measurements was pressurized to one atmosphere by equipment similar to that used in the experimental system.

The in situ ozone monitor was similar to the one used in the experimental system. The condensation nuclei counter operated like a cloud chamber, i.e., water was condensed on any particle larger than about 0.003 micrometers in diameter. The number of nuclei in the resulting cloud was determined by measuring the attenuation of a light beam passing through a cloud. Measurements were made at the rate of one per second.

The carbon monoxide monitor was a single beam non-dispersive infrared absorption analyzer using a dual-isotope fluorescence technique. The instrument was periodically zeroed by passing the sample air through a heated catalytic filter which oxidized the carbon monoxide. The light scattering particle counter collected near-forward light to count the number of particles and to separate them into various size ranges.

RESULTS AND DISCUSSION

Experimental System - Ozone: The latitudinal ozone distribution is shown plotted in figure 1. For all altitudes from 8.8 to 11.9 kilometers the ozone concentration is quite low (below 50 ppbv) for the latitudes from 25° North to 25° South. At the higher latitudes, ozone concentrations are generally higher as expected. Concentrations above about 150 ppbv are an indication of flight in stratospheric air. The ozone data have been corrected for losses in the sample inlet train. Data are plotted at 15 minute intervals.

Light Scattering Particles: Figure 2 shows the latitudinal distribution of particles greater than 0.3 micrometers in diameter. The distribution is

somewhat similar to the ozone distribution in that lower concentrations are generally found at the tropical latitudes with higher concentrations at the higher latitudes. The flagged points indicate data taken while the aircraft was flying through clouds. When the aircraft is flying through clouds, water droplets are registered as particles. The shaded points indicate flight in the stratosphere. Higher concentrations generally occur during flight in the stratosphere. Fewer data with concentration greater than 1 particle per cubic centimeter were found in the Southern Hemisphere. Concentrations below 0.03 particles per cubic centimeter were only found in the tropical latitudes. A typical particle size distribution is shown in figure 3. Slope of the distribution range from -2.8 to -5.2 which is indicative of a well-aged aerosol.

Water Vapor: The latitudinal variations in water vapor concentrations are shown in figure 4. As expected, the highest water vapor concentrations were recorded in the tropical latitudes. The lowest water concentration recorded was 11 ppmw at 75° north latitude at an altitude of 10.1 km. The line in Figure 4 connects the minimum values of measured water vapor. In general, its shape indicates the regions where the Hadley cell and the other circulation cells interact, transporting large scale air masses up and down in the Earth's atmosphere.

Nitrous Oxide: Considerable variation exists in the data which may partially be explained by a gradual decrease in the sensitivity of the instrument during the course of each flight. Efforts are now being made in the laboratory to determine the cause of this gradual decrease in sensitivity. As a result, it is hoped that some of the data may eventually be retrievable.

Carbon dioxide: After flight 7 the sensitivity of the instrument decreased such that most of the data was far below published concentration values. Analysis of data on the first 7 flights is continuing.

UVS: A limited amount of total ozone data is now available. These data are listed in table 1. Detailed analysis of the balance of the UVS data will be made after a computer program is developed.

Automated System - The computer operated automatic system obtained data on ozone, condensation nuclei, the chlorofluoromethanes, carbon monoxide, light-scattering particles, and meteorological data. In addition, tropopause pressure height data (Ref. 3) will be coded into the GASP data when it is archived at the NCC.

Ozone data were recorded for the entire mission. The data for flights 1-4 were invalid due to an instrument failure. After an instrument replacement, predominantly tropospheric levels of ozone were measured during the remainder of the mission. Notable exceptions were during flights 9 and 11 when the ozone mixing ratios reached 300 to 400 ppbv levels, respectively. Figure 5 shows a vertical ozone profile for 4 - 11 km measured during flight 10, which coordinated with the Australian "Hibal" balloon flight from Mildura. Each data point is a computed mean value.

Data on condensation nuclei (CN) particles were obtained during the entire mission. Figure 6 shows a five minute segment of flight 14 where the CN count was abnormally high. Calibration of the instrument revealed poor sensitivity below 300 particles/cm^3 counting rates. Approximately 80% of the data were below a level of 300 particles/cm^3.

SUMMARY OF RESULTS

The latitudinal distributions of various atmospheric constituents were measured during the NASA CV-990 Latitude Survey Mission as part of the GASP Program. Data and instrumentation information were obtained for a number of species. The results from preliminary analyses were as follows:

1. Latitudinal distributions were obtained for ozone, water vapor, and particles. Each distribution exhibited expected equatorial minima and near polar maxima.
2. Distributions were obtained for total ozone with the prototype UV spectrophotometer.
3. Data for distributions of nitrous oxide, carbon dioxide, carbon monoxide, and F-11 were obtained. Problems with calibration or instrument operation make the obtained data either difficult or impossible to retrieve.

REFERENCES

1. Reck, Gregory M; Briehl, Daniel; and Perkins, Porter J: Flight Tests of a Pressurization System Used to Measure Minor Atmospheric Constituents From an Aircraft. NASA TN D-7576, 1974.

2. Perkins, Porter J.: Global Measurements of Gaseous and Aerosol Trace Species in the Upper Troposphere and Lower Stratosphere from Daily Flights of 747 Airliners. NASA TM X-73544, 1976.

3. Holdeman, J. D., and Humenik, F. M.: NASA Global Atmospheric Sampling Program (GASP) Data Report for Tape VL0004. NASA TM X-73574, 1976.

TABLE I - Ultraviolet Spectrophotometer Data
Taken On-Board the CV-990 Aircraft

Flight	GMT	Lat.	Long.	Alt, km	Total Ozone,*Atm-cm
5	1808	19.75N	155.58W	10.7	.230
9	2155	40.18S	144.18E	6.4	.303
9	2241	42.35	147.30	11.7	.288
9	2319	37.98	145.98	11.9	.278
11	0006	43.10	147.70	10.7	.283
11	0151	54.49	159.53	10.7	.314
11	0327	46.30	169.90	11.3	.321
12	0329	47.10	169.00	10.1	.322
13	0119	41.10	175.12	10.1	.336

* Data has not been corrected for amount of ozone below aircraft.

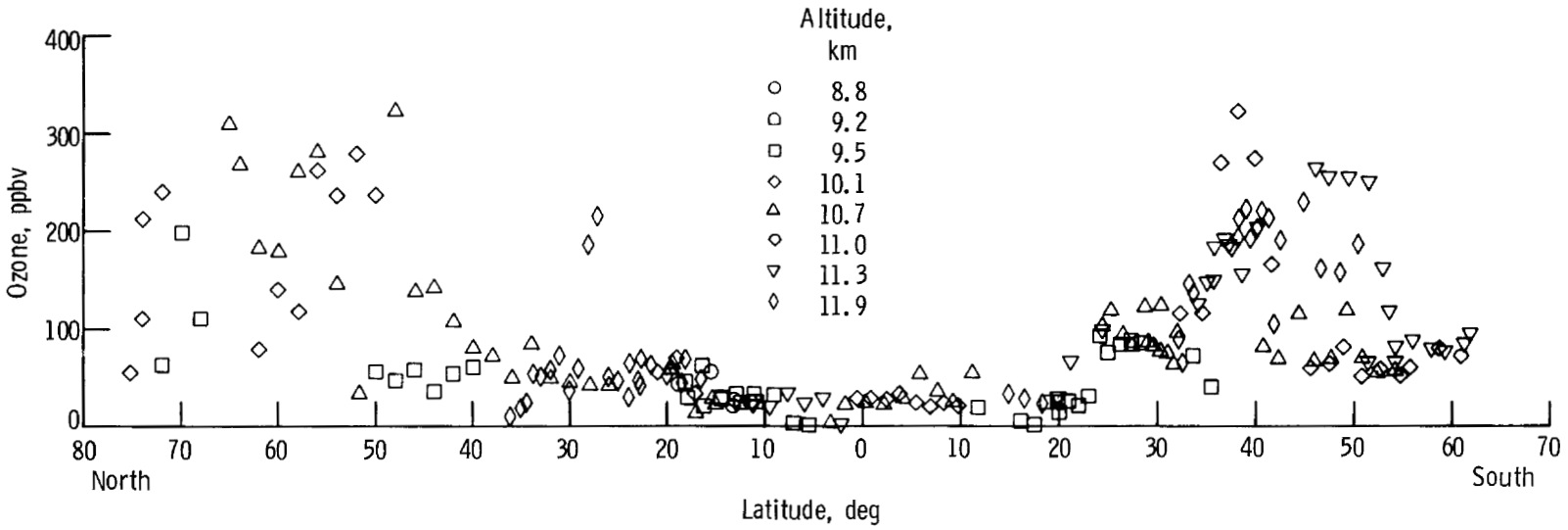

Figure 1. - Latitudinal ozone distribution.

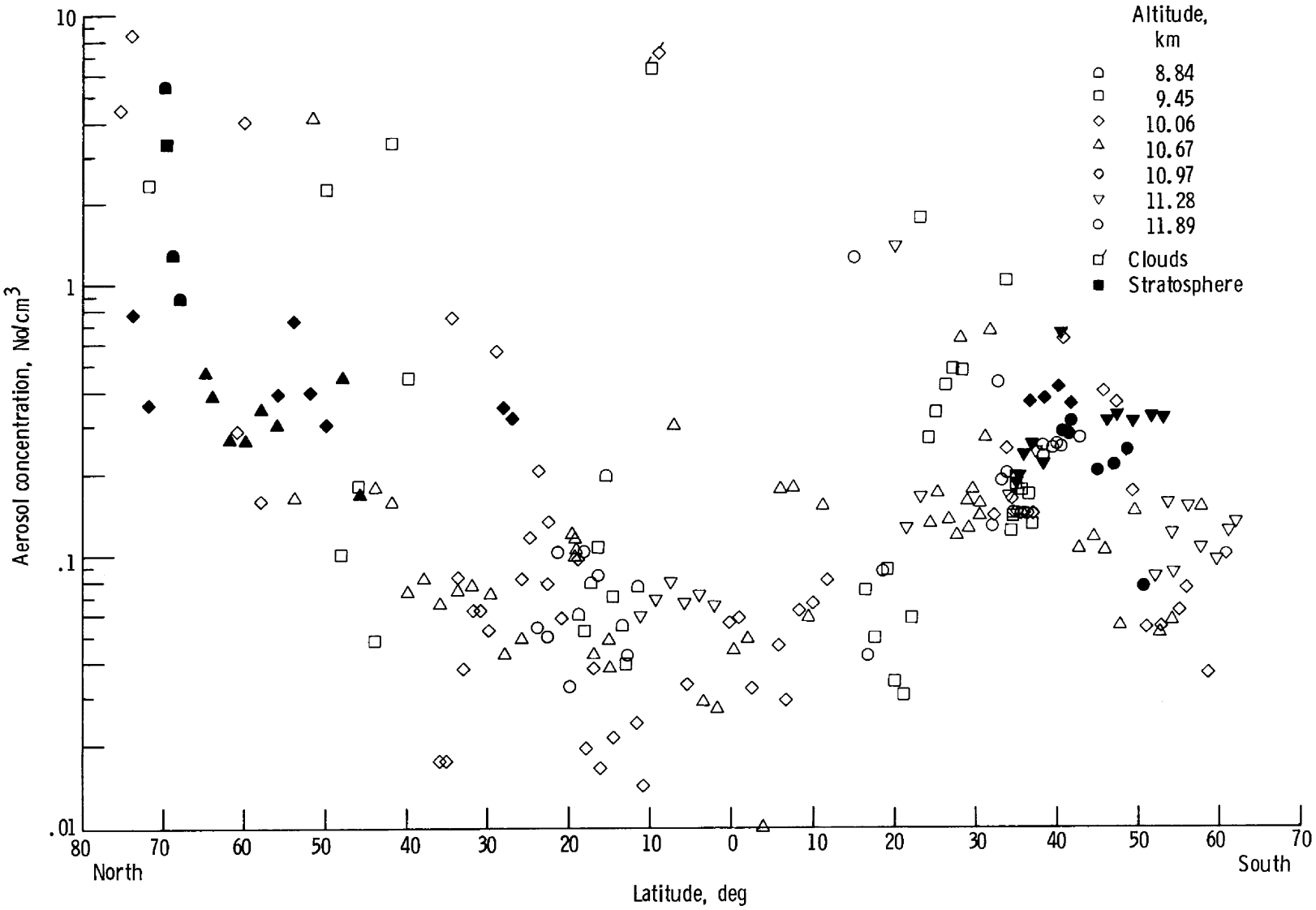

Figure 2. - Latitudinal distribution of particles >0.3 μm diameter.

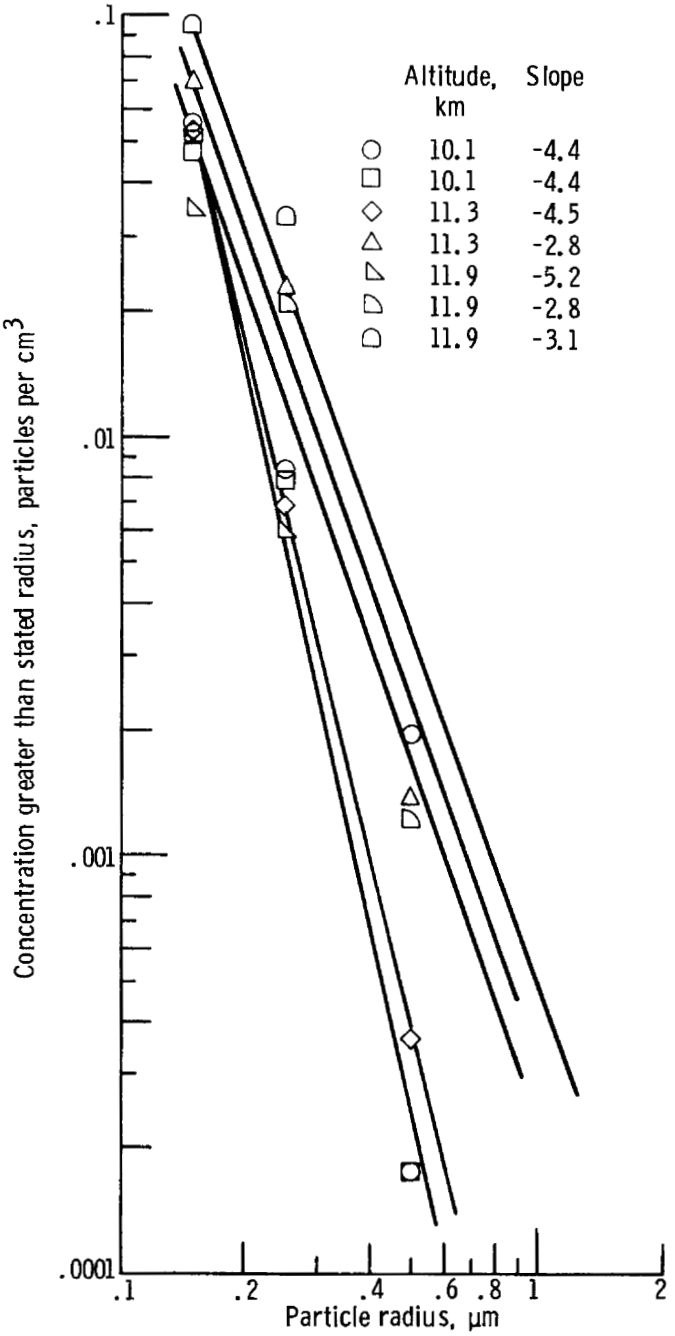

Figure 3. - Particle size distribution from flight 14, Pago Pago to Honolulu.

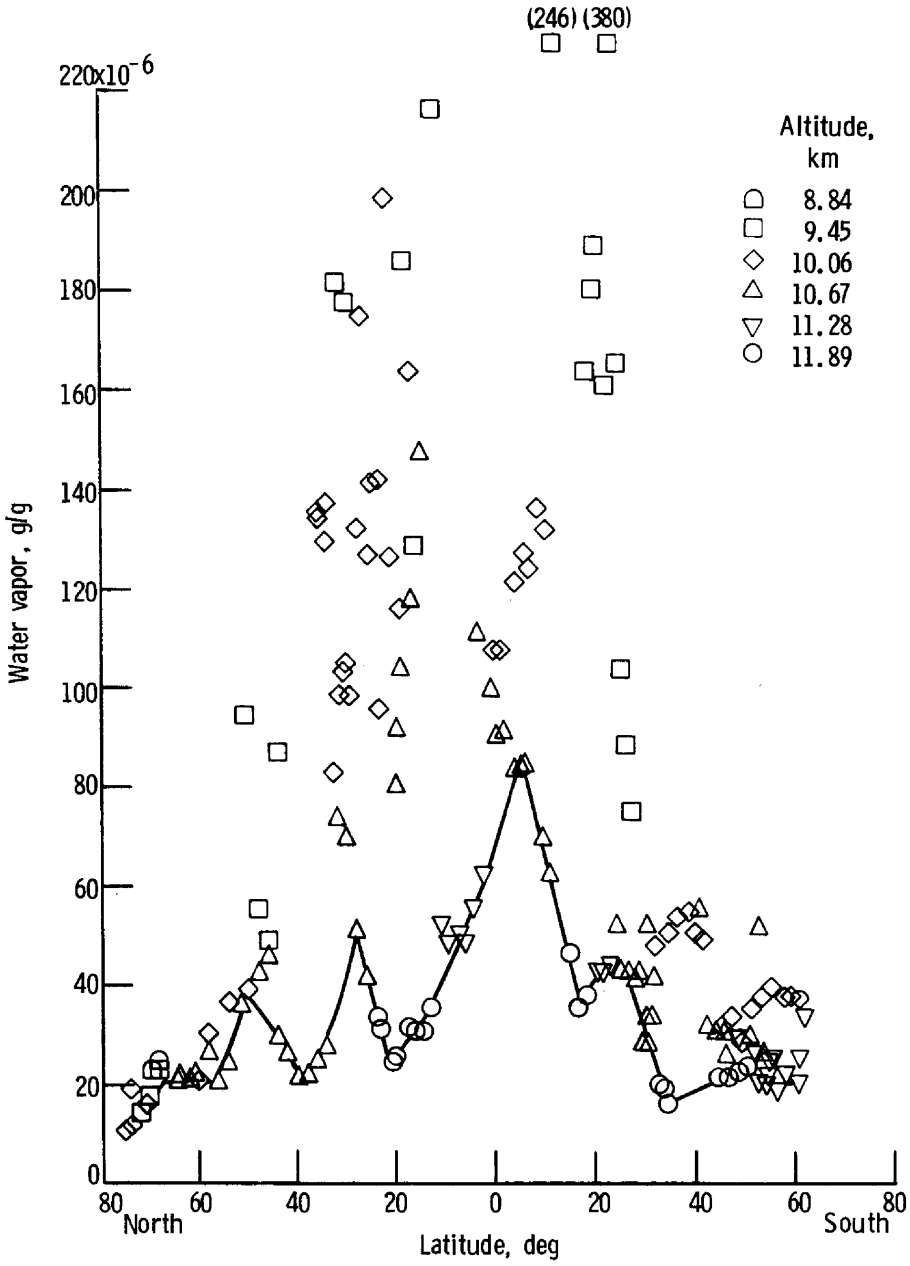

Figure 4. - Latitudinal distribution of water vapor.

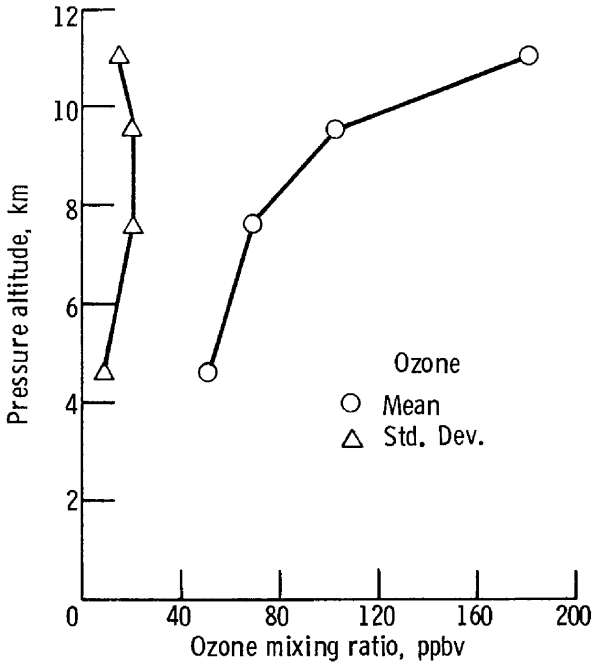

Figure 5. - Mean ozone vertical profile. In-situ measurements during CV-990 Latitudinal Survey flight 10. 34° S latitude, 142° E longitude.

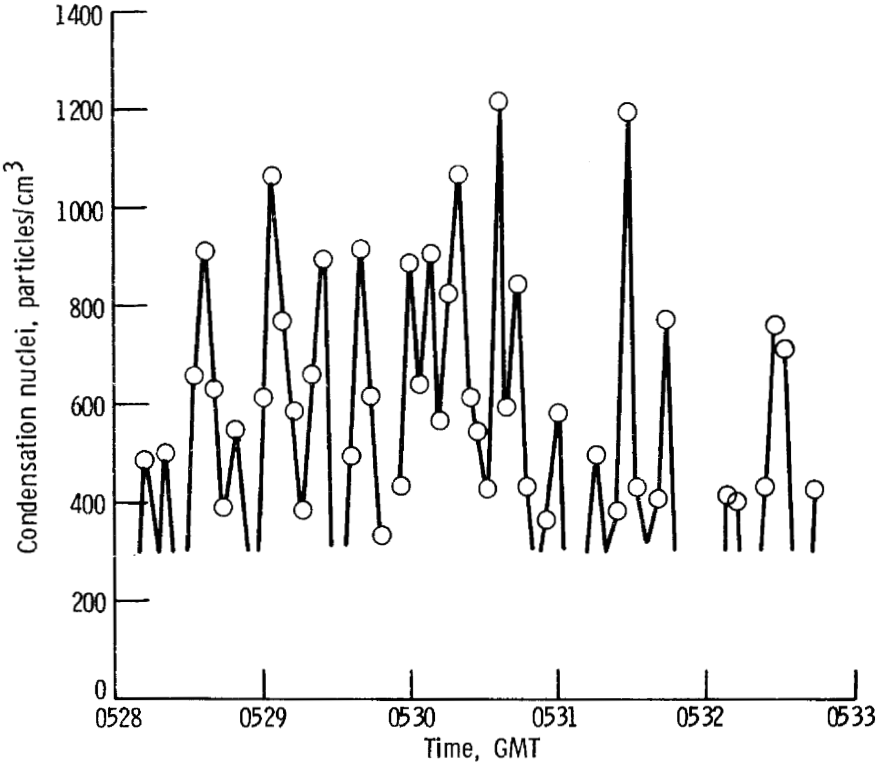

Figure 6. - Condensation nuclei concentration. In-situ measurements during CV-990 Latitudinal Survey flight 14. (14.75^0 S latitude, 169.6^0 W longitude at 11.8 km.)

THE MICROWAVE LIMB SOUNDER EXPERIMENT: OBSERVATIONS OF STRATOSPHERIC AND MESOSPHERIC H_2O

by

J. W. Waters[1], J. J. Gustincic[2], R. K. Kakar[1], A. R. Kerr[3],

H. K. Roscoe[1], and P. N. Swanson[1]

[1]Jet Propulsion Laboratory, Pasadena, California 91103
[2]Consulting Engineer, Marina Del Rey, California 90291
[3]Goddard Institute for Space Studies, New York, New York 10025

SUMMARY

The Microwave Limb Sounder (MLS) experiment was operated continuously on all fifteen flights of the 1976 NASA CV-990 Latitude Survey Expedition. All the MLS objectives for the expedition were accomplished.

The principal objective of the MLS on the expedition was to measure water vapor in the upper stratosphere and mesosphere from observations of thermal emission by its rotational transition at 183 GHz (1.64 mm wavelength). Approximately 90% of the available measurement time was devoted to this objective. Preliminary analysis indicates that the altitude variation in H_2O predicted by current photochemical models is consistent with the MLS measurements. The measured emission from H_2O in the upper stratosphere decreased slightly from polar to tropical latitudes, with slightly less emission observed in the southern hemisphere.

Other MLS objectives included (1) measurement of the 184 GHz O_3 line, (2) engineering measurements with the instrument tuned for the 167 GHz $Cl O$ line, and (3) comparison of variations in water vapor observed by the MLS and by Dr. Peter Kuhn's infrared radiometer. The 184 GHz O_3 line was measured with good signal to noise during the flight coincident with an ozonesonde launched from the CSIRO station in Aspendale, Australia. This will allow comparison of the ozonesonde and MLS ozone measurements. Engineering data for the 167 GHz $Cl O$ measurement were taken during the local flight from Honolulu; instrumental baselines were encouraging for a measurement of $Cl O$ to be attempted by the MLS on the CV-990 ASSESS-II mission in May 1977. The MLS and infrared signals from Dr. Kuhn's radiometer for H_2O were simultaneously

recorded on a dual-channel strip chart recorder and, during clear sky conditions above the aircraft, the correlation was excellent.

INTRODUCTION

The Microwave Limb Sounder (MLS) is an experiment being developed to remotely sense the composition and temperature of Earth's stratosphere, mesosphere, and lower thermosphere. The ultimate application of the experiment is for research and monitoring of these regions of the atmosphere on a global scale from a satellite or Space Shuttle platform. The first step in the MLS development was the construction of an aircraft version of the instrument for measurements of H_2O and O_3. Development of this instrument is part of NASA's Advanced Applications Flight Experiments (AAFE) program. The Upper Atmospheric Research Program at NASA has supported extension of the operating range of the instrument to cover the spectral range for $C\ell O$ and aircraft measurements with the instrument, including those described in this report.

The measurement of upper stratospheric and mesospheric water vapor was chosen as the principal objective for the MLS on the Latitude Survey Expedition because:

1. In the altitude region sensed by the MLS ($\sim$ 25-80 km), water vapor is thought to be produced by the reactions (references 1, 2)

$$OH + CH_4 \rightarrow H_2O + CH_3$$

$$OH + HO_2 \rightarrow H_2O + O_2$$

involving the OH and HO_2 radicals which are important in stratospheric ozone chemistry, and is destroyed, at the higher levels sensed, by solar ultraviolet.

2. Few measurements of H_2O in this region have been previously made, and none with as wide an altitude and latitude coverage as would be possible with MLS on the expedition. Consequently the MLS measurements of H_2O over this range were expected to improve our knowledge of the hydrogen chemistry of the stratosphere and mesosphere.

3. The signal from water vapor is sufficiently strong that the probability of success in performing the measurement was quite high, an important consideration for an expedition as unique as the Latitude Survey. Although some of the other molecules which should be detectable with the MLS (e.g., $C\ell O$,

H_2O_2) are perhaps of more immediate importance for present problems of stratospheric chemistry than is H_2O, the signals from these molecules are sufficiently weak that it was decided to use upcoming local flights, rather than the Latitude Survey, to attempt their measurement.

MEASUREMENT TECHNIQUE

The MLS observes thermal radiation from the atmospheric limb in certain discrete bands at millimeter wavelengths. These bands are chosen to cover spectral regions in which the thermal radiation is principally due to particular molecules of interest. The observed signal depends both upon the abundance of the molecule and its temperature. By choosing the observing direction and spectral band such that the atmospheric path being observed is optically thin (i.e., total attenuation through it is small), then the observed signal depends mainly upon the abundance of the molecule.

For limb measurements made from platforms above the atmospheric region being sensed, altitude resolution can be obtained by having an instrument with a highly directional field of view. In this case the altitude resolution is given by the field of view of the instrument.

For measurements made from platforms below the atmospheric region being sensed, as is the case for the aircraft MLS measurements, altitude resolution can be obtained by observing the shape of atmospheric emission or absorption lines. At microwave and millimeter wavelengths broadening of atmospheric lines is dominated by collisions throughout the stratosphere and into the mesosphere. In this region the line width decreases drastically with altitude; if a spectral line is observed to be narrower than a certain amount, it must have originated at altitudes higher than a certain value. The altitude resolution which can be achieved by the method is somewhat limited, being approximately two atmospheric scale heights for a uniformly mixed gas (reference 3). At sufficiently high altitudes Doppler (thermal) broadening of spectral lines dominates the collisional broadening; at these altitudes the spectral shape contains little information about the altitude distribution of the gas because the Doppler width is a very weak function of altitude.

Figure 1 shows the collisional and Doppler line width parameters (half width at half intensity) for the $3_{13} \rightarrow 2_{20}$ 183.310 GHz H_2O line which was

observed by the MLS on the Latitude Survey Expedition. Collisional broadening of this line dominates up to approximately 70 km, and the line shape gives altitude information to this altitude. Above approximately 70 km only the total column abundance of H_2O molecules is obtained. Also shown in Figure 1 are the positions of the MLS channels as configured for the expedition. These channel positions allow a coarse altitude profile of H_2O to be determined between approximately 25 and 70 km, and column abundance of H_2O above 70 km. More details of measuring H_2O from observations of its 183 GHz line are given in reference 4.

INSTRUMENTATION AND OBSERVATION PROCEDURE

The MLS aircraft instrument consists of: (1) a millimeter-wavelength receiver which receives the atmospheric radiation, down-converts its frequency, and amplifies it such that the signal can be processed by conventional electronics; (2) a system which performs spectral analysis of the signal from the receiver; and (3) a data handling system which performs calibration, averaging, and recording of the signals from the spectrum analyzer.

The receiver is a Dicke-switched double-sideband superheterodyne system which combines the signal and local oscillator quasi-optically (reference 5), and incorporates a new low-noise mixer design (reference 6). A phase-locked klystron is used for the local oscillator. The first frequency down-conversion is to 1.42 GHz with a first stage room temperature parametric amplifier. The receiver contains internal calibration targets at ambient and liquid nitrogen temperatures. The liquid nitrogen target is also used as the reference of the Dicke-switch; a mirror within the receiver switches the receiver input between the atmosphere and this target at 4 Hz switching frequency. Observations of the atmospheric radiation were performed through a specially-constructed polyethylene window with measured 9% loss at 183 GHz. The receiver was mounted on top of a standard NASA CV-990 lowboy rack and observed through a passenger window port which contained the polyethylene window. Optics within the receiver formed a beam of 4 degrees width; the entire receiver could be tilted such that this beam could receive atmospheric emission between elevation angles of 0° and 25°. Figure 2 shows the receiver and associated local oscillator electronics.

Spectral analysis of the signal from the receiver is performed by a 15 channel filter bank and a 256 channel Fourier transform spectrometer operating in parallel. The filter bank covers a total bandwidth of 160 MHz, with resolution varying from 1 MHz at center to 32 MHz at the edge of its band. The Fourier transform spectrometer has 0.04 MHz resolution over a total band of 10 MHz; during operation three adjacent resolution elements were averaged to give a net resolution of .12 MHz.

A desk calculator with cassette recorder was used to perform all data handling and recording. Averaged and calibrated spectra were printed out in real time on a small line printer. The calculator, line printer, and spectral analysis system are shown in Figure 3.

The observational procedure used for the H_2O measurements was to take data in five minute blocks with the receiver switching between the atmosphere at 20° elevation and the liquid nitrogen target. At the elevation angle of 20°, the atmospheric absorption was sufficiently small (as long as the aircraft operated in the stratosphere) that signals from higher altitudes were not substantially attenuated; this attenuation was measured, approximately once per flight, by observing the H_2O emission line as a function of elevation angle. After approximately three five-minute observations, the receiver was calibrated and observations resumed. This procedure was followed throughout the expedition.

RESULTS

We here discuss results of preliminary analysis of the MLS measurements of water vapor in the upper stratosphere and mesosphere. Other results also obtained by the MLS during the expedition are mentioned in the summary of this report.

Figure 4 shows examples of measurements of the 183 GHz H_2O and 184 GHz O_3 lines. As can be seen the H_2O line is significantly narrower than the O_3 line. This implies there is relatively more H_2O than O_3 at higher altitudes.

In order to determine the range of H_2O profiles which are consistent with the MLS measurements, we performed calculations of emission from the 183 GHz H_2O line for the mixing ratio profiles shown in Figure 5. Profiles B, C, and BB′ are indicative of mixing ratios which have been measured at altitudes below 50 km (reference 7) and are consistent with photochemical calculations above

50 km (reference 2). Some of the measurements below 50 km indicated a decreasing H_2O mixing ratio with altitude at the highest altitudes measured; profile A was thus chosen to determine whether a continually decreasing mixing ratio above 50 km is consistent with our measurements. A recent ground-based microwave measurement of H_2O in the mesosphere (reference 8) suggested an H_2O mixing ratio of more than 10^{-5} between 50 and 80 km; profile D was thus also chosen to determine whether such an increase in mixing ratio from the stratosphere to the mesosphere is consistent with our measurements.

Figure 6 compares results of the calculations with the MLS measurements made in three latitude bands during the expedition. The measurements suggest that the H_2O profile lies between C and B. Profiles A and D are inconsistent with the measurements. Although a standard temperature profile was used for the calculations, uncertainties in the temperature (now under investigation) are not expected to change these preliminary conclusions.

Figure 7 shows the observed latitude variation in the H_2O emission arising principally from two levels in the upper stratosphere. This variation suggests that during the time of the expedition the upper stratospheric water vapor decreased slightly from the sub-polar to sub-tropical latitudes with slightly less in the southern hemisphere. However, temperature variations could be responsible for some of the observed variation in the emission. A cursory examination of temperature data from the Pressure Modulator Radiometer experiment on the Nimbus 6 satellite (kindly supplied by Professor J. T. Houghton of Oxford, U.K.) suggests that temperature cannot explain all of the observed variation in the H_2O emission.

The results given here should be considered as quite preliminary. A more complete analysis of the measurements is now underway.

REFERENCES

1. McConnell, J. C.; McElroy, M. B.; and Wofsy, S. C.: Natural Sources of Atmospheric CO. Nature, vol. 233, 1971, p. 187.
2. Anderson, J. G.; and Donahue, T. M.: The Neutral Composition of the Stratosphere and Mesosphere. Jnl. Atmos. Terres. Phys., vol. 37, 1975, p. 865.
3. Waters, J. W.: Ground-Based Microwave Spectroscopic Sensing of the Stratosphere and Mesosphere., Ph.D. Thesis, Massachusetts Institute of Technology, 1971.

4. Waters, J. W.: Remote Sensing of Atmospheric O_3 and H_2O to 70 km by Aircraft Measurements of Radiation at 1.64 mm Wavelength. Proc. 8th Int. Symp. Remote Sensing of Environment, Environmental Research Institute of Michigan, 1972, p. 467.

5. Gustincic, J. J.: A Quasi Optical Radiometer. Digest of Second Int. Conf. on Submillimeter Waves (IEEE Cat. No. 76 CH 1152-8 MTT), San Juan, 1976, p. 106.

6. Kerr, A. R.; Mattauch, R. J.; Grange, J.: A New Mixer Design for 140-220 GHz. In press, 1977.

7. Harries, J. E.: The Distribution of Water Vapor in the Stratosphere. Rev. Geophys. and Space Phys., vol. 14, 1976, p. 565.

8. Radford, H. E.; Litvak, M. M.; Gottlieb, C. A.; Gottlieb, E. W.; Rosenthal, S. K.; Lilley, A. E.: Mesospheric Water Vapor Measured from Ground-Based Microwave Observations. Jnl. Geophys. Res., 1977, in press.

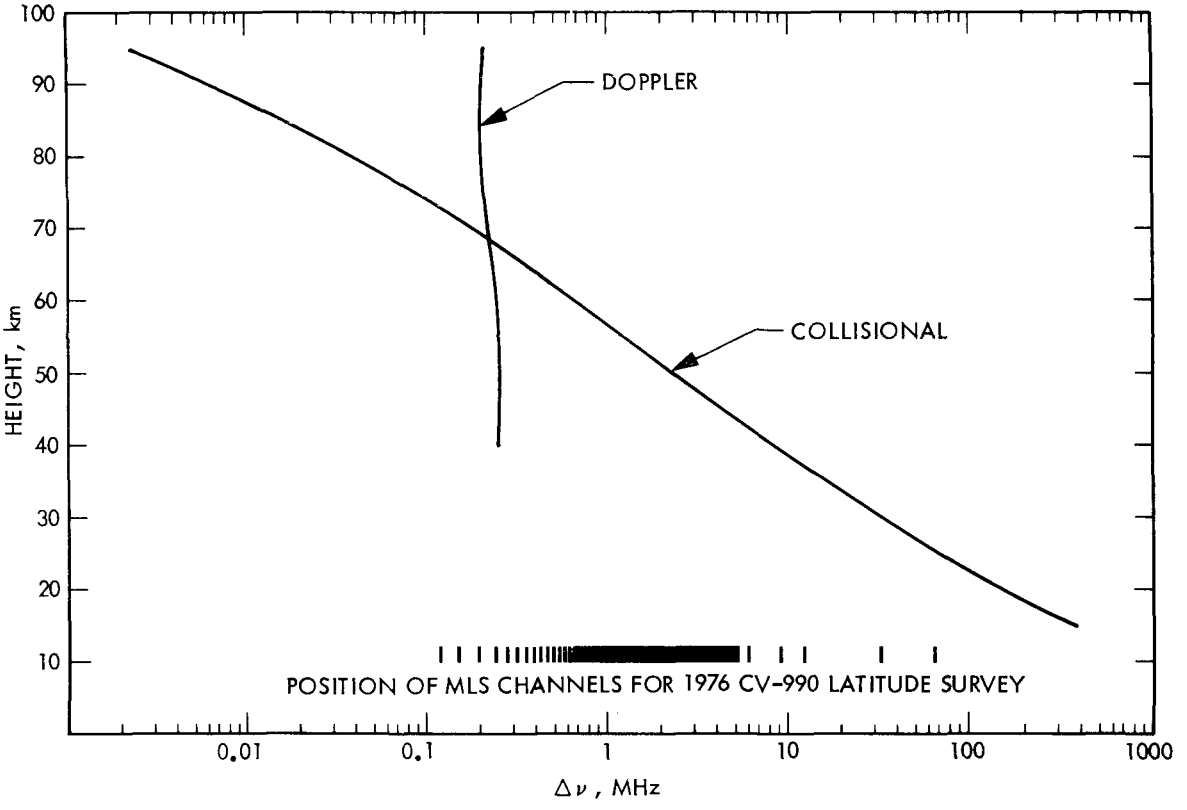

Figure 1. Doppler and collisional linewidth parameters $\Delta\nu$ for the 183 GHz H_2O line as a function of height. The linewidth parameter is the half-width at half-maximum-intensity of the spectral line. The values were calculated using measured molecular parameters and the U.S. Standard Atmosphere.

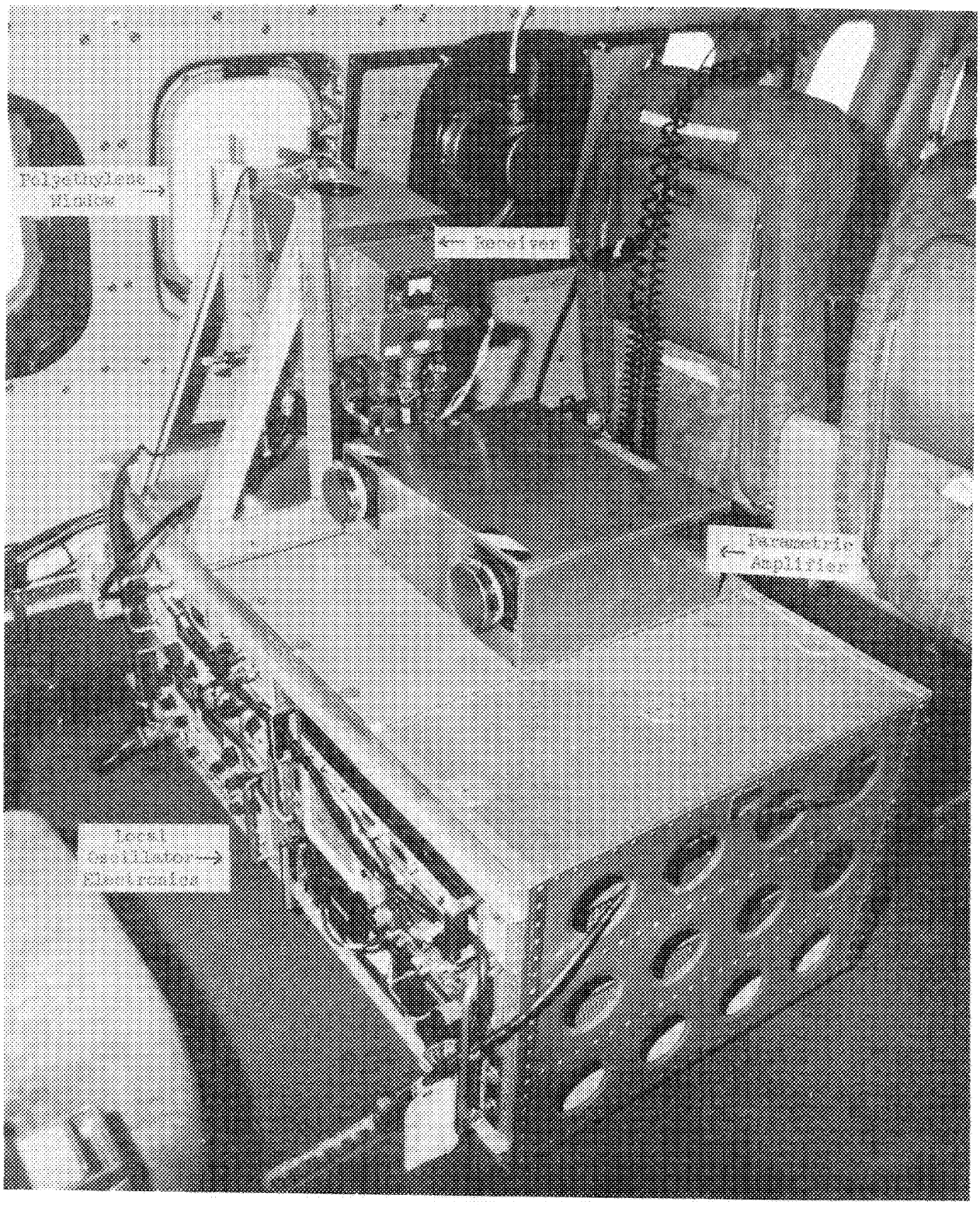

Figure 2. The MLS Receiver and Local Oscillator Electronics.

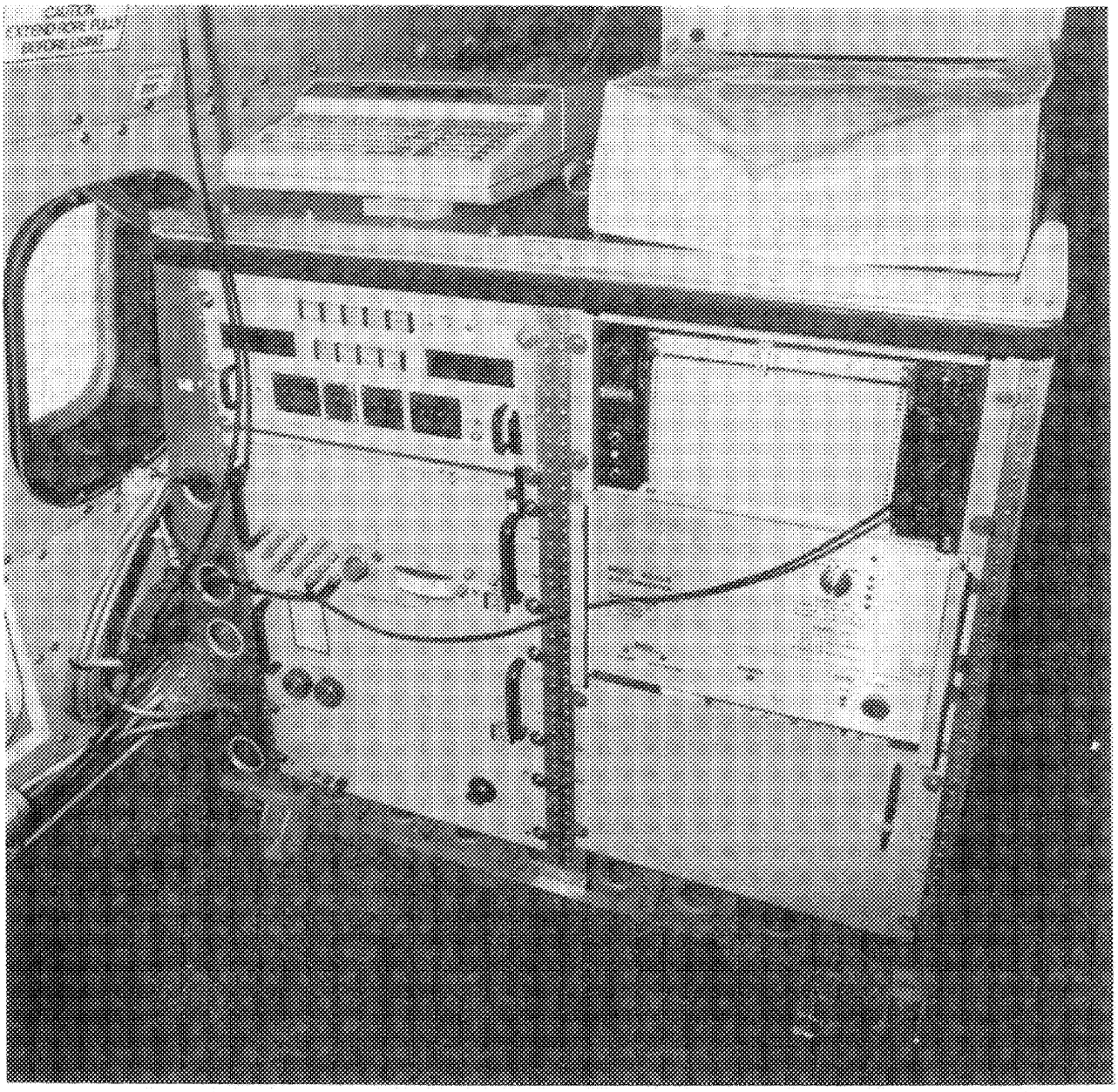

Figure 3. The MLS Spectral Analysis and Data Handling Systems.

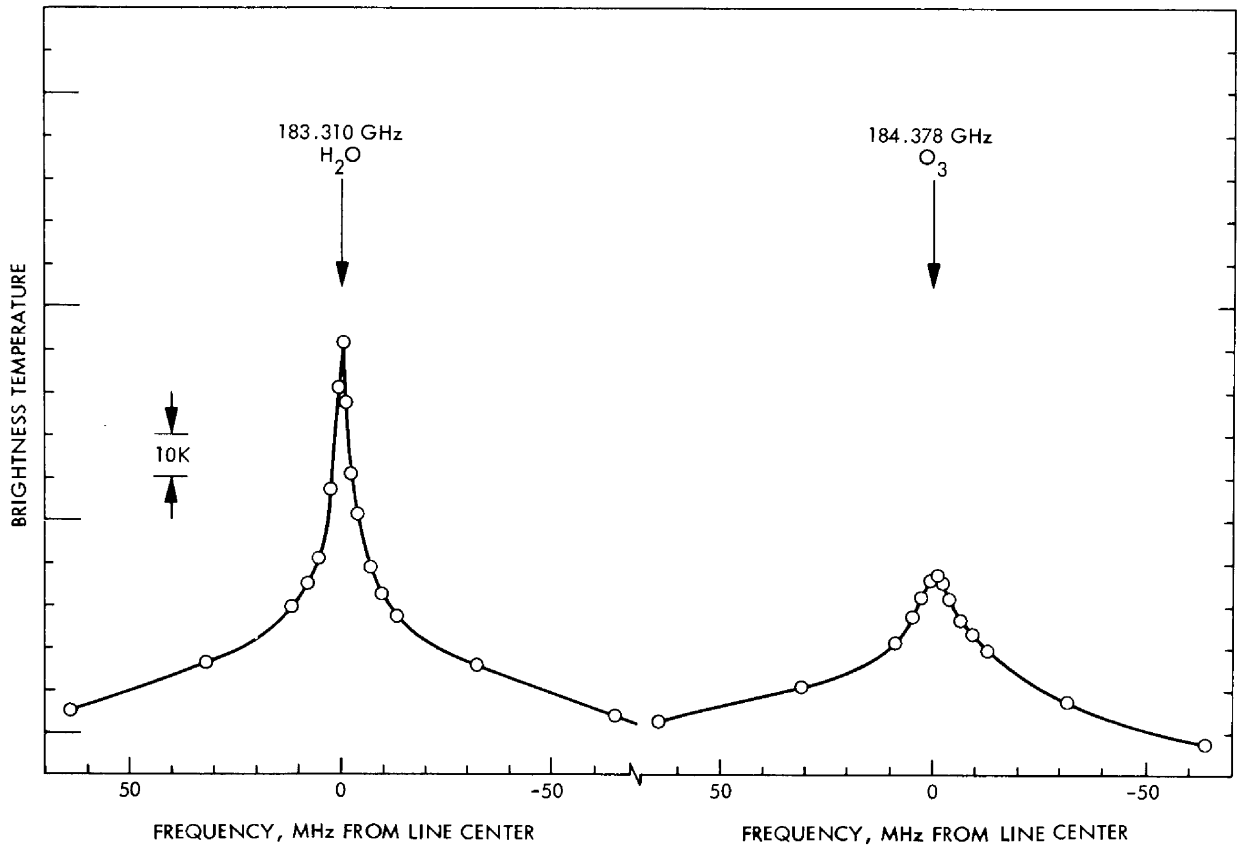

Figure 4. The 183 GHz H_2O line and 184 GHz O_3 line as measured by the MLS. These measurements were made on the local flight out of Melbourne, Australia, during daytime on 11 November 1976. The elevation angle was 20° and the integration time was approximately ten minutes each.

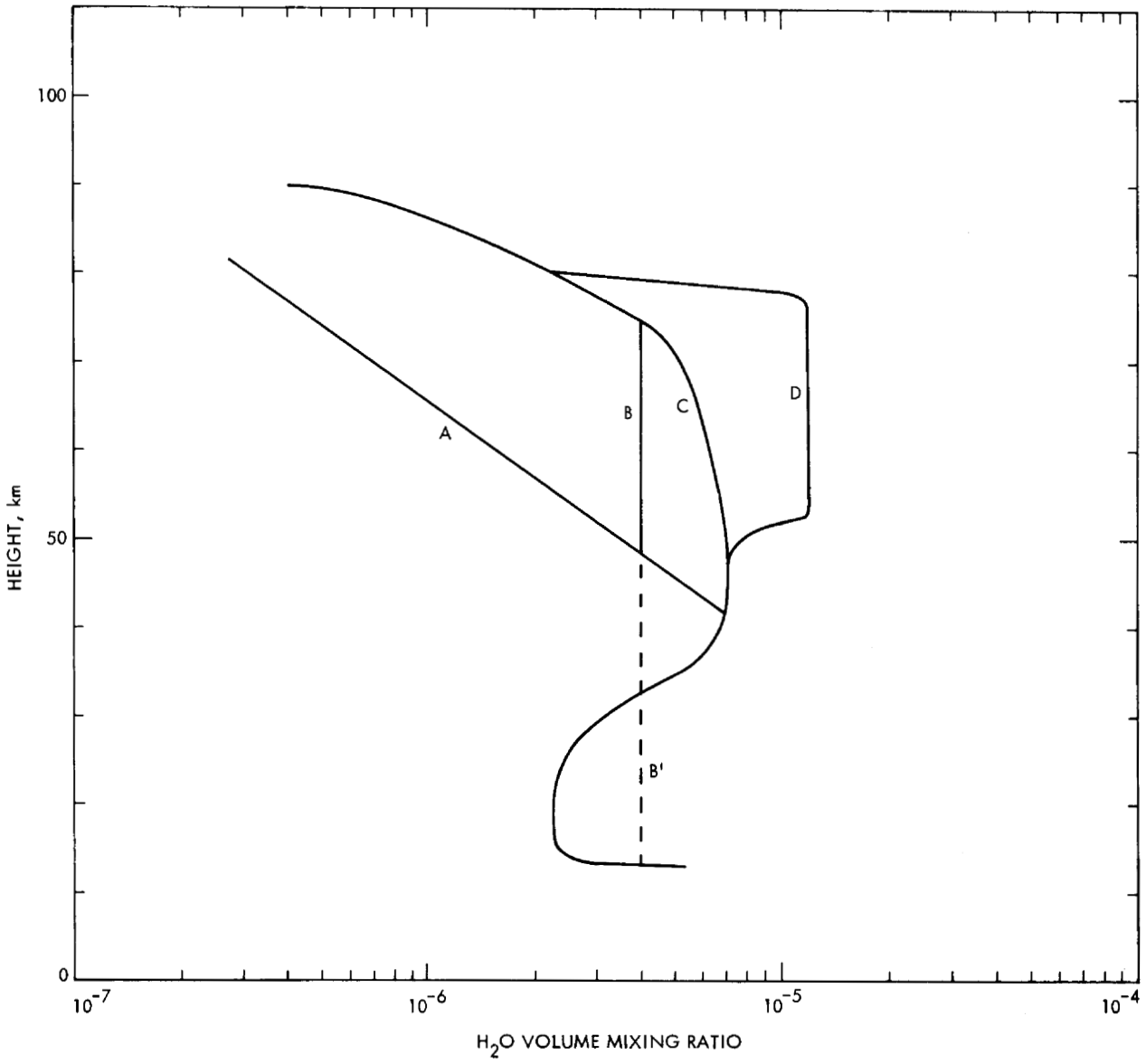

Figure 5. H_2O mixing ratio profiles used for calculations.

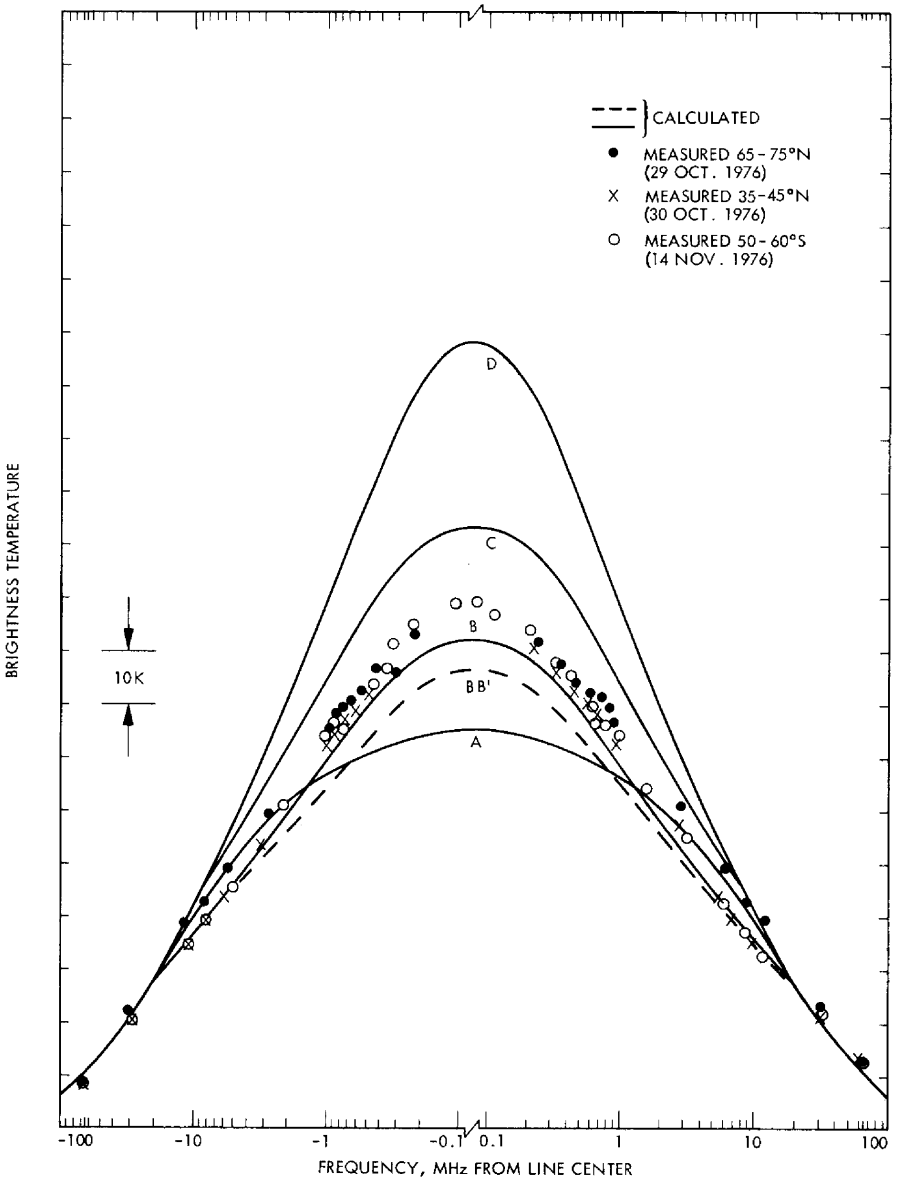

Figure 6. Calculated and measured emission from the 183 GHz H_2O line. The calculated lines correspond to similarly-labeled H_2O profiles shown in Figure 5; the U.S. Standard atmosphere temperature profile was used. The zero level is arbitrary and the calculated and measured curves have been shifted slightly ($\leq$ 10 K) to coincide at 100 MHz from line center. Measurements within 0.2 MHz of center are not available in the two northern hemisphere bands because of interference in those channels.

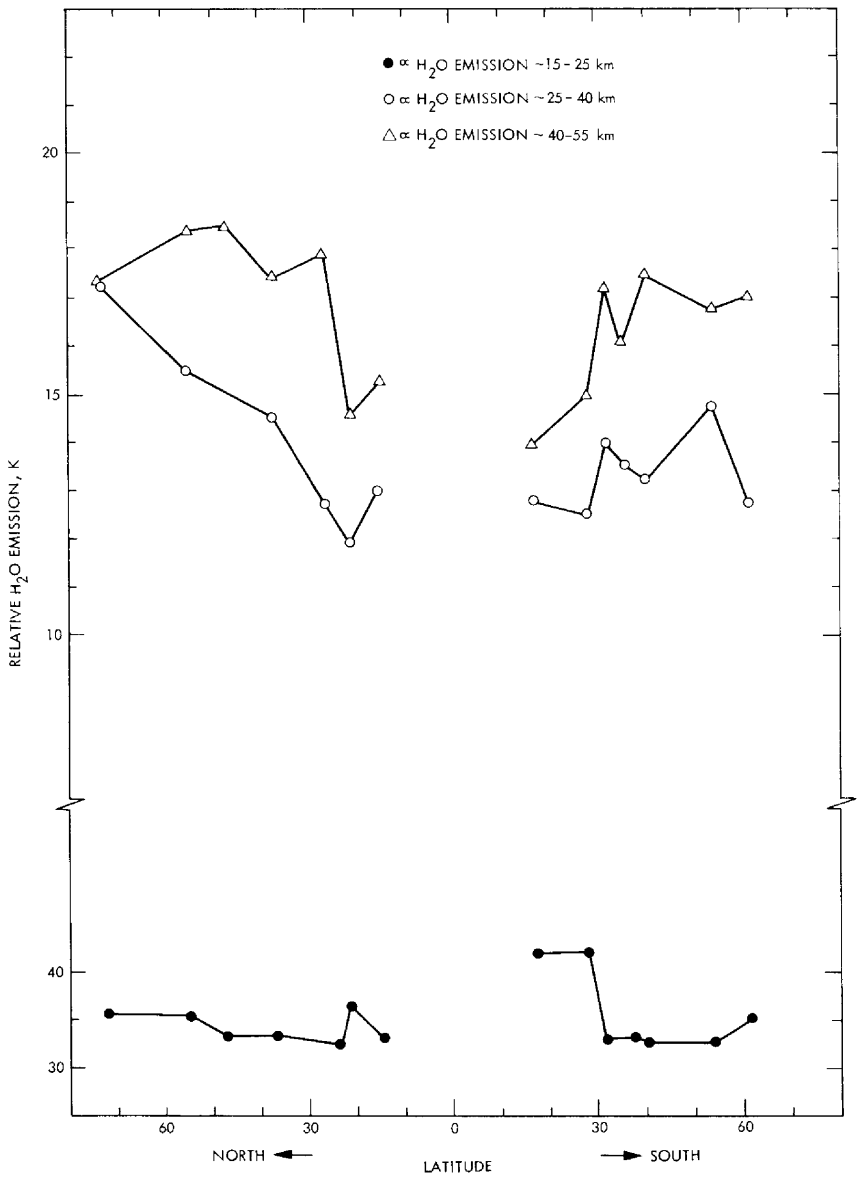

Figure 7. Observed Latitude Variation in Emission from Upper Stratospheric Water Vapor. The points indicated for emission between 40 and 55 km are differences between filters 1 MHz and 9 MHz from line center; those for the 25-40 km region are differences between filters 9 and 64 MHz from center. The points indicated for emission between 15 and 25 km are absolute values of the filters 64 MHz from center, and indicate that variation in absorption by the lower altitude H_2O is not severe. Data in the tropics is not shown because it was significantly affected by tropospheric H_2O above the aircraft.

NASA CV-990 LATITUDE SURVEY

November 1976

STRATOSPHERIC AND UPPER TROPOSPHERIC WATER VAPOR EXPERIMENT

P. M. Kuhn
National Oceanic and Atmospheric Administration
Atmospheric Physics and Chemistry Laboratory
Environmental Research Laboratories
Boulder, Colorado 80302

INTRODUCTION

The NOAA - NASA water vapor observation program commenced in 1970 aboard NASA Ames Research Center's Airborne Science Office (now Medium Altitude Mission Branch) CV-990 jet laboratory. In January 1974 this program centered on the Kuiper Airborne Observatory C-141-A jet observatory as an on-line routine support observation ancillary experiment to the Astronomy program of the aircraft. Observations have averaged approximately two and one-half times each week covering a region bounded by 165^{o} W. and 90^{o}W longitudes and 10^{o} to 50^{o} north latitude. Results of the program through July of 1976 have been reported by Kuhn, et al (1976) and Kuhn (1975).

During the 1976 Latitude Survey expedition an infrared water vapor radiometer similar to that carried aboard the C-141, but of slightly less minimum signal detectivity, was flown on the CV-990. Basically the procedure for water vapor burden determination involves observations of radiant power in the rotational band of the water vapor spectrum (270-520 cm^{-1}) and a transfer calculation.

Following the radiative transfer calculation it is compared (computer comparison as well as calculation) with the observation. The calculation is iterated following stepwise increase of the water vapor burden via a water vapor profile increase until observation and calculation agree within the noise equivalent change in radiance of the radiometer. It is here that one exhibits the water vapor burden. Prior to discussing the results of the latitude survey water vapor burden observations a brief discussion of the infrared water vapor radiometer is in order followed by a short description of the method of water vapor inference.

INSTRUMENTATION

The radiometer employed in these observations is a chopper system with a speed of response of 20 ms. The electronic signal is AC from a temperature controlled, deuterated triglycine sulfate pyroelectric detector, referenced to the black chopper. The temperature of the chopper blade is monitored by a thermistor bead embedded in the chopper. Connections to the thermistor are made through redundant slip rings.

The radiometer forward lens is KRS-S. The aft interference filter is an optical flat of coated silicon with a cut-on frequency of 512 cm^{-1} and a peak transmission of 0.58 decreasing to 0.05 at 270 cm^{-1}. The noise equivalent radiance (N.E.Δ.N.) of the radiometer system was measured to be 2.1×10^{-7} w cm^{-2} sr^{-1} at the detector. Electronic output is -10.0 to + 10.0 VDC. This corresponds to a water vapor burden minimum detectable observation of 0.25×10^{-4} gm cm^{-2}.

METHOD

Water Vapor Burden

The following five equations with appropriate directions are the technique by which we proceed from observed radiance, to calculated radiance, to inferred water vapor burden. Before following the plan of the inference we should state three basic assumptions:

1. A temperature profile above the aircraft is assumed using the nearest sounding station, but based on an observed flight level temperature.
2. The latest water vapor transmission functions (Wark, et al. 1974) are employed as valid for the atmosphere.
3. The water vapor mixing ratio lapse with height above observational level follows a power law (Smith, 1966).

Basically an iterative routine is employed to minimize the difference between the observed downward radiance $N_o\downarrow$ and the calculated radiance $N_c\downarrow$. It follows that

$$(N_c\downarrow - N_o\downarrow)\Delta\nu \quad N.E.\Delta N.(2.1 \times 10^{-7} \text{ w cm}^{-2} \text{ sr}^{-1}), \tag{1}$$

where $\Delta\nu$ is the radiometer response frequency interval, 270-520.

Calculated or observed downward radiance may be expressed as:

$$N\downarrow = \int_{\nu}\int_{p} \phi(\nu)\ B(\nu,\ T(p)\ldots)\frac{\partial\tau(u,(p),\nu)}{\partial p}\ dp d\nu \ (\text{w cm}^{-2}\ \text{sr}^{-1}) \tag{2}$$

where p is pressure (mb),

ϕ is radiometer system transmission

B is the Planck function,

τ is the transmission function of water vapor (270-520 cm^{-1}),

u is the optical mass of water vapor (g cm^{-2}),

T is the absolute temperature (^{o}K), and

ν is the frequency (cm^{-1}).

Defining the temperature profile above flight level it is possible to vary the downward radiance $N\downarrow$, by varying u(p), since,

$$\tau = \tau(u,k). \tag{3}$$

Here k is the water vapor absorption coefficient, (g cm^{-2}).

The optical mass, u, is varied by changes in the flight level mixing ratio, q_o, in the mathematical approximation for u, (g cm^{-2})

$$u = \frac{1}{g}\int_p \bar{q}\, dp \simeq \frac{1}{gp_o^{\lambda}} \sum_i q_o p_i^{\lambda} \Delta p, \text{ (g cm}^{-2}\text{)} \tag{4}$$

where g is the acceleration of gravity (cm sec^{-2})

q is the water vapor mass mixing ratio (g g^{-1})

"o" subscript refers to flight or reference level, and

λ is a power law exponent, 1.8 (Smith, op.cit.)

The choice of non-zero value for λ eliminates the assumption of a uniform mixing ratio with height. Thus (4) reduces to,

$$u = q_o C \tag{5}$$

where λ,Δ and p_o are fixed. In effect Δp is fixed as one assigns 10 mb intervals to Δp upward to 0.1 mb from the pressure, p, at flight level. It is therefore, necessary to change only q_o as part of an iterative convergence routine for $N_c\downarrow$ and $N_o\downarrow$. The technique used is a modified Newton-Ralphson solution (to alter u from the i-th to i+1-th iteration). It is due to Ralston and Wilf (1967).

In essence, then, one defines a temperature profile above radiometer flight level, makes an educated first guess of q_o at flight level, p, and proceeds to minimize the difference between $N_c\downarrow$ and $N_o\downarrow$ via the iterative calculation to which we alluded.

RESULTS

Real Time Infrared Water Vapor Observation:

Due to dynamic range of the water vapor radiometer and since it was designed for operation at or above 13 km it is necessary to multiply printed results of zenith water vapor by 1.5 at flight level 330 (10.8 km) and by 1.2 at flight level 360 (11.8 km). All observations above flight level 360 (11.8 km) are correct as printed. Obviously intermediate altitudes between flight levels 330 and 360 may be scaled appropriately. The dynamic range of the water vapor radiometer precludes its use below flight level 320 (10.5 km).

Prior to considering singular observational events of the expedition we note only invalid data which is to be omitted from the large bulk of valid data. The list follows:

REPORT: LATITUDE SURVEY

REAL TIME INFRA RED WATER VAPOR OBSERVATIONS

Delete only following Latitude Survey Water Vapor Data Zenith H_2O.
All other water vapor data is valid.

FLT.NO.	JULN DATE	TIME(HMS UT)	COMMENTS
1	300	No water vapor burden data available this flight	
2	302-303	Delete all water vapor data due to incorrect bandwidth setting.	
3	303-304	Delete all water vapor data due to incorrect bandwidth setting.	
4	304	163907 - 165554	Several high values of Zenith H_2O are due to clouds above aircraft. These data values may easily be detected by user.
		210625-End of Flight	Clouds above aircraft flight level and descending below operating level of instrument.
5	306	Lift Off - 169233	Climbing to Flight Level 320
		170133 - 170503	Clouds above
		171433 - 171733	Clouds above
		172403 - 173803	Cirrus overhead
		181504 - END	Descending below operating level of instrument and into clouds.
6	308	Lift Off - 202602	Climbing to Flight Level 320
		204233 - 210933	Cirrus overhead
		211503 - 213703	Cirrus overhead
		213933 - 215133	Cirrus overhead
		215633 - 220333	Cirrus overhead
		220733 - 222333	Cirrus overhead
		224907 - END	Descending below operating level of instrument

FLT.NO.	JULN DATE	TIME (HMS UT)	COMMENTS
7	312-313	Lift Off - 210455	Climbing to F.L. 310
		211255 - 212255	Cirrus overhead
		212425 - 213825	Cirrus overhead
		214455 - 214725	Cirrus overhead
		220455 - 224855	Immersed in dense cirrus
		225225 - 230155	Immersed in dense cirrus
		004626 - 005026	Cirrus overhead
		012956 - END	Descending below operating level of instrument
8	313-314	Lift Off - 214001	Climbing to FL 300
		215032 - 215832	Thin clouds overhead
		220903 - 221733	Thin clouds overhead
		225533 - 225933	Thin clouds overhead
		230703 - 231603	Thin clouds overhead
		014433 - 015533	Thin clouds overhead
		025733 - END	Descending
9	315	Lift off - 184455	Climbing to FL 315
		184925 - 185155	Thin cirrus overhead
		185425 - 190825	Thin cirrus overhead
		213825 - 222655	Thin cirrus overhead
		232356 - END	Descending
10	316-317	Lift Off - 200749	Climbing to FL 360
		214220 - END	Descending
11	317-318	Lift Off - 234450	Climbing to FL 350
		034521 - END	Descending

FLT.NO.	JULN DATE	TIME (HMS UT)	COMMENTS
12	319	Lift Off - 030357	Climbing to FL 320
		075228 - END	Descending
13	321	Lift Off - 010331	Climbing to FL 300
		043920 - 044420	Cirrus clouds overhead
		053921 - END	Descending
14	322-323	Lift Off - 224514	Climbing to FL 348
		225844 - 225944	Cirrus overhead
		235914 - 001544	Cirrus overhead
		035514 - END	Descending
15	323	Lift Off - 190217	Climbing to FL 342
		203348 - 205148	Cirrus overhead
		220548 - 221848	Cirrus overhead
		225148 - END	Descending

During the southernmost flight track on Latitude Survey Flight No. 12, the occurrence of a tropopause break or fold was evident in the sharp decrease in the water vapor burden south of approximately 51^{o} south. The burden dropped from approximately 14 microns at 49^{o} south to 8.0 microns at 52^{o} south. New Zealand Meteorological Service analyses did in fact show the tropopause break.

In this brief summary report three interesting observations are discussed, briefly, out of numerous research oriented situations.

Fig. 1 summarizes water vapor burden results from 40^{o}N latitude to 40^{o} south latitude at flight level 370 or approximately 12.1 km. The burden, averaged for the flight tracks, ranges from 14 microns (12×10^{-4} g cm^{-2}) at 40^{o} North to 7.0 microns at 40^{o} South, suggesting an Antarctic moisture sink. This is so in view of the disparity between the overhead burdens at 40^{o} North and South.

The obvious effects of strong upward vertical transport along the ITCZ are evident at approximately 10^{o} North where the burden reaches 20 microns.

The average water vapor burden after the radiometer stabilized at flight level 360 (approximately 10 km) during Latitude Survey Flight # 10 during the Mildura Balloon run was approximately 10.0 microns compared with the balloon run value of 18 microns. This disparity may be due to an air mass change as a value of 18 microns appears somewhat high. However the general agreement is good and further research into the difference is planned.

Real Time Infrared Surface Temperature Observations

Aside from obvious instances of surface to cloud and cloud to surface changes and lags in switching range in "scene" and resulting abrupt changes in the radiatively inferred temperatures the data is accurate.

Real Time Infrared Free Air Temperature Observations

Instances of aircraft roll and lags in changing range switch, both of which are obvious in the data train, no errors occur in the IR air temperature results.

REFERENCES

Kuhn, P. M., 1975, Zonal profiles of atmospheric water vapor. NOAA Tech Rept., ERL 319-APCL 33, 11 pp.

Kuhn, P. M., E. Magaziner, and L. P. Stearns, 1976, Stratospheric areal distribution of water vapor burden and the jet stream. Geo. Res. Letters, Vol. 3, 9, 529-532.

Ralston, A., and H. Wilf, 1967, Multipart iteration function. Mathematical Methods for Digital Computers, 2, John Wiley & Sons, Inc.

Smith, W. L., 1966, Note on the relationship between total precipitable water and surface dew point. J. Appl. Meteor., 5, 726-727.

Wark, D.Q., J. H. Liensch, and M. P. Weinreb, 1974, Satellite observations of atmospheric water vapor. Appl. Optics, 13, 507-511.

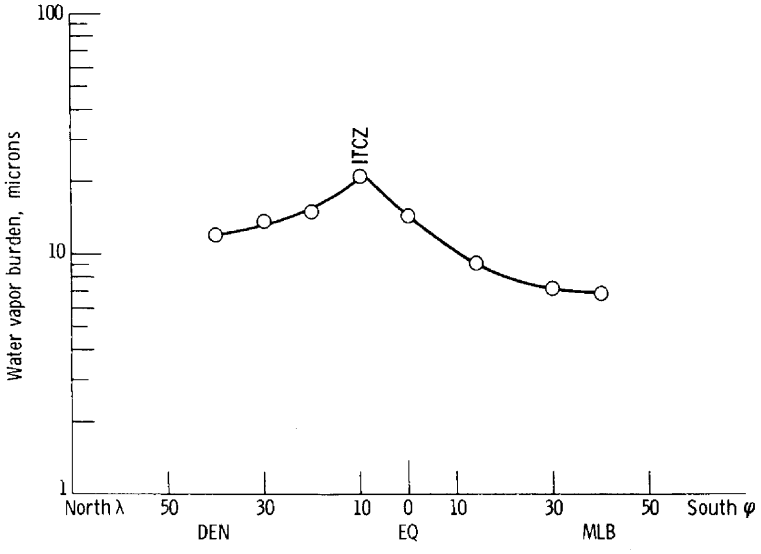

Figure 1. - Latitude survey - water vapor burden; 12.1 km.

INFRARED HETERODYNE SPECTROMETER MEASUREMENTS of ATMOSPHERIC OZONE USING THE CV 990 AIRBORNE PLATFORM

by

B.J. Peyton,* J. Hoell,** R.A. Lange*
R.K. Seals, Jr.,** M.G. Savage* and F. Allario**

SUMMARY

The remote sensing of the concentration and vertical distribution of an atmospheric species has been demonstrated using a dual-laser, multi-channel infrared heterodyne spectrometer (IHS) that was mounted in the CV 990 NASA test aircraft. Ground-based solar viewing measurements using the IHS were previously performed (reference 1) at selected laser LO transitions for ammonia (NH_3) and ozone (0_3).

Ozone was the selected atmospheric species for the airborne flight measurements because of the scientific interest in this atmospheric species, the availability of in situ monitors, the coordinated ozone measurements, and the availability of ground truth data. The IHS was operated in: (1) the solar viewing mode to determine ozone distributions in the stratosphere, and (2) the nadir viewing mode to determine the ozone distribution in the troposphere. Airborne atmospheric propagation measurements also were carried out at selected CO_2 laser transitions.

INTRODUCTION

A dual-laser, multi-channel infrared heterodyne spectrometer (IHS) was mounted in the CV 990 NASA test aircraft and used to measure remotely the concentration and vertical distribution of atmospheric ozone (0_3). The

---

*AIL, a division of Cutler-Hammer, Melville, N.Y. 11746
**NASA Langley Research Center, Hampton, Virginia 23665

IHS utilizes two PV:HgCdTe photomixers and two CO_2 laser local oscillators, which can be tuned to overlap selected transitions of ozone (0_3) in the 9.6-μm spectral region. The IHS ozone channel has a 2.2-GHz spectral bandwidth, which is divided into four, 500-MHz channels. The high specificity ($\Delta\nu \sim 3 \times 10^{-2}$ cm^{-1}) and the nearly quantum-noise-limited sensitivity of the IHS (references 2-4) provide the capability of scanning individual atmospheric signature lines. These features are of particular significance in remote gas sensing applications where low-level signals often exist in a background of other interfering atmospheric gases.

The potential of utilizing heterodyne measurements to infer pollutant gas profiles from satellite measurements of atmospheric emissions (references 5 and 6) and from measurements of reflected laser (hot source) absorption (references 7 and 8) previously have been reported.

It is well known that the stratospheric ozone layer shields the earth's surface from harmful ultraviolet radiation, is a contributor to stratospheric energy balance studies, and also is an important climatological parameter. The latitude survey mission permitted stratospheric ozone measurements over a wide range of global latitudes. Tropospheric measurements also are significant, since atmospheric ozone accounts for much of the pollution injury to vegetation (reference 9) and excessive 0_3 levels are considered evidence of photochemical smog formation (reference 10).

The IHS includes a pollutant (ozone) and a "clear" reference infrared channel. The reference channel is used to cancel the continuum and near-continuum attenuation and interfering gas effects in the solar absorption mode, and minimize the effects of ground brightness temperature variations in the nadir radiance mode.

IHS INSTRUMENTATION

The IHS (Figures 1 and 2) utilizes two PV:HgCdTe photomixers, two grating tunable $C^{12}0_2{}^{16}$ laser local oscillators (LO's), four IF networks with RF filters which spectrally channelize the incident irradiance, two blackbody sources for measurement reference and absolute calibration, four radiometer processing channels, and appropriate analog and digital recorders. The Dicke type IHS processor is used when the source and reference temperatures are nearly identical (nadir radiance mode). The automatic nulling gain

modulation type processor is used in the solar absorption mode when the source temperature is much greater than the reference temperature (reference 11).

An optical Dicke switch alternately switches the receiver field-of-view (FOV) between a collecting telescope and a reference blackbody, and supplies synchronizing signals to the processing channels. A common collecting aperture, reference blackbody, and Dicke switch are used for the matched photomixers to: (1) provide a common receiver field-of-view, and (2) minimize the effects of laser LO instabilities. A blackbody source can be inserted between the collecting aperture and the optical Dicke switch for absolute IHS calibration.

The PV:HgCdTe photomixers have 3-dB cutoff frequencies of greater than 1000 MHz, and heterodyne sensitivites of less than 1.5×10^{-19} W/Hz at IF frequencies of less than 500 MHz. The 500-MHz IF bandwidths of the IHS pollutant channels can be centered at IF offsets of ±400, ±900, ±1400, and ±1900 MHz with respect to the laser LO frequency. The IHS reference channel has a bandwidth of 680 MHz which is centered at an IF offset of ν_{LO} ±360 MHz. The post-detection integration time is discretely selectable between 1 and 30 seconds. The nadir radiance mode blackbody sources can be varied between 260 and 350 K, while the solar absorption mode blackbody sources can be varied between 350 and 1300 K.

The ozone profiling measurements were carried out using the P (20) transition of the $C^{12}0_2{}^{16}$ laser LO at 1046.8452 cm^{-1} for the pollutant channel and the P(24) transition of the $C^{12}0_2{}^{16}$ LO at 1043.1633 cm^{-1} for the reference channel. The P(18) and P(26) $C^{12}0_2{}^{16}$ laser LO transitions at 1048.6608 and 1041.2791 cm^{-1} also are suitable wavelengths for remotely monitoring atmospheric ozone in the SA mode. The calculated transmittance spectra between 1040 and 1055 cm^{-1} for a ground level to 10-km path, and the overlap of the $C^{12}0_2{}^{16}$ laser LO with discrete ozone signature lines is given in Figure 3.

The IHS was mounted in the NASA CV 990 test aircraft. A 7-inch diameter, anti-reflection coated germanium window and gyrostabilized mirror were used to direct the solar energy into the IHS (Figure 4). A near infrared vidicon/television display was used to maintain the solar disc within the IHR field-of-view.

A 4-inch diameter anti-reflection coated germanium window and 45 degree, external mirror were used to direct the nadir radiation into the IHS. The IHS control panel is shown in Figure 5.

The atmospheric ozone profiles were derived from the measured radiances in the IHS channels using an iterative inversion process (references 5 and 6). Vertical temperature profiles and measured pollutant absorption coefficients are used to determine the absorption coefficient for the inversion calculation. An initial guess of the pollutant profile is used to initiate the inversion process and successive profile adjustments are made using prediction algorithms until the selected convergence criteria is satisfied. Onboard ozone retrivals can be obtained using the CV 990 Addas II computer system.

MEASURED OZONE CONCENTRATIONS

Stratospheric ozone measurements were performed over a wide range of latitudes. Typical retrieved profiles for 18^{O}N and 55^{O}N latitudes are given in Figure 6. Seasonally averaged profiles obtained from chemical balloon soundings at 10^{O}N and 60^{O}N latitudes are given in Figure 7. The IHS retrieved profiles and the absolute magnitudes appear to be consistent with the chemical sounding data.

The IHS permits stratospheric ozone profiling on a regional/global basis from an airborne platform. The sun was observed for approximately 60 minutes per day. Whenever possible, IHS calibrations were carried out at calibration temperatures larger and smaller than the effective temperature of the source to allow an accurate determination of the relative solar energy reaching the IHS in each of the four IF channels. The IHS was calibrated every 5 minutes during a solar measurement period, and ozone measurements on up to three pollutant laser LO transitions were possible during a 60-minute measurement period.

Initial investigations indicate that the IHS retrievals at the aircraft altitude are within a factor of 1.5:1 of the in situ ozone measurements. A more detailed analysis of the stratospheric ozone profiles will be performed after the correlation measurements are obtained from the ozone sounding stations.

Some initial nadir radiance measurements were carried out during the latitude survey flight mission. Most of the mission flight paths were over water and very little flight time was available over urban centers. A series of nadir measurements were carried out over northern Alaska to determine

whether the IHS reference channel output tracks the actual ground temperature (provided by the onboard surface temperature radiometer). The results, shown in Figure 8 for a ground temperature variation of 20°C,* indicate that the IHS reference channel appears to track the ground temperature over the 3-minute measurement period. Therefore, it appears that the reference channel will be effective in minimizing the effects of changes in the ground brightness temperature.

ATMOSPHERIC PROPAGATION MEASUREMENTS

The IHS has been utilized to make vertical path atmospheric attenuation measurements at the P(24) transition of the $C^{12}O_2^{16}$ laser. The logarithms of the measured solar energy [$P(\nu)$] at the IHS input versus secant θ_s is shown in Figure 9 for θ_s between approximately 4 and 11 degrees, where θ_s is the solar viewing angle. The slope of the log $P(\nu)$ versus secant θ_s is equal to $\alpha_a(\nu)$ h, where $\alpha_a(\nu)$ is the atmospheric attenuation coefficient at the selected LO transition and h is the vertical height of the atmosphere (references 11 and 12).

The measured atmospheric transmission data indicates that the vertical path atmospheric transmission at the selected $C^{12}O_2^{16}$ isotope laser transitions (1043.1633 cm^{-1}) is 0.89 (-0.5 dB) above the aircraft altitude of 39,000 ft.

Ground-based IHS measurements indicated that the vertical path atmospheric transmission is 50 to 60 percent at the P(20) transition of the CO_2 laser at 944.1904 cm^{-1} (references 11 and 12). The increased atmospheric transmission measured during the latitude survey mission can be attributed to the lower concentration of CO_2 ahd H_2O molecules in the solar viewing path.

CONCLUSIONS

Airborne infrared heterodyne spectrometer measurements have demonstrated the feasibility of obtaining vertical profiles of stratospheric ozone on a regional/global basis. Nadir radiance measurements indicate that the

*The ice-covered terrain is expected to provide a nearly constant emissivity.

reference channel of the IHS will correct for changes in the earth's brightness temperature due to aircraft motion. Propagation measurements through the upper atmosphere indicate that the vertical path transmissions near 9.6 μm can approach 90 percent for an airborne platform at 39,000 ft. Additional data reduction and analysis are planned as well as correlation with other sources of ozone measurement data.

REFERENCES

1. "Infrared Heterodyne Spectrometer Measurements of the Vertical Profile of Tropospheric Ammonia and Ozone," AIAA Conference, Los Angeles, California, January 1977.

2. Peyton, B.J., et al, "High Sensitivity Receiver for Infrared Laser Communication," IEEE J. Quantum Elec, QE-8, p 252-263, February 1972.

3. Teich, M.C., "Infrared Heterodyne Detection," Proc, IEEE, No. 56, p 37-46, January 1968.

4. Arams, F., et al, "Infrared 10.6-Micron Heterodyne Detection with Gigahertz IF Capability," IEEE J. Quantum Elec, QE-3, p 484-492, November 1967.

5. Seals, R.K. and Peyton, B.J., "Remote Sensing of Atmospheric Pollutant Gases Using an Infrared Heterodyne Spectrometer," Proceedings of the International Conference on Environmental Sensing and Assessment, Vol 1, p 10-4, September 1975, Las Vegas, Nevada.

6. Seals, R.K., Jr., "Analysis of Tunable Laser Heterodyne Radiometry: Remote Sensing of Atmospheric Gases," AIAA J. No. 12, p 1118-1122, August 1974.

7. Seals, R.K., Jr. and Bair, C.H., "Analysis of Laser Differential Absorption Remote Sensing Using Diffuse Reflection From Earth," Second Joint Conf. on Sensing of Environmental Pollutants, ISA JSP 6675, p 131-137, December 1973.

8. Menzies, R.T. and Chahine, M.T., "Remote Atmospheric Sensing With an Airborne Laser Absorption Spectrometer," Appl Optics, No. 13, p 2840-2849, December 1974.

9. Marx, J.L., "Air Pollution: Effects on Plants," Science, No. 187, p 731-733, February 1975.

10. "Air Quality Criteria for Photochemical Oxidants," Chapter 3, U.S. Department of Health, Education, and Welfare, Washington, D.C., 1970.

11. Peyton, B.J., et al, "An Infrared Heterodyne Radiometer for High-Resolution Measurements of Solar Radiation and Atmospheric Transmission," IEEE J. Quantum Elec, QE-11, August 1975.

12. S.R. King, D.T. Hodges, T.S. Hartwick and D.H. Baker, "High Resolution Atmospheric-Transmission Measurement Using a Laser Heterodyne Radiometer," Appl Optics, Vol 112, p 1106, June 1973.

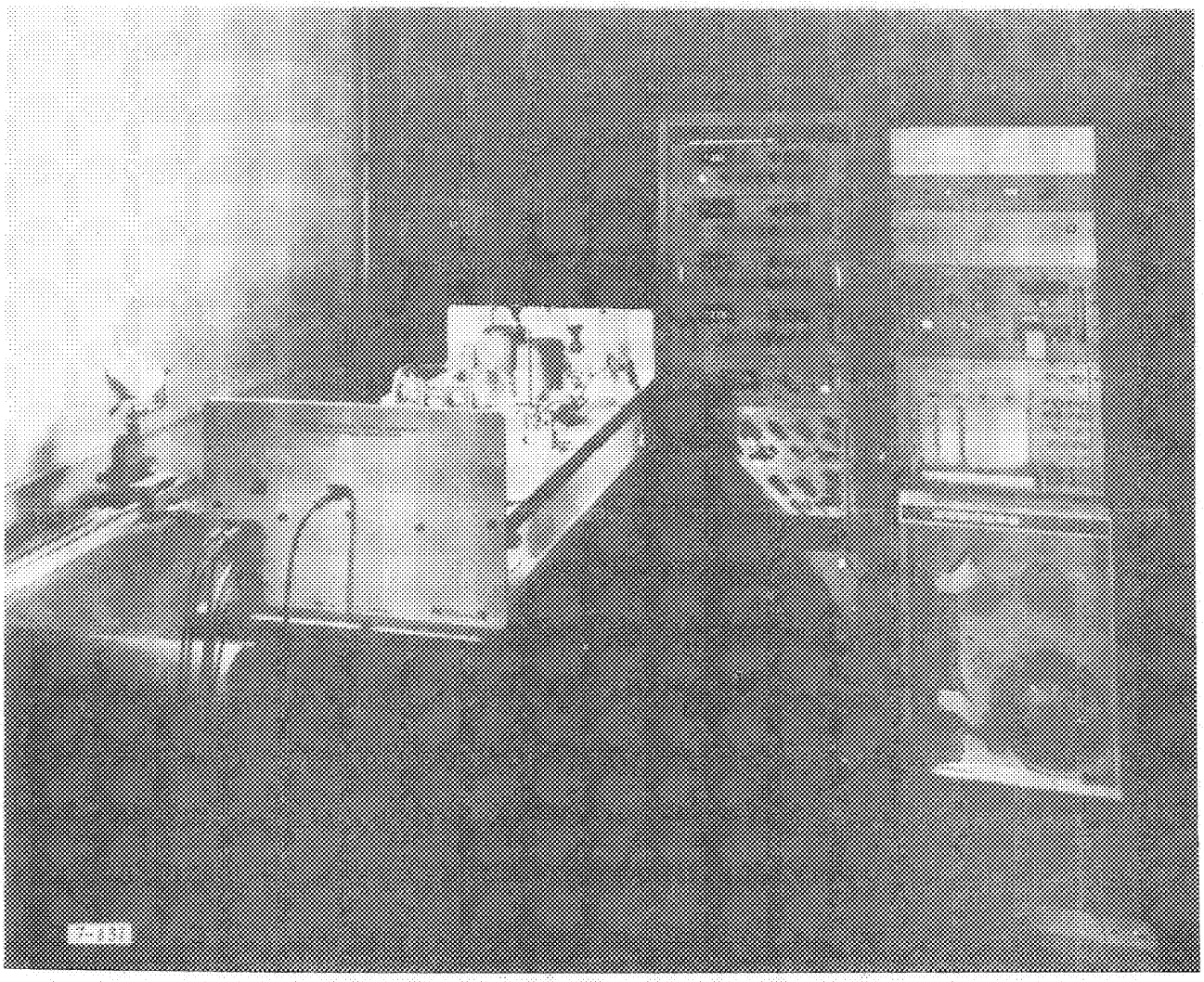

Figure 1. Dual-Laser, Multi-IF Channel, Dicke-Switched IHS

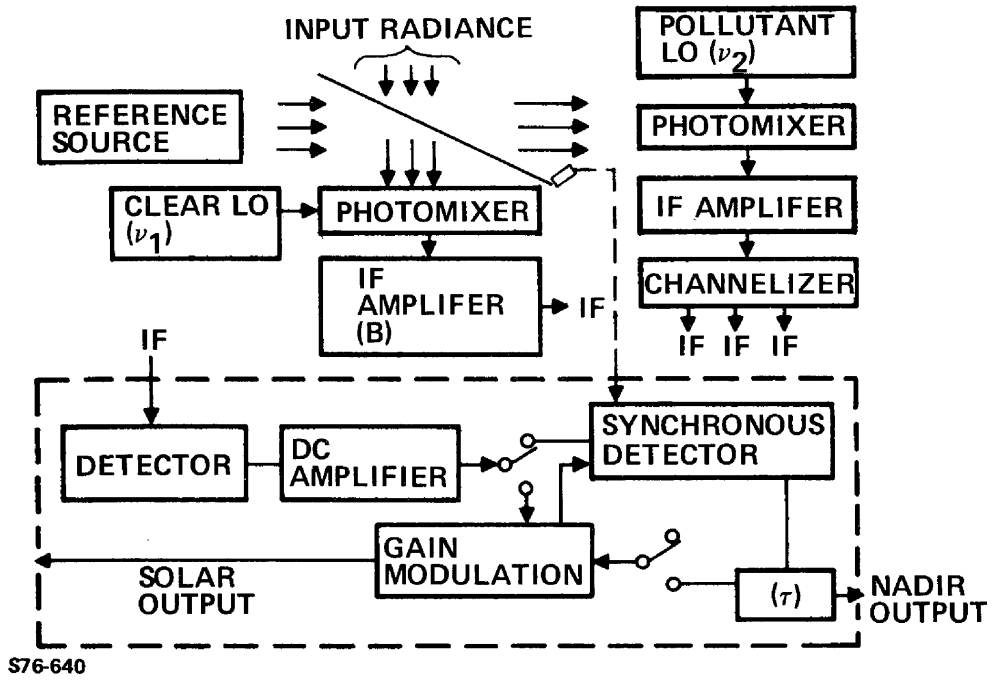

Figure 2. Simplified Block Diagram of Dual-Laser, Multi-IF Channel, Dicke Switched IHS

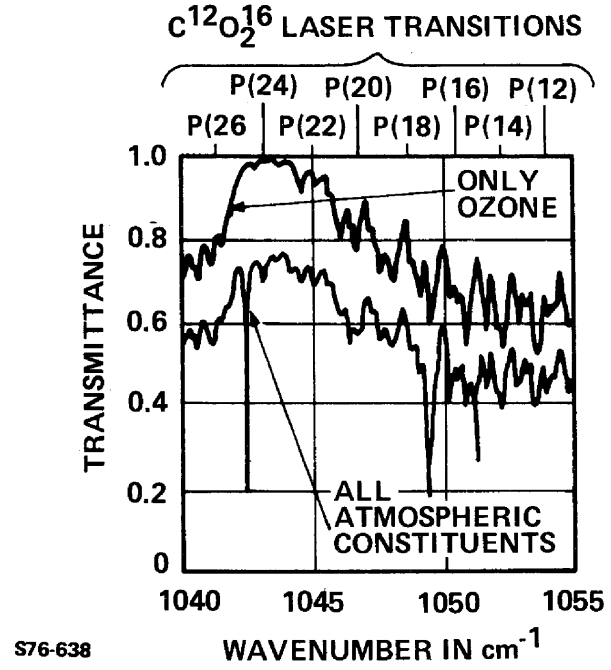

Figure 3. Calculated Atmospheric Transmittance

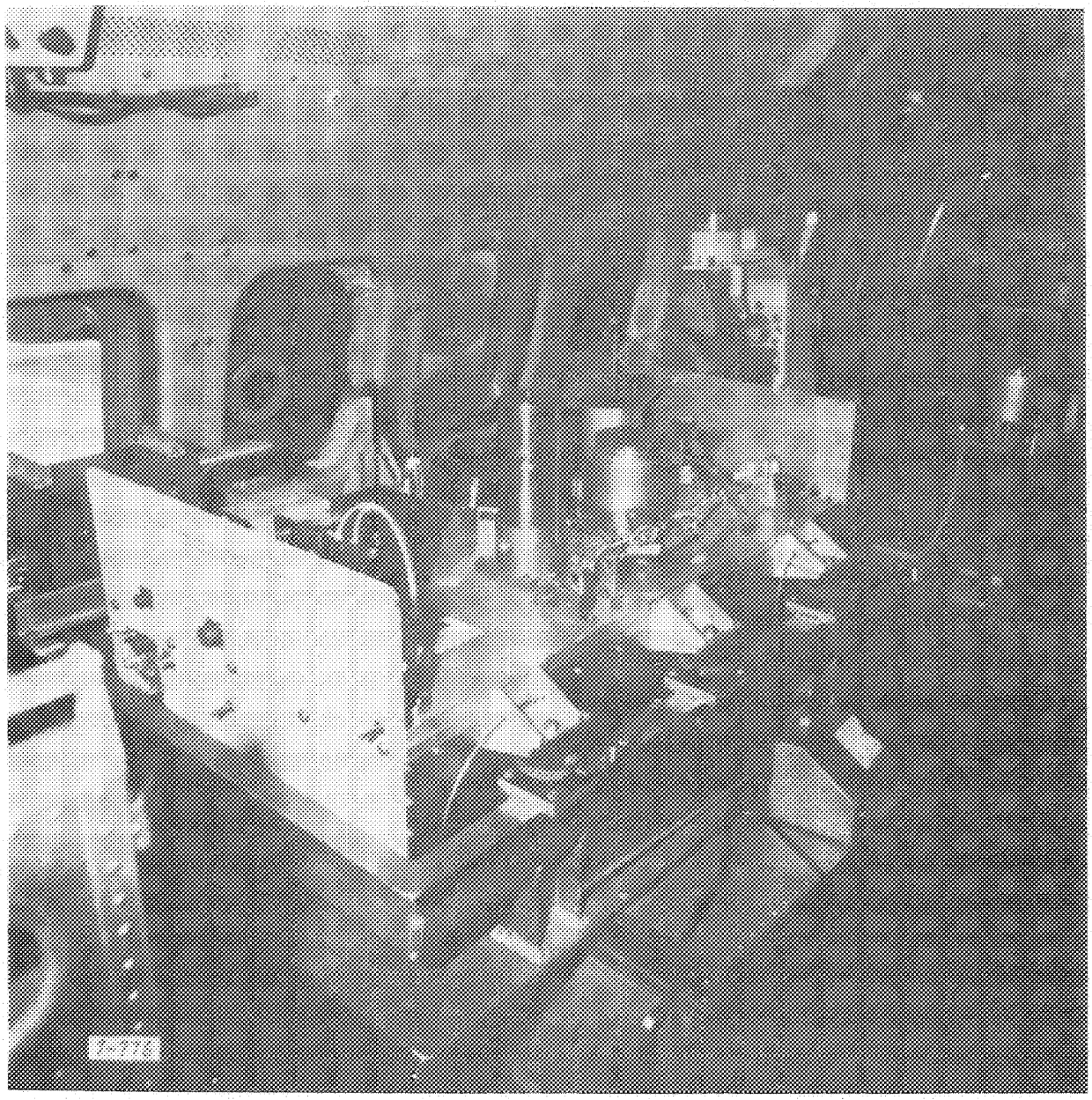

Figure 4. IHS Mounted in the NASA CV 990 Test Aircraft

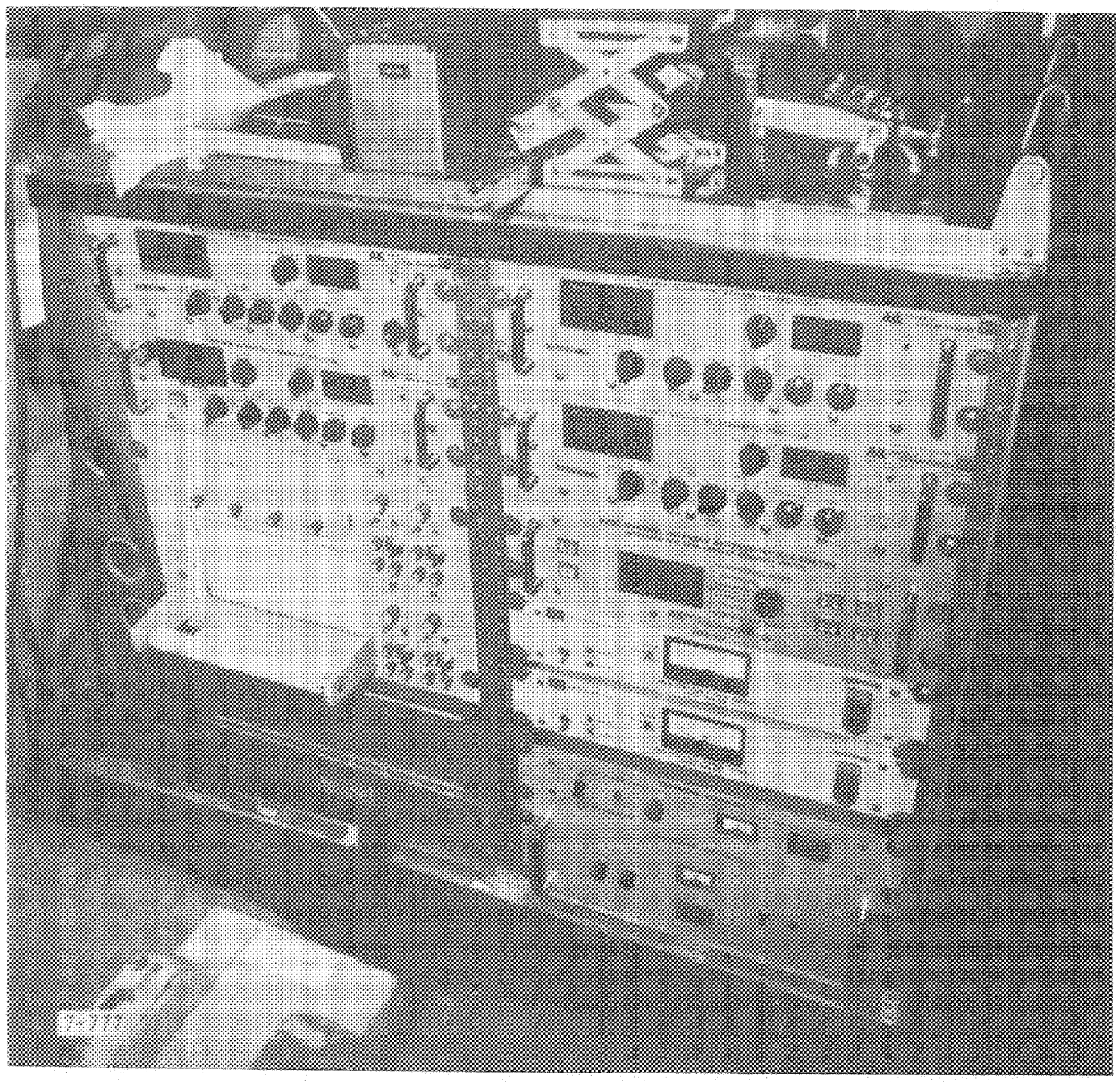

Figure 5. IHS Monitor and Control Package

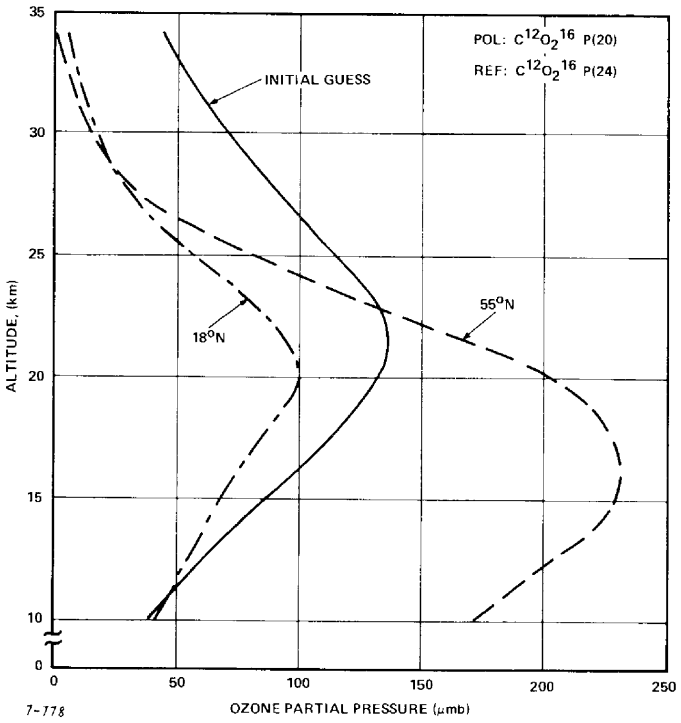

Figure 6. Preliminary Ozone Distribution for IHR Solar Absorption Measurements at Two Selected Latitudes

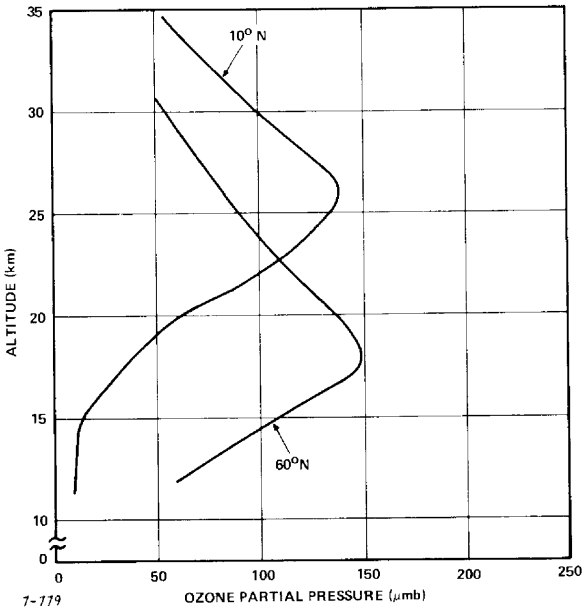

Figure 7. Seasonally Averaged Ozone Distribution From Chemical Balloon Soundings at Two Selected Latitudes

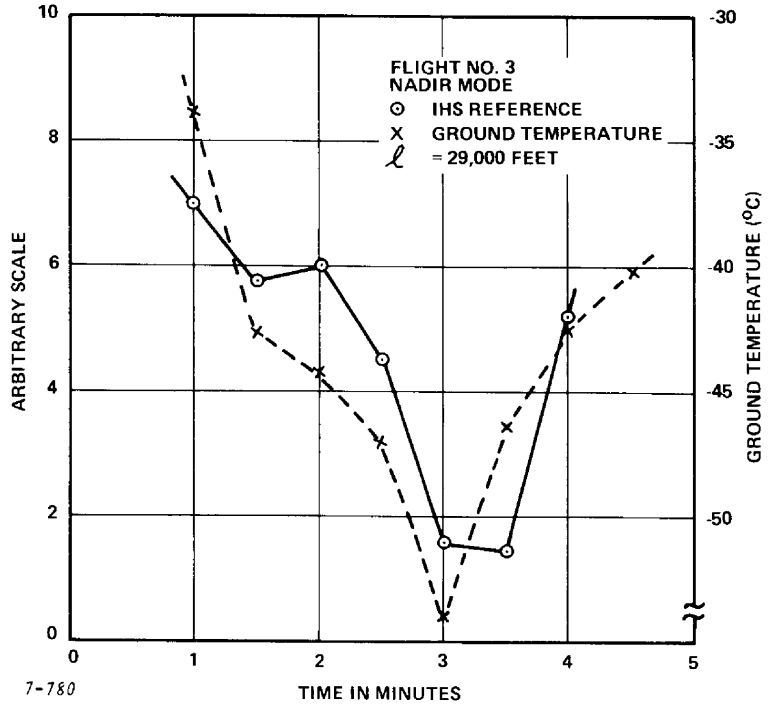

Figure 8. Measured Variation of IHS Reference Channel and Ground Temperature Versus Time in Nadir Radiance Mode

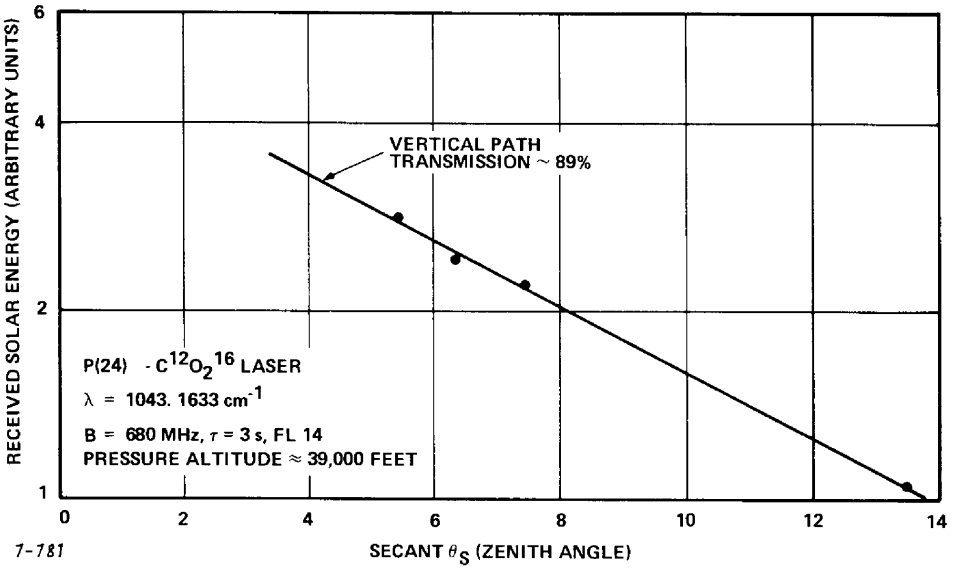

Figure 9. Variation of Solar Energy Collected at IHS Versus Secant of the Solar Angle

STUDY OF TRACE CONSTITUENTS IN THE ATMOSPHERE BY ABSORPTION SPECTROMETRY*

by A. Girard and J. Besson

Office National d'Etudes et de Recherches Aérospatiales (ONERA) 92320 Châtillon (France)

SUMMARY

Measurements were done by infrared absorption spectrometry, using the sun as a source a sunset or at sunrise. The instrument, which is essentially a spectrometer associated with a sun tracker automated through a control module, is briefly described.

The program of measurement was practically unchanged all along the mission. Five spectral intervals were scanned, with a view to measuring : NO, NO_2, HCl, HNO_3, O_3, CH_4 and H_2).

A preliminary survey of the data collected over seven of the ten flights performed shows that valuable numerical data can be derived from most of the spectra, although a residual vibration noise frequently limits the signal/noise ratio in the records. The present effort of data reduction is focused on the measurement of NO_2 and HNO_3.

A set of typical spectra obtained for these two species is shown. A first result concerning HNO_3 is given for the flight Moffett-Field-Fairbanks. For a solar zenith angle equal to 90°, the total column density is near 10^{18} mol.cm^{-2}. The local number density at a flight altitude of 10.6 km is $(1.4 \pm 0.4) \cdot 10^{10}$ mol.cm^{-3}.

1 – INTRODUCTION

A great amount of observational data on atmospheric trace constituents has been collected during the last years, following the efforts developed for facing hazards of ozone depletion by human activity (high flying jets, sprays, fertilizers).

In terms of local number density and for a given altitude, these data frequently extend, for each reactive species, over more than one order of magnitude, so that an adequate data base for modeling is still lacking.

In fact, a large natural variability has been demonstrated for several important species, e.g. NO, with respect to climatic seasonal and meteorological conditions, but a major difficulty still exists for a global evaluation : the part due to the instrumental inaccuracy cannot be isolated from the natural variability, by comparing non simultaneous measurements. This is why, at the present state of knowledge, the pressing need is for correlated measurements which are considered as far more valuable than independent ones.

---

* NO_2, HNO_3, HCl, NO, CH_4, H_2O, O_3 measurements by absorption spectrometry.

This is specially valid for the range of altitude where the troposphere and the stratosphere are strongly coupled.

2 – PURPOSE AND PRINCIPLE OF THE MEASUREMENTS

The purpose of the automatic spectrometer operation is the measurement of the minor atmospheric constituents concentration for various climatic and/or geographic conditions.

The principle of the measurement is infrared absorption spectrometry from an aircraft platform, using the sun as a source. For a given value of the solar elevation, the number of absorbing molecules through the optical path (column density) is calculated from the depth of the absorption characteristic lines. At sunrise or sunset, the optical path is maximal and the method reaches the ultimate sensitivity.

The experimental package has been designed with a view to measuring many trace constituents during the same flight : for this purpose, a narrow spectral range (a few wave numbers) has been selected for each species, which includes at least one strong and reasonably well isolated absorption feature considered as an unambiguous spectral signature of this species.

The concerned molecules and the respective selected spectral intervals are listed in Table I. For each experiment, a program of measurements is established and the instrument is operated automatically by the control module according to this program.

Table I – Atmospheric gases and pollutants.

Molecule	Center of the selected spectral interval		Molecule	Center of the selected spectral interval	
	λ (μm)	σ (cm^{-1})		λ (μm)	σ (cm^{-1})
O_3	4.7 5.8 9.6	2130 1712 1042	NH_3 (1)	10.1 9.55 6.1	985 1046 1640
NO	5.2	1915	SO_2 (1)	4 7.4 8.7	2500 1360 1150
NO_2	6.25	1600	HCl	3.4	2945
N_2O	3.9 4.6	2576 2210	$CF\,Cl_3$	11.8 9.1	845 1100
HNO_3	5.8 7.5	1726 1326	CF_2Cl_2	10.9 9.1	920 1100
CO	4.7	2132	$C\,Cl_4$	6.6	1520
CH_4	3.45 6.15 7.7	2900 1550 1300	CH_3Cl (1)	9.25	1080
HCHO (1)	3.6 5.7	2780 1765	CO_2	4.3 5	2320
C_2H_2 (1)	7.4	1350	H_2O	2.7 6.2	3800 1606
C_2H_4 (1)	5.3 7.14	1900 1400	HF	2.5	4039

(1) Species unidentified at the present time in the atmosphere (at least by infrared spectrometry)

3 – INSTRUMENTATION

The automatic spectrometer is essentially a grille spectrometer associated with a sun tracker. These elements are automated through a module which ensures the control of the internal servo-loops and the sequence of the various phases of the experiment.

The optical scheme is indicated on figure 1.

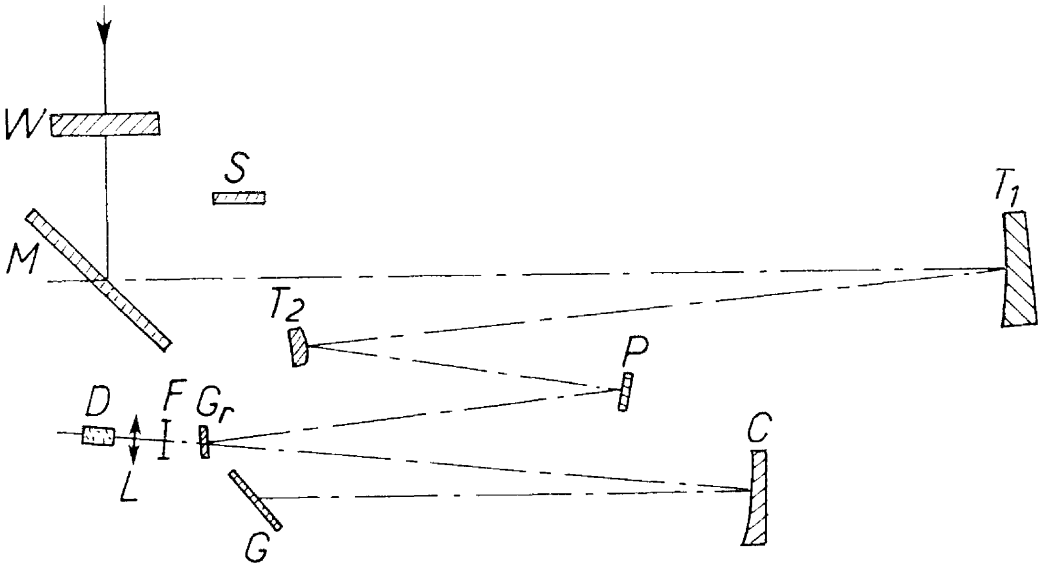

Figure 1. Optical scheme of the automatic spectrometer.

W : Infrared window (F_2Ca)
M : Plane mirror, servo controlled by the sun tracker S
S : Sun tracker
T_1, T_2 : Primary and secondary mirrors of the telescope
P : Plane mirror
G_r : Grille, placed in the focal plane of the telescope
C : Oscillating collimator (F = 180 Hz)
G : Diffraction grating
F : Interference filter
L : Ge lens
D : Photoconductive MCT detector.

The main numerical values are the following :

- The wavelength range of the instrument spreads from 3 to 15 μm (during the CONVAIR 990 mission, it was limited to 8 μm by the calcium fluoride window).
- Grille area : 15 x 15 mm
  equivalent slit width : 0,15 mm.
- Diffraction grating. Ruled area : 65 x 130 mm
  60 grooves per millimeter
  blaze angle : 64°.
- Focal length of the collimator C : 600 mm.

– Detector : HgCdTe. Sensitive area : 0,6 x 0.6 mm.

– Filters. The selection of the different orders of the grating is achieved by a set of six interference filters mounted on a rotating wheel.

The Figure 2 represents the block diagram of the instrument.

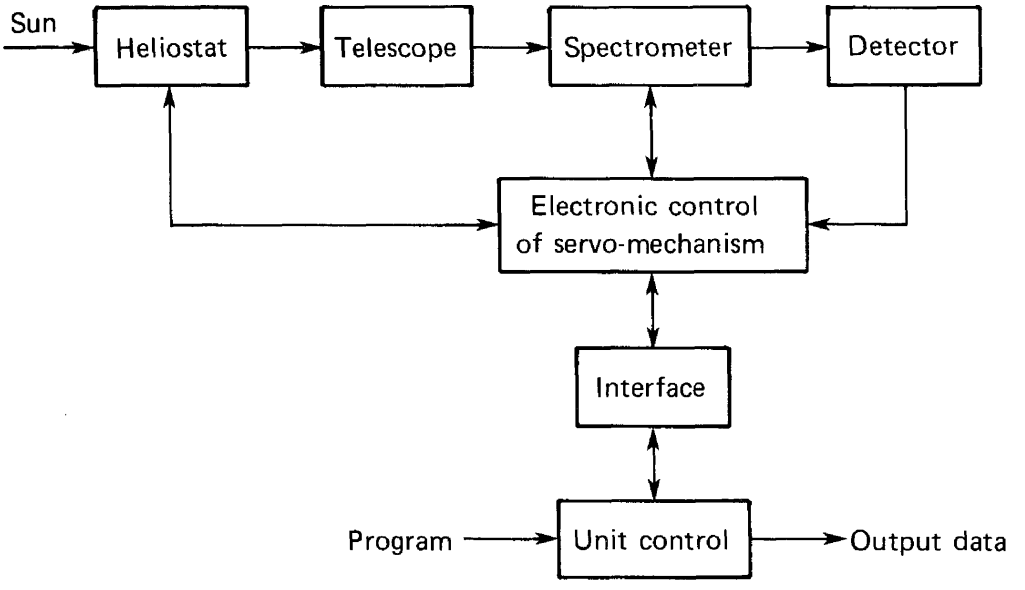

Figure 2.

An experiment is constituted by the analysis of a number of chemical constituents, in a given order:

For each species of interest, the specific parameters are entered, once and for all, in the memory of the control unit. These parameters are :

– the convenient filter for the selected order of the grating,
– the mean position of the grating and the spectral interval to be scanned by the rotation of the grating.

The specific parameters for an experiment are entered by an operator, through a specialized keyboard, into the control module (HP 2105).

These parameters are :

– the names of the constituents to be analyzed,
– the order in which these analyses should be performed,
– the number of analyses to be performed on each constituent,
– the number of times the total sequence of analysis should be performed.

4 – PROGRAM OF MEASUREMENTS

During the "Latitude survey mission", the program of measurement was practically unchanged all along the mission. Five spectral intervals were scanned, with a view to measuring : NO NO_2, HCl, HNO_3, O_3, CH_4 and H_2O. The limits of these intervals are given in Table II. The program of a sequence of measurement is given in Table III. The duration of one sequence is 4 minutes. An overview of the observation periods along the mission is given in table IV.

Table II – Spectral intervals scanned during a sequence of measurement.

Main constituent	Spectral interval (cm^{-1})	Other constituent with specific absorption features in the same interval
NO	1910 – 1920	CO_2
NO_2	1600 – 1610	H_2O
HCl	2940 – 2949	CH_4
HNO_3	1321 – 1329	CH_4, N_2O
O_3	1723 – 1730	HNO_3

Table III – Sequence of measurement.

Main constituent	Number of scans
NO	5
NO_2	3
HCl	3
HNO_3	3
O_3	4
HNO_3	2
HCl	2
NO_2	2

Table IV – Overview of the observation periods.

Flight number	Taking off and landing points	Duration of measurements (mn)	Latitude*	Sunset (SS) or Sunrise (SR) or Constant =	Range of solar elevation (degrees)	
1	Moffett-field - Moffett-field	30	36-39°N	SS	3	−1
2	Moffett-field - Fairbanks	55	58-64°N	SS	3	−1.5
3	Fairbanks-Fairbanks	30	75-74°N	=	1	
3bis	Fairbanks-Fairbanks	30	71-71°N	=	4	
4	Fairbanks-Honolulu	60	60-54°N	SR	−0.5	6
5	Honolulu-Honolulu	50	22-14°N	SR	0.5	12
9	Melbourne-Melbourne	40	32-38°S	SR	1	8
12	Christchurch-Christchurch	60	52-44°S	SS	8	1
13	Christchurch-Pago Pago	30	20-16°S	SS	9	2
14	Pago Pago-Honolulu	60	14-21°N	SS	11	0

* During the period of measurement.

It can be noticed that the observations are limited to values of solar zenith angle smaller than 90°, except for flights n° 1, 2 and 4. For the lowest values of the solar elevation, the observations were frequently limited by clouds.

It is well known that a vertical profile of local concentration can hardly be derived from spectral observations above the altitude of the instrument.

Consequently the results will be generally presented in terms of total column density (mol. cm^{-2}) with respect to solar elevation, which leads to a mean value of the mixing ratio above the altitude of observation and for the most favorable cases, to plausible vertical profiles in the vicinity of the altitude of flight.

During the experiments, the altitude of the aircraft varied between 9.3 km and 11.7 km, so that the aircraft was generally inside the troposphere. However, the aircraft was clearly inside the stratosphere during the periods of observation n° 2, 3 and 3bis.

5 – PRELIMINARY RESULTS FROM OBSERVATIONAL DATA

The equipment has been operated during the mission without failure except for a trouble coming from the magnetic tape during flights n° 3bis, 5 and 14. Therefore, a qualitative preliminary study of the spectra has been carried out for flights n° 1, 2, 3, 4, 9, 12 and 13. It will be extended to the flights n° 3bis, 5 and 14 as soon as digital data will be made available from the Airborne Digital Data Acquisition System (ADDAS), since the spectral data were simultaneously recorded in analogue form on the magnetic tape included in our equipment and digitally on an ADDAS tape.

From this preliminary study, it can be stated that meaningful spectral data have been obtained on the five spectral channels (Table III) during these seven flights, and that this will be probably extended to the whole set of 10 periods of observation.

It appears also that valuable numerical data can be extracted from a number of spectra recorded on each flight, although a residual vibration noise frequently limits the signal/noise ratio on the records. This restriction holds in particular for flight n° 4. For this experiment, and possibly for two others, the numerical data will be probably limited to HNO_3, O_3, CH_4, H_2O* and NO_2, excluding HCl and NO, because of the weakness of the absorption features observed for these species.

The large amount of data (more than 7 hours of records) will necessitate a period of about nine months before presentation of the final results.

---

* For H_2O the possible effect of the water vapor inside the aircraft will have to be estimated since the instrument did not work in airtight conditions.

The present effort of data reduction is directed toward extraction of valuable informations on NO_2 and HNO_3 in the shortest time possible.

A set of typical spectra obtained for these two species during 6 flights are shown on figure 3. Over two hundred similar spectra are available for these two species (excluding the data concerning flights n° 3bis, 5 and 14, as indicated above). Each couple of NO_2 and HNO_3 spectra shown on the figure 3 has been obtained within a period of time shorter than one minute so that a single value of the solar elevation can be associated with the couple.

A first example of data reduction is given for HNO_3, on figure 4. It concerns flight n° 2. The calibration is based upon laboratory data previously performed at room temperature by Fontanella et al. [1]. These laboratory data have been compared with previous ones (Goldman et al. [2]). They have yet to be improved by temperature corrections. This will be allowed by a theoretical and instrumental investigation presently performed with a view to application to atmospheric studies by a team conducted by Pr Jouve (University of Reims).

A local concentration of $1.4 \cdot 10^{10}$ mol.cm^{-3} has been deduced from the data shown on figure 4, at 10.6 km altitude. This high value is coherent with previous observations performed in July 1974 at high altitude (65 °N) in the lower stratosphere [3].

Our participation in the NASA Latitude Survey Mission has been supported by CNES (Centre National d'Etudes Spatiales).

The authors wish to mention L. Gramont and J. Marcault for their basic role as participants in the preparation of the mission and during the mission itself. We also wish to thank many other people at ONERA, who have played a crucial role building and adjusting the equipment in a very short time.

Finally, it is a pleasure to thank NASA Ames Medium Altitude Missions Branch and chiefly L.C. Haughney for their help and their friendly cooperation before and during the whole mission.

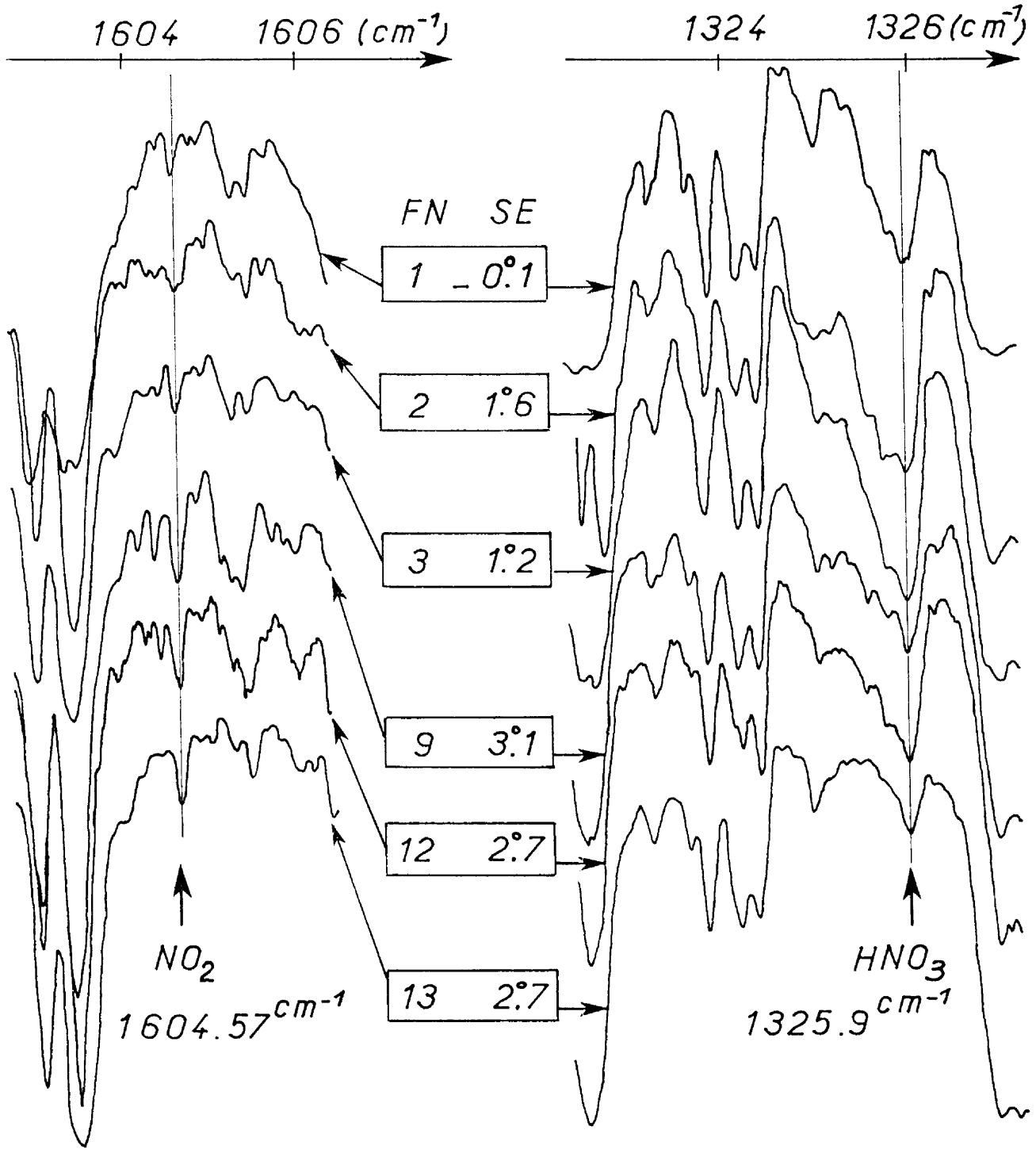

Figure 3. Typical NO_2 and HNO_3 spectra obtained during various flights.
FN : Flight Number SE : Solar Elevation

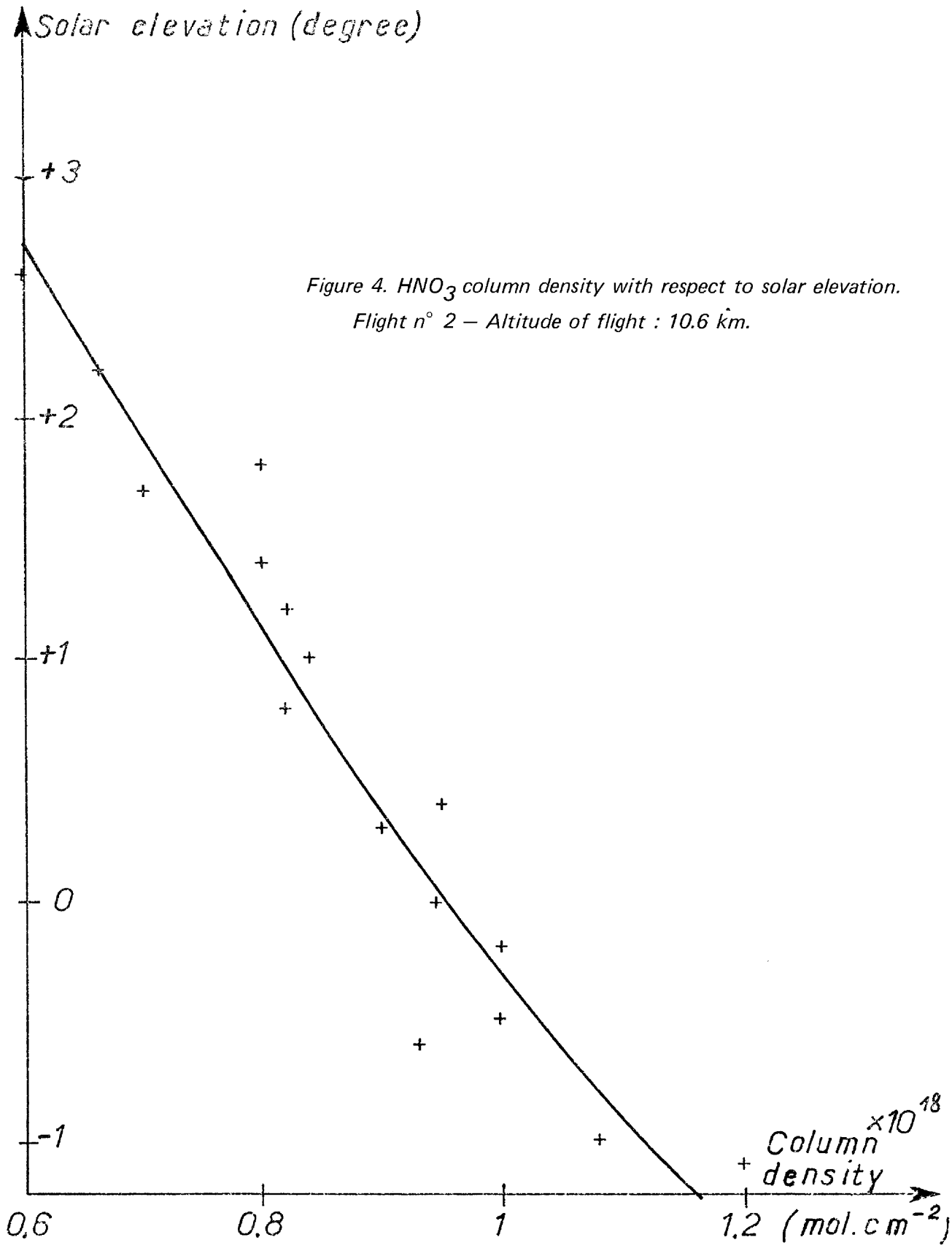

Figure 4. HNO_3 column density with respect to solar elevation.
Flight n° 2 — Altitude of flight : 10.6 km.

REFERENCES

1. Fontanella, J.C., Girard, A., Gramont L., Louisnard, N. Vertical distribution of NO, NO_2 and HNO_3 as derived from Stratospheric Absorption infrared Spectra. Applied Optics, vol. 14 No 4, 825-839, 1975. Proc. Third Conf. CIAP, p. 217-233.

2. Goldman A., Kyle, T.G., Bonomo, F.S. Statistical Band Model Parameters and Integrated Intensities for the 5.9 μm, 7.5 μm, 11.3 μm bands of HNO_3 vapor. Applied Optics, vol. 10, No 1, 65-74, 1971.

3. Girard, A., Fontanella, J.C., Giraudet, R., Louisnard, N. Simultaneous measurements of nitrogen dioxide and nitric acid in the lower stratosphere (to be published in Journal de Chimie-Physique, 1977).

ATMOSPHERIC HALOCARBON EXPERIMENT

Edward C. Y. Inn, Bennett J. Tyson,
and John C. Arvesen

NASA Ames Research Center
Moffett Field, CA 94035

INTRODUCTION

The catalytic decomposition of stratospheric ozone by photolysis products of chlorofluoromethanes predicted by Molina and Rowland (ref. 1) is of major worldwide concern. The measurement of the global distribution of these halocarbons, which are anthropogenically released in the troposphere and then carried up into the stratosphere, should provide important quantitative background information required in any theoretical formulation of the photochemistry of ozone. On the basis of four sets of measurements reported by others, Rowland and Molina (ref. 2) deduce that the south-north hemisphere ratio of $CFCl_3$ (Freon 11) concentration in the troposphere is about 0.8. There is clearly a need for more measurements of the global distribution of halocarbons in order to determine the eventual fate of these anthropogenically released constituents.

In this experiment, in situ measurements of minor atmospheric constituents are made by means of an Automated Gas Chromatograph (AGC) on board the Convair 990 aircraft. The objectives then are: (1) measure the latitude and altitude distribution of minor atmospheric constituents throughout the CV-990 flightpath, and (2) rendezvous with a U-2 stratospheric cryogenic sampling experiment at a location near the Hawaiian Islands for a coordinated set of measurements of the same air mass. It is appropriate to consider a third objective; namely, to assess the performance of the AGC system under flight conditions prior to its ultimate use on board a U-2 aircraft for in situ stratospheric measurements. In the present experiment, the measurements are directed at the following minor constituents: $CFCl_3$ (Freon 11), CF_2Cl_2 (Freon 12), $C_2F_3Cl_3$ (Freon 113), $C_2F_4Cl_2$ (Freon 114), CCl_4 (carbon tetrachloride), CH_3Cl (methylchloride), CH_3CCl_3 (methylchloroform), N_2O (nitrous oxide), SF_6 (sulfur hexafluoride).

DESCRIPTION OF EXPERIMENT

A schematic diagram of the measurement system, the plumbing constructed with stainless steel parts, is shown in Figure 1. The inlet scoop of the air sampling system is a 2.54-cm-diameter tube that is welded to a stainless steel aircraft window. The standoff distance of the inlet part from the window is 25.4 cm, which is substantially beyond the boundary layer over the fuselage. The aircraft window is located topside on the fuselage at an elevation angle 65° from the horizontal.

The direction of flow of the sampled air is shown (in fig. 1) flowing under ram pressure from the inlet scoop to C, a stainless steel bellows compressor pump. V_3 is a throttling valve that controls the rate of pressurization of air entering the sample loop of the gas chromatograph. The maximum pressure of the sampled gas is regulated by the relief valve, R, which is preset for a pressure of about 3 atmospheres. For pressure measurements the transducer, T, is used, and a digital

printout of the pressure is provided for each sample of air analyzed. The flowing air is exhausted beyond the three-way solenoid valve, V_5, into the cabin atmosphere; the flow rate is monitored by the flow meter, M.

A source of calibration gas is coupled to the inlet system that leads to the gas chromatograph, as shown in Figure 1. V_2 is a three-way solenoid valve that is used to isolate the calibration gas supply, G, and the gas chromatograph from the inlet line, and V_1 is the flow control valve.

An auxiliary pumping system is included in this arrangement for evacuating the sample loop of the gas chromatograph, thereby providing a convenient method for adjusting the zero reading of the pressure transducer. V is a small rotary vacuum pump (25 liters/min). To prevent contamination by backstreaming pump oil, a trap, T, which consists of silica gel, a molecular sieve, and charcoal, is placed between V_5 and the vacuum pump.

The analytical instrument is an automated gas chromatograph (Hewlett-Packard Model 5840A) that uses an electron-capture detector with a 15 millicurie Ni^{63} source. Included in this system is a microprocessor, which controls the analysis, computes and displays the results on a printed record. The solenoid valves shown in Figure 1 are also controlled by the microprocessor. Thus, the analysis procedure may be programmed from the microprocessor keyboard or input from a preprogrammed magnetic tape. Dual electron-capture detectors are used, each coupled to separate columns and each column connected to a separate sample loop (5 cm^3). With this arrangement for each complete cycle of measurement, one column (Porosil A) and one detector are used in the analysis for N_2O, SF_6, Freon 12, and Freon 114 during one-half cycle, and the other column (DC200 silicone oil) and detector are used to determine the remaining constituents during the other half-cycle. During the period of analysis of the sample in one loop, the other loop is flushed and filled, ready to be analyzed upon the completion of the first analysis. A methane-argon mixture is used as the carrier gas.

In view of the sampling procedure described above, the gas chromatograph measurements of the atmospheric constituents while airborne are quasi-continuous. The measured concentrations of each constituent thus corresponds to the air mass sampled during the time that the gas chromatograph sample loop is being filled. Therefore, for each measurement half-cycle, the altitude and coordinates of the air mass are determined by the position of the aircraft during the time that the sample loop is being filled.

RESULTS AND DISCUSSION

The data for N_2O, CF_2Cl_2, $CFCl_3$, and CCL_4 are presented in Table I. The altitudes listed in the table are pressure altitudes based on the 1962 Standard Atmosphere. The meridional distribution of these compounds in the troposphere of both hemispheres are plotted in Figures 2 and 3. The data plotted in these figures represent all measurements obtained in the troposphere for the altitude range of 9.14 to 11.9 km. Thus, data obtained for those measurements made at tropopause altitudes and above are not plotted in the figures. The concentrations were calculated based on post-flight laboratory calibrations with the equipment in the same configuration as during actual flights. The error in the in-flight measurements is estimated to be about ±15%. This estimate is based on variable operating conditions encountered in use of the gas chromatograph in an aircraft where cabin pressure cannot be controlled to 1.013×10^5 Pa (760 torr) and because of calibration uncertainties. These variables affect the sensitivity of the measurement because of changes in detector exit pressure, changes in carrier gas flow rate, and changes in sample pressure. The influence of these three variables will be examined in more detail and discussed in the final report. Further calibrations will be performed and an assessment of the operational variations will be made in order to minimize the uncertainties of the measurements.

Intercalibrations on the ground in Melbourne, Australia, between Washington State University, C.S.I.R.O. Aspendale, Australia, and Ames Research Center showed good agreement to within 7% for calibration mixtures of CF_2Cl_2, $CFCl_3$, and CCL_4. Post-flight calibrations confirmed the CF_2Cl_2 and $CFCl_3$ correlations but we obtained a 20% higher value for CCl_4. An intercalibration comparison was not made on N_2O.

The average concentrations of each of the compounds measured in the two hemispheres are listed in Table II. These averages were derived from the data plotted in Figures 2 and 3. The concentrations of the compounds measured between the two hemispheres show no concentration gradients in the troposphere within the limits of error. This is evident from the average values listed in Table II. If it is assumed that the zonal distribution of these compounds is uniform, then these results support previous studies of interhemispheric tropospheric gradients and indicate mixing in the troposphere is rapid.

The results of the coordinated measurements with the U-2 cryogenic samplers are discussed in the section on Stratospheric Halocarbon Experiment.

REFERENCES

1. Molina, M. J.; and Rowland, F. S.: Stratospheric Sink for Chlorofluoromethanes: Chlorine Atom-Catalyzed Destruction of Ozone. Nature, vol. 252, 1974, pp. 292-294.

2. Rowland, F. S.; and Molina, M. J.: Estimated Future Atmospheric Concentrations of CCl_3F (Fluorocarbon 11) for Various Hypothetical Tropospheric Removal Rates. J. Phys. Chem., vol. 80, 1976, pp. 2049-2056.

TABLE I. CV-990 MERIDIONAL SURVEY RESULTS - FALL, 1976

Run #	Latitude	Longitude	Altitude (km)	F-11 pptv	CCl_4 pptv	N_2O ppbv	F-12 pptv
A. Flight #2 - Moffett Field to Fairbanks, 10/28/76							
1	38° 18'N	122° 54'W	5.03	123			
	39° 51'N	123° 12'W	9.14			315	211
2	42° 02'N	122° 58'W	9.14	141	169		---
	43° 48'N	123° 16'W	9.14			350	---
3	45° 59'N	123° 52'W	9.14	144	161		
	47° 33'N	124° 23'W	9.14			327	234
4	49° 08'N	125° 50'W	9.14	148	174		
	50° 12'N	127° 28'W	9.14			332	230
5	53° 52'N	132° 27'W	10.7			311	239
	52° 38'N	130° 55'W	9.14	141	148		
6	55° 31'N	134° 11'W	10.7[a]	123	164		
	56° 53'N	135° 43'W	10.7			300	200
7	58° 40'N	137° 46'W	10.7[a]	126	175		
8	61° 58'N	141° 42'W	10.7[a]	120			
	63° 32'N	143° 33'W	10.7			306	222
B. Flight #3 - Fairbanks, 10/29/76							
1	69° 03'N	144° 11'W	9.45[b]	125	177		
	71° 26'N	143° 19'W	9.45[b]			269	212
2	72° 58'N	142° 52'W	10.1[b]	131	202		
	74° 44'N	142° 14'W	10.1[b]			282	213
3	75° 12'N	148° 28'W	10.1[b]	124	214		
	74° 52'N	154° 43'W	10.1[b]			282	197
4	74° 10'N	161° 59'W	10.1[b]	125	179		
	74° 03'N	155° 52'W	10.1[b]			280	213
5	72° 37'N	151° 49'W	10.1[b]	118	176		
	71° 33'N	151° 43'W	10.1[b]			277	209
6	71° 40'N	157° 52'W	11.3[b]	118	161		
	71° 38'N	163° 33'W	11.3[b]			269	197
7	71° 32'N	160° 37'W	6.40	141	185		
	71° 35'N	156° 33'W	6.40			302	---
8	71° 24'N	156° 33'W	1.07		185		
	72° 08'N	155° 36'W	1.07			307	229
9	71° 34'N	156° 25'W	0.33	132	194		
	70° 52'N	156° 01'W	7.62			271	230

a Tropopause height - 10.7 km. b Tropopause height - 9.45 km.

TABLE I. CONTINUED

Run #	Latitude	Longitude	Altitude (km)	F-11 pptv	CCl_4 pptv	N_2O ppbv	F-12 pptv
C. Flight #4 - Fairbanks to Honolulu, 10/30/76							
1	50° 07'N	156° 03'W	10.1	125	166		
	49° 00'N	156° 00'W	10.1			293	221
1	45° 20'N	156° 00'W	10.7	128	190		
	44° 14'N	156° 00'W	10.7			283	240
2	42° 36'N	156° 00'W	10.7	154	187		
	41° 34'N	156° 00'W				---	---
3	40° 54'N	156° 00'W	10.7	141	158		
	39° 47'N	156° 00'W	10.7			291	222
5	36° 03'N	156° 02'W	10.7	137	171		
	35° 01'N	156° 03'W	10.7			294	249
6	33° 06'N	156° 07'W	10.7	131	168		
	32° 02'N	156° 07'W	10.7			305	240
10	23° 49'N	156° 18'W	11.9	125	88		
	22° 42'N	156° 28'W	11.9			277	209
D. Flight #5 - Honolulu, 11/1/76							
2	23° 32'N	155° 12'W	10.1	135	153		
	22° 30'N	155° 25'W	10.1			289	241
3	19° 42'N	156° 10'W	10.1	129	172		
	18° 40'N	156° 26'W	10.1			276	204
4	16° 18'N	156° 52'W	10.1	126	171		
	15° 18'N	157° 03'W	11.0			286	224
5	15° 05'N	156° 53'W	10.7	149	150		
	16° 11'N	156° 41'W	11.0			305	223
6	18° 22'N	156° 17'W	10.7	150	158		
	19° 26'N	156° 01'W	10.7			305	232
7	20° 17'N	155° 26'W	6.4	144	188		
	19° 24'N	155° 34'W	6.4			288	234
8	19° 21'N	155° 34'W	4.57	161	172		
	20° 03'N	155° 27'W	4.57			303	219
9	19° 16'N	155° 40'W	3.35	137	174		
	19° 01'N	155° 34'W	3.35			315	221
10	19° 54'N	155° 04'W	0.43	131	173		
	20° 10'N	155° 37'W	0.49			299	203
11	20° 46'N	156° 54'W	2.44	137	202		
	21° 00'N	157° 31'W	2.07			288	215

TABLE I. CONTINUED

Run #	Latitude	Longitude	Altitude (km)	F-11 pptv	CCl_4 pptv	N_2O ppbv	F-12 pptv
E. Flight #6 - Honolulu, 11/3/76							
1	18° 47'N	158° 17'W	9.14	137	165		
	17° 42'N	158° 45'W	9.14			320	226
2	15° 31'N	159° 40'W	9.45	134	169		
	14° 31'N	160° 04'W	9.45			299	231
3	12° 27'N	160° 52'W	9.45	135	161		
	11° 25'N	161° 15'W	9.45			325	210
5	12° 28'N	160° 59'W	9.45	138	174		
	13° 30'N	160° 33'W	9.45			346	213
6	15° 35'N	159° 40'W	9.45	134	174		
	16° 35'N	159° 16'W	9.45			327	224
7	19° 07'N	158° 15'W	9.45	138	175		
	20° 05'N	157° 59'W	6.1			322	190
F. Flight #7 - Honolulu to Pago Pago, 11/7/76							
6	15° 06'N	159° 51'W	9.45	140	185		
	14° 07'N	160° 14'W	9.45			275	175
7	12° 15'N	160° 57'W	9.45	131	170		
	11° 15'N	161° 19'W	9.45			309	191
9	9° 15'N	162° 04'W	9.45	133	182		
	8° 16'N	162° 26'W	9.45			302	197
10	6° 03'N	163° 14'W	9.45	135	179		
	4° 59'N	163° 38'W	9.45			281	188
11	2° 39'N	164° 28'W	10.7	141	177		
	1° 35'N	164° 51'W	10.7			312	197
13	0° 25'S	165° 34'W	10.7	136	177		
	1° 29'S	165° 57'W	10.7			310	187
14	3° 56'S	166° 51'W	10.7	133	166		
	4° 58'S	167° 13'W	10.7			311	189
15	6° 57'S	167° 57'W	10.7	128	178		
	8° 00'S	168° 20'W	10.7			306	190
16	10° 54'S	169° 24'W	10.7	129	182		
	11° 53'S	169° 46'W	10.7			301	223
17	13° 47'S	170° 35'W	4.57	129	179		
	14° 26'S	170° 28'W	3.35			332	196
18	14° 29'S	170° 30'W	0.94	128			
	14° 14'S	170° 34'W	0.98			322	229

TABLE I. CONTINUED

Run #	Latitude	Longitude	Altitude (km)	F-11 pptv	CCl_4 pptv	N_2O ppbv	F-12 pptv
G. Flight #8 - Pago Pago to Melbourne, 11/8/76 and 11/9/76							
2	17° 54'S	175° 13'W	9.45	129	164		
	18° 34'S	176° 05'W	9.45			309	181
3	19° 47'S	177° 43'W	9.45	126	163		
	20° 24'S	178° 34'W	9.45			322	212
4	21° 36'S	179° 46'E	9.45	121	168		
	22° 10'S	178° 57'E	9.45			302	182
5	23° 18'S	177° 18'E	9.45	122	165		
	23° 50'S	176° 29'E	9.45			294	183
6	25° 12'S	174° 22'E	9.45	128	166		
	25° 46'S	173° 28'E	9.45			303	171
7	27° 16'S	170° 59'E	9.45	128	173		
	27° 48'S	170° 04'E	9.45			309	193
8	28° 50'S	168° 15'E	10.7	130	169		
	29° 14'S	167° 22'E	10.7			264	229
9	30° 27'S	164° 25'E	10.7	127	165		
	30° 53'S	163° 28'E	10.7			345	232
10	31° 39'S	160° 46'E	10.7	126	176		
	31° 59'S	159° 44'E	10.7			308	207
11	32° 35'S	157° 52'E	11.9[a]	123	166		
	32° 51'S	156° 55'E	11.9[a]			292	304
12	33° 24'S	154° 55'E	11.9[a]	120	166		
	33° 38'S	153° 51'E	11.9[a]			318	197
13	34° 29'S	150° 44'E	6.7	130	153		
	34° 58'S	149° 57'E	6.7			297	182
14	35° 59'S	147° 59'E	6.7	127	171		
	36° 24'S	147° 02'E	6.7			267	202

a Tropopause height - 11.9 km.

TABLE I. CONTINUED

Run #	Latitude	Longitude	Altitude (km)	F-11 pptv	CCl_4 pptv	N_2O ppbv	F-12 pptv
H. Flight #9 - Melbourne, 11/10/76							
5	35° 01'S	143° 58'E	9.45	133	187		
	34° 00'S	143° 42'E	9.45			300	192
6	32° 02'S	142° 59'E	10.7	142	170		
	33° 01'S	142° 42'E	10.7			338	236
7	35° 03'S	142° 10'E	11.3	126	168		
	36° 04'S	141° 56'E	11.3			463	264
8	38° 10'S	141° 20'E	11.3	107	156		
	37° 10'S	141° 31'E	11.3			402	229
9	38° 54'S	141° 57'E	11.3	115	170		
	34° 54'S	142° 23'E	11.3			366	256
10	36° 30'S	143° 52'E	11.3	115	178		
	36° 46'S	144° 05'E				376	238
11	39° 21'S	145° 01'E	11.3	127	183		
	40° 22'S	144° 46'E				398	228
13	40° 23'S	144° 48'E	6.40	115	173		
	40° 01'S	144° 51'E	6.40			421	243
14	41° 08'S	145° 12'E	3.05	119	188		
	41° 50'S	146° 02'E	3.05			362	264
15	42° 07'S	147° 16'E	11.9[a]	116	178		
	41° 06'S	146° 55'E	11.9[a]			399	297
16	39° 17'S	146° 01'E	11.9	118	170		
	38° 24'S	145° 31'E	11.9			375	203
17	37° 55'S	145° 00'E	7.62	120	175		
	38° 41'S	145° 40'E	7.62			417	217
18	38° 03'S	145° 08'E	3.05	117	175		
	37° 33'S	144° 47'E	3.05			383	204

a Tropopause height - 11.3 km.

TABLE I. CONTINUED

Run #	Latitude	Longitude	Altitude (km)	F-11 pptv	CCl_4 pptv	N_2O ppbv	F-12 pptv
I. Flight #10 - Melbourne, 11/11/76							
1	35° 32'S	141° 53'E	11.0	118	164		
	35° 02'S	142° 27'E	11.0			349	204
2	35° 13'S	142° 25'E	11.0	120	166		
	34° 14'S	142° 37'E	11.0			300	198
3	35° 36'S	142° 00'E	11.0	118	155		
	36° 43'S	141° 55'E	11.0			310	190
4	36° 05'S	142° 15'E	9.44	125	173		
	35° 00'S	142° 28'E	9.44			301	183
5	34° 49'S	142° 03'E	7.62	116	166		
	34° 14'S	142° 18'E	6.40			299	196
6	35° 17'S	142° 33'E	4.57	122	169		
	36° 01'S	143° 24'E	4.57			295	195
J. Flight #11 - Melbourne to Christchurch, 11/12/76							
1	38° 29'S	145° 36'E	6.71	121	164		
	39° 32'S	145° 23'E	9.14			321	195
2	41° 58'S	146° 44'E	10.7	123	165		
	42° 56'S	147° 35'E	10.7			324	217
3	45° 18'S	149° 25'E	10.7	122	163		
	46° 16'S	150° 13'E	10.7			---	241
4	48° 10'S	151° 55'E	10.7	127	212		
	49° 07'S	152° 49'E	10.7			304	209
5	51° 00'S	154° 44'E	10.7	126	169		
	51° 52'S	155° 43'E	10.7			315	195
6	53° 37'S	157° 50'E	10.7	126	170		
	54° 30'S	159° 00'E	10.7			320	215
7	53° 54'S	162° 36'E	10.7	126	170		
	53° 33'S	164° 25'E	11.3			311	216
9	49° 30'S	168° 44'E	11.3[a]	115	158		
	48° 20'S	168° 35'E	11.3			308	200
10	46° 12'S	169° 08'E	11.3	117	161		
	45° 30'S	170° 20'E	11.3			303	230
11	43° 48'S	172° 08'E	2.74	115	161		
	43° 18'S	172° 36'E	1.52			292	

a Tropopause height - 11.0 km.

TABLE I. CONTINUED

Run #	Latitude	Longitude	Altitude (km)	F-11 pptv	CCl_4 pptv	N_2O ppbv	F-12 pptv
K. Flight #12 - Christchurch, 11/14/76							
4	47° 00'S	166° 22'E	10.1	119	159		
	48° 03'S	168° 26'E	10.1			273	198
5	50° 23'S	168° 37'E	10.1	114	163		
	51° 29'S	168° 42'E	10.1			293	159
6	53° 38'S	168° 52'E	10.1	122	155		
	56° 04'S	169° 06'E	10.1			303	201
7	56° 55'S	169° 10'E	10.1	117	164		
	58° 01'S	169° 17'E	10.1			308	199
8	60° 44'S	169° 51'E	11.3	121	159		
	61° 46'S	170° 44'E	11.3			281	188
9	59° 30'S	172° 24'E	11.3	121	156		
	58° 30'S	172° 59'E					
11	56° 16'S	174° 12'E	11.3	---	164		
	53° 14'S	174° 43'E	11.3			283	169
12	53° 04'S	175° 42'E	11.3	117	163		
	52° 00'S	175° 42'E	11.3			277	229
13	49° 56'S	174° 10'E	11.3[a]	113	193		
	48° 54'S	173° 26'E	11.3[a]			294	188
14	46° 58'S	172° 03'E	11.9[a]	114	150		
	45° 57'S	171° 18'E	11.9[a]			291	188
a Tropopause height - 11.3 km.							
L. Flight #13 - Christchurch to Pago Pago, 11/16/76 - 11/15/76							
1	41° 21'S	174° 48'E	10.1	109	153		
	40° 29'S	175° 51'E	10.1[a]			303	190
2	38° 28'S	178° 04'E	10.1	107	146		
	37° 23'S	178° 44'E	10.1[a]			271	171
3	35° 16'S	179° 56'E	10.1	120	155		
	34° 05'S	179° 45'W	10.1			282	190
4	31° 50'S	179° 21'W	10.1	120	164		
	30° 39'S	179° 09'W	10.1			282	199
5	27° 05'S	174° 04'W	10.7	117	159		
	26° 24'S	172° 54'W	10.7			367	183
6	26° 50'S	173° 39'W	10.7	125	164		
	26° 09'S	172° 30'W	10.7			301	208
7	24° 41'S	170° 10'W	10.7	124	175		
	24° 15'S	169° 04'W	10.7			292	183
8	22° 49'S	167° 54'W	11.3	127	166		
	21° 58'S	167° 59'W	11.3			288	208
9	19° 56'S	168° 18'W	11.3	129	166		
	19° 00'S	168° 29'W	11.3			286	199
10	17° 02'S	168° 54'W	11.9	131	168		
	16° 06'S	169° 01'W	11.9			283	193
a Tropopause height - 9.4 km.							

TABLE I. CONTINUED

Run #	Latitude	Longitude	Altitude (km)	F-11 pptv	CCl_4 pptv	N_2O ppbv	F-12 pptv
M. Flight #14 - Pago Pago to Honolulu, 11/17/76							
2	13° 36'S	170° 26'W	4.57	116	170		
	12° 44'S	170° 06'W	10.1			345	190
3	10° 16'S	169° 10'W	10.1	129	173		
	9° 23'S	168° 30'W	10.1			331	197
4	7° 52'S	167° 07'W	10.1	127	171		
	7° 03'S	166° 21'W	10.1			220	199
5	5° 11'S	164° 40'W	10.1	127	178		
	4° 21'S	163° 55'W	10.1			298	189
6	2° 39'S	162° 23'W	10.1	122	163		
	1° 51'S	161° 40'W	10.1			303	189
7	0° 10'N	159° 56'W	10.1	123	170		
	1° 12'N	159° 31'W	10.4			322	178
8	3° 19'N	158° 41'W	11.3	127	175		
	4° 20'N	158° 16'W	11.3			309	189
9	6° 22'N	157° 20'W	11.3	128	173		
	7° 22'N	156° 50'W	11.3			312	203
10	9° 21'N	155° 50'W	11.3	129	175		
	10° 22'N	155° 18'W	11.3			326	172
11	12° 25'N	154° 10'W	11.9	132	175		
	13° 25'N	153° 37'W	11.9			312	208
13	18° 20'N	154° 33'W	11.9	131	178		
	19° 13'N	154° 56'W	11.9			305	197

TABLE I. CONCLUDED

Run #	Latitude	Longitude	Altitude (km)	F-11 pptv	CCl_4 pptv	N_2O ppbv	F-12 pptv
N. Flight #15 - Honolulu to Moffett Field, 11/18/76							
15	21° 20'N	157° 27'W	3.05	121	142		
	21° 51'N	156° 38'W	7.01			332	220
1	23° 15'N	154° 16'W	10.1	115	153		
	23° 54'N	153° 12'W	10.1			325	206
2	25° 08'N	151° 05'W	10.1	118	156		
	25° 44'N	150° 00'W	10.1			312	252
3	26° 55'N	147° 51'W	10.1	119	155		
	27° 29'N	146° 46'W	10.1			329	186
4	28° 33'N	144° 40'W	10.1	119	150		
	29° 06'N	143° 31'W	10.1			327	223
5	30° 14'N	141° 05'W	10.1	120	150		
	30° 47'N	139° 50'W	10.1			338	211
6	31° 52'N	137° 17'W	10.1	124	151		
	32° 24'N	135° 58'W	10.1			338	214
7	33° 23'N	133° 23'W	10.1	122	158		
	33° 52'N	132° 01'W	10.1			334	202
9	36° 03'N	125° 05'W	10.1	120	153		
	36° 40'N	123° 50'W	7.01			306	217

TABLE II. CONCENTRATIONS IN TROPOSPHERE BETWEEN 9.14 KM AND 11.9 KM

Compound	Concentration		Number of Samples	
	Northern Hemisphere	Southern Hemisphere	Northern Hemisphere	Southern Hemisphere
F-11	132 ± 9 pptv	124 ± 6 pptv	41	51
CCl_4	167 ± 11 pptv	166 ± 8 pptv	40	54
F-12	218 ± 19 pptv	204 ± 22 pptv	32	53
N_2O	306 ± 21 ppbv	314 ± 39 ppbv	27	52

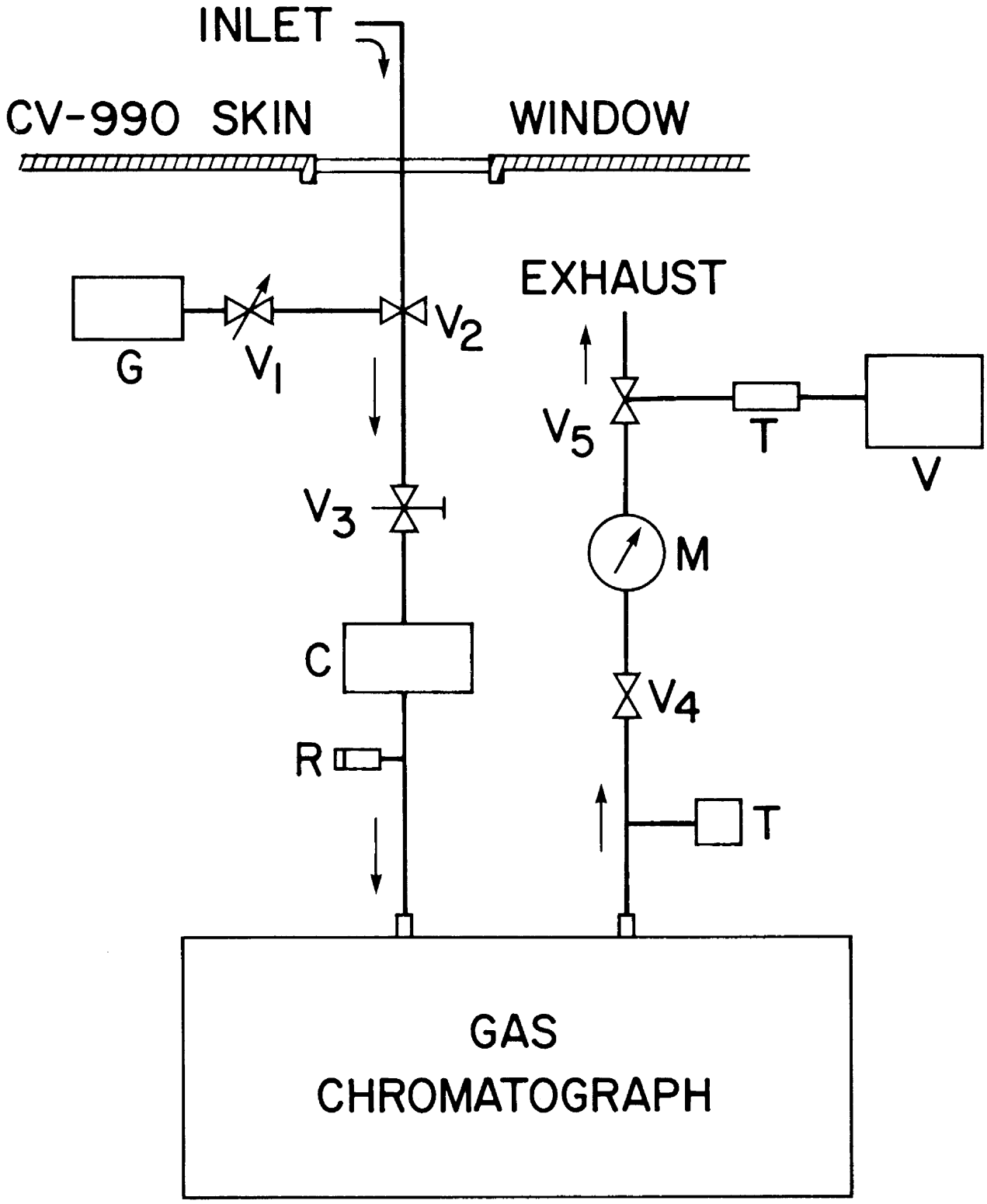

Figure 1.- Schematic diagram of the gas sampling system.

FIGURE 2
CONCENTRATION VS LATITUDE
9.14 km to 11.89 km

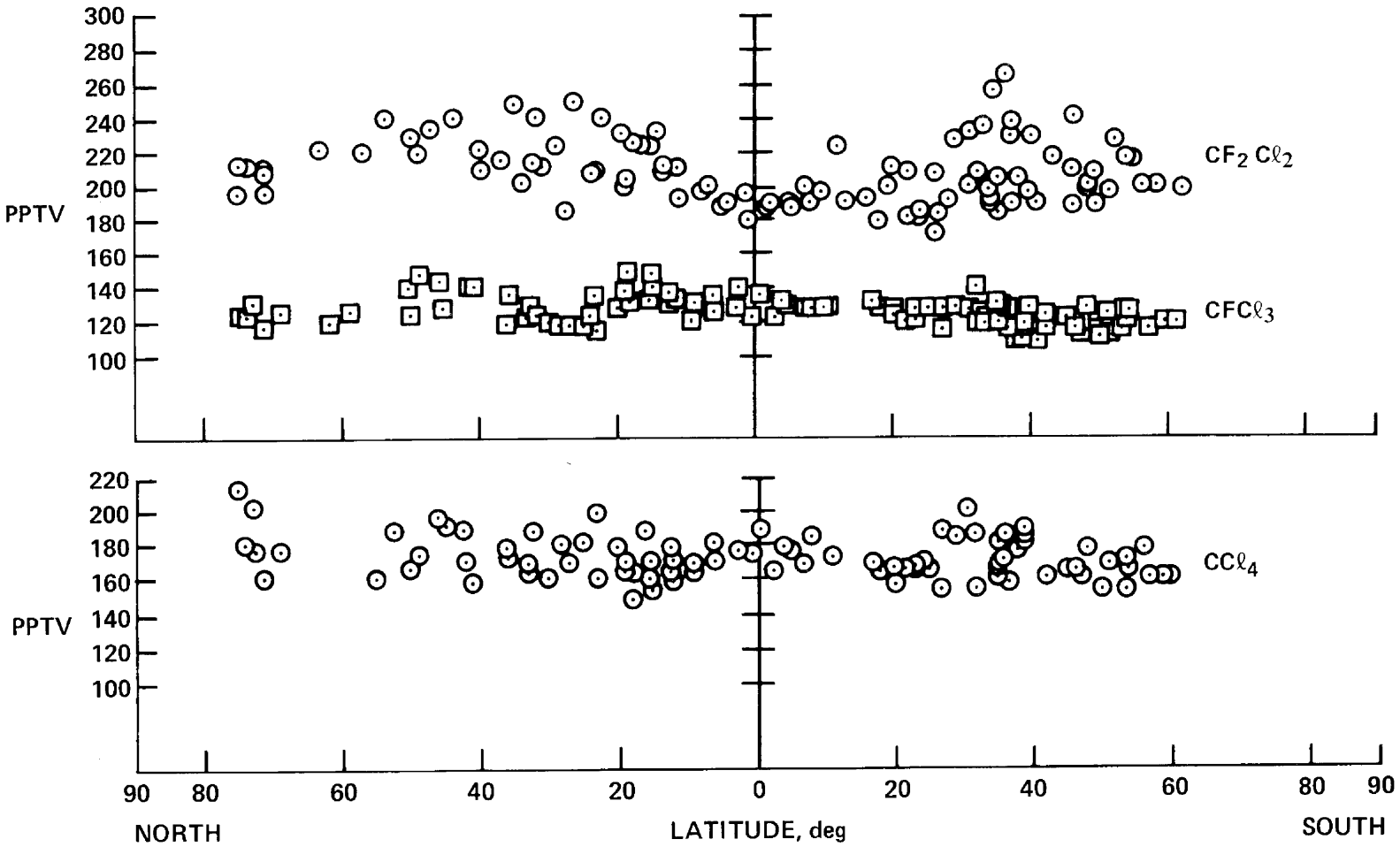

FIGURE 3
N_2O CONCENTRATION VS LATITUDE

9.14 km to 11.89 km

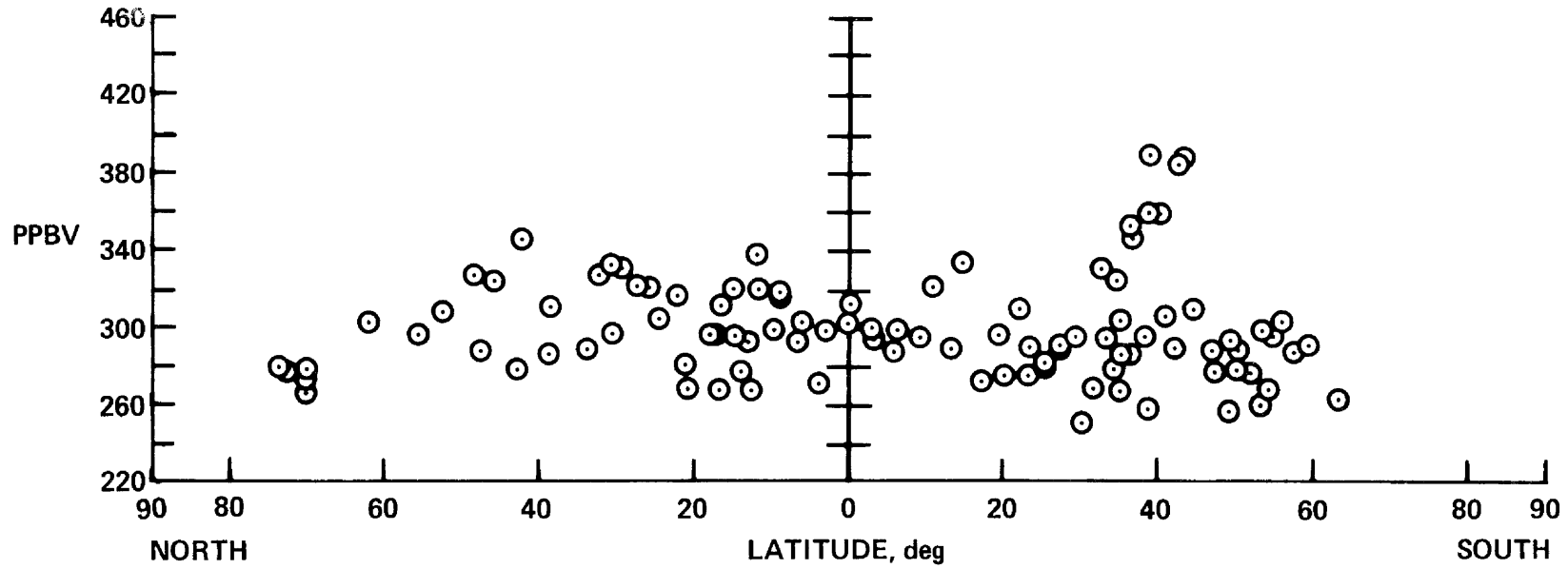

GASP Latitudinal Survey Flight

WSU Preliminary Results

R. A. Rasmussen & J. Krasnec
Air Pollution Research Section
Chemical Engineering Branch
College of Engineering
Washington State University
Pullman, Washington 99164

OBJECTIVES

The objectives of Washington State University's participation in the GASP Latitudinal Survey flight are:

1. Intercomparison with NASA-Lewis measurements of fluorocarbons scheduled to be collected via their automated flask system and WSU's air canister system.

2. Measure in flight the concentration distributions of fluorocarbons -12, -11, and -113, as well as the chlorocarbons -- chloroform, methyl chloroform, and carbon tetrachloride. Nitrous oxide will also be measured.

3. Collect whole-air samples with WSU's passivated stainless steel air canister collection system for more detailed analysis of the halocarbons; methyl chloride, dichloromethane, carbon tetrachloride, trichloroethylene, and tetrachloroethane. In addition, non-methane hydrocarbon measurements will be made on a selected number of samples.

4. Comparison of the data obtained on the November GASP survey flight will be made with the data obtained during WSU's June 1976 flights between Alaska and New Zealand. The data will also be used as a baseline for comparison with subsequent flights made across the same wide latitudinal zones at later dates.

BACKGROUND

The need for conducting interlaboratory comparisons as cooperative studies was suggested in the discussion panel recommendations of the NBS-NASA-NSF Halocarbon Workshop (Boulder Colorado, March 22-23, 1976) as a means of achieving better data comparisons. Two such cooperative studies are scheduled for the GASP survey flight. The first study is an intercomparison of WSU's manually-operated whole air collection system with NASA-Lewis's automated flask sampling system for fluorocarbon collections. The data will provide a better understanding of the limits of intercomparison related to analysis techniques as well as possible surface adsorption-desorption effects. The second study concerns the joint real time airborne measurement of a selected number of halocarbons using electron-capture gas chromatographs (EC-GC). Both WSU and NASA-Ames have successfully operated their respective EC-GC systems in the test flights of the Convair 990.

In summary, the GASP survey flight provides a unique opportunity to conduct parallel experiments for both real time intercomparisons as well as subsequent laboratory measurements on collected air samples. The exchange of samples between WSU and the NASA-Lewis studies will greatly serve to reinforce the validity of the data obtained through independent analyses and cross-calibrations.

The in-depth analysis of the collected air samples is very important if the more difficult species to measure such as

CH_3Cl, CH_2Cl_2, F-22, F114, $CHCl{=}CCl_2$, and C_2Cl_4 are to be measured accurately. The above species have all been measured in mid- to upper-tropospheric air samples obtained using WSU's air sample canisters in March 1976. The use of a gas chromatograph-mass spectrometer has been necessary to achieve many of these measurements because of the low response of these species to the conventional electron capture detector and their much lower atmospheric concentrations compared to F12, F11, and CCl_4.

Originally the light hydrocarbons C_2 - C_5 (especially ethane, ethylene, and acetylene) were to be measured as analysis and sample priorities allowed. However, because of the recent interpretations of preliminary WSU data for measureable amounts of the C_2 hydrocarbons (especially ethane) in the lower stratosphere, a concerted effort will be made to make careful hydrocarbon measurements. It is possible that ethane may be as effective as methane in terminating chlorine reactions in the stratosphere at a concentration of 0.5 to 1 ppb.

The need to compare WSU cross equatorial trans-Pacific flight halocarbon measurements with the present GASP latitudinal survey flight over the same flight route is believed to be very important. The need for repetitive halocarbon concentration distribution profiles of an interhemispheric nature is critical in determining the possible fate of the fluorocarbons in the troposphere. The closeness in time between the two flights is sufficient to enable WSU to compare with high precision the GASP November data with WSU's June data. This is possible by using

the same calibration gases used for the June expedition. Preliminary in-house results suggest that a $\pm$ 2% relative precision has been maintained using the same calibration gas over a six-month period. This type of precision has not been available to previous halocarbon measurements studying the temporal or latitudinal variation in the atmospheric concentration distributions of the halocarbons. The opportunity to apply this high-precision calibration for comparing fluorocarbon measurements over a six-month period for interhemispheric measurements is believed to be a very important reason for joining the experiment.

EXPERIMENTAL DESCRIPTION

WSU Instrumentation Installed in Convair 990

1. A commercial PE 3920 electron capture-gas chromatograph with dual channels dedicated to real-time automated atmospheric analysis of nitrous oxide and halocarbons.
2. WSU's whole-air pressurized sample collection system operated for the collection of large-volume samples (6 ℓ) for subsequent laboratory study.
3. Dedicated ram air probe designed for a high volume flow split between EC-GC sample needs and whole-air sample collections.
4. Special rack configurations were built to accommodate WSU's air sampling canisters.

AIRCRAFT SPACE REQUIREMENTS

A. Upright Rack (standard type)

1. Constant-Pressure sampling system. (two shelves)
2. WSU Canisters, 60 cans assigned to the survey flight. Twelve canisters available per flight leg in one rack. Replacement cans carried in cargo for resupply needs.
3. Recorders (2), HP 7127, rack mountable.
4. Weight items 1 through 3, 400 pounds.

B. Special Low Boy Rack

1. Bench shock-mounted for PE 3920 dual-channel gas chromatograph. Dimensions 30 inches x 60 inches, support weight of 220 pounds on shock mounts.
2. Cylinder support for inert Argon carrier gas and calibration gas cylinder.
3. Weight items 1 and 2, 400 pounds.

RESULTS

The GASP Latitudinal Survey Flight took place in the latter part of October through Mid-November 1976. The area covered was from 76°N to 62°S. There were fifteen research flights lasting typically 5-6 hrs. each. The flight altitudes were generally between 31,000 to 35,000 ft. with some vertical profiles made as low as 1500 ft. On several occasions (extreme northern and southern latitudes) the tropopause was penetrated for periods of a few hours allowing the lower stratosphere to be studied. During the survey flight WSU collected 75 air samples for halo-

carbon and hydrocarbon analyses and made 100 real-time halocarbon and N_2O measurements with the electron capture-gas chromatograph installed on the aircraft.

The data obtained from both the real-time analyses and the air samples collected appears to be valid. That is, no contamination problems are apparent in the data. In this sense the flight was very successful because in many of WSU previous flights intermittent on-line contamination has been a problem. This is especially true when many different experiments are being conducted on board the aircraft from the same manifold. The separate ram air intake probe dedicated to WSU's sole use is probably responsible for maintaining the integrity of the air sampling system. Two operational problems were encountered that while serious did not adversely affect the overall achievement of the project's objectives. The first problem was the need to isolate the electron capture detectors from responding to changes in the cabin pressure. This was accomplished during the extended lay-over in Hawaii. Beginning with flight leg #7 the real-time EC-GC analyses provided data that could be reliably standardized during the flight against WSU's calibration air at the beginning, middle and end of the flight profiles. In this way the relative accuracy and precision of the analyses could be maintained within and between subsequent flights.

The second operational problem was an electrical short in the gas chromatograph's amplifier experienced just before take-off on the flight #11 between Melbourne, Aust. and Christchurch,

N.Z. This resulted in WSU's science package including the air sampling system being inoperative. This is the only leg of the flight where WSU was not able to obtain data. The resourcefulness of Mr. S. Ferguson, Head of the Electronics Shop in the Chemistry Department of the University of Canterbury in Christchurch, N.Z. resulted in the problem being identified and repaired in time to continue the real-time EC-GC analyses on the subsequent return flight legs to CONUS.

The intercomparison of halocarbon data was accomplished in a special interlaboratory exchange of calibration gases during the layover in Melbourne, Aust. Dr. P. S. Fraser of CSIRO participated in this study with WSU and the NASA-Ames scientists. The results are shown in table 1. The results show only small differences between laboratories which is important as further indepth comparisons of the data obtained on the local flight #9 out of Melbourne in which CSIRO participated is planned.

While it is too soon after the flight to submit a complete documentation of the data obtained there are several conclusions that can be made.

1. The fluorocarbon-12 and 11 concentration distributions obtained on the GASP flight are consistent with the data obtained on WSU's earlier Cross Equatorial Trans-Pacific flights from 80°N to 60°S. Both data sets indicate a much smaller interhemispheric difference than expected. The present difference indicated is only 10-12%. In addition, no steep gradient for F-12 and F-11 was observed in the

northern hemisphere from 70°N to the equator. Likewise, neither was there a marked falloff in the F-12 and F-11 concentrations through the intertropical convergence zone (ITCZ). Rather the data show a homogeneous concentration distribution for the northern hemisphere and a gradual decrease in the fluorocarbons from the ITCZ (8°N) through to 33°S. The smaller-than-expected difference observed in these data would indicate that the world's atmosphere is mixing more quickly and more efficiently than previously thought. It also suggests that pollutants are spread more easily than presently modeled across the world.

2. No interhemispheric differences were observed for the concentration distributions of N_2O (330 ± 3 ppb).

3. The data presented in table 2 are from the analyses of the air samples collected between 32°N to 60°S. These data are given rather than the results for the real-time EC-GC analysis because better precision was obtained from the analysis of the collected samples than from the real-time measurements. The GASP latitudinal flight showed conclusively that while the potential value of the EC-GC for airborne real-time measurements is considerable, the precision of the method is not adequate in its present state of development to show the small differences that exist for the fluorocarbons over the latitudes studied. Therefore, only the results from collected samples are included in this preliminary report.

Figure 1 is a plot of concentration vs. latitude for the data given in table 2. It shows a falloff in the fluorocarbons beginning in the area of the ITCZ and continuing to about 36°S. The tropospheric concentration distribution further southward to 60°S shows no significant further falloff. Likewise, the tropospheric concentrations of the fluorocarbons between 32°N and 12° to 8°N are reasonably stable. The large scatter in the data collected in the vertical flights over Hawaii is shown by the stacked points at 20°N. A summary of the interhemispheric differences observed from the real-time measurements is given in table 3 for comparison.

TABLE 1

CV990 SURVEY FLIGHT INTERLABORATORY CALIBRATION

	F-12 ppt	F-11 ppt	CCl_4 ppt	N_2O ppb
WSU Standard K-3				
WSU Data	238	144	137	330
NASA-Ames Data	235	133	134	295
NASA-Ames Standard				
WSU Data	241	109	--	NM†
NASA-Ames Data	251	106	*	256
CSIRO Standard (VZ608)				
WSU Data	*	248	126	*
NASA-Ames Data	*	261	124	*
CSIRO Data	*	266	103	*
CSIRO Standard (705)				
WSU Data	*	125	64	*
NASA-Ames Data	*	125	57	*
CSIRO Data	*	144	54	*

*Compound not included in the standard
†Not Measured

Table 2

GASP Convair-990 Flight Collected Samples Data

Date	Altitude feet	Latitude	Longitude	F-11 ppt	F-12 ppt	N_2O ppb
11/1/76	36000	19°35'N	156°57'W	230	138	330
	25000	19°43'	155°30'	233	137	332
	15000	19°43'	155°30'	232	140	328
	11000	20°	155°	235	138	333
	1500	20°04'	155°21'	237	142	333
	6000	20°86'	157°24'	234	140	331
11/3/76	31000	14°30'N	160°05'W	227	138	332
	31000	11°25'	161°15'	227	134	331
11/7/76	31000	09°50'N	161°50'W	227	135	331
	31000	07°55'N	162°47'	228	138	329
	31000	04°55'N	164°40'	222	132	327
	35000	00°04'S	164°00'	225	132	328
	35000	05°05'S	167°27'	222	130	326
	31000	13°02'S	170°20'	221	130	325
11/8/76	31000	20°35'S	179°03'W	220	130	330
	31000	25°05'	174°10'	218	129	329
	35000	29°20'	166°25'	217	128	326
	39000	33°02'	155°30'	212	124	320
	33000	33°42'	152°45'	216	126	328
	22000	36°18'	147°10'	214	127	327
11/11/76	37000	36°53'S	146°12'W	209	122	320
	21000	41°50'	144°32'	220	130	328
	10000	40°50'	144°53'	220	130	327
	39000	40°10'	146°25'	209	120	320
	25000	38°54'	146°	218	132	326
11/14/76	33000	50°05'S	168°37'W	216	126	326
	33000	53°02'	168°50'	218	128	328
	33000	56°10'	169° E	219	129	328
	34000	60°00'	169°35'	218	128	404
	37000	61°20'	171°20'	218	127	328
	39000+	48°12'	172°53'	206+	119+	318+
	39000+	46°00'	171°05'	204+	116+	317+
	23000	44°15'	171°46'	216	127	327
	6500	43°30'	172°22'	217	126	335

+ Lower stratosphere

TABLE 3

INTERHEMISPHERIC DIFFERENCES
REAL-TIME EC-GC MEASUREMENTS
Convair-990 GASP Survey Flight
October 12 - November 19, 1976

Location	Altitude	F-12 ppt	F-11 ppt	$CHCCl_3$ ppt	CCl_4 ppt	N_2O ppb
45°S	35,000'	212	127	88	125	332
47°N	25,000'	238	144	104	137	330
Difference		11%	12%	15%	9%	1%
60°S	37,000'	217	125	94	130	330
64°N	35,000'	244	141	128	143	328
Difference		11%	11%	27%	9%	1%

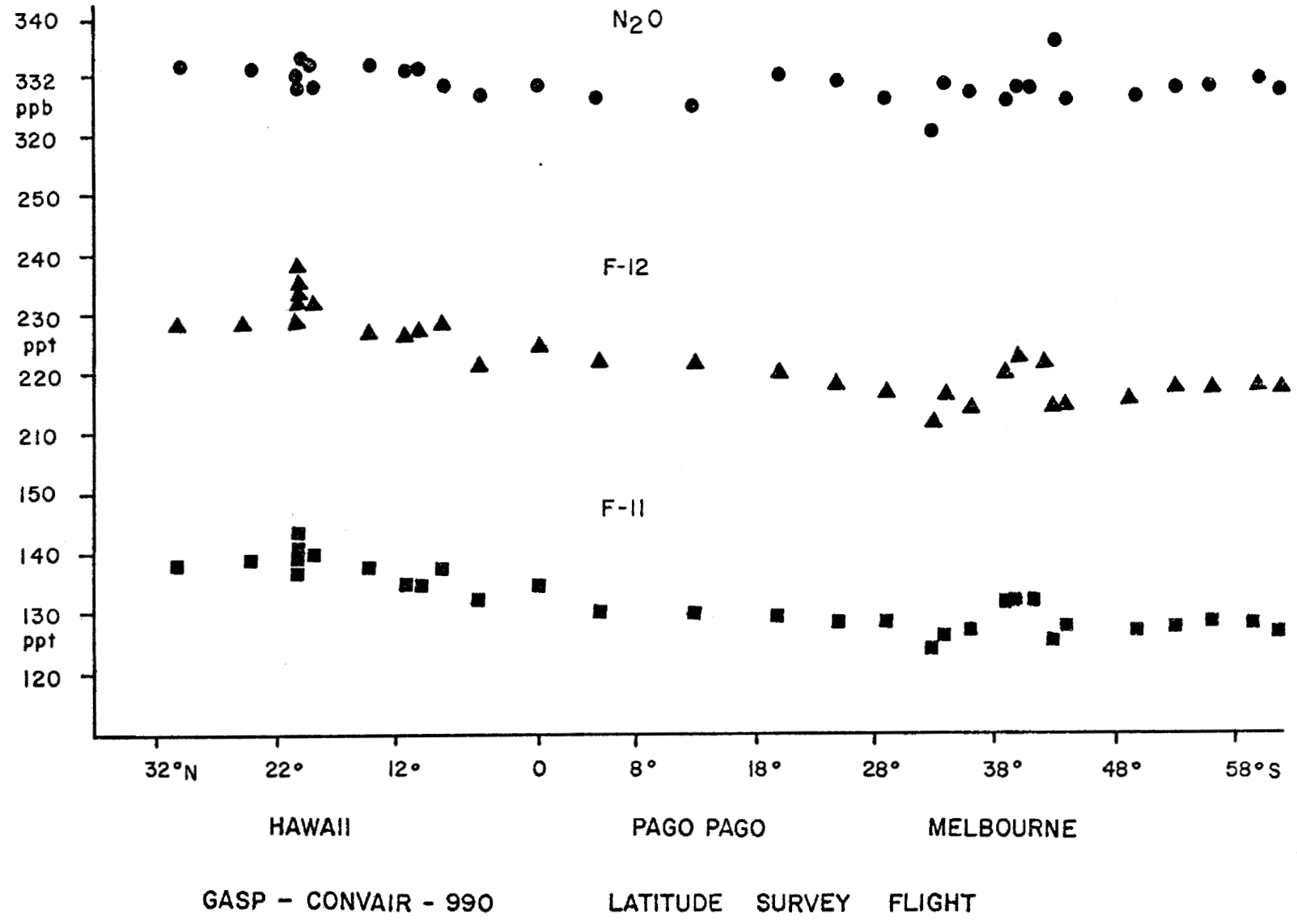
340
332
ppb
320
250
240
230
ppt
220
210
150
140
130
ppt
120
N2O
F-12
F-11
32°N
22°
12°
0
8°
18°
28°
38°
48°
58°S
HAWAII
PAGO PAGO
MELBOURNE
GASP – CONVAIR - 990 LATITUDE SURVEY FLIGHT

Figure 1.

BRIEF REPORT ON RADIATION DOSE RATE MEASUREMENTS DURING THE 1976 LATITUDE SURVEY MISSION

J. E. Hewitt,[1] C. A. Syvertson,[1] L. Hughes,[1] R. H. Thomas,[2] L. D. Stephens,[2] J. B. McCaslin,[2] A. S. Bunker,[3] and A. B. Tucker[3]

INTRODUCTION

The authors are engaged in a collaborative study to define the flux and energy spectrum of atmospheric neutrons more precisely than has been possible in the past. Discrepancies between theoretical calculations and experimental data exist in the literature. In particular, there is uncertainty about the fraction of the total neutron spectrum which lies between 1 and 15 MeV. This energy range is particularly important for dosimetry purposes since it contributes most of the neutron dose to aircraft passengers.

The neutron flux is sensitive to geomagnetic latitude, altitude, and time in the solar cycle. Our purpose in the present series of flights was to measure the latitude effect over a large span of latitudes within a reasonably short period of time. In addition, we wished to compare the results with the effect of latitude on the ionizing component of the cosmic ray secondaries.

INSTRUMENTATION

Because of restricted space we decided to measure only the intensity of the neutron component, using a moderated BF_3 proportional counter. The more complete neutron spectrum analysis would have required flying a set of large

---

[1]Ames Research Center, Moffett Field, CA 94035

[2]Health Physics Dept., Lawrence Berkeley Laboratory, University of California, Berkeley, CA 94720

[3]Physics Dept., San Jose State University, San Jose, CA 95192

Bonner spheres and a liquid scintillation detector. However, we expect to be able to relate the BF_3 readings closely to the total spectrum at a later time. The counter used in the experiment is 5.1 cm in diameter by 22.9 cm active length. It is filled with 96% enriched ^{10}B to 20 cm Hg. A 6.4-cm-thick paraffin moderator surrounded by 0.8-mm (0.03-in.) cadmium is used as the jacket for the BF_3 counter and provides a reasonably flat response to 0.02- to 20-MeV neutrons.

A Reuter-Stokes (RSS-111) environmental radiation monitor measured the ionizing component. It is a sensitive gamma-exposure monitoring system designed to measure and record low-level exposure rates such as those due to fallout and natural background radiation at ground level. To measure the higher exposure levels at aircraft altitudes, the instrument was modified by the manufacturer to extend its range to 1000 μR/hr.

The use of the two instruments permitted the simultaneous measurement of the ionizing and neutron components of the secondary cosmic radiation. Together, the instruments act as a crude spectrometer for the primary proton spectrum since their relative response depends on the energy distribution in the spectrum.

PRELIMINARY RESULTS

Figure 1 shows the variation of both the neutron component and the ionizing component as a function of geomagnetic latitude. The data are plotted as a percentage of the highest readings. These were 275 μR/h for the RSS-111 meter and 730 counts/min for the BF_3 neutron counter.

The expected dependence of the dose rates on geomagnetic latitude was obtained. The highest intensities were measured in the polar regions and the lowest at the equator. The greatest changes occurred between 20 to 55 degrees. The readings are symmetric with distance north and south of the geomagnetic equator. The neutron dose rates are more sensitive to latitude changes than those of the

ionizing component. The latter are produced by primaries of high energy which are not easily deflected by the earth's magnetic field.

Altitude profiles from sea level to 39,000 feet were measured at six different latitudes. The dose rates from both components increase exponentially with altitude, as measured in pressure units. The neutron dose rate increases more rapidly.

When all the data have been reduced, the results will be analyzed in terms of the latitude effect to be expected for the time in the solar cycle at which the flight was made. The relationship between the two components will be compared and possible inferences about the primary spectrum will be drawn. Altitude profiles will be plotted and compared. Finally, the variation in the contribution of each component to the total radiation dose and dose-equivalent as a function of latitude will be evaluated.

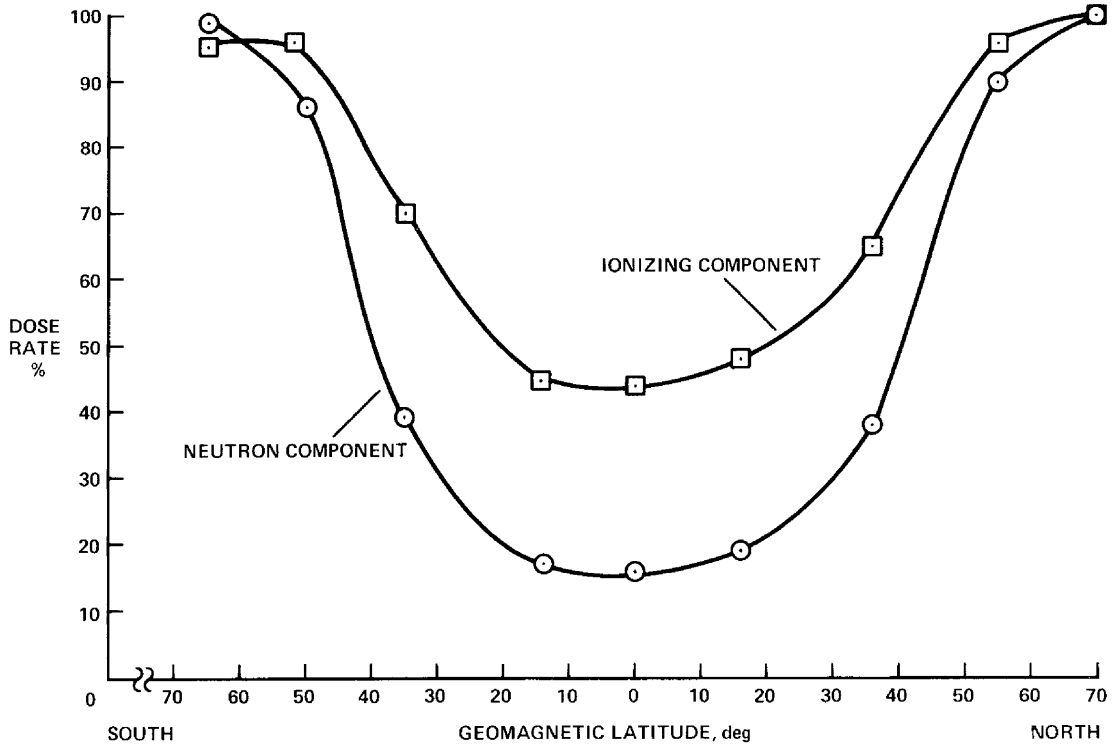

FIGURE 1

PERCENTAGE DOSE RATE VERSUS GEOMAGNETIC LATITUDE AT 33,000 FEET

STRATOSPHERIC HALOCARBON EXPERIMENT

E. C. Y. Inn, J. F. Vedder, B. J. Tyson,
R. B. Brewer, and C. A. Boitnott

NASA Ames Research Center
Moffett Field, CA 94035

INTRODUCTION

In a recent review Rowland and Molina (Ref. 1) discuss the important consequences of the presence of chlorofluoromethanes in the stratosphere. Thus, the predicted catalytic decomposition of stratospheric ozone by Cℓ, produced by photolysis of these halocarbons, may seriously affect the ozone balance in our atmosphere. The intrusion of these anthropogenically released halocarbons into the stratosphere has been demonstrated in sampling measurements reported by a number of investigators (Ref. 2). Stratospheric measurements at various locations are needed to reveal the global distribution of these minor constituents and to monitor the increase in concentration with time.

Halocarbon measurements reported here are made by acquiring stratospheric air samples using a cryogenic trapping method in a sampling system mounted in a U-2 aircraft. In this experiment stratospheric halocarbon concentrations at U-2 altitudes (lower stratosphere) are determined from samples acquired over a wide range of latitude, namely, at about 10^{o}N, 35^{o}N, 60^{o}N, and 80^{o}N, all at about 160^{o}W. A second objective is to determine halocarbon concentrations from samples acquired within the Intertropical Convergence Zone (ITCZ) and to compare these with samples obtained nearby, but outside the ITCZ. A third objective is to make stratospheric measurements that are coordinated, in a rendezvous, with in situ tropospheric measurements from onboard the CV-990 (see section on Atmospheric Halocarbon Experiment). The recovered stratospheric samples are analyzed with a ground-based gas chromatograph optimized to measure $CFC\ell_3$ (Freon 11), $CF_2C\ell_2$ (Freon 12), $C_2F_3C\ell_3$ (Freon 113), $C_2F_4C\ell_2$ (Freon 114), $CC\ell_4$ (carbon tetrachloride), $CH_3CC\ell_3$ (methylchloroform), N_2O (nitrous oxide), and SF_6 (sulfur hexafluoride). Grab samples are also obtained from which CH_4 (methane) is determined.

DESCRIPTION OF EXPERIMENTAL METHOD

The cryogenic sampling system is supported on an aluminum rack that is mounted in the instrument bay (called Q-Bay) of the U-2 aircraft. The Q-Bay is located on the underside of the aircraft and just aft of the pilot compartment. A schematic diagram of the sampling system is shown in Figure 1. All the plumbing consists of stainless steel parts, except for those noted below. The inlet and outlet tubes, both 2.54 cm in diameter, are mounted with the respective ports located beyond the boundary layer about 25.4 cm from the skin of the aircraft. The sampled air moves under ram pressure through the system, with the air directed to any of the sampling containers, C, depending on the setting of the various valves. The bypass valve, B, is used to flush out the inlet, I, and outlet, O, manifolds. The Venturi meter, M, measures the flow rate, which is

derived from the measured pressure, pressure differential, and temperature of the flowing air through M. Typical flow rates range from 10 to 25 liters/minute.

The sampling technique is a flow-through cryogenic trapping method in which all condensable constituents in the flowing air are retained in the cooled container. Two types of cryogenic samplers are used in this experiment. One consists entirely of stainless steel (about 4 liters), as shown in Figure 2. The other type is shown in Figure 3, consisting of a helical coil of 20-mm-OD pyrex tubing (about 0.5 liters) mounted in a stainless steel container. Liquid nitrogen is the coolant in both types of samplers and, under the conditions maintained in the Q-Bay during flight, the sampler temperature is held to about 68°K. To ensure high trapping efficiency coarse steel wool is packed in the stainless steel samplers, whereas the glass samplers are made with numerous re-entrant dimples. The stainless steel samplers have measured trapping efficiencies greater than 99% and the glass samplers 85%. Thus, in these configurations it is possible to sample a large volume of stratospheric air depending on the flow rate and the duration of flight at altitude (up to about 4 hours).

A gas chromatograph (Hewlett Packard Model 5803) is used in the analysis of the samples acquired during each flight. Dual electron capture detectors are each connected to separate columns; one column (Porosil A) is used for N_2O, SF_6, and Freon 12 determinations, and the second column (DC 200 silicone oil) is used for the remaining constituents (see above). A single sample loop ($5\ cm^3$) is switched from one column to the other during one cycle of complete analysis of all constituents. Methane-argon is used as the carrier gas.

RESULTS

The data on all the trace species analyzed are presented in Table I. Missing entries in the table represent constituents that were not recovered during the gas chromatographic analysis. A conservative estimate of the error in the measurements is 15-20%, except for those with the lowest concentrations. Quantitative recovery of CCl_4 was a problem encountered in these experiments, especially for samples collected in the stainless steel samplers (2 and 3); hence, rather larger errors may be expected. Two values of $CFCl_3$, both from sampler 2, are anomalously low and are most probably a retention problem associated with the stainless steel sampler. In the November 3 flight, the magnetic tape jammed during the collection of the first sample. Therefore, the flows for the other samples on that flight were assumed to be the same as on the November 8 flight, where the conditions were nearly the same. Past experience had shown that the flow on different flights varies little for a given sampler at given altitude. Errors in the reported concentrations arise in the sampling and analysis. Those of sampling originate from measurement of the total volume of sampled air and the collection efficiency of the samplers. The sources of error in gas chromatographic analysis are in the determination of the fraction of the total sample injected into the column and in the calibration using primary and secondary standards. The altitudes in Table I are pressure altitudes based on the 1962 Standard Atmosphere. The U-2 flight tracks during the sampling periods at altitude were nearly linear except for those near 61°N latitude, which were segments of an elongated race track path. The pyrex samplers (1 and 4) were normally opened for about 28 minutes (horizontal distance

360 km) at a sampling rate of 15 S.T.P. liters/minute. The sampling time for the stainless steel samplers (2 and 3) was about 14 minutes (180 km) at a rate of 25 S.T.P. liters/minute. The tabulated latitudes and longitudes are for the midpoints of the sampling track and are probably accurate within a radius of 60 km. Some of the data are presented graphically in Figures 4, 5, 6, and 7. Appropriate data from the CV-990 aircraft mission are also shown.

CONCLUDING REMARKS

The three objectives noted in the introduction were successfully accomplished. The atmospheric samples in the lower stratosphere were collected at five different latitudes from 8°N to about 78°N. The analyses indicate a definite trend of decreasing concentration with increasing latitude at a given altitude as shown in Figure 7. The two flights south of Hawaii (Nov. 3 and 8) reached the ITCZ, centered near $7\frac{1}{2}^{\circ}$N latitude. The cloud cover in the zone was moderate at the time. No significant differences in concentrations near 8°N and 16°N latitude were noted. The flights south from Hawaii were also rendezvous flights with the CV-990 aircraft. On the November 3 flight, the U-2 carried out an overflight above the CV-990 on the southern leg of the rendezvous. However, on November 7, the CV-990 made tropospheric measurements in the region of the ITCZ at about 8°N, whereas the second U-2 flight in this area took place a day later on November 8. The CV-990 results on these rendezvous flights are plotted along with the corresponding U-2 flights in Figures 4, 5, and 6.

REFERENCES

1. Rowland, F. S.; and Molina, M. J.: Chlorofluoromethane in the Environment. Rev. of Geophys., vol. 13, 1975, pp 1-35.

2a. Heidt, L. E.; Lueb, R.; Pollock, W.; and Ehhalt, D. H.: Stratospheric Profiles of CCl_3F and CCl_2F_2. Geophys. Res. Lett., vol. 2, 1975, pp 445-447.

b. Schmeltekopf, A. L.; Goldan, P. O.; Henderson, W. R.; Harrop, W. J.; Thompson, T. L.; Fehsenfeld, F. C.; Schiff, H. I.; Crutzen, P. J.; Isaksen, I. S. A.; and Ferguson, E. E.: Measurements of Stratospheric CCl_3F, CCl_2F_2, and N_2O. Geophys. Res. Lett., vol. 2, 1975, pp 393-396.

c. Krey, P. W.; Lagomarsino, R. J.; and Frey, J. J.: Stratospheric Concentrations of CCl_3F in 1974. J. Geophys. Res., vol. 81, 1976, pp 1557-1560.

TABLE I

MIXING RATIOS FROM U-2 SAMPLING FLIGHTS- FALL, 1976

Date 1976	Sampler	Vol (ℓ)	Alt. (km)	Lat. N	Long. W	CO_2 ppmv	N_2O ppbv	CF_2Cl_2 pptv	$CFCl_3$ pptv	CCl_4 pptv	$C_2F_4Cl_2$ pptv	$C_2F_3Cl_3$ pptv	CH_3CCl_3 pptv	SF_6 pptv	CH_4 ppm
1 Oct	4	365	21.3	73.5	156.5	320	155	60	7.0	4.7	2.6	3.4	1.5	--	
	3	397	20.7	78.0	156.5	298	140	62	7.4	3.0	2.6	2.5	5.6	--	
	1	447	15.2	77.5	156.5	274	240	140	65	91	7.8	15.5	32	0.3	
	2	335	12.2	74.0	156.5	342	286	216	10.1	--	4.9	--	--	--	
	G														1.0
8 Oct	4	358	21.3	61.0	156.5	283	128	52	5.5	4.1	3.0	3.0	8.9	--	
	2	501	18.3	60.5	156.5	291	210	129	29	4.9	3.5	1.8	0.4	--	
	1[a]	452	15.2	60.5	156.5	--	--	--	--						
	G														1.2
14 Nov	1	298	21.3	29.5	158.0	305	232	136	38	40	4.2	4.1	0.7	--	
	3	342	21.3	33.0	158.0	289	205	125	31	12	4.2	3.9	3.8	--	
	2	280	18.3	33.0	158.0	293	271	177	16	--	4.6	--	--	--	
	4	324	15.2	30.0	158.0	308	303	224	106	89	7.6	10.4	35	0.4	
	G														1.0
3 Nov	1[b]	284	21.3	9.0	160.0	321	290	201	86	70	6.6	9.7	1.1	0.3	
	3[c]	--	21.3	16.0	159.5	--	--	--	--	--	--	--	--	--	
	4[b]	441	18.3	8.0	159.0	285	278	194	91	81	6.7	8.5	34	0.4	
	2	469	18.3	16.0	159.5	334	305	221	68	3.7	5.4	2.4	--	--	
	G														1.25
8 Nov	1	305	21.3	8.0	162.0	300	286	167	63	67	5.6	6.5	17	0.2	
	3	344	21.3	16.0	159.5	303	258	169	60	34	5.3	5.8	9	--	
	4	530	18.3	7.0	162.5	291	280	178	96	79	5.4	8.6	30	0.3	
	2	330	18.3	16.5	159.5	316	304	221	71	16	5.7	3.2	3.4	--	
	G														1.1

a Sampler developed a leak during analysis.

b Data system failed; flow estimated from similar samplings.

c Cryogen lost prior to completion of sampling.

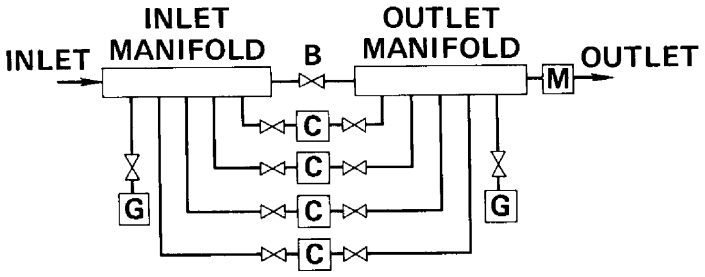

FIGURE 1. CRYOGENIC SAMPLING SYSTEM

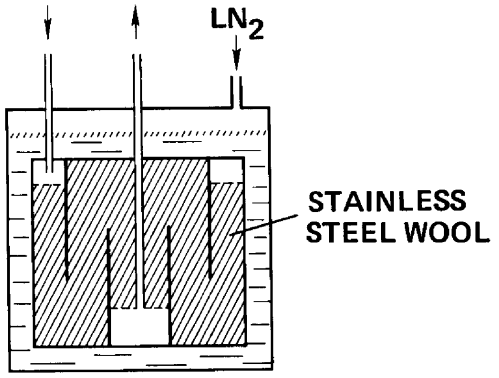

FIGURE 2. STAINLESS STEEL CRYOGENIC SAMPLER

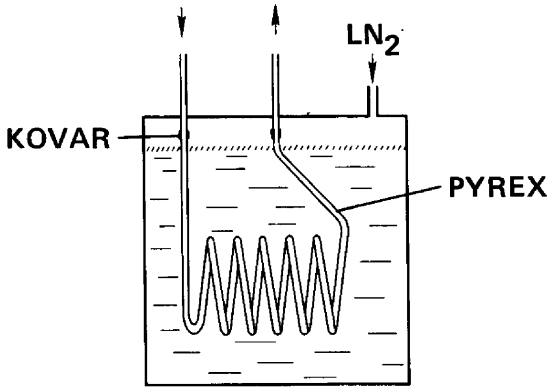

FIGURE 3. PYREX CRYOGENIC SAMPLER

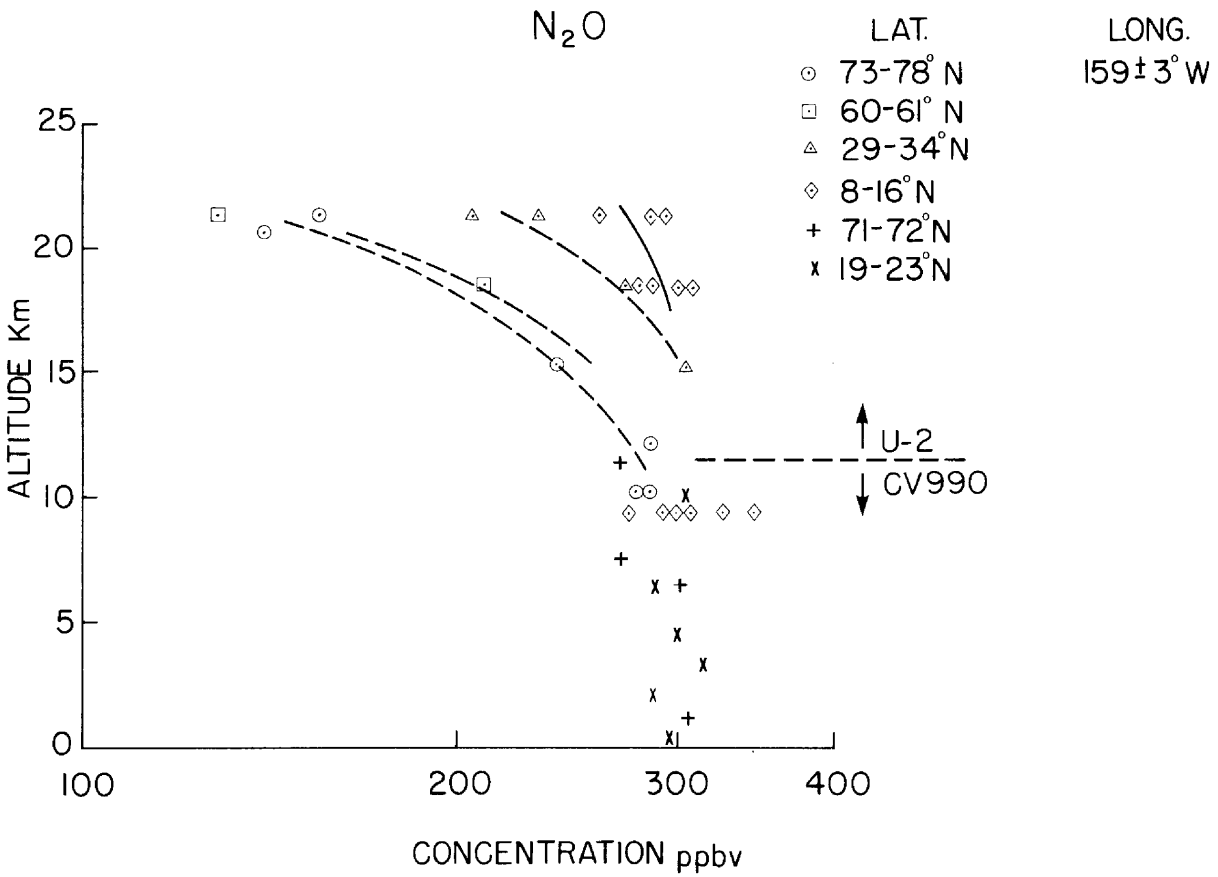

FIGURE 4. ALTITUDE AND LATITUDE DEPENDENCE OF N_2O

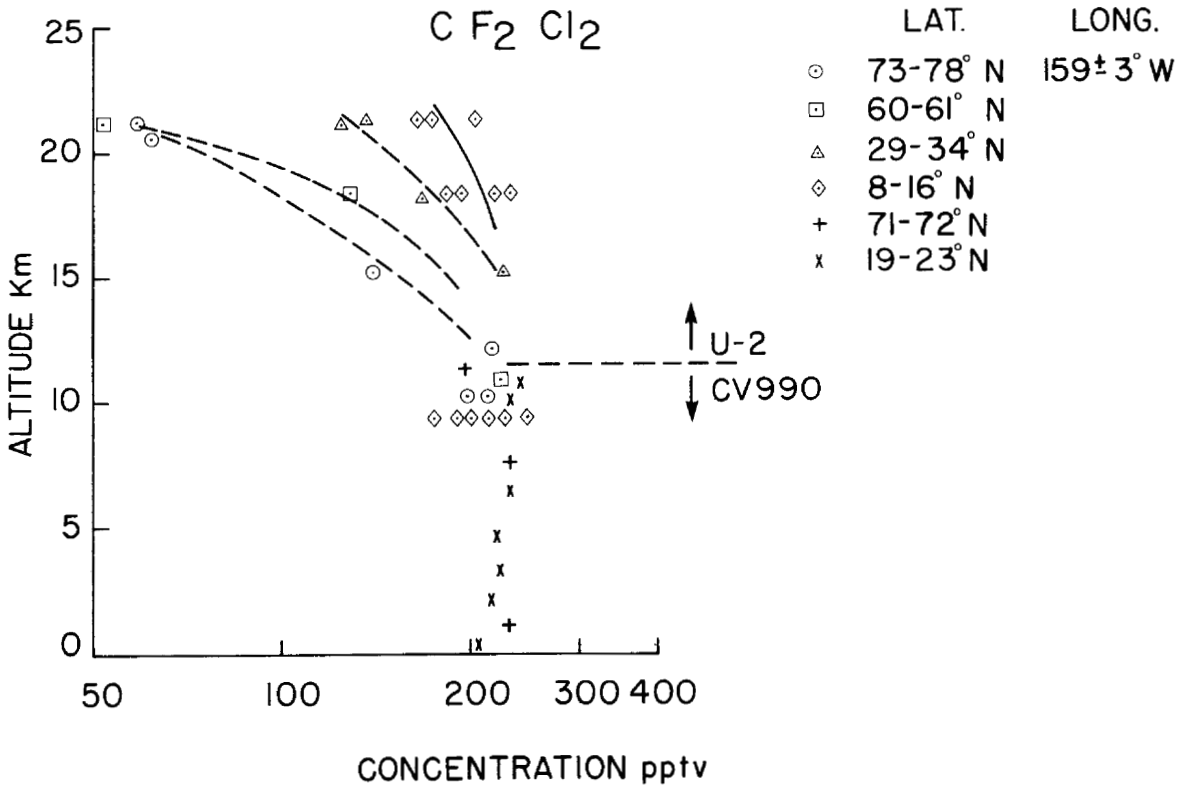

FIGURE 5. ALTITUDE AND LATITUDE DEPENDENCE OF CF_2Cl_2

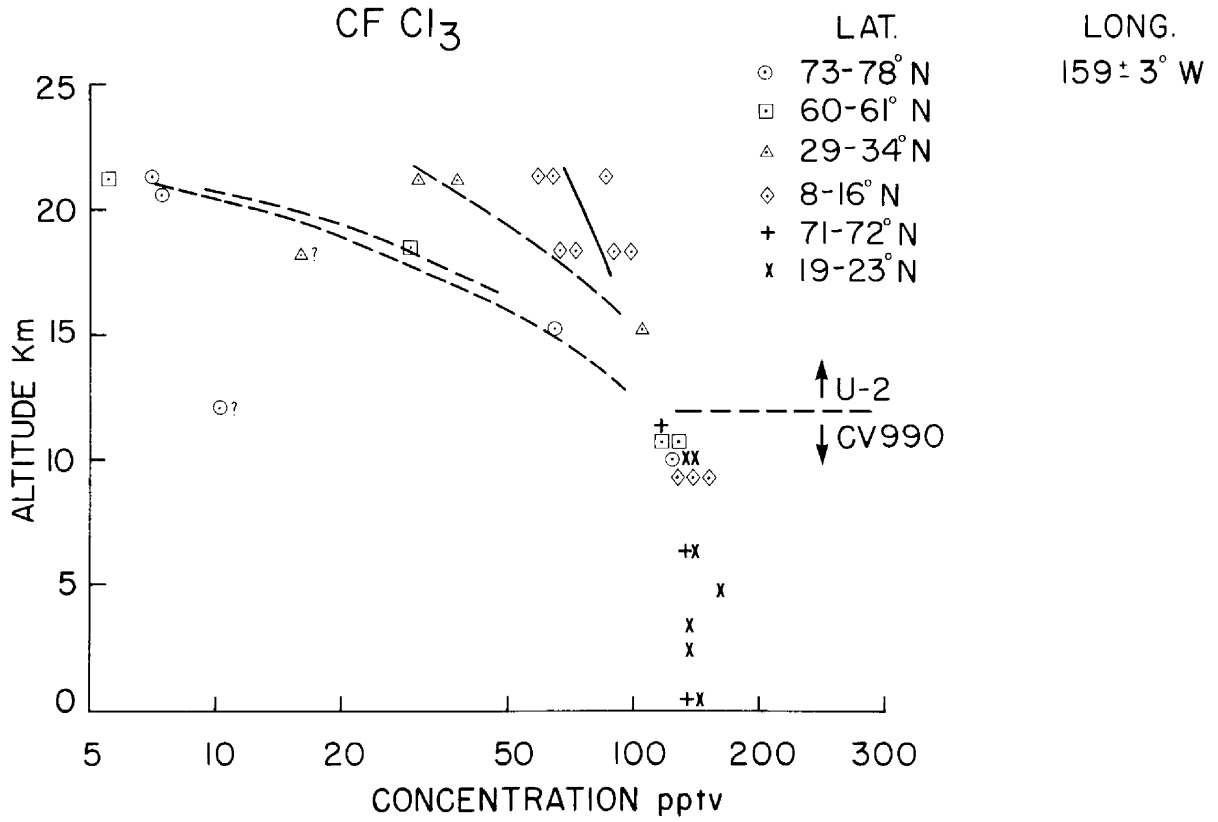

FIGURE 6. ALTITUDE AND LATITUDE DEPENDENCE OF $CF Cl_3$

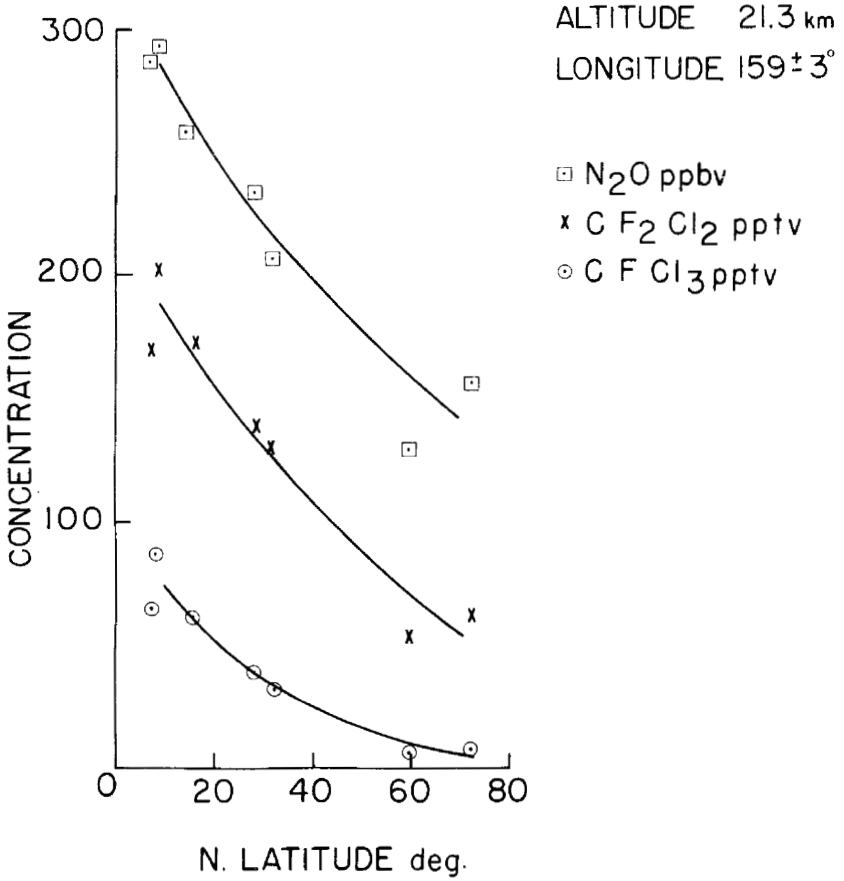

FIGURE 7. LATITUDE DEPENDENCE OF N_2O, CF_2Cl_2 AND $CFCl_3$

COLLECTION AND ANALYSIS OF STRATOSPHERIC AEROSOLS

by

Guy V. Ferry and Neil H. Farlow
NASA Ames Research Center
Moffett Field, CA 94035

and

Homer Y. Lem and Dennis M. Hayes
LFE Corporation
Richmond, CA 94804

SUMMARY

Stratospheric aerosols were collected by a U-2 aircraft at several altitudes along meridians extending to the north and south through Hawaii and Alaska. Laboratory analyses were made on the samples to obtain particle size distributions and concentrations versus altitude and location, physical state information and insoluble nuclei content. These data are presented in this preliminary report and will be compared later with aerosol information obtained from CV 990 aircraft flights at lower altitudes and similar latitudes.

INTRODUCTION

Variations in the size, concentration, and composition of stratospheric aerosols may affect the Earth's climate by changing the absorption and scattering of solar radiation in the lower stratosphere (ref. 1). Long-term studies are underway to determine the variations of aerosol features versus time and location from perturbing events such as volcanic eruptions. Aerosol measurements in the stratosphere are being obtained by U-2 aircraft flights for comparison with those obtained from upper tropospheric flights of the CV 990. This comparison enables assessments to be made of the size-concentration differences in the two regions so modelers can evaluate solar radiation absorption and scattering contributions.

Aerosol particles are being collected on the U-2 aircraft by a device which places collecting surfaces into the airstream below the wing and beyond the boundary layer (ref. 2). The collecting surfaces are specially made thin films supported on electron microscope screens, and thin (75 μm dia.) palladium wires that are carbon coated to prevent spreading of fluid particles. Impaction of aerosol particles larger than 0.1 μm is assured by the aircraft's speed in the stratosphere. Collection surfaces are projected from and returned to a vacuum sealable flight module that is processed before and after flight within the laboratory's class 100 clean room. Because of the sealable module design, the collected samples are returned to the laboratory vacuum sealed from the stratosphere without exposure to moisture in the lower atmosphere. Special treatment of the flight-exposed grids can then be made in controlled environmental chambers.

The carbon-coated wire collector and the two types of thin film collecting surfaces are flown simultaneously. One of the thin film surfaces is a conventional

nitrocellulose film vacuum coated with carbon to add strength. The other is one developed in our laboratory to absorb liquid and soluble materials in collected particles without chemical reaction or recrystallization. This type of collector is used to isolate insoluble nuclei contained in the stratospheric particles. This is done by a polyvinyl alcohol film absorbing soluble portions so they are not visible in the electron microscope. The conventional nitrocellulose film is used to provide unaltered aerosol particles for physical state and electron diffraction studies. Size distributions and concentration measurements are obtained from the carbon-coated palladium wires which are very efficient collectors of all particle sizes.

RESULTS AND DISCUSSION

Stratospheric aerosols were collected from 79° to 7° North latitude using the U-2 aircraft. Table 1 summarizes the geographical locations where each sample was obtained as well as the altitude and collection date. In addition, pertinent data about insoluble nuclei and aerosol concentrations, as discussed below, are shown. Each collection provided sufficient data to construct particle size concentration curves for each altitude and location, and information on the physical state and nuclei content of the particles. These results are presented in the following sections.

Particle Concentration-Size Distributions. Particle concentration-size distributions for several altitudes are compared in figure 1 to see if there is any trend in the concentration-size distributions at northern latitudes. Figure 2 compares distributions at temperate latitudes, and figure 3 compares them for tropical latitudes. Because there is considerable variation not only in the shapes of the curves but also in the magnitude of the collections, no general trend of altitude dependence is apparent in any of the latitude ranges.

To see if the particle concentration-size distributions vary with latitude at a given altitude, the distributions at different latitudes are compared for 12, 15, 18, and 21 km altitudes in figures 4, 5, 6, and 7. Again, no general trend in the data is apparent.

The wide variation in concentration-size distributions from day to day at the same altitude or latitude tends to obscure any general trends. However, a comparison of the total concentration of particles collected at the various altitudes and latitudes (see table 1) permit three generalizations.

First, although there is considerable variation in day to day data or even in data collected on the same day, the collections made at 18 km altitude typically have higher particle concentrations than collections made at other altitudes.

Second, the aerosol layer occurs at lower altitudes in polar regions. Collections made at 12 km altitude and 75°N latitude and at 15 km and 79°N showed unusually high concentrations of particles. On the other hand, a collection made at 18 km and 65°N showed no particles. While occasional collections with few or no particles have been made in the past as well as during this set of collections, this was the first such collection at 18 km. It seems significant that it was made in an area that shows high concentrations of particles at unusually low altitudes.

Third, the greatest concentrations of particles appear to occur at tropical latitudes. More particles were found on surfaces exposed at 18 km altitude and 7° and 8°N latitude than on any other collection in this series. In addition, for 21 km altitude, the number of particles collected was greater at 8°N latitude than any other latitude at that altitude.

These results are consistent with current circulation models which indicate upwelling into the stratosphere near the equator and circulation of stratospheric air down into the troposphere at the poles. Because of the high variability of particle concentrations, these conclusions must be tentative and more measurements of particle concentrations should be made at both high and low latitudes.

Physical State and Insoluble Nuclei. The physical state of the particles is best observed on the nonabsorbing nitrocellulose films. On these films in the electron microscope, the particles appear to be composed of a somewhat volatile slurry mixture of crystalline-like material in a liquid matrix. Variations in the relative amounts of liquid at different times cause changes in particle fluidity. Although all particles contain a significant portion of the crystalline material, they are fluid in the atmosphere in the altitude range 12 to 20 km and are physically similar at all geographic locations from latitude 79°N to 7°N. No evidence of frozen particles has been found even at low stratospheric temperatures. Examples of these particles are seen in figure 8. These results are similar to those obtained from previous U-2 and balloon flights that extended over wider geographic and altitude ranges (ref. 3).

Insoluble nuclei are found, on the average, in less than half of the aerosol particles that have been absorbed into the soluble polyvinyl alcohol films (see table 1). This supports the conclusions found in a previous study of these nuclei (ref. 3). In that study, the data indicated such nuclei were probably not active nucleating agents for stratospheric aerosol formation. Rather, hypotheses that suggest nucleation on soluble sulfate crystals or by gas phase reactions are more likely. Furthermore, as in the former study (ref. 3), we find that the nuclei listed in table 1 usually contain only the elements sulfur and sodium or undetectable light elements ($Z < Na$). As before, we conclude that volcanic silicate ash is not a typical component of stratospheric aerosols except, perhaps, during a brief time after a major eruption.

However, some differences in the nuclei count were found in these present samples compared to the earlier study. Several collections contained insoluble nuclei in every slurry particle (see table 1, samples C-46, C-47, and C-41). And an average of a little less than one-half of the slurry particles contained some nuclei in the present study, whereas only one-third did in the former one. Whether these features represent a significant change in stratospheric conditions or merely a statistical variation is not known.

The appearances of the nuclei (fig. 8) are not substantially different than those observed before. Again we have the single nucleus which is centered in the soluble particle spread area in the PVA film (figs. 9a, 9b), and also the multi-nuclei configurations (figs. 9c, 9d); and the needle-like artifacts (figs. 9e, 9f). Therefore, we feel these collections are substantially the same as those we have made before, with perhaps some small statistical variations influencing the nuclei population.

As before, the cause of the needle-like artifacts in the PVA film is not known (figs. 9e, 9f). One conjecture is that the crystals form in the PVA film from a slurry particle solution that becomes saturated as the film dries. We have found an example, however, where needle-like crystals are visible in an unabsorbed slurry particle on a nitrocellulose film (fig. 8e). These needle-like crystals can be compared with those in figure 9f (PVA film) as both collections were made simultaneously (sample C-51, table 1). Usually, however, such needle crystals are not visible in slurry particles on nitrocellulose films. For example, particles in figures 9e (PVA film) and 8d (nitrocellulose film) were collected simultaneously (sample C-56) but only the PVA film exhibited needle-like artifacts. Thus conclusions about these artifacts must await more detailed analyses.

No obvious differences can be seen between collections at northern latitudes and those near the equator, but there is a tendency for particles collected at higher altitudes to contain more liquid and fewer nuclei per slurry particle. This trend seems more apparent at northern latitudes than at southern locations. However, the sampling is too small to merit positive conclusions.

REFERENCES

1. Pollack, J. B.; Toon, O. B.; Sagan, C.; Summers, A.; Baldwin, B.; and Van Camp, W.: Volcanic Explosions and Climatic Change: A Theoretical Assessment. J. Geophys. Res., vol. 81, 1976, pp. 1071-1083.

2. Ferry, G. V.; and Lem, H. Y.: Aerosols at 20 Km Altitude. Presented at the Second Conference on Environmental Impact of Aerospace Operations in the High Atmosphere, Am. Meteorol. Soc., San Diego, CA, 1974.

3. Farlow, N. H.; Hayes, D. M.; and Lem, H. Y.: Insoluble Nuclei in Stratospheric Aerosols. Poster paper, Intnl. Conf. on the Stratosphere and Related Problems, Utah State Univ., Logan, UT, September 15-17, 1976.

TABLE 1. SUMMARY OF 1 MIN. AEROSOL COLLECTIONS AT VARIOUS LOCATIONS AND ALTITUDES

Sample Number	Location (Lat. °N-Long. °W)		Altitude (km)	Collection Date	Aerosol Concentration (No/cm^3)	Aerosols with Nuclei		
						No. Particles/ Grid Opening	Number with Nuclei	Fraction with Nuclei
C-43	75	157	12	1 Oct 76	4.13	62	22	0.35
C-46	65	147	12	29 Sept 76	1.43	12	12	1.00
C-37	37	122	12	18 Oct 76	---	10	0	0
C-67	37	122	11	2 Dec 76	0	--	0	0
C-63	21	158	12	5 Nov 76	0	--	--	---
C-44	79	157	15	1 Oct 76	3.20	50	36	.72
C-47	65	147	15	29 Sept 76	2.12	20	20	1.00
C-38	37	122	15	18 Oct 76	---	39	11	.28
C-66	37	122	15	2 Dec 76	---	21	6	.29
C-50	31	158	15	14 Nov 76	0.32	--	--	---
C-51	21	158	15	2 Nov 76	0.70	--	--	---
C-56	21	158	15	3 Nov 76	2.70	36	--	---
C-48	65	147	18	29 Sept 76	0	--	--	---
C-58	52	128	18	28 Sept 76	2.23	81	30	.37
C-57	52	128	18	28 Sept 76	2.41	53	8	.15
C-42	51	128	18	11 Oct 76	3.28	58	24	.41
C-41	51	128	18	11 Oct 76	2.67	17	17	1.00
C-39	37	122	18	18 Oct 76	---	--	--	---
C-65	37	122	18	2 Dec 76	---	48	9	.19
C-49	34	158	18	14 Nov 76	4.19	--	--	---
C-52	21	158	18	2 Nov 76	2.07	15	3	.20
C-54	8	158	18	5 Nov 76	7.68	25	--	---
C-62	7	158	18	3 Nov 76	5.97	--	--	---
C-59	53	130	21	28 Sept 76	1.45	75	46	.61
C-61	34	158	21	14 Nov 76	1.25	--	--	---
C-60	21	158	21	2 Nov 76	2.36	23	7	.30
C-53	8	158	21	5 Nov 76	2.58	--	--	---
C-55	7	158	21	3 Nov 76	---	--	--	---

PARTICLE CONCENTRATION-SIZE DISTRIBUTIONS AT NORTHERN LATITUDES

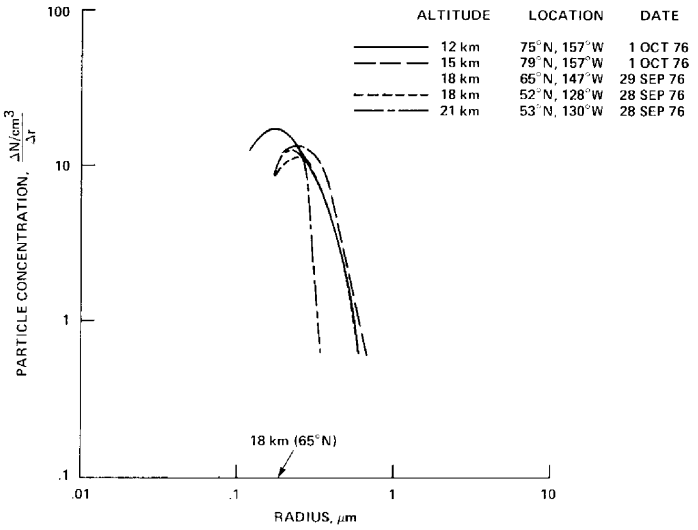

FIGURE 1

PARTICLE CONCENTRATION-SIZE DISTRIBUTIONS AT TEMPERATE LATITUDES

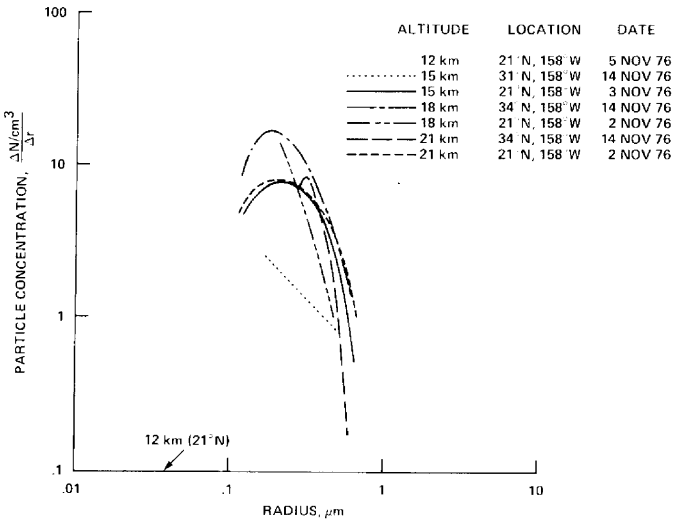

FIGURE 2

PARTICLE CONCENTRATION - SIZE DISTRIBUTIONS AT TROPICAL LATITUDES

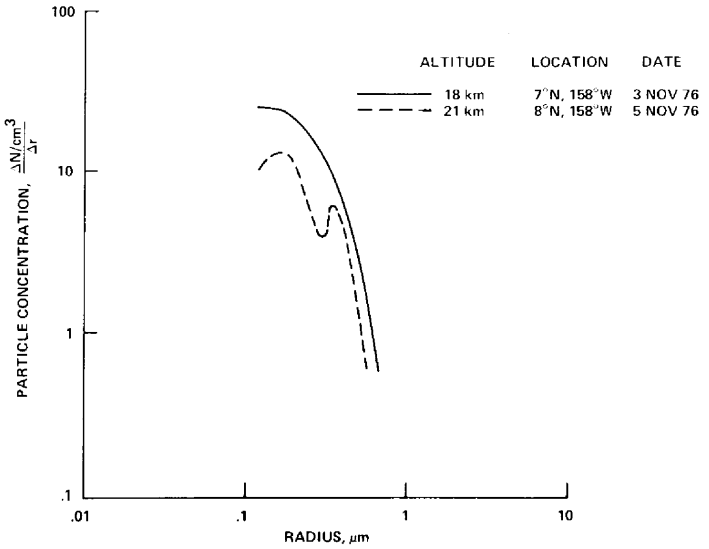

FIGURE 3

PARTICLE CONCENTRATION-SIZE DISTRIBUTIONS AT 12km ALTITUDE

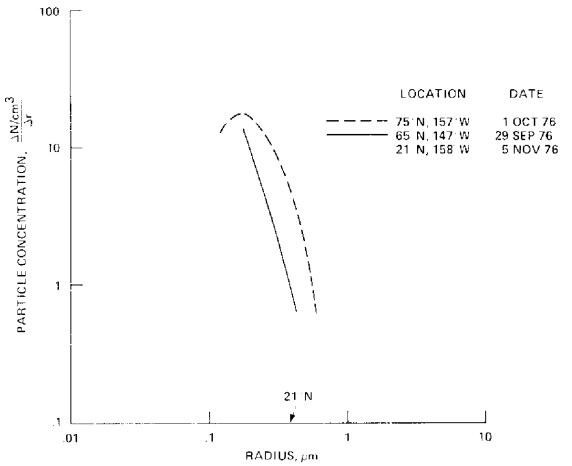

FIGURE 4

PARTICLE CONCENTRATION-SIZE DISTRIBUTIONS AT 15km ALTITUDE

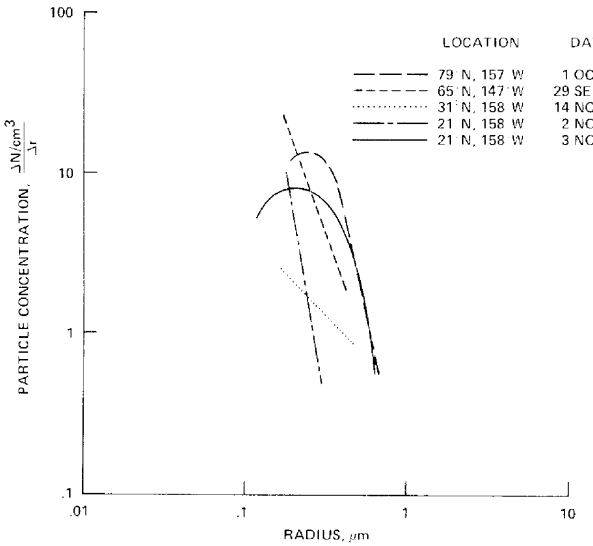

FIGURE 5

PARTICLE CONCENTRATION-SIZE DISTRIBUTIONS AT 18km ALTITUDE

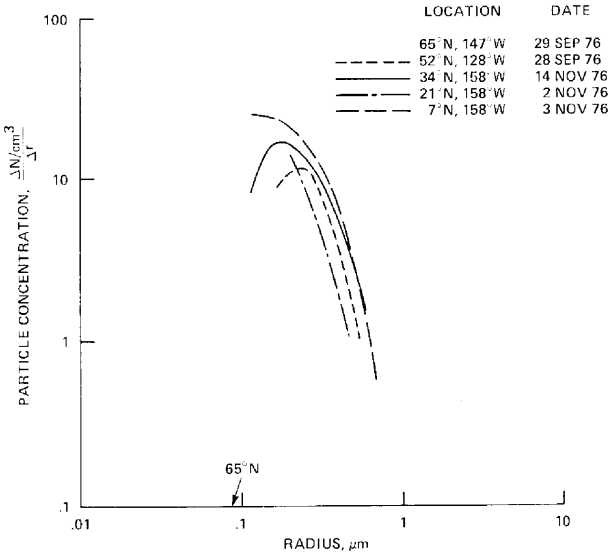

FIGURE 6

PARTICLE CONCENTRATION-SIZE DISTRIBUTIONS AT 21km ALTITUDE

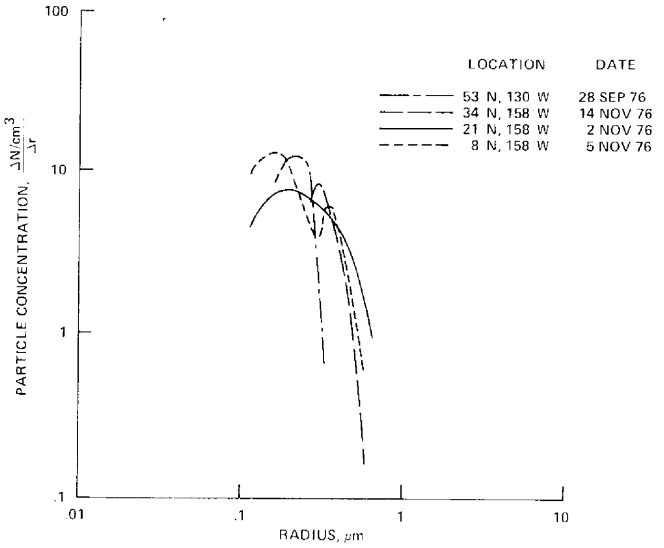

FIGURE 7

STRATOSPHERIC AEROSOL PARTICLES ON NITROCELLULOSE FILMS

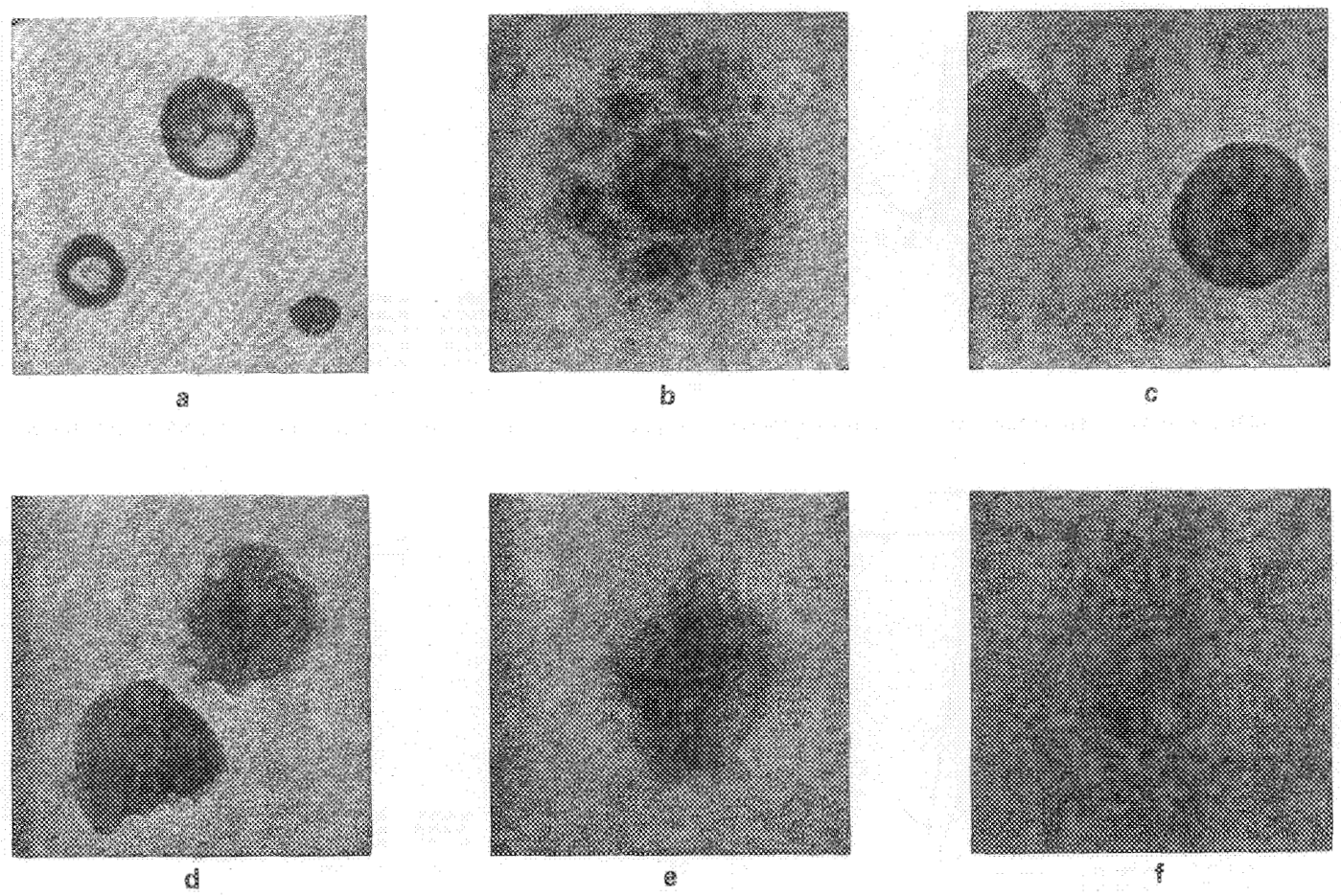

Figure 8. Stratospheric aerosol particles on nitrocellulose films showing fluid and crystalline features. (a) C-43:75°N, 157°W; (b) C-41:51°N, 128°W; (c) C-46:65°N, 147°W; (d) C-56:21°N, 158°W; (e) C-51:21°N, 158°W; (f) C-66: 37°N, 122°W. Diameters of circular areas are 1-2 μm.

STRATOSPHERIC AEROSOL PARTICLES DISSOLVED IN POLYVINYL ALCOHOL FILMS

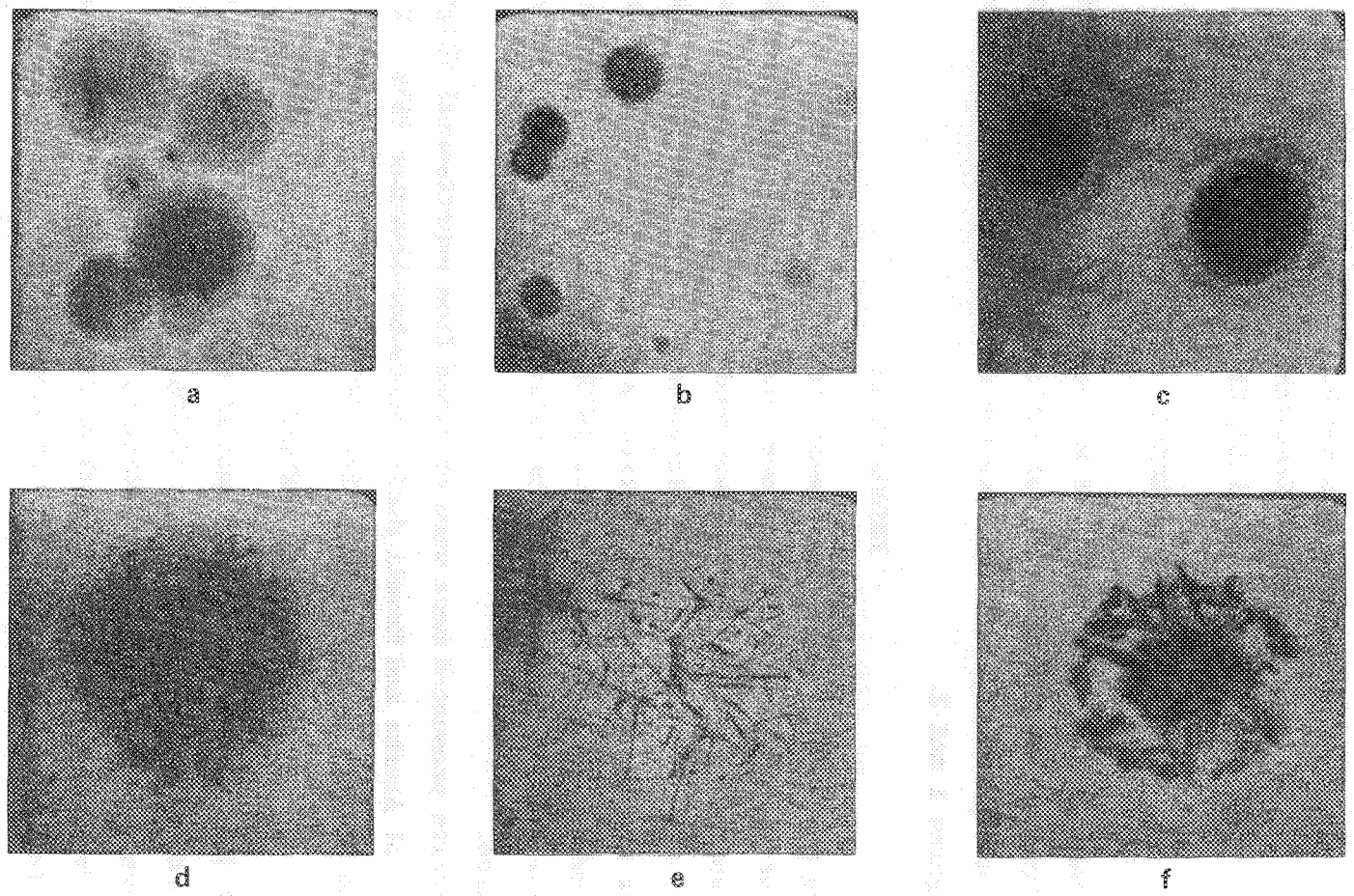

Figure 9. Stratospheric aerosol particles dissolved in polyvinyl alcohol films showing undissolved nuclei and needle-like artifacts. (a) C-39:37°N, 122°W; (b) C-44:79°N, 157°W; (c) C-46:65°N, 147°W; (d) C-50:31°N, 158°W; (e) C-56:21°N, 158°W; (f) C-51:21°N, 158°W. Nuclei are 0.1 - 0.3 μm.

MEASUREMENTS OF O_3 AND NO AT 18.3 AND 21.3 KM IN THE VICINITY OF ALASKA AND HAWAII, SEPTEMBER-NOVEMBER 1976

by

M. Loewenstein and W. L. Starr

NASA-Ames Research Center

Moffett Field, CA 94035

SUMMARY

Meridional measurements of O_3 and NO, concentrations were carried out in September, October and November 1976 at altitudes of 18.3 and 21.3 km, using in-situ measuring techniques. The observed mixing ratios vs latitude are shown in figures 1 and 2.

INTRODUCTION

In this preliminary report we present the latest results of a continuing program undertaken to determine the lower stratospheric mixing ratios of O_3 and NO as functions of latitude. Measurements are made in-situ by instruments carried on a U-2 aircraft flying at altitudes up to 21.3 km. The chemiluminescence-type sensor used for both species is similar to the NO sensor described elsewhere (Loewenstein, et al., 1975). The O_3 sensor is identical to the NO sensor with the exception of the role reversal of the detected and reactant gases.

The results presented here were obtained from experimental flights in the vicinity of Alaska and Hawaii during September-November 1976. The latitudes of the flights covered a range from 10° to 70°N.

RESULTS

The 18.3 km NO data is nearly constant up to 50°N and declines rather abruptly north of that. At 21.3 km a rising trend is seen in the NO data up to 50°N, with a decline above that latitude, but less abrupt than at the lower altitude. Up to about 45°N and at both altitudes the NO trends and magnitudes are quite similar to the observations of June-July 1975 (Loewenstein and Savage, 1975). The June-July data show a continuing increase in marked contrast to the September-November data set. It is possible that in the latter data set we are

observing the decrease of NO associated with the onset of the polar night.

The ozone data trends are quite similar to those observed in June-July 1975. This is to be expected since the ozone is largely transport dominated and the onset of polar night would have little effect on O_3 measured at these altitudes.

CONCLUDING REMARKS

We have presented data on the meridional distribution of O_3 and NO in the altitude range 18 to 21 km. These are results of a program undertaken to determine the global distribution of important stratospheric minor constituents. In the near future, measurement capability for NO_2 and HNO_3 will be added to the airborne in-situ sampling system to allow simultaneous measurements of all the abundant odd nitrogen species.

REFERENCES

1. Loewenstein, M., H. F. Savage, and R. C. Whitten, 1975: Seasonal variations of NO and O_3 at altitudes of 18.3 and 21.3 km, J. Atmos. Sci., 32, 2185-2190.
2. Loewenstein, M. and H. F. Savage, 1975: Latitudinal measurements of NO and O_3 in the lower stratosphere from 5° to 82° North, Geophys. Res. Lett., 2, 448-450.

OZONE MIXING RATIO vs LATITUDE AT 18.3 km

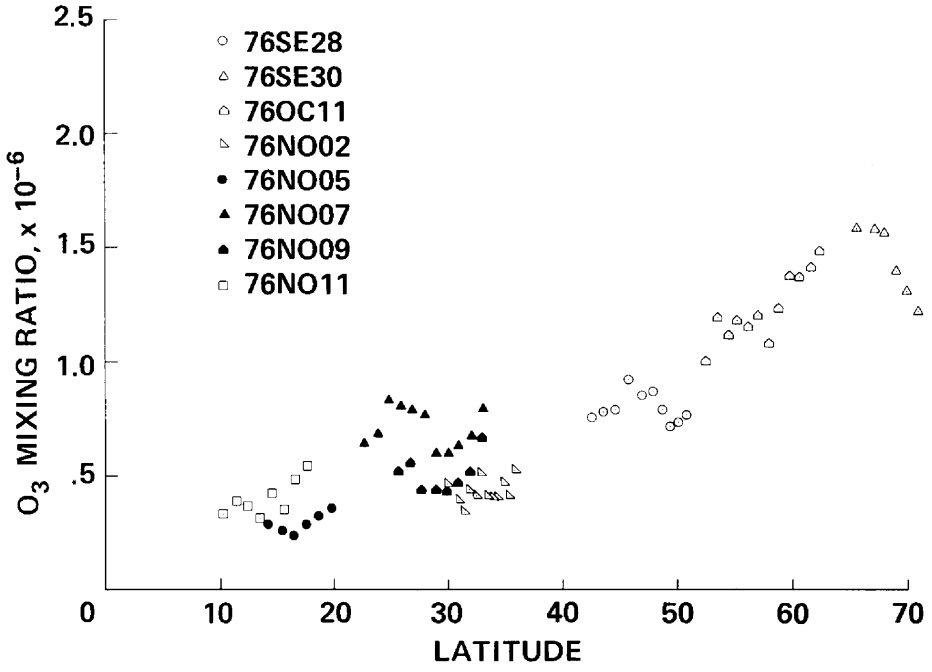

NITRIC OXIDE MIXING RATIO vs LATITUDE AT 18.3 km

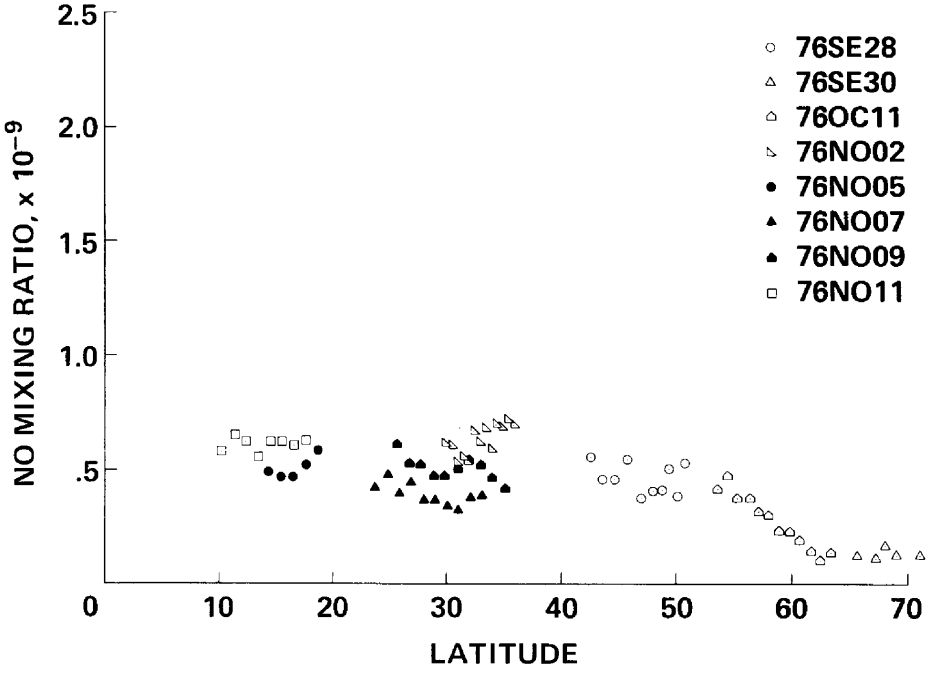

OZONE MIXING RATIO vs LATITUDE AT 21.3 km

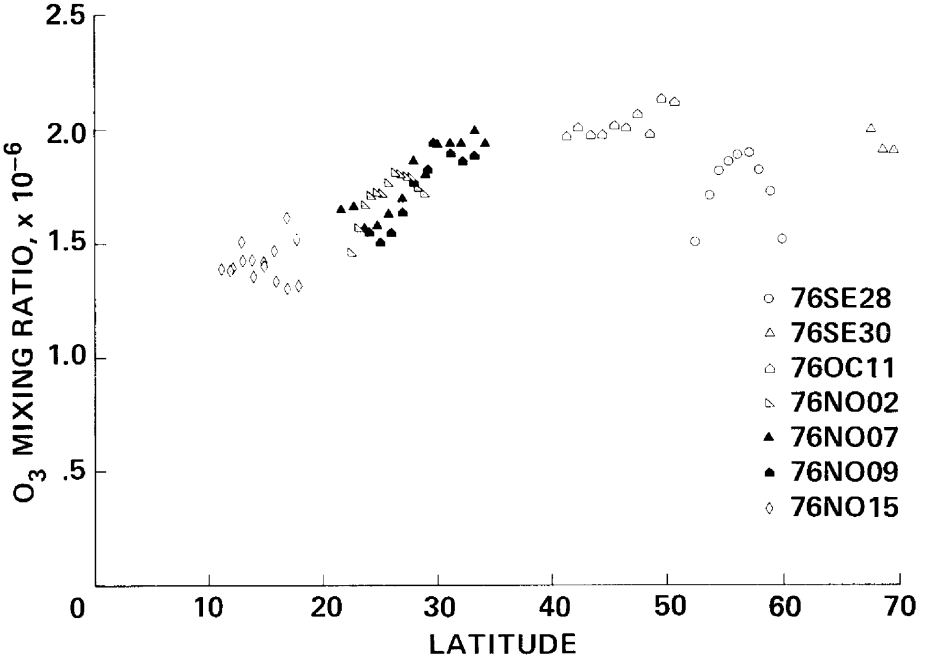

NITRIC OXIDE MIXING RATIO vs LATITUDE AT 21.3 km

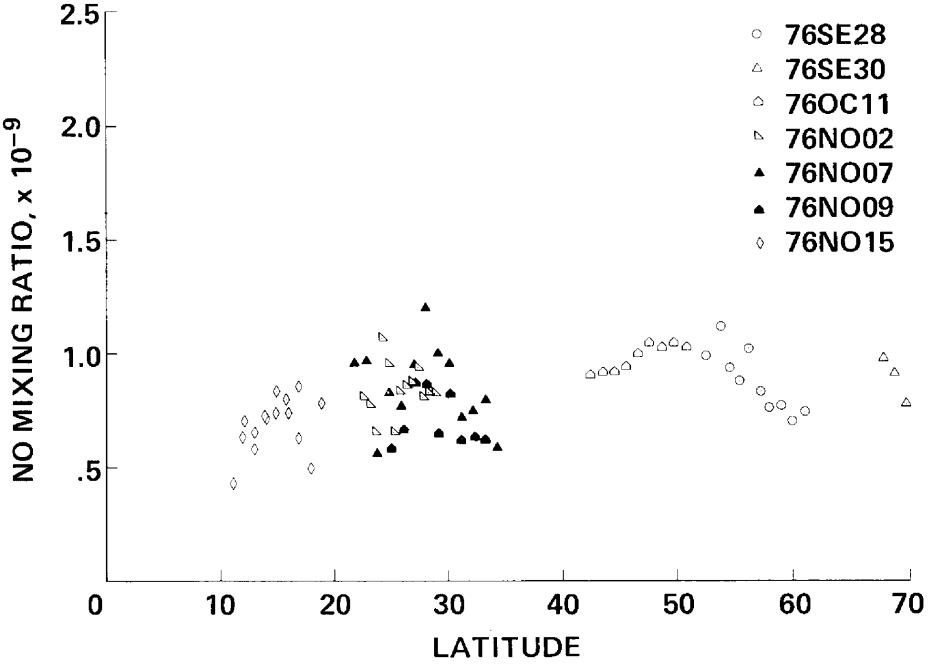

LATITUDINAL VARIATION OF HNO_3 COLUMN DENSITY DERIVED FROM SPECTRAL RADIOMETRIC MEASUREMENTS

by D. B. Barker, W. J. Williams and D. G. Murcray

Department of Physics and Astronomy, University of Denver
Denver, Colorado 80208

INTRODUCTION

Infrared radiometry is an effective technique for remote sensing of trace concentrations of atmospheric gases. Stratospheric concentrations of a number of these constituents are currently of interest scientifically and environmentally. Both the total column density and the altitude density profile are of interest, along with the diurnal, seasonal and latitudinal variation of these densities. Derivation of the concentration of a constituent from infrared radiometric measurements requires a knowledge of theoretical molecular modeling with substantial laboratory data, as well as knowledge of the atmospheric infrared background the constituent is to be observed against. HNO_3 profiles derived from data obtained with an infrared spectral radiometer flown aboard a NASA U-2 aircraft are presented in this paper. The instrument is briefly described and the derived profiles are compared with earlier results.

INSTRUMENTATION

A liquid helium cooled, grating spectrometer was designed and constructed at the University of Denver to measure the spectral emission from minor atmospheric constituents of the stratosphere. The design parameters of

Resolution	$1\ cm^{-1}$
Spectral Range	3-30μm total, in selected intervals
Scan Time	1/2-2 min, possibly adjustable
External F.O.V.	$1/2\text{-}1^{o}$ in the vertical
N.E.R.	$10^{-8}\text{-}10^{-9}$ w cm^{-2} sr^{-1} μm^{-1}
Optics	Low emissivity and low temperature (instrument emission should be low relative to data)

and the capability of remote operation, low power operation (to avoid a heat load on cryogenics), a 12 hour minimum operating time, operation at stratospheric temperatures and pressures, sustaining 15-20 g's shock in any plane and mechanically operating and maintaining optical alignment at LHe temperature and in vacuum make the spectrometer suitable for unattended operation in reconnaissance type aircraft.

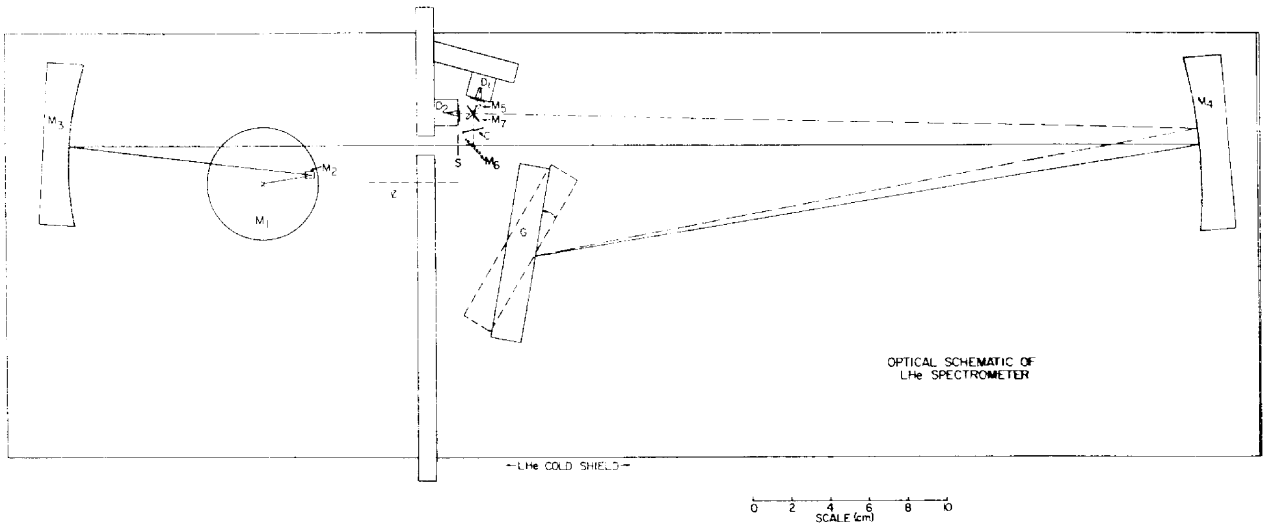

Figure 1. Optical schematic of LHe spectrometer.

A Littrow type mount was selected for the grating because it can be mounted in a smaller volume than other optical configurations for the same grating size and spectrometer focal length. Figure 1 shows the selected optical schematic of the spectrometer. There are several features in this design which are related to the low level of signals intended to be measured. The optical beam is dispersed twice (double passed) by the grating and optically chopped after the first pass. This not only improves the spectral purity but provides a radiometric reference at 4 K which, for all purposes here, is zero. In addition, the image plane after the first pass is displaced from the slit-detector plane by the height of the slit such that no direct radiation from the first pass falls onto the detectors (even though unchopped). Large amounts of dc radiation on the detector can change the noise and responsivity.

Two Ge:Cu detectors, observing two different spectralregions, are heat sinked to the LHe reservior through a copper block. One advantage of the spectrometer design is that separate vacuum dewars for the detectors are not necessary, which reduces the instrument size and eliminates the need for optical adjustment between the exit slit image and the detector position. The dark resistance of these detectors is approximately 5×10^{11} ohms. An electrometer type pre-amplifier with a high input impedance shunted with a very low capacitance is therefore required for impedance matching of the signal transfer circuit. The input radiance is interrupted (chopped) at a 260 Hz rate with a tuning fork type chopper.

To reduce the microphonic noise generated by tuned or vibrating leads between the detector and the pre-amp and the capacitance produced by long leads, the detector pre-amp was physically mounted as close as possible to the detector inside a thermally isolated case. From the pre-amp, the detector signal is buffered with a voltage follower mounted external to the dewar,

passed through a variable gain amplifier controlled by binary switches, synchronously rectified using a phase reference signal from the tuning fork chopper, fed to two low pass active filters and recorded on an on-board digital recorder.

The grating is driven axially with a direct drive torque motor. Also directly coupled to the grating drive shaft is a tachometer used for position and velocity control in the closed loop drive system circuit. The signal to drive the grating is a ramp function derived from a binary controlled D to A converter driven from a 100 kHz clock. This type of ramp generator features many options: 7 scan periods, programmed or command controlled scan stop mode, programmable speed-up or slow-down mode during the scan and an externally adjustable scan length. Because of the hostile environment the grating drive system operates in, special Bemol self-lubricating Fernalon AW polyimide ball bearings were selected for axial support. This torque motor-tack-ramp combination is reliable, versatile, accurate, efficient, low power (typically 20 mw) low mass grating drive system that has operated successfully at 4.2 K.

The spectrometer is oriented such that the slit length is horizontal. The center of the optical axis passes radially through the center of the vacuum dewar and changes in the observational height angle may be accomplished by rotating the dewar.

DATA REDUCTION

The signal voltage as measured is proportional to the difference in the incident spectral radiance from both the atmosphere and the dewar window and the reference blackbody radiance at the temperature of the instrument. Since the internal temperature is < 10 K the internal radiance is taken as zero. The window used in the dewar (Zn Se) is chosen for low emissivity, and operates at ambient air temperature; however, at the higher altitudes this emission becomes a significant portion of the observed signal in the 11μm region. The data are reduced using calibration factors determined from pre- and post-flight instrument calibrations. The window radiance is calculated on the basis of its temperature and a curve of emissivity versus wavelength determined from laboratory calibrations, and subtracted from the total measured radiance data. The remaining radiance is due to atmospheric gases and particulates.

Once the data have been obtained in this form, two additional steps are required to determine the HNO_3 column density above the aircraft. The first step is to determine the emissivity at 11.2μm and the second is to determine the HNO_3 amount from the emissivity. The amount of HNO_3 present above the aircraft is small and the radiance observed at the aircraft comes from all altitudes above the aircraft. The mean height of the HNO_3 column density was determined for the profiles derived from the balloon flight data. This mean height was 22 km with very little variation with latitude or time of year. In

view of this, the total HNO_3 above the aircraft was assumed for the calculation to be 22 km and the temperature at that altitude was determined from rawinsonde data obtained at various stations close to the aircraft flight path. Using a blackbody radiance for this temperature, it is possible to determine the HNO_3 emissivity from the data. Since the HNO_3 emissivity is small, it lies in the linear absorption region and the total column density of HNO_3 above the aircraft is directly proportional to the emissivity. The constants of proportionality have been determined in laboratory measurements (Reference 1).

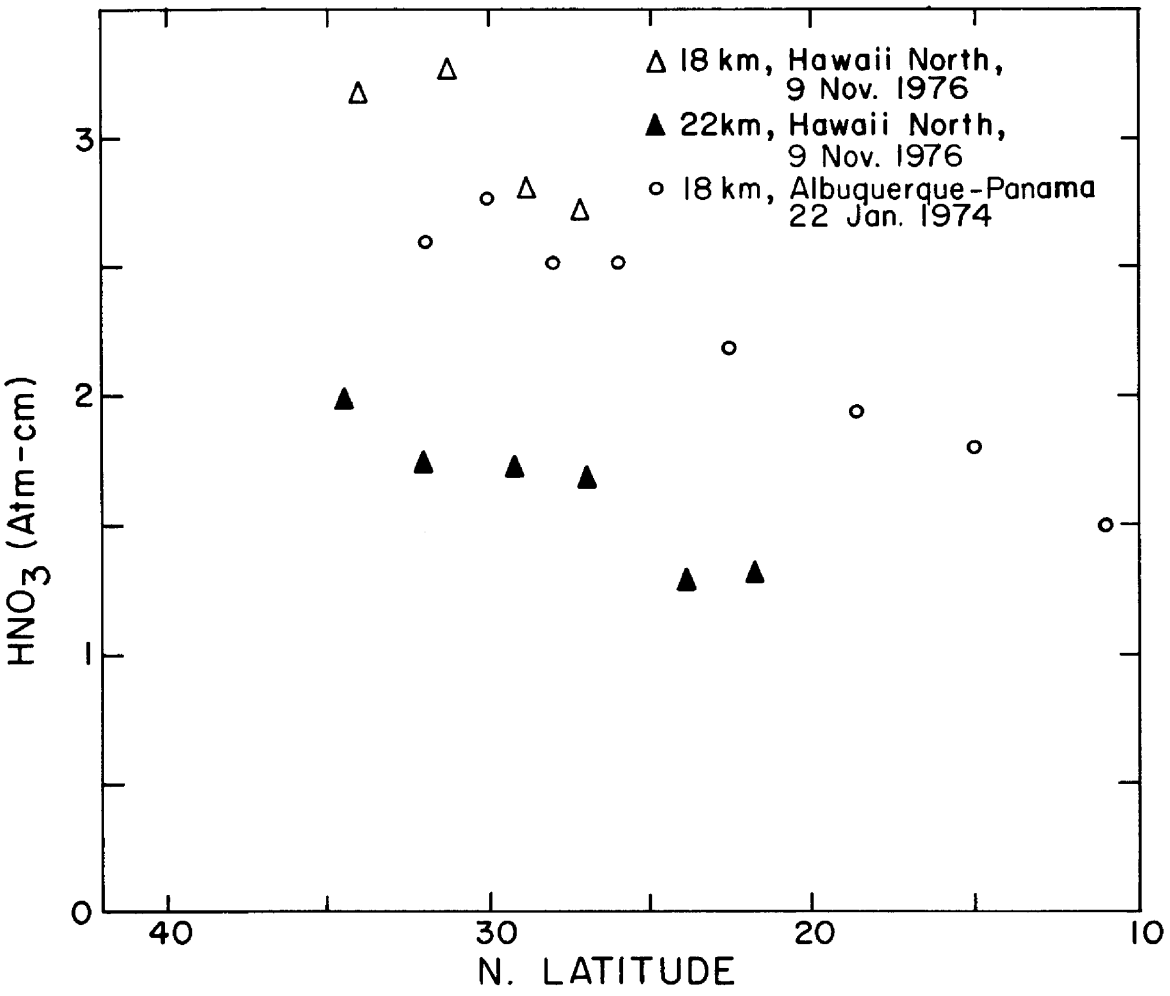

Figure 2. Variation of HNO_3 Column Density with Latitude

FLIGHT RESULTS

The spectrometer was flown in the right wing pod of the U-2, NASA 708, on 9 November 1976 (Flight 76-187). The flight track was north along 158 W. Longitude to 35 N. Latitude; outbound at 18 km altitude and back at 22 km. The spectrometer and digital recorder operated satisfactorily.

The data were reduced as described using temperatures of 198K at 18 km and 212 K at 22 km as indicated by the 2315Z Rawinsonde from Lihue, Hawaii. The calculated column densities of HNO_3 are plotted in Figure 2 along with results from an RB-57 flight of the DOT Airstream series. The latitudinal variation is comparable to that measured on previous flights.

REFERENCES

1. Goldman, A., T. G. Kyle and F. S. Bonomo, Statistical band model parameters and integrated intensities for the 5.9μ, 7.5μ and 11.3μ bands of HNO_3 Vapor, Appl. Opt., 10, 65-73, 1971.

MEASUREMENTS FROM GEOPHYSICAL MONITORING FOR CLIMATIC CHANGE BASELINE STATIONS

Gary A. Herbert
Air Resources Laboratory
Environmental Research Laboratories
NOAA - Boulder, Colorado 80302

1. CATALOG OF OBSERVATIONS

As part of the NASA Latitude Survey Mission, performed by the CV990 aircraft, fly-by comparisons were made at the GMCC observatories at Point Barrow, AK, Mauna Loa, HI and Cape Matatula, American Samoa. The data presented in this section are those taken at the observatories during the time of the comparison. While the individual values have been checked, in some cases the quality of the data is hard to assure in short, detached, samples such as these. For this reason the continuous measurements of carbon dioxide and ozone will not be included in this report. All measurement programs that were active during the intercomparison, are cataloged in Table 1.

2. LOCAL METEOROLOGICAL CONDITIONS

Surface meteorological conditions are determined by measurements of wind speed and direction, station pressure, and air temperature. The wind is measured at a height of 10 meters using a propeller type anemometer (Bendix aerovane model 120). Station pressure is measured at a height of about 3-4 meters above the local terrain, employing a static pressure transducer (Rosemount Inc. model 1201C). A linearized thermistor (Yellow Springs Instrument Company, model 44212) is used to sense the temperature at a height of 3 meters. The thermometer is enclosed in an aspirated radiation shield (R. M. Young Company, model 43406). The data in Table 2 are the average values for the hour beginning at the times listed. In the case of the winds, the resultant wind speeds and directions are reported.

3. SURFACE AEROSOLS

The concentrations of Aitken nuclei in the atmosphere were measured with two instruments at Pt. Barrow and at the Mauna Loa Observatory. Continuous

TABLE 1

CONSTITUENT	SENSING INSTRUMENTATION	GMCC OBSERVATORIES	BARROW	MAUNA LOA	AMERICAN SAMOA
		DESIGNATION	199	031	191
		LATITUDE (Deg. Min)	71 19N	19 32N	14 15S
		LONGITUDE (Deg. Min)	156 36W	155 35W	170 34W
		ELEVATION (Meters)	11	3397	82
TOTAL OZONE	DOBSON OZONE SPECTRO-PHOTOMETER		NO DATA TAKEN (Low Sun)	4 OBSERV. TAKEN	4 OBSERV. TAKEN
SURFACE OZONE CONCENTRATION	DASIBI-TYPE OZONE ANALYZER		DATA IS AVAILABLE	DATA IS AVAILABLE	DATA IS AVAILABLE
CARBON DIOXIDE CONCENTRATION	NON-DISPERSIVE INFRARED ANALYZER		DATA IS AVAILABLE	DATA IS AVAILABLE	DATA IS AVAILABLE
CARBON DIOXIDE CONCENTRATION	FLASK SAMPLES		3 FLASKS ANALYZED	3 FLASKS ANALYZED	2 FLASKS ANALYZED
AITKEN NUCLEI CONCENTRATION	GARDNER COUNTER		NOT IN OPERATION	NOT IN OPERATION	10 READINGS
AITKEN NUCLEI CONCENTRATION	CONTINUOUS NUCLEI COUNTER (GECNC)		DATA IS AVAILABLE	DATA IS AVAILABLE	NO DATA (Not yet installed)
AEROSOL SIZE DISTRIBUTION	NEPHELOMETER (4λ)		INOPERATIVE	DATA IS AVAILABLE	NO DATA (Not yet installed)
HALOCARBON-11 CONCENTRATION	EXTERNAL FLASK SAMPLES		3 FLASKS ANALYZED	1 FLASK ANALYZED	3 FLASKS ANALYZED

measurements were made with a condensation nuclei counter (General Electric Company, model 112L428G30). The data from this instrument are reported as hourly average values. The values are assigned to the beginning of the hour. The second set of Aitken nuclei counts was obtained from a Pollak counter, which is a more accurate instrument than the continuous condensation nuceli counter. The Pollak counter is not a continuous instrument, therefore the data apply only at the time listed. Aitken nuclei concentrations are listed in Table 3.

TABLE 2

ONE-HOUR AVERAGE VALUES OF WEATHER PARAMETERS

STATION: DATE 1976	TIME (GMT)	WIND DIRECTION (DEG)	WIND SPEED (ms^{-1})	STATION PRESSURE (mb)	AIR TEMPERATURE (^{o}C)
PT. BARROW, ALASKA					
10/29	2300	353	7.6	1012.1	-14.7
10/30	0000	004	6.4	1012.0	-15.3
10/30	0100	014	5.7	1012.3	-16.2
10/30	0200	010	5.8	1012.5	-17.2
10/30	0300	348	5.1	1012.5	-17.6
MAUNA LOA OBSERVATORY, HAWAII					
11/1	1400	201	4.4	681.7	2.3
11/1	1500	203	4.4	681.8	2.2
11/1	1600	208	4.9	682.1	2.6
11/1	1700	219	4.5	682.5	6.0
11/1	1800	260	3.9	682.7	9.6
CAPE MATATULA, AMERICAN SAMOA					
11/7	2300	155	5.9	999.7	24.8
11/8	0000	154	4.7	999.9	24.2
11/8	0100	163	4.0	999.2	24.8
11/8	0200	142	5.3	998.2	25.5
11/8	0300	144	4.9	998.0	25.9

TABLE 3

AEROSOL MEASUREMENTS

STATION / DATE 1976	TIME (GMT)	AEROSOL COUNT (nuclei cm^{-3})	POLLAK READING (nuclei cm^{-3})
PT. BARROW, ALASKA			
10/29	2300	105	128
10/30	0000	110	94
10/30	0100	107	91
10/30	0200	105	109
10/30	0300	107	121
MAUNA LOA, HAWAII			
11/1	1400	154	140
11/1	1500	156	137
11/1	1600	148	115
11/1	1700	138	188
11/1	1800	140	181
11/1	1900	152	215

The scattering characteristics of the aerosols can be estimated from the integrating nephelometer. A 4-wavelength nephelometer (Meteorology Res. Inc. model 1559A) was in operation at the Mauna Loa Observatory during the fly-by. The data in Table 4 are the average integrated backscatter coefficients for the specified hour at the specific wavelengths listed.

TABLE 4

INTEGRATED AEROSOL SCATTERING

MAUNA LOA OBSERVATORY, HAWAII

DATE 1976	TIME (GMT)	INTEGRATED SCATTERING 450 nm (m^{-1})	550 nm (m^{-1})	700 nm (m^{-1})	850 nm (m^{-1})
		$x10^{-7}$	$x10^{-7}$	$x10^{-7}$	$x10^{-7}$
11/1	1400	1.04	0.65	0.43	0.55
11/1	1500	1.00	1.08	0.50	0.57
11/1	1600	1.03	1.18	0.48	0.55
11/1	1700	1.20	0.95	0.54	0.51
11/1	1800	1.44	1.00	0.46	0.90
11/1	1900	2.00	1.05	0.44	0.77

At Cape Matatula a special set of Aitken nuclei counts was made with a longtube counter. (Gardner Assoc. Inc., model cn). The extended tube increases the sensitivity of the counter to low aerosol concentrations of about 100 nuclei cm^{-3}.

The prevailing winds at all three observatories, for three hours in advance of and at the time of the fly-by, were from directions generally found to be free from local pollution. The changes in wind direction were small and the speed remained steady throughout this period. Changes in atmospheric pressure were also small indicating a generally steady weather situation. The relatively low aerosol count observed at each station substantiates the conclusion that the air passing the station at the time of the comparison was relatively free from local pollution.

TABLE 5

AITKEN NUCLEI CONCENTRATIONS

CAPE MATATULA, AMERICAN SAMOA

DATE 1976	TIME (GMT)	CONCENTRATION (nuclei cm^{-3})
11/8	0050	105
11/8	0055	124
11/8	0100	138
11/8	0105	138
11/8	0115	139
11/8	0120	127
11/8	0130	135
11/8	0135	122
11/8	0140	127
11/8	0145	149

4. CARBON DIOXIDE FROM FLASK SAMPLES

Three glass flasks were exposed upwind of each station before and after the comparison fly-by. The samples were sent to Boulder and analyzed for carbon dioxide content. The values in the adjoining table are the result of this analysis. They are mole fractions based on the Scripps 1959 Adjusted Index Scale.

TABLE 6

CARBON DIOXIDE OBSERVATIONS

STATION 1976	DATE (GMT)	TIME OF SAMPLE (GMT)	CARBON DIOXIDE CONCENTRATION (ppm) SAMPLE 1	SAMPLE 2	SAMPLE 3
BRW	10/29	2325	324.7	324.8	324.5
BRW	10/30	0130	324.6	324.6	324.7
MLO	11/1	1535	339.9	323.9	
MLO	11/1	2020	323.8	325.6	
SMO	11/8	0050	326.3	326.4	
SMO	11/8	0235	326.7	326.6	326.4

5. HALOCARBON - 11

The estimates of halocarbon-11 (CCl_3F) are made from flask samples taken upwind of the station. The flasks are made of stainless steel with a volume of 300 ml. The samples are analyzed on a variable frequency gas chromatograph. The overall uncertainty in the concentration is estimated to be ± 25%.

TABLE 7

HALOCARBON-11 OBSERVATIONS

STATION 1976	DATE (GMT)	TIME OF SAMPLE (GMT)	AVERAGE HALOCARBON-11 CONCENTRATION (ppt)
BRW	10/29	2215	193.2
BRW	10/29	2330	193.2
BRW	10/30	0135	194.7
MLO	11/1	2020	182.5
SMO	11/8	0050	157.4
SMO	11/8	0150	166.7
SMO	11/8	0240	157.2

6. TOTAL OZONE

Observations of total ozone were made with Dobson spectrophotometers, at Samoa and Mauna Loa, at the time of the aircraft fly-by. Due to the low sun angle at Pt. Barrow during the end of October, Dobson measurements were not possible. Observations are reported for two different modes, A-D direct sun (ADDS); and A-D zenith cloud (ADZC). The A-D direct sun measurement is the more accurate of the two methods. The airmass is computed for each observation.

TABLE 8

TOTAL OZONE OBSERVATIONS

DATE 1976	TIME (GMT)	TOTAL OZONE (milli Atm -cm)	AIRMASS	MODE
MAUNA LOA, HAWAII				
11/1	1753	.265	2.96	ADDS
11/1	1757	.265	2.85	ADDS
11/1	1947	.246	1.50	ADDS
11/1	1951	.246	1.48	ADDS
11/1	2033	.265	1.32	ADDS
11/1	2036	.266	1.32	ADDS
CAPE MATATULA, AMERICAN SAMOA				
11/8	0014	.296	1.04	ADZC
11/8	0016	.295	1.05	ADZC
11/8	0313	.268	1.94	ADDS
11/8	0315	.267	1.97	ADDS

NASA CV 990 Interlatitude Survey

November 1976

Australian Support Data

ATMOSPHERIC CCl_3F, CCl_4 and CH_3CCl_3 CONCENTRATIONS OVER SOUTH EAST AUSTRALIA DURING NOVEMBER 1976

P.J. Fraser
G.I. Pearman
CSIRO
Division of Atmospheric Physics
Aspendale, Victoria
Australia.

INTRODUCTION

The CSIRO Division of Atmospheric Physics has been monitoring levels of various halocarbons, namely trichlorofluoromethane CCl_3F, carbontetrachloride CCl_4 and 1,1,1-trichloroethane CH_3CCl_3, in the atmosphere of south-east Australia since early 1976. In situ measurements of all three gases are made regularly at both Aspendale, Victoria and Cape Grim, Tasmania. Air samples, collected routinely in glass and stainless steel flasks as part of the carbon dioxide monitoring programme of this Division (Pearman and Garratt, 1973), are now analysed for CCl_3F. Flask contaminations problems do exist for all three compounds and these are discussed briefly in this report.

The purpose of the present study was to compare our data for CCl_3F, CCl_4 and CH_3CCl_3 obtained during November 1976 with measurements made on board the NASA CV 990 during its interlatitude survey. The data consist of four parts:

(a) routine measurements made on flask samples collected from commercial and govenment aircraft during November 1976;

(b) measurements made on flask samples collected from a light aircraft which flew over Cape Grim and Aspendale within a few hours of the CV 990's flight number 9 on November 11, 1976.

(c) measurements made on flask samples collected from the Washington State University (WSU) air intake onboard the CV 990 during flight number 9.

(d) surface measurements made in situ at Cape Grim, Tasmania and at Aspendale, Victoria.

Figure 1 shows the position of the various locations mentioned in the text.

INSTRUMENTATION, CALIBRATION AND SAMPLING

The gas chromatographs used at Cape Grim and Aspendale were supplied by J.E. Lovelock, Bowerchalke, Salisbury, Wiltshire and contain 2m x 0.6cm I.D.

stainless steel columns, packed with 100-120 mesh Chromosorb W coated with 12% dimethyl silicone fluid. The electron capture detectors contain tritium sources and are operated in a pulsed mode. The carrier gas used is nitrogen with 1% hydrogen, purified by passing through palladized asbestos at 400°C and 5A molecular sieve. The Lovelock gas chromatographs are designed to be used in a coulometric mode (Lovelock, 1974). However we have also found it necessary to use tanks of air as calibration standards. Two tanks have been used in this study - one at Aspendale, code number VZ068, and one at Cape Grim, code number AAC144. Two intercalibrations on VZ068 (3/9/76, WSU, M. Campbell; 12/11/76; WSU, J. Krasnec and NASA-Ames, J. Arvesen and B. Tyson) have shown that the CCl_3F and CCl_4 concentrations in VZ068 are slowly drifting. The data presented in this report have been corrected for these drifts. Regular intercomparisons between VZ068 and AAC144 have been made. Unfortunately AAC144 has a low CCl_4 concentration (approx. 20 pptv) and therefore concentrations of CCl_4 determined at Cape Grim could be unreliable. Also neither standard appears to contain CH_3CCl_3. However the intercalibration on 3/9/76 showed that the Cape Grim detector was approximately 30% coulometric in measuring CH_3CCl_3. Approximate CH_3CCl_3 concentrations were obtained by multiplying the observed coulometric concentrations by 3.37.

Air samples were collected from cabin air outlets (turbine compressed) or rammed air intakes, using peristaltic or stainless steel bellows pumps (see Table 1 for details). Low altitude samples were dried before collection using magnesium perchlorate. Half litre glass flasks were first flushed for 2-5 mins and then the sample was compressed to approximately 1 atmosphere above cabin pressure.

RESULTS AND COMMENTS

In Table 2 we have listed all of the aircraft CCl_3F data collected from the routine CSIRO air sampling programme during November 1976. The results of analyses made on flasks collected on the day of the CV990 flight 9 are shown in Table 3. The exact position of the CV990 can be obtained from the flight records using the recorded time of sampling. For the purpose of this presentation we have grouped the CV990 and PA39 measurements according to geographical area. Table 4 lists the coulometric and calibrated concentrations of CCl_3F, CCl_4 and CH_3CCl_3 made at Cape Grim during November 1976, while Table 5 lists the calibrated concentrations of CCl_3F and CCl_4 observed at Aspendale during November 1976.

In Figure 2 the aircraft and surface data for CCl_3F are plotted as a function of altitude above MSL for November 11, 1976. Concentrations of CCl_4 obtained from the flask samples averaged in excess of 200 pptv, which is considerably higher than concentrations measured in situ at Aspendale (136 pptv) and at Cape Grim (156 pptv). This latter figure could be in error due to the fact that the calibration gas (AAC144) used had a low CCl_4 concentration (approximately 20 pptv).

Concentrations of CCl_3F obtained from the flask samples averaged 132 pptv for the Tasmanian area which is 10 pptv higher than the concentration observed at Cape Grim on November 11, and 17 pptv higher than the November average con-

centration observed at Cape Grim. Table 6 shows that there is a fairly consistent difference of, on average, 19 pptv between flask and in situ measurements taken at Cape Grim. The cause of this contamination is, at present, unknown. The CCl_3F concentrations observed in situ at Cape Grim on November 11 averaged 122 pptv which is 7 pptv higher than the November average. At Cape Grim local surface winds were from the east on November 11 and this higher than average concentration probably represents some local surface contamination. This higher than average CCl_3F concentration on November 11 is also observed in flask measurements at Cape Grim compared to flask measurements taken on board the CV990.

On the day of flight 9, south eastern Australia generally experienced near northerly winds in the lower kilometre of the atmosphere whereas in the middle and upper troposphere winds were generally in the west (see flight record and Figure 3). The effect of the low level northerlies on the vertical profile of CCl_3F measured south of Melbourne is apparent in Figure 2, with high urban like concentrations of CCl_3F observed below approximately 1 km.

REFERENCES

Pearman, G.I. and Garratt, J.R. 1973: Space and time variations of tropospheric CO_2 in the southern hemisphere. Tellus 25: 309-311.

Lovelock, J.E. 1974: The electron capture detector - theory and practice. Journal of Chromatography 99: 3-12.

Table 1

Details of aircraft and sampling techniques used

Aircraft	B707 Boeing 707	F27 Fokker Friendship	PA39 Piper Commanche	CV 990 Convair 990
Agency	Qantas	Dept. of Transport	Private Hire	NASA
Altitudes	10-12 km	3-5 km	0-5 km	3-12 km
Collection	Cockpit air-conditioning outlet. Pressurization with peristaltic pump.	Cabin air conditioning outlet. Air dried with magnesium perchlorate and pressurized with peristaltic pump.	Rammed air intake with drying and pressurization as for F27.	Rammed air intake with pressurization with s.s. bellows pump. (WSU system).

DATE	AIRCRAFT	FLIGHT NO.	FLASK	TIME (Z)	LOCATION				ALTITUDE	CCl_3F
1976					Sect.	Dist.	Dir.	DME	(km)	
Nov. 8	F27	D137	37	2349	1	91	2	16	4.25	134
9	"	D137	29	0637	1	161	5	7	3.95	134
15	"	D138	33	2308	1	93	1	1	4.55	125
16	"	D138	38	0110	1	93	4	42	4.85	123
22	"	D139	29	2238	1	163	1	1	4.55	132
23	"	D139	37	0039	1	194	8	44	4.85	135
30	"	D140	34	0430	2	132	8	12	4.05	137
	"	D140	36	0434	2	102	8	12	4.05	132
										132 (5)

Table 2 - Details of routine CSIRO air sampling flights and measured CCl_3F concentrations for NOVEMBER 1976.
Location code: SECT - Sector as in Figure 1
DIST - Distance in km from DME station
DIR - Direction from DME station (1-North, 2-NE, 3-East, etc.)
DME - Distance measuring equipment station number (see Figure 1 for location of stations)

TIME	AIRCRAFT TYPE	HEIGHT ABOVE M.S.L. (km)	CCl_3F CONC. (pptv)
NORTH-WEST TASMANIA AREA			
2132	CV990	11.29	133
2154	"	6.41	126
2205	"	3.10	131
2236	PA39	0.91	137
2243	"	1.52	130
2249	"	2.13	135
2258	"	3.05	133
2316	"	4.27	130
2325	"	3.66	134
2333	"	2.74	134
2345	"	1.52	133
0002	"	0.30	134
0007	"	0.15	133
0010	"	0.11	134
0013	"	1.01	135
0019	"	1.52	134
TASMANIA SECTOR - OUTSIDE N-W AREA			
2229	CV990	8.54	133
2244	"	11.90	124
MELBOURNE-WESTERNPORT AREA			
2112	CV990	11.29	134
2319	"	11.90	131
2331	"	7.61	134
2336	"	7.62	135
2352	"	3.12	134
2359	"	3.11	133
0335	PA39	1.22	136
0339	"	0.61	259
VICTORIAN SECTOR - OUTSIDE MELBOURNE-WESTERNPORT			
2039	CV990	11.28	131

Table 3 - CCl_3F measurements made on air samples collected on November 10th and 11th (Z time) during the CV990 flight 9 and PA39 flight.

DATE	CCl_3F (pptv)		CCl_4 (pptv)		CH_3CCl_3 (pptv)	
	COULOMETRIC	CALIBRATED	COULOMETRIC	CALIBRATED	COULOMETRIC	CALIBRATED
Nov.4	74 (4)	118 (6)	111 (3)	138 (4)	8 (2)	27 (7)
5	84 (4)	114 (5)	125 (4)	124 (4)	9 (1)	30 (3)
6	82 (4)	125 (6)	120 (8)	183 (12)	10 (1)	34 (3)
7	84 (5)	122 (7)	123 (4)	153 (5)	9 (1)	30 (3)
8	88 (3)	118 (4)	130 (4)	172 (5)	9 (1)	30 (3)
9	94 (3)	122 (4)	136 (5)	193 (7)	9 (1)	30 (3)
10	101 (5)	114 (6)	134 (6)	148 (7)	8 (2)	27 (7)
11	99 (5)	122 (6)	139 (3)	172 (4)	10 (1)	34 (3)
12	104 (5)	114 (5)	144 (4)	151 (4)	10 (1)	34 (3)
13	104 (5)	106 (5)	145 (5)	131 (5)	10 (1)	34 (3)
14	105 (3)	98 (3)	146 (2)	133 (2)	10 (1)	34 (3)
15	117 (11)	114 (11)	152 (3)	126 (2)	10 (1)	34 (3)
16	100 (2)	121 (2)	144 (8)	137 (8)	9 (1)	30 (3)
17	105 (2)	114 (2)	146 (3)	172 (4)	10 (1)	34 (3)
18	107 (4)	121 (5)	153 (3)	152 (3)	10 (1)	34 (3)
19	112 (3)	117 (3)	153 (2)	191 (3)	11 (2)	37 (7)
20	117 (7)	109 (7)	155 (2)	172 (2)	10 (2)	34 (7)
21	116 (3)	117 (3)	158 (6)	151 (6)	12 (2)	40 (7)
22	118 (3)	117 (3)	162 (3)	147 (3)	11 (1)	37 (3)
23	117 (5)	109 (5)	160 (5)	140 (4)	12 (2)	40 (7)
24	122 (8)	113 (7)	164 (11)	153 (10)	13 (3)	44 (10)
25	120 (2)	117 (2)	167 (7)	209 (9)	14 (2)	47 (7)
26	118 (5)	116 (5)	165 (7)	132 (6)	15 (1)	51 (3)
29	81 (2)	116 (3)	133 (5)	157 (6)	9 (2)	30 (7)
30	90 (3)	113 (4)	143 (3)	169 (4)	9 (1)	30 (3)
Monthly mean	102 (14)	115 (6)	144 (15)	156 (23)	10 (2)	35 (6)

Table 4 - Coulometric and calibrated concentrations of CCl_3F, CCl_4 and CH_3CCl_3 measured at Cape Grim during November 1976. Each value represents a mean of, on average, 9 measurements between approximately 0800 and 2000 hrs. Concentrations are calibrated against standard tank AAC144. Numbers in parentheses represent one standard deviation.

DATE	CCl_3F (pptv)	CCl_4 (pptv)
Nov.1	183	131
8	182	131
9	158	133
10	145	128
11	287	136
18	141	152
19	161	145
22	130	134
23	141	141
24	146	155
25	157	339
29	562	127

Table 5 - CCl_3F and CCl_4 concentrations observed at Aspendale during November 1976 between 1200 and 1700 hrs. Concentrations are calibrated against standard tank VZ068.

DATE	IN SITU CCl_3F (pptv)	NO. OF SAMPLES	FLASK CCl_3F (pptv)	NO. OF SAMPLES	DIFFERENCE
Sept.13	110	7	129	3	19
Oct. 11	110	5	128	2	18
12	115	10	130	3	15
Nov. 4	118	13	137	3	19
5	114	9	137	3	23
11	122	13	139	4	17
12	114	10	137	2	23
15	114	7	135	1	21
17	114	7	133	2	19
19	117	4	137	2	20
26	116	6	130	6	14
				MEAN	19 (3)

Table 6 - Comparison of flask and in situ measurements of CCl_3F at Cape Grim, Tasmania.

Figure 1

Map of south eastern Australia showing localities mentioned in the text. Each numeral represents a station equipped with distance measuring equipment (DME) from which sampling points are located in Table 2.

DME Station Number	Location	DME Station Number	Location
1	Wynyard (Tas.)	12	Mount Gambier (S.A.)
3	Meningie (S.A.)	16	King Island (Tas.)
5	Sydney (N.S.W.)	42	Wonthaggi (Vic.)
7	Melbourne (Vic.)	44	Launceston (Tas.)

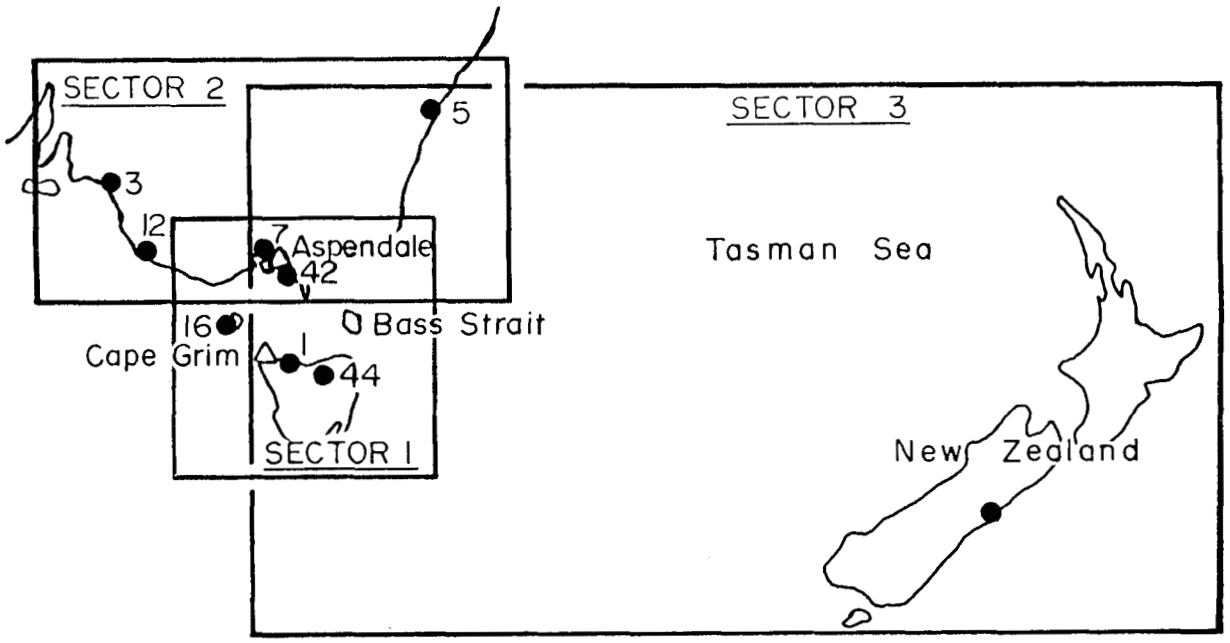

FIG. 2 Variation of CCl_3F with height – 11th Nov. 1976

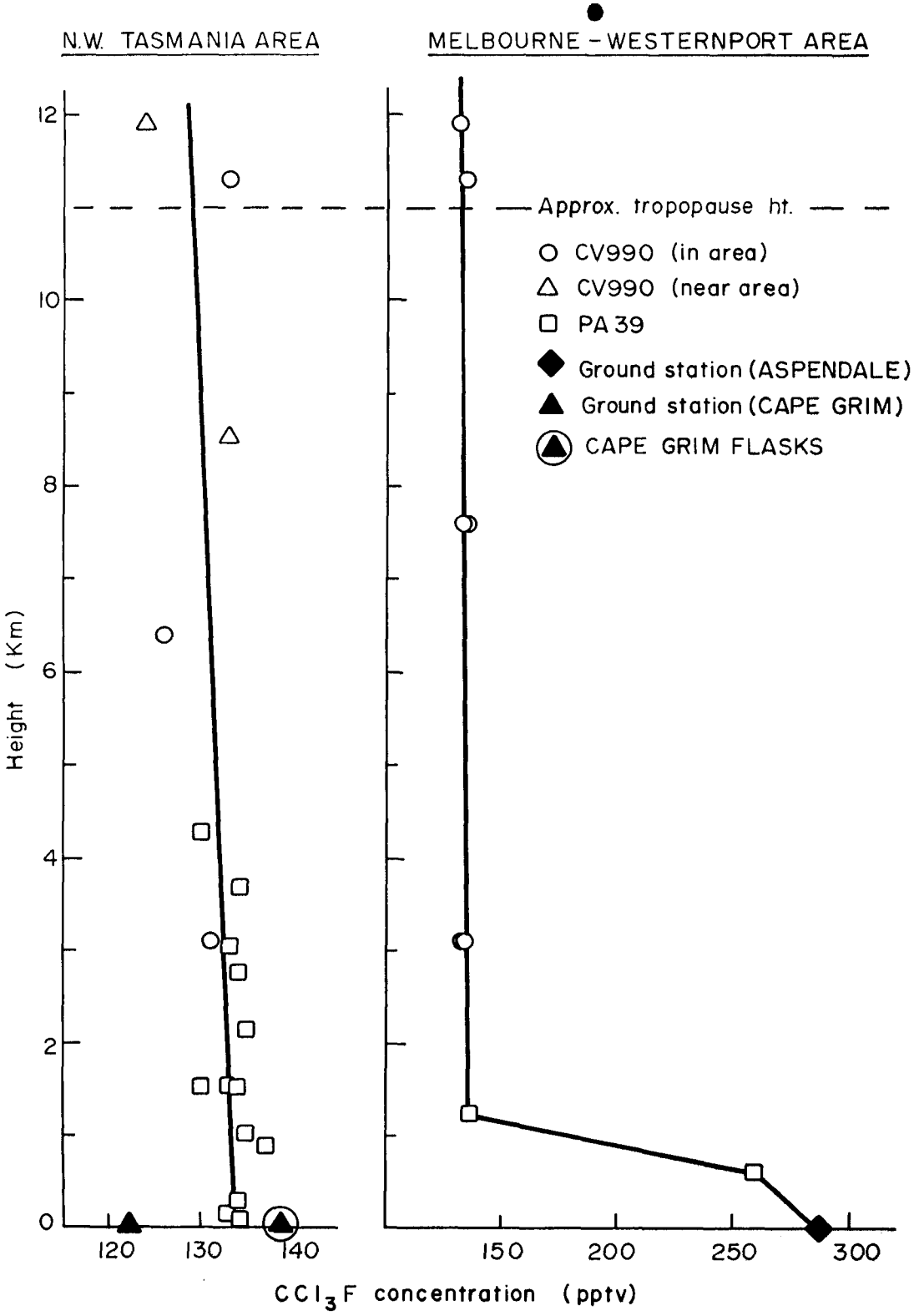

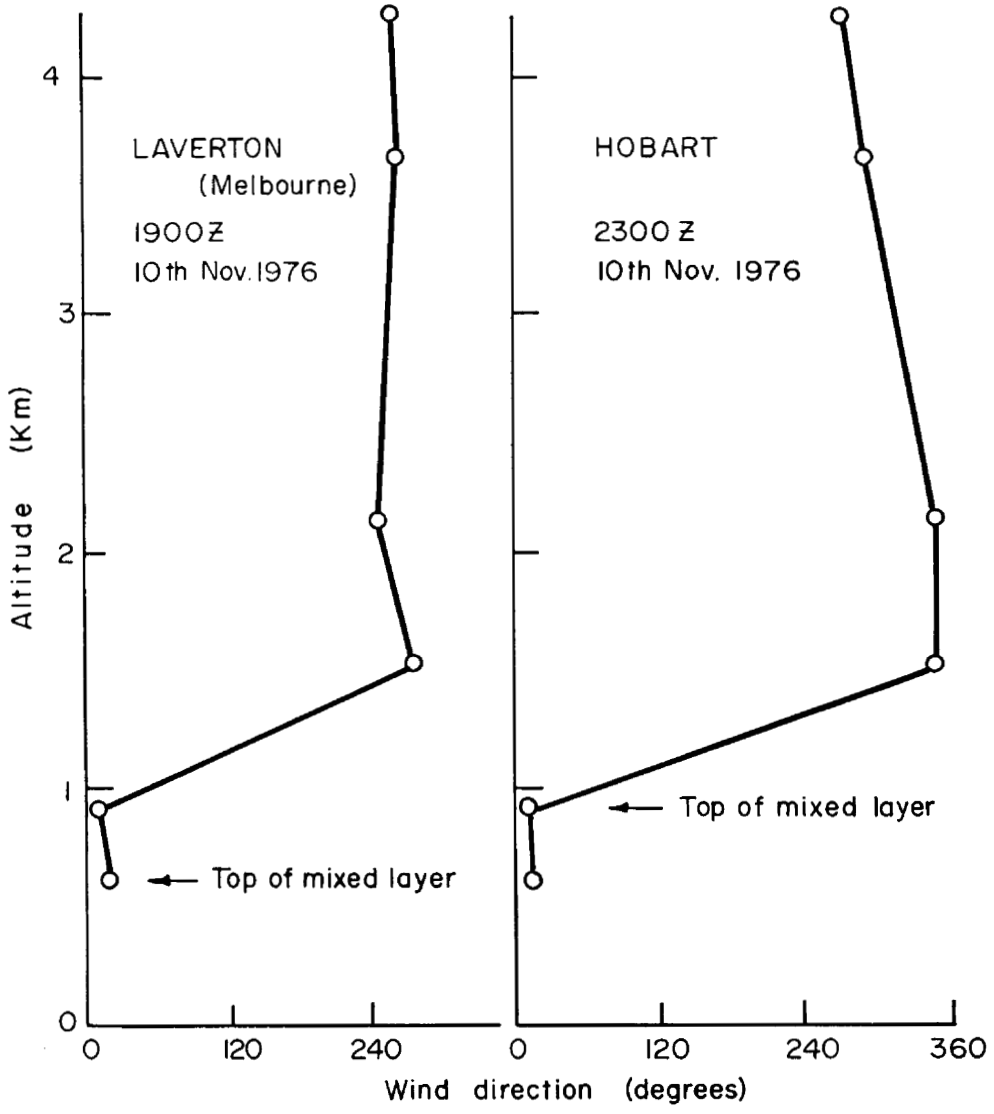

FIG. 3 Wind direction at different altitudes over Melbourne and Hobart on the day of CV990 Flight 9.

NASA CV-990 INTERLATITUDE SURVEY

November 1976

Australian Support Data

Total Ozone and Ozonesonde Data

R.N. Kulkarni

Total ozone data were obtained from stations at Aspendale, Hobart, Cairns, Brisbane, and Macquarie Island. An ozonesonde obtained data during an ascent from Aspendale.

TABLE I. - OZONESONDE ASCENT MADE FROM ASPENDALE - AUSTRALIA ON 11th NOVEMBER 1976 - RELEASE AT 0034 GMT

VALUES HAVE BEEN CORRECTED FOR MEAN TOTAL - OZONE OF 322 m. atm. cm.

SIGNIFICANT LEVELS (mb)	CORRECTED PARTIAL PRESSURE OF OZONE (mb)	SIGNIFICANT LEVELS (mb)	CORRECTED PARTIAL PRESSURE OF OZONE (mb)
1004.5	43.4	89.0	43.9
960.0	48.0	80.0	78.7
900.0	29.4	71.0	94.8
860.0	27.9	67.0	106.1
840.0	23.2	58.5	124.1
790.0	27.9	53.0	147.0
692.0	27.9	49.5	152.3
604.0	26.3	45.0	173.9
440.0	26.3	42.5	166.3
360.0	18.6	38.0	175.3
320.0	15.5	33.4	163.4
230.0	15.5	30.5	167.6
212.0	31.0	27.0	162.2
191.0	31.0	25.5	134.6
174.0	23.2	23.0	142.2
151.0	38.7	19.2	133.9
130.0	21.7	16.0	116.9
116.0	21.8	15.5	105.2
99.0	31.3	11.0	76.6

TABLE II. - TOTAL OZONE VALUES - AUSTRALIA *

in m-atm-cm

ASPENDALE (Lat. 38° 0S'S Long. 145° 06E')

9 Nov. 1976		10 Nov. 1976		11 Nov. 1976		12 Nov. 1976		13 Nov. 1976	
TIME	OZONE	TIME	OZONE	TIME	O_3	TIME	O_3	TIME	O_3
0758	337	0819	333	0658	322	0658	321	0911	317
0954	336	1000	329	0712	324	0754	319	1052	324
1307	346	1500	330	0729	315	0758	326		
1614	347	1549	327	0726	314	1617	327		
1642	347			0826	318	1702	335		
				1545	323				
				1622	326				
				1634	330				

HOBART (Lat 42° 54'S 147° 20'E)

9 Nov. 1976		10 Nov. 1976		11 Nov. 1976		12 Nov. 1976		13 Nov. 1976	
TIME	O_3	TIME	O_3	TIME	O_3	TIME	O_3	TIME	O_3
0758	351	0812	355	0658	336	0739	324	1057	328
1052	323	1002	344	0806	332	0906	316	1205	294
1320	318	1313	345	0904	326	1008	310	1301	286
1547	356	1512	361	1006	317	1322	302	1510	319
1628	355			1057	311	1517	319		
1704	347			1202	317				
1745	347			1410	325				
				1508	326				
				1609	330				
				1716	339				

(*All times are in Eastern Standard Time (E. S. T.), to get G. M. T., subtract 10 hours.)

TABLE II. (cont.)

CAIRNS (Lat. 16° 55'S 145° 44'E)

9 Nov. 1976		10 Nov. 1976		11 Nov. 1976		12 Nov. 1976		13 Nov. 1976	
TIME	O_3	TIME	O_3	TIME	O_3	TIME	O_3	TIME	O_3
0944	295	1000	289	1100	292	1133	312	1133	294
0955	297	1009	269	1120	294	1143	299	1147	294
1345	296	1415	286	1300	292	1400	300	1259	295
1405	295	1430	279	1328	291	1410	295	1326	294

BRISBANE (Lat. 27° 28'S Long. 153° 02'E)

9 Nov. 1976		10 Nov. 1976		11 Nov. 1976		12 Nov. 1976		13 Nov. 1976	
TIME	O_3	TIME	O_3	TIME	O_3	TIME	O_3	TIME	O_3
1100	330	1035	272	1256	355	1255	307	1032	328
1132	338	1053	265	1312	356	1317	301	1059	328
1202	302	1108	286	1049	350	0923	312	1130	328
1212	312	1118	282	1107	342	0940	309	1204	328

MACQUARIE ISLAND (Lat. 54° 29 S 158° -58'E)

10 Nov. 1976		11 Nov. 1976		12 Nov. 1976		13 Nov. 1976		14 Nov. 1976	
TIME	O_3	TIME	O_3	TIME	O_3	TIME	O_3	TIME	O_3
		0554	399	0541	377	0542	365	0542	372
0603	387	0702	377	0712	371	0740	358	RAIN	
0715	387	1026	359	1210	347	1004	347		
1012	365	1351	363	1400	372	1053	358		
1315	330	1514	376	1520	362				
1539	376								

15 Nov. 1976	
TIME	O_3
0538	355
0715	358
0947	328
1230	355
1511	321

NASA CV-990 Interlatitude Survey

November 1976

Australian Support Data

ATMOSPHERIC CARBON DIOXIDE CONCENTRATIONS OVER SOUTH EAST AUSTRALIA DURING NOVEMBER 1976

G.I. Pearman
D.J. Beardsmore
CSIRO
Division of Atmospheric Physics
Aspendale.

INTRODUCTION

The CSIRO Division of Atmospheric Physics has conducted an extensive aircraft air sampling programme since 1972, primarily for the purpose of investigating the space and time variations of carbon dioxide (CO_2) in the troposphere and lower stratosphere (Pearman and Garratt, 1973). The purpose of the present study was to provide a data base for comparison with measurements made on board the CV 990 Galileo II, by the GASP (Global Atmospheric Sampling Program) CO_2 instrument. The data base consists of four parts:

(a) Routine measurements made on air samples collected from commercial and government aircraft during November.

(b) Measurements made on 16 samples collected from a light aircraft which flew over Cape Grim and Aspendale within a few hours of the CV 990's flight number 9 on November 11th.

(c) Measurements made on 12 samples collected from the WSU halocarbon air intake on the CV 990 during flight number 9.

(d) Surface measurements made by in situ analysis equipment at Cape Grim and Aspendale.

Figure 1 shows the position of the various locations mentioned in the text.

SAMPLING AND MEASUREMENT

Air samples were collected from cabin air outlets (turbine compressed) or rammed air intakes, using peristaltic or bellows pumps (see Table 1 for details). Low altitude samples were dried before collection using magnesium perchlorate. Half litre glass flasks were first flushed for 2-5 mins and then the sample was compressed to $\sim$1 atmosphere above cabin pressure.

All samples were returned to Aspendale for analysis using a UNOR 2

(Maihak, Hamburg) non-dispersive infrared CO_2 gas analyser. This is a differential instrument with a range of ±20 ppmv (parts per million by volume) about a reference gas and a resolution of <0.2 ppmv. All measurements were made by comparison of the sample air with CO_2/N_2 (nitrogen) gas mixtures contained in 50 lt tanks at pressures of 100-150 atmospheres. These tanks were in turn calibrated before and after the measurements by comparison with WMO secondary standard CO_2/N_2 mixtures provided by the Scripps Institution of Oceanography. Before presentation of all data, the necessary conversions to the WMO 1974 CO_2 calibration scale were made and the corrections for the instrument carrier gas error applied (see Pearman and Garratt, 1975 and Pearman, 1977 for a discussion of the international CO_2 calibration system and the carrier gas error). The precision of the CO_2 data presented below is better than 1 ppmv.

In situ measurement at Aspendale were made using an air intake above the roof of the laboratory (∿10m) and the same instrument as used for the flask measurements. A second UNOR 2 is permanently installed at Cape Grim, the temporary location of the Australian baseline air monitoring station. This instrument operates continuously, being calibrated automatically each hour. The Cape Grim data was also corrected as described above before presentation.

RESULTS AND COMMENTS

In table 2 we list all of the CO_2 data collected from the routine CSIRO air sampling programme during November 1976. These demonstrate the lack of large time and space variations in CO_2 concentration in the middle and upper troposphere. The mean concentration of 33 samples collected from the F27 aircraft during November was 331.3 ppmv (σ = 0.3) and during October, 331.2 (σ = 0.6, N = 22). Data collected on these flights since 1972 have shown an annual cycle of monthly mean concentration of ∿1 ppmv with an annual increase in concentration of ∿0.8 ppmv. One standard deviation about the monthly means is always <1 ppmv.

The results of analyses made on flask samples collected on the day of the CV 990 flight 9 are shown in Table 3. The exact position of the CV 990 can be obtained from the flight records using the recorded time of samping. For the purpose of this presentation we have grouped the CV 990, PA 39 and ground station measurements according to geographical area.

The coherence of the data from these three sources is demonstrated in Figure 2 where they are plotted against collection altitude above MSL.

On the day of flight 9, south eastern Australia generally experienced near northerly winds in the lower kilometer of the atmosphere whereas in the middle and upper troposphere winds were generally in the west (see flight record and Figure 3). At Cape Grim local surface winds were from the east. Thus air arriving at both Cape Grim and Aspendale had traversed land and as might be expected, was influenced by the activity of the surface vegetation. Figure 2 shows how surface concentrations at Aspendale decreased from 332.6 ppmv at 2340 Z (0940 EST) to 324.5 ppmv at 0338 Z (1338 EST). A similar day time drawdown in concentration occurred at Cape Grim. A discussion of the vegetation effects on boundary layer CO_2 concentrations is given by Garratt and

Pearman (1973).

The upper altitude samples were taken at about tropopause heights, which could account for the concentration of these samples being slightly lower than that for middle tropospheric samples.

REFERENCES

Garratt, J.R. and Pearman, G.I. 1973. CO_2 concentrations in the atmospheric boundary-layer over south-east Australia. Atmos. Environ. 7: 1257-1266.

Pearman, G. I. and Garratt, J.R. 1973: Space and time variations of tropospheric CO_2 in the southern hemisphere. Tellus 25: 309-311.

Pearman, G.I. and Garratt, J.R. 1975: Errors in atmospheric CO_2 concentration measurements arising from the use of reference gas mixtures different in composition to the air sample. Tellus 27: 62-65.

Pearman, G.I. 1977: Further studies of the comparability of baseline atmospheric CO_2 measurements. Tellus 28: In Press

Table 1

Details of aircraft and sampling techniques used

Aircraft	B707 Boeing 707	F27 Fokker Friendship	PA39 Piper Commanche	CV 990 Convair 990
Agency	Qantas	Dept. of Transport	Private Hire	NASA
Altitudes	10-12 km	3-5 km	0-5 km	3-12 km
Collection	Cockpit air-conditioning outlet. Pressurization with peristaltic pump.	Cabin air conditioning outlet. Air dried with magnesium perchlorate and pressurized with peristaltic pump.	Rammed air intake with drying and pressurization as for F27.	Rammed air intake with pressurization with s.s. bellows pump. (WSU system).

Date 1976	Air-craft	Flight No.	Flask	Time (Z)	LOCATION SECT.	DIST.	DIR.	DME	Altitude (km)	CO_2 (ppmv)
Nov. 6	B707	Q99	20	0400	3	930	4	5	10.06	331.2
			19	0400	3	930	4	5	10.06	331.0
			16	0400	3	930	4	5	10.06	330.8
Nov. 8	F27	D137	39	2338	1	131	2	16	4.25	331.6
			38	2345	1	117	2	16	4.25	331.7
			37	2349	1	91	2	16	4.25	331.5
			36	2352	1	77	2	16	4.25	331.5
			34	2356	1	58	2	16	4.25	331.6
Nov. 9	F27	D137	33	0632	1	60	1	16	3.95	330.9
			30	0635	1	73	1	16	3.95	331.4
			29	0637	1	161	5	7	3.95	331.3
			28	0640	1	139	5	7	3.95	331.0
			27	0643	1	119	5	7	3.95	331.1
Nov. 15	F27	D138	27	2244	1	128	5	7	4.55	331.3
			28	2249	1	159	5	7	4.55	331.3
			29	2258	1	155	1	1	4.55	331.3
			30	2303	1	124	1	1	4.55	331.2
			33	2308	1	93	1	1	4.55	331.5
Nov. 16	F27	D138	34	0054	1	142	8	44	4.85	331.1
			36	0100	1	186	8	44	4.85	331.4
			37	0105	1	131	4	42	4.85	331.4
			38	0110	1	93	4	42	4.85	331.3
			39	0115	1	66	4	42	4.85	331.4
Nov. 22	F27	D139	27	2232	1	197	1	1	4.55	331.3
			28	2235	1	181	1	1	4.55	331.2
			30	2246	1	115	1	1	4.30	331.3
			33	2249	1	95	1	1	3.90	331.3
Nov. 23	F27	D139	34	0030	1	130	8	44	4.85	331.4
			38	0043	1	140	4	42	4.85	331.6
			39	0047	1	109	4	42	4.85	331.7
Nov. 30	F27	D140	27	0410	2	18	8	3	4.05	331.5
			28	0414	2	16	4	3	4.05	331.2
			29	0418	2	44	4	3	4.05	330.5
			30	0422	2	67	4	3	4.05	330.2
			33	0426	2	99	4	3	4.05	331.2
			36	0434	2	102	8	12	4.05	330.7

TABLE 2

Details of routine CSIRO air sampling flights and measured carbon dioxide concentrations for November 1976.
Location code: SECT - Sector as in Figure 1
DIST - Distance in km from DME station.
DIR - Direction from DME station (1-North, 2-NE, 3-East, etc.)
DME - Distance measuring equipment station number (see Figure 1 for location of stations).

Time (Z)	Aircraft Type	Height Above M.S.L. (km)	CO_2 Concentration (ppmv)
NORTH WEST TASMANIA AREA			
2132	CV 990	11.29	331.5
2154	"	6.41	332.4
2205	"	3.10	331.5
2236	PA 39	0.91	330.3
2243	"	1.52	330.8
2249	"	2.13	331.1
2258	"	3.05	331.3
2313	"	4.27	331.9
2316	"	4.27	332.0
2325	"	3.66	331.6
2333	"	2.74	331.2
2345	"	1.52	331.7
0002	"	0.30	330.5
0007	"	0.15	330.6
0010	"	0.11	331.3
0013	"	1.01	330.9
0019	"	1.52	331.2
2300	BASELINE	0.09	330.8
0000	STATION	0.09	330.5
0100	CAPE GRIM	0.09	329.4
TASMANIA SECTOR-OUTSIDE N.W. area			
2229	CV 990	8.54	332.4
2244	"	11.90	331.4

Time (Z)	Aircraft Type	Height Above M.S.L. (km)	CO_2 concentration (ppmv)
MELBOURNE-WESTERNPORT AREA			
2112	CV 990	11.29	331.9
2319	"	11.90	331.7
2331	"	7.61	332.1
2336	"	7.62	332.5
2352	"	3.12	330.2
2359	"	3.11	330.3
0335	PA 39	1.22	331.6
0339	"	0.61	327.5
2340 ± 20	GROUND STATION ASPENDALE	0	332.6
0338 ± 8		0	324.5
VICTORIAN SECTOR-OUTSIDE MELB-W/PORT			
2039	CV 990	11.28	331.9
VIC-TAS SECTORS MONTHLY MEAN CO_2 CONCENTRATIONS			
OCT 1976	F 27	3.65-4.30	331.2 (N=22, σ=0.6)
NOV 1976	"	3.90-4.85	331.3 (N=33, σ=0.3)

Table 3

Carbon dioxide measurements made on air samples collected on November 10th and 11th (Z time) during the CV 990 flight 9 and PA 39 flight. Surface measurements at Cape Grim and Aspendale (Melbourne-Westernport area) are included together with monthly mean concentrations measured during routine sampling in October and November.

Figure 1

Map of south eastern Australia showing localities mentioned in the text. Each numeral represents a station equipped with distance measuring equipment (DME) from which sampling points are located in Table 2.

DME Station Number	Location	DME Station Number	Location
1	Wynyard (Tas.)	12	Mount Gambier (S.A.)
3	Meningie (S.A.)	16	King Island (Tas.)
5	Sydney (N.S.W.)	42	Wonthaggi (Vic.)
7	Melbourne (Vic.)	44	Launceston (Tas.)

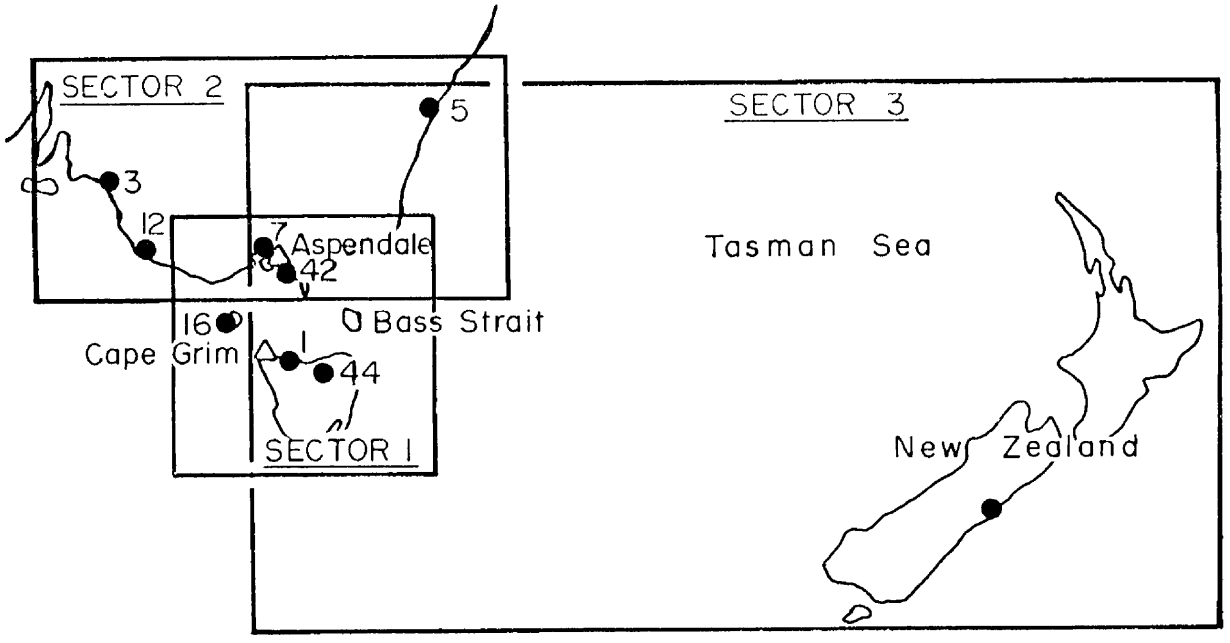

FIG. 2 Variation of CO_2 concentration with height — 11th Nov. 1976

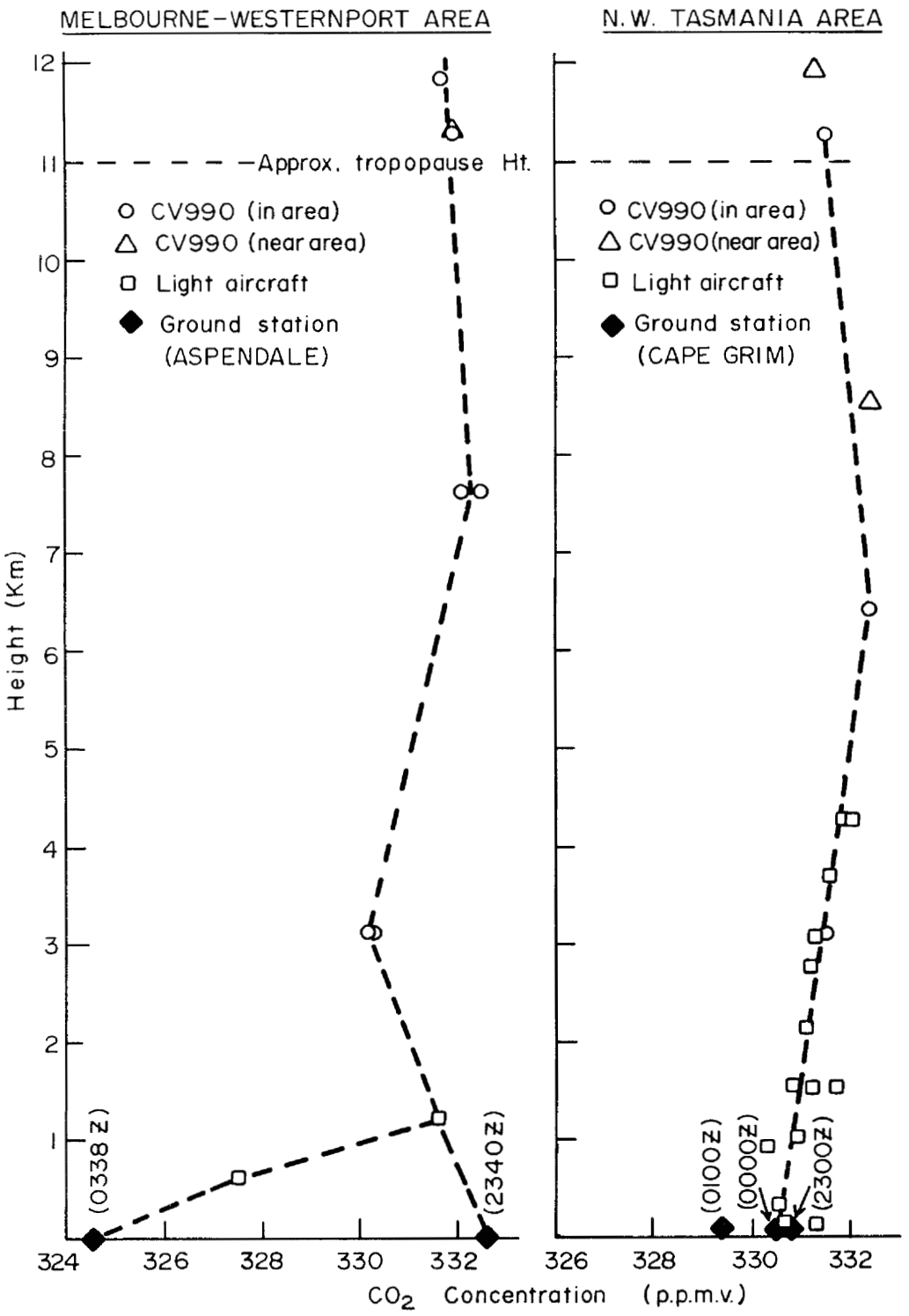

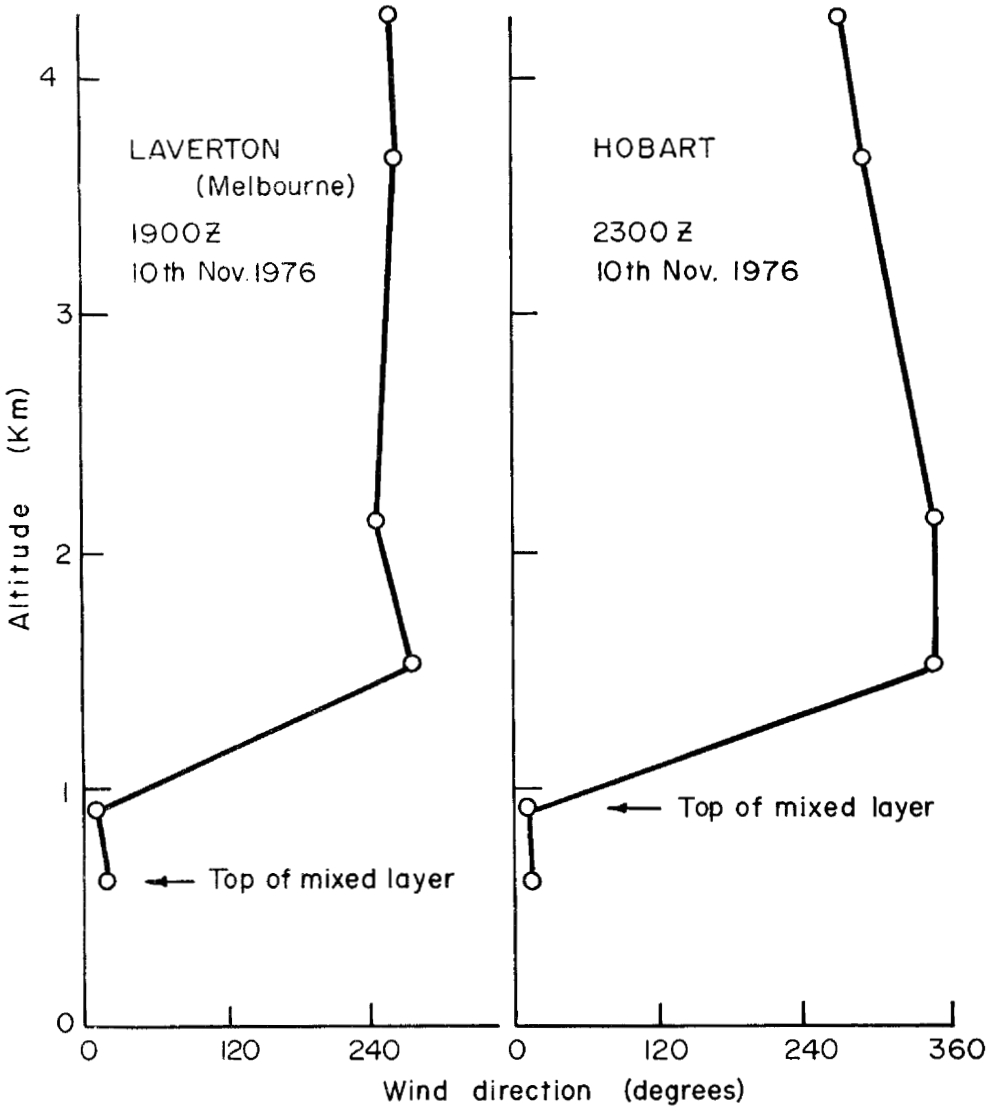

FIG. 3 Wind direction at different altitudes over Melbourne and Hobart on the day of CV990 Flight 9.

NASA CV 990 Interlatitude Survey

November 1976

Australian Support Data

STRATOSPHERIC WATER VAPOUR

P. Hyson
CSIRO
Division of Atmospheric Physics
Aspendale

INTRODUCTION

The CSIRO stratospheric water vapour monitoring program was initiated in the early 1970's to obtain data on the stratospheric water vapour content over Australia and observe seasonal and latitudinal and secular variations.

Measurements were commenced in November 1972 and have taken place on approximately a bi-monthly basis. The program is supported by the Australian HIBAL balloon launching facility in Mildura.

Under the auspices of the Climatic Assessment Program an intercomparison flight took place at Laramie, Wyoming, USA in July 1974. Data from the instrument were compared with those from a "Panametrics" aluminum oxide sensor. The results were reported by Laby et al. 1974.

A second instrument (Mark 2) of slightly different dimension, but of identical design concept has been flown for comparison and replacement purposes.

Hibal flight 664, launched on 11th November 1925 Z was undertaken to coincide with NASA CV 990 flight 10 for comparison of water vapour, carbon dioxide, and halocarbon data (our Division of Atmospheric Physics) as well as aerosol data (CSIRO Division of Cloud Physics, Sydney). The grab sample collection program for carbon dioxide and halocarbons is in the initial stages. The samples still appear to be contaminated and will therefore not be submitted for this comparison. This report deals with the stratospheric water vapour data only.

METHOD

The instrument is an infrared radiometer, which measures the emission of radiation by water vapour in the far infrared (40-200μ) from two zenith angles (nominally 45° and 70°). A Golay cell senses the difference between the radiation at these zenith angles and that just below the horizon sequentially at a rate of approximately once per minute. The emission below the horizon serves as a reference black body emission at ambient temperature.

The signal is amplified, rectified and recorded on a Rustrak and/or cassette recorder (the later after frequency modulation of the ac signal).

The data is used to compute a parameter "Q", where $Q = \frac{S_{45}-S_{70}}{S_{45}+S_{70}}$, and S is the difference between the below horizon emission and that at one of the zenith angles. The Q parameter is then compared with computed values of the reduced water path based on Goody's random model absorption data (Goody 1964) for a range of water vapour mixing ratios and a temperature of 216°C, and the best fit is adopted as the observed reduced water path, from which the precipitable water and mixing ratio may be deduced. A detailed description of the instrument and method of data reduction may be found in Hyson and Platt 1974.

RESULTS

The data obtained on the 12th November 1976 from instrument Mark I is shown in Fig. 1, where the Q parameter is displayed versus height. Fig. 2 shows the theoretical data of the reduced water path u_o above the instrument for various higher zenith angles (the other zenith angle is a constant 22° lower) to allow for deviations of the higher zenith angle from the nominal 70°. Since the actual zenith angle was 68° the values of the reduced water path may be obtained by interpolation from Fig. 2. These values are plotted in Fig. 3 and converted to precipitable water in Fig. 4. The oblique lines indicate constant mixing ratios. The corresponding mixing ratios computed over 1 km intervals are displayed in Fig. 5.

Instrument Mark 2 returned a set of data which was clearly erroneous in that the deduced precipitable water would have to be increasing with height over the interval between 14 and 20 km. The reason for the failure of the instrument has not yet been established.

COMMENTS

1. The indicated tropopause level is 14.5 km on the basis of 0000 Z sonde flights from Adelaide and Cobar. On this flight the mixing ratio reached its first minimum at tropopause level.

2. Below the tropopause, the scale height for water vapour is approximately 2.4 km. The height over which the precipitable water decreases by 1/e is approximately 1.1 km. The value for λ (Louis and McQueen 1970) is approximately 4.0.

3. The precipitable water amount of CV 990 flight level 36000' was about 34μm, and the local mixing ratio 30 ppm.

REFERENCES

Laby, J.E., P. Hyson, J.M. Rosen & D.J. Hofmann, "Stratospheric flight comparison of aluminum oxide and infrared radiometric water vapour sensor." Report # GM-23, Department of Physics and Astronomy, University of Wyoming, August 1974.

Goody, R.M. "Atmospheric Radiation, Part I", Oxford University Press, London, 1964.

Hyson, P. & C.M.R. Platt, 1974, "Radiometric measurements of stratospheric water vapour in the Southern Hemisphere" J.G.R. 79, pp. 5001-5005.

Louis, J.F. & R.M. McQueen, 1970 "Spectroscopic observations of water vapour near the tropopause" J. Appl. Meteor. 9. pp. 722-724.

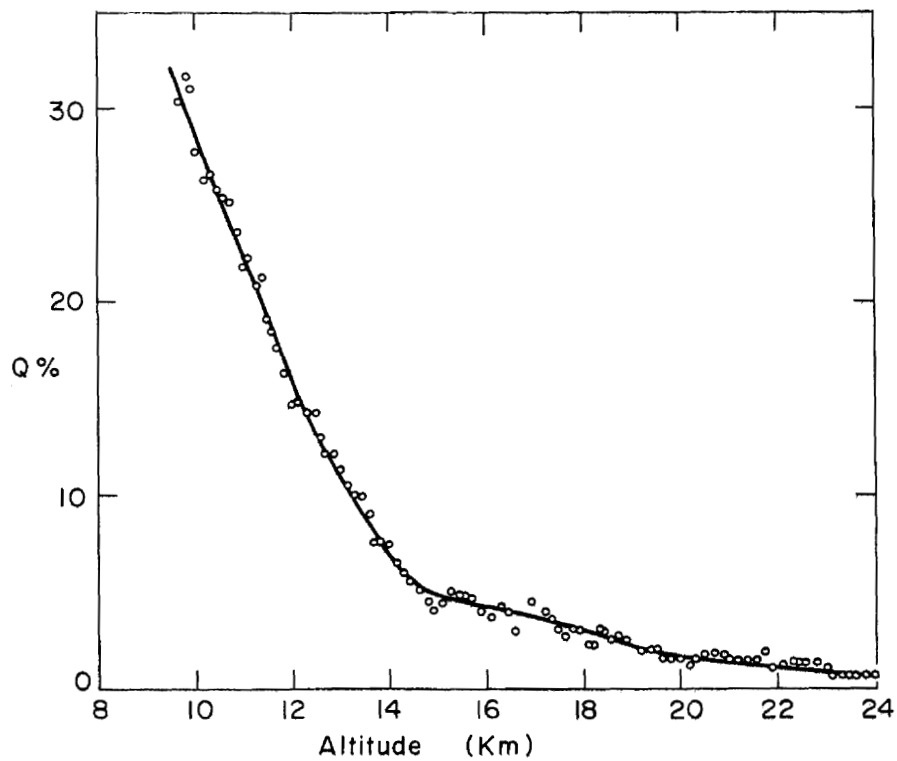

Figure 1. - Data points of Q parameters versus altitude, Hibal flight 664, November 12th 1976.

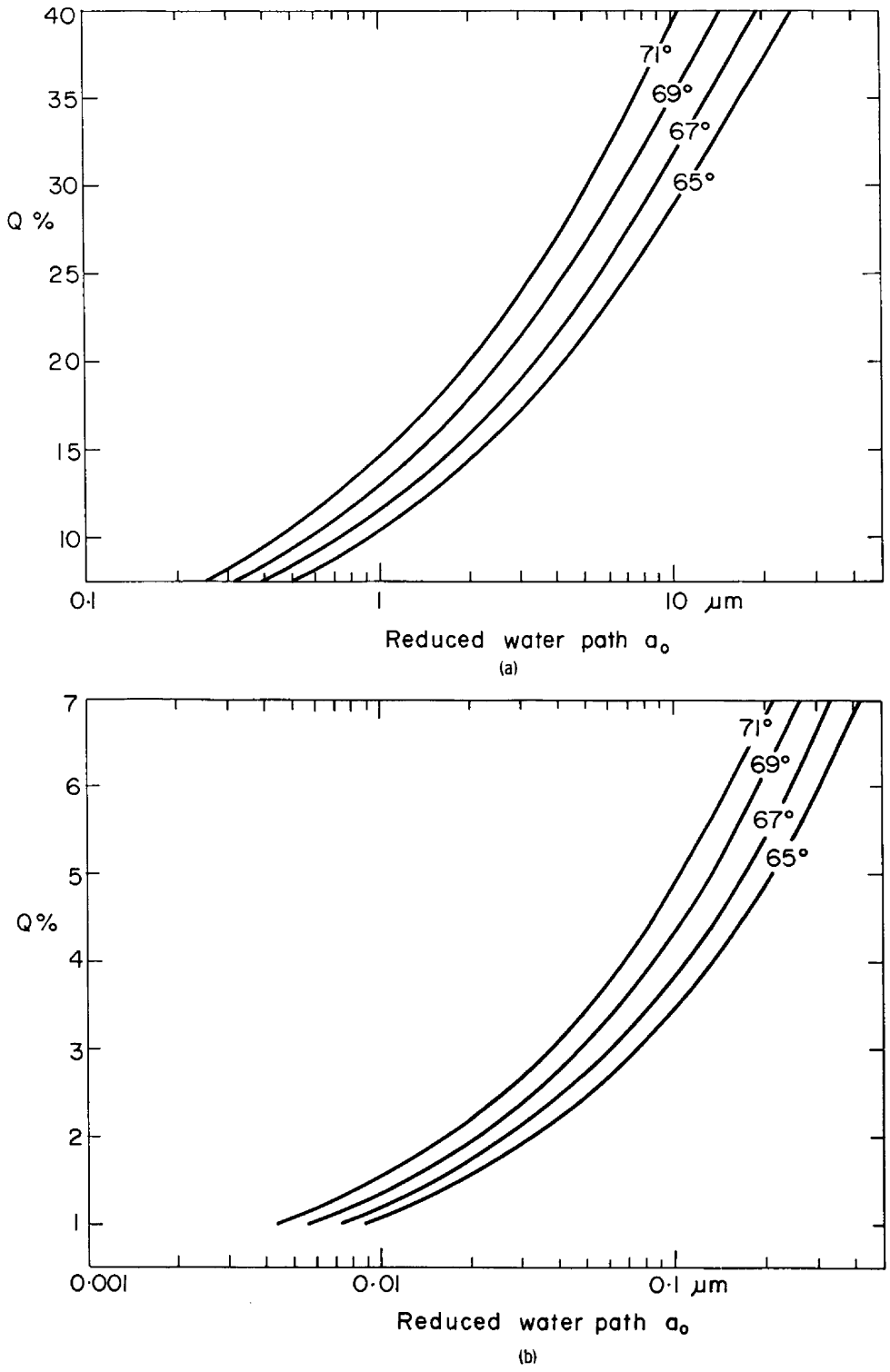

Figure 2. - Computed values of Q parameter versus reduced water path (a_0) for various zenith angles.

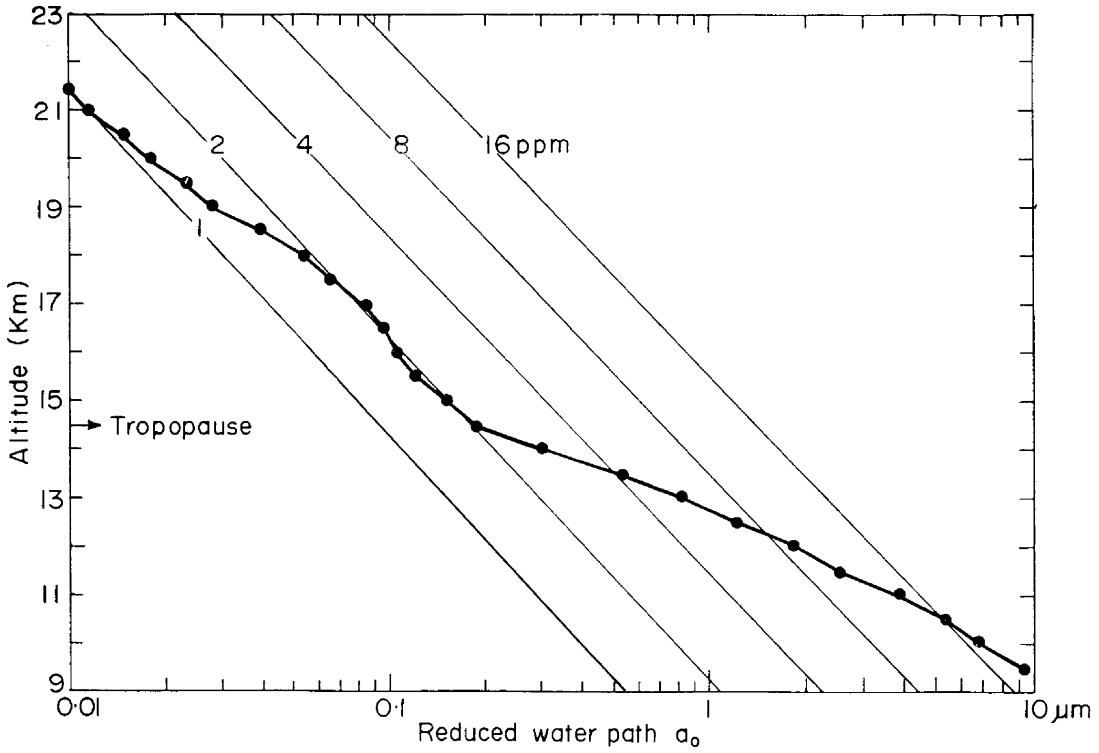

Figure 3. - Deduced reduced water path (a_0) versus altitude. The oblique lines are isopleths of constant mixing ratio.

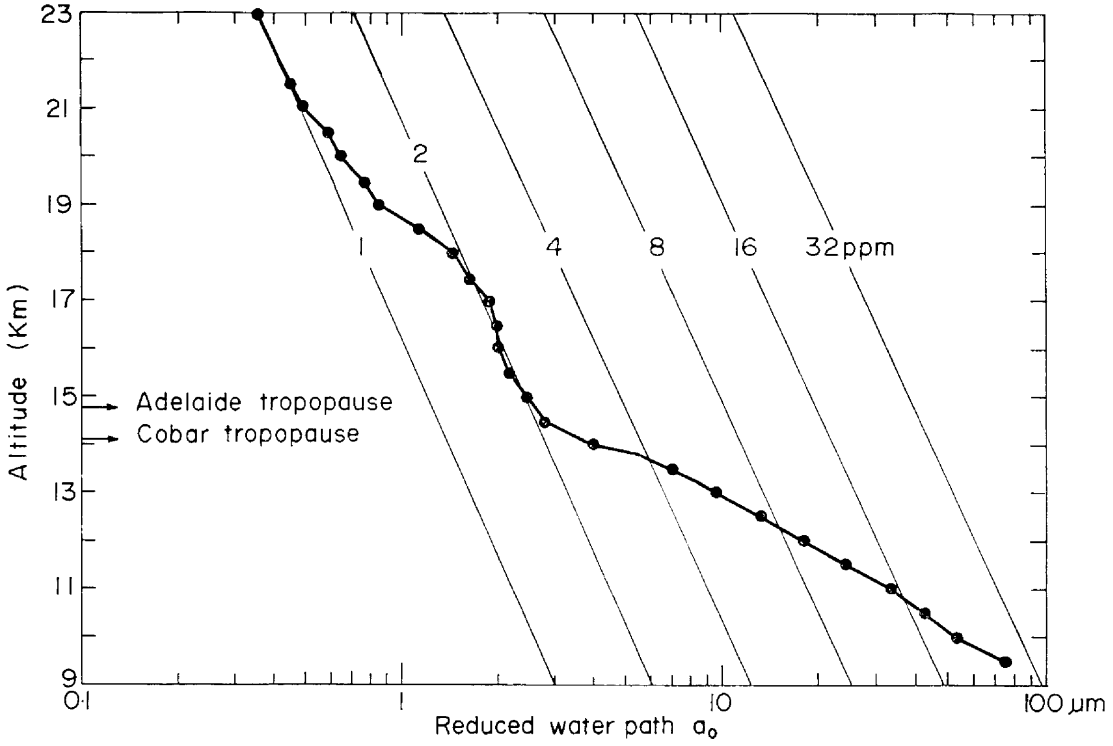

Figure 4. - Precipitable water (a) versus altitude. Mildura November 12th 1976.

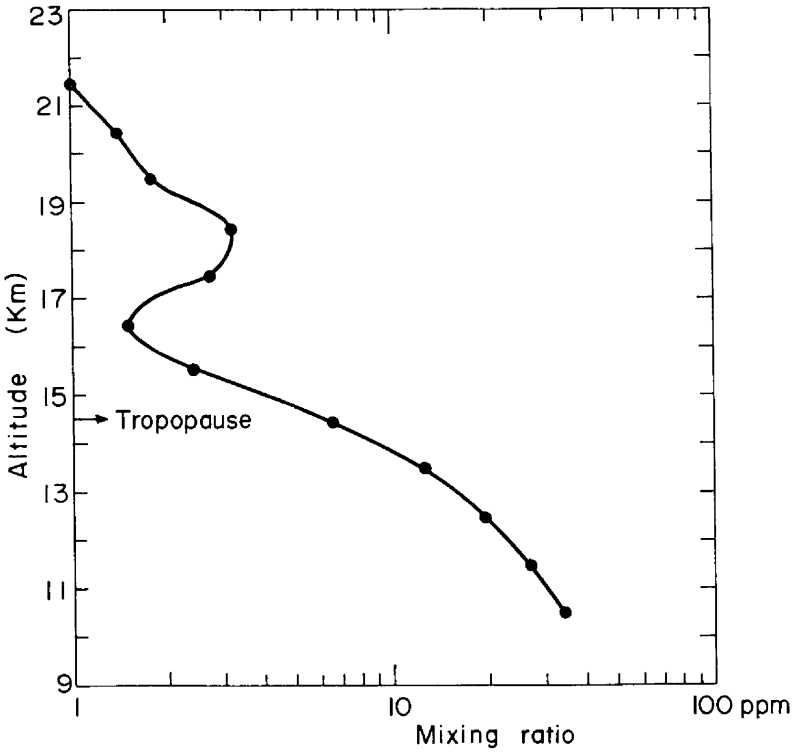

Figure 5. - Mixing ratio versus altitude. Mildura November 12th 1976.

NASA CV 990 Interlatitude Survey

November 1976

Australian Support Data

LIDAR MEASUREMENTS OF TROPOSPHERIC AEROSOLS

A.C. Dilley
CSIRO
Division of Atmospheric Physics
Aspendale

INTRODUCTION

The measurements described in this paper were made with a view to obtaining lidar derived vertical profiles of the aerosol backscatter coefficient and the aerosol extinction coefficient and comparing these, where appropriate, with profiles of aerosol properties derived from measurements made on board the NASA CV 990 aircraft. Such comparisons provide, firstly, a basis for assessing the validity of the methods of measurement and analysis employed, and, secondly, experimental data on which empirical relationships can be based and against which theoretical models can be tested.

METHODS

(a) The Instrument The lidar system employed here is the tenth in a series of systems developed and constructed by Stanford Research Institute. Its main features are summarized in Table I. A few of these require some explanation. The energy monitor records the integral of the output power envelope as sensed by a HP 4203 pin photo-diode located in the transmitter. The PMT modulated gain control used in the measurements reported here compensates for the inverse-range-squared decrease of the return signal in the range 0 - 7,500 m. The Biomation 8100 digitizer samples the analogue return signal over 2 nS intervals and stores an 8-bit digital representation of its value into one of 2048 memory locations at a maximum rate of 1 sample per 10 nS. The recording process is initiated when the pin photo-diode senses a laser pulse. At the conclusion of the recording interval all data relevant to the firing are transferred under computer control to the magnetic tape unit.

(b) Procedure The lidar was sited at Aspendale, Victoria (38°02'S, 145°06'E). A total of 111 shots were fired between 0024Z and 0056Z (1124 and 1156 EST) on the morning of the CV 990 overflight (11th November, 1976). Eighty of these shots were part of 5 separate scanning sequences in which the lidar was stepped in 5° increments from 15° elevation to 90° elevation. The first 2 such sequences were recorded with the lidar being fired towards the North, the remaining sequences with it being fired towards the East. Four of the scanning sequences were recorded with a maximum range of 15 km and one with a maximum range of 3 km. The remaining shots were fired at angles and ranges selected to give additional data on specific features in the profile.

(c) Analysis The equation describing a lidar return signal may be written

$$v_r = KE_t r^{-2} \beta_r \, e^{-2\int_0^r \sigma(r')dr'} \tag{1}$$

where v_r is the voltage developed across a fixed load resistance by the signal from a range r

K is a system constant

E_t is the energy of the transmitted light pulse

β_r is the backscatter coefficient at range r

$\sigma(r')$ is the extinction coefficient as a function of range

In the past, the system constant, K, of the lidar system employed here has been determined by making the assumption that the atmosphere was free of aerosols at some height, c, where the signal was very small (hence β_c = Rayleigh backscatter coefficient) and using separate measurements to determine the integrated backscatter coefficient. The present set of measurements could be used similarly to give a more soundly based estimate of K. Success in this approach depends on whether a layer of sufficiently clean air was encountered above the lidar site during the overflight and whether ancilliary measurements are available which would yield a sufficiently accurate estimate of the integrated extinction coefficient.

Hamilton (1969) has suggested a method which allows both backscatter and extinction profiles to be calculated from a series of lidar returns for which the angle of elevation of firing, θ, has been varied. The equation describing such returns may be written

$$v_h = KE_t (h \operatorname{cosec} \theta)^{-2} \beta_h \, e^{-2\int_0^h \sigma(h')\operatorname{cosec}\theta \, dh'} \tag{2}$$

$$h = r \sin \theta \tag{3}$$

Hence,

$$\ln\left(\frac{v_h h^2 \operatorname{cosec}^2 \theta}{KE_t}\right) = \ln \beta_h - 2 \operatorname{cosec} \theta \int_0^h \sigma(h')dh' \tag{4}$$

Thus, provided β_h and $\int_0^h \sigma(h')dh'$ are constant, i.e., the atmosphere is horizontally uniform, the plot of $\ln\left(\frac{v_h h^2 \operatorname{cosec}^2\theta}{KE_t}\right)$ against 2 cosec θ has an inter-

cept on the vertical axis of ln β_h and slope of $\int_0^h \sigma(h')dh'$. If the variation of temperature with height is known, the Rayleigh component of the backscatter and extinction coefficients can be calculated and subtracted to give vertical profiles of the aerosol coefficients.

RESULTS

Lidar data are currently being analysed along the lines outlined above. To date, however, no profiles of aerosol properties have been produced.

A representation of a typical return is shown in Fig. 1. The background information relevant to this shot is contained in Table 2. Since the elevation angle is 90° the range converts directly to height. The return shows a low level peak in backscattered energy at about 320 m. A second broad band of enhanced backscattering lies between 1,450 m and 5,650 m with relatively cleaner air lying beneath and between the cloud layers centred on 7,900 m and 9,000 m. A third minor band of enhanced scattering can be seen lying in the height range 9,900 m to 10,900 m.

REFERENCE

Hamilton, P., 1969. Lidar measurement of backscatter and attenuation of atmospheric aerosol. Atmos. Environment, 3, pp. 221-223.

TABLE 1. SRI MK X LIDAR DETAILS

Transmitter:	ruby laser, Q switched through Pockels cell.	
	peak energy	2.0 J
	wavelength	694.3 nm
	pulse duration	20-30 ns
	pulse divergence	∿0.5 mR
	energy monitor	
Receiver:	Schmidt - Cassegrain telescope	
	mirror diameter	36 cm
	narrow-band-pass filter	0.9 nm
	acceptance angle	0.5 - 15 mR
	RCA 7265 PMT (S20 spectral response) with modulated gain control for range compensation	
Recorder:	Biomation 8100 fast transient digitizer	
	Hewlett-Packard 7970 B 7-track magnetic tape unit	
	Hewlett-Packard 2100 computer with 16K memory	

TABLE 2. DETAILS OF PLOT OF LIDAR DATA SHOWN IN FIG. 1

x - axis:	digitizer memory locations	
y - axis:	digitizer memory contents	
Scaling:	multiply x-ordinate by 10^3	
	multiply y-ordinate by 10^2	
Date:	11th November, 1976	
Time:	0041 Z (1141 EST)	
Shot no.:	64	
Elevation:	90^o	
Range:	Digitizer memory location	range m
	400	2,644
	800	5,642
	1,200	8,640
	1,600	11,638
	2,000	14,636

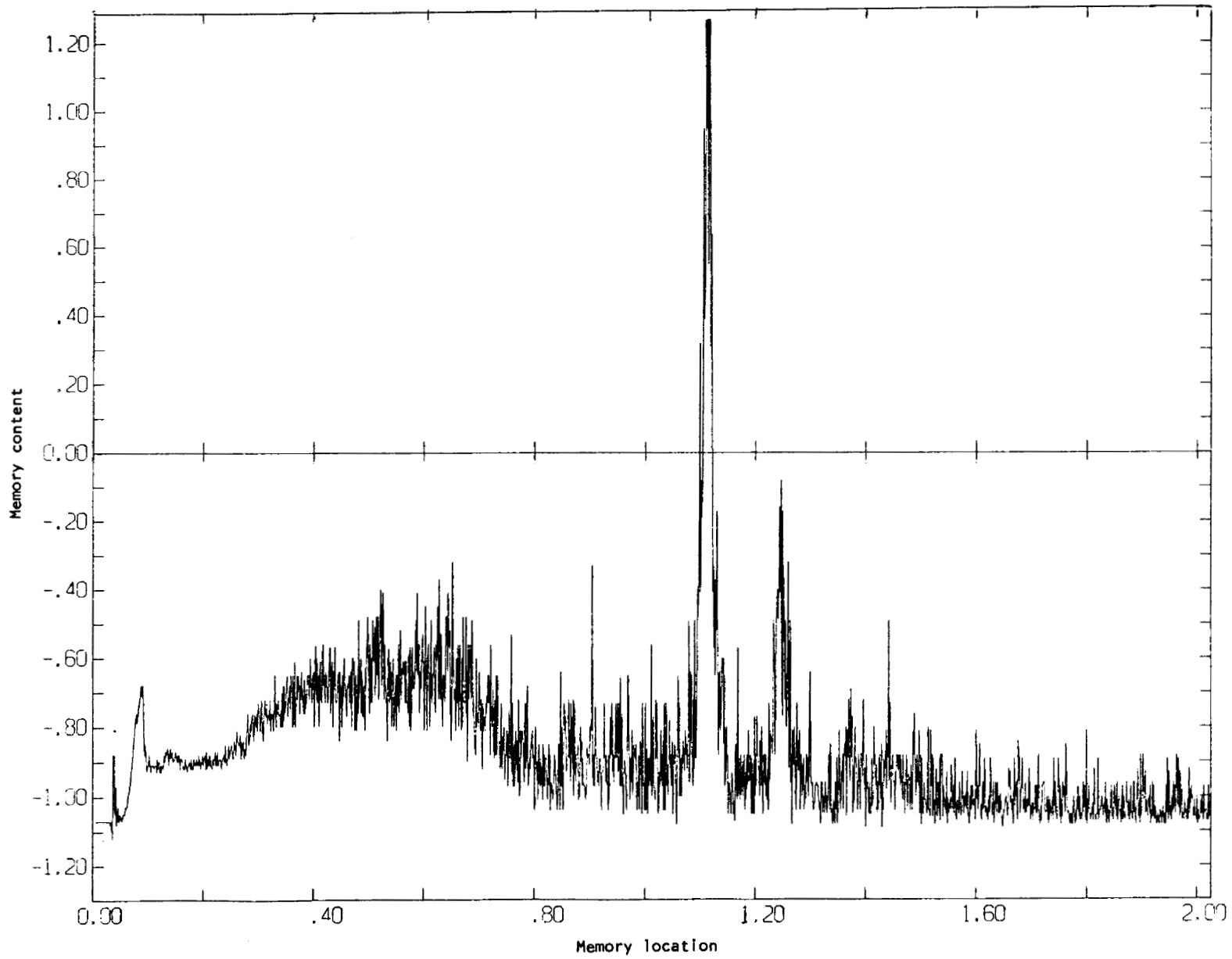
1.20
1.00
.80
.60
.40
.20
0.00
-.20
-.40
-.60
-.80
-1.00
-1.20
Memory content
0.00
.40
.80
1.20
1.60
2.00
Memory location

Figure 1

NASA CV 990 Interlatitude Survey

November 1976

Australian Support Data

DIRECT SAMPLING OF ATMOSPHERIC AEROSOLS

J. L. Gras
CSIRO
Division of Cloud Physics
Sydney, N.S.W.

Jean Laby,
Physics Dept. (RAAF Academy)
University of Melbourne
Melbourne, Vic.

The Division of Cloud Physics and the Physics Dept. (RAAF Academy) University of Melbourne have collaborated since early 1975 on an investigation of the southern hemisphere stratospheric aerosol. This has taken the form of approximately bi-monthly balloon soundings from Mildura Australia (34.2°S 142.1°E). On these flights aerosol concentrations are determined independently using two fundamentally different techniques.

The CSIRO technique is to impact the aerosol, using a jet impactor, onto specially prepared electron microscope screens for laboratory analysis after collection. This analysis involves size sorting and counting as well as some simple chemical testing. This method is sensitive to aerosols in the size range of approximately r=0.05μm to 1μm at 10Km however, the lower size limit improves with increasing altitude. For example, at 21Km particles with radii greater than 0.006μm are collected at greater than 50% efficiency. For a more detailed description of the method of collection and analysis techniques as well as some recent results refer to Bigg (1975) or Gras (1976).

The University of Melbourne group uses an in situ optical counter to classify aerosol into two size ranges. This gives the concentration of particles with $r > 0.15\mu m$ and of particles with $r > 0.25\mu m$. This counter is the same construction as those used extensively by the University of Wyoming atmospheric physics group. The methods of operation and calibration and the analysis techniques have been well described in the literature; see for example Hofmann et al. (1975).

For the intercomparison with the NASA CV990 flight 9 a sounding (flight 663, 1.8 million cubic ft., Winzen) was scheduled for November 10, 1925 Z. The flight was aborted as a result of parachute shroud lines fouling the launch arm, and a second flight was scheduled to coincide with CV990 flight 10. This flight (664, 1.8 million cubic ft., Winzen) was successfully launched on November 11, 1925 Z by the B.L.S. crew and reached a maximum altitude of 34.7Km (114Kft).

The CSIRO impactor operated from an altitude of 10Km to the maximum altitude (also on descent) and the University of Melbourne counter operated from ground level to maximum altitude (also on descent).

Atmospheric temperature, wind strength and wind direction were also determined for the flight. Analysis of all results is proceeding.

REFERENCES

Bigg, E.K. Stratospheric Particles. J.Atmos.Sci., 32, 910-917. (1975)

Hofmann, D.J., J.M. Rosen, T.J. Pepin and R. G. Pinnick. Stratospheric Aerosol Measurements I: Time Variations at Northern Mid-Latitudes. J.Atmos.Sci., 32, 1446-1456. (1975)

Gras, J.L. Southern Hemisphere Mid-Latitude Stratospheric Aerosol after the 1974 Fuego Eruption. Geophys. Res. Lett., 3, 533-536. (1976)

NEW ZEALAND METEOROLOGICAL SERVICE

DATA REPORT FROM THE NEW ZEALAND REGION, NASA CV-990 LATITUDINAL SURVEY MISSION, NOVEMBER 1976

E. Farkas

GENERAL:

Flight-routes of the CV-990 instrumented aircraft passed over New Zealand regions on the 13, 14 and 16 November. Ground-based supporting observations on these days consisted of vertical temperature and humidity soundings at various New Zealand Meteorological Stations near the times of the fly-over of the aircraft, combined vertical ozone, temperature and humidity soundings at Wellington, total ozone measurements at Wellington and Invercargill, and observations of vertical ozone distribution by the Umkehr method at Invercargill. For the three days, tabulations of hourly mean values of atmospheric CO_2 concentrations measured near Wellington were supplied by the Institute of Nuclear Sciences, Department of Scientific and Industrial Research, to be incorporated in this report.

PROGRAM DETAILS:

The following list gives details about the observing stations, instruments used, and times of observations.

Campbell Island (93944), 52°33'S, 169°07'E, 14.9 m AMSL
Combined Radiosonde/Radarwind flight.
Radiosonde type: VIZ Model 1092 ESSA Type 1680 MHZ
Release time: 14 Nov 0400 GMT.

Invercargill (93844), 46°25'S, 168°20'E, 0.3 m AMSL
Combined Radiosonde/Radarwind flights
Radiosonde type: Plessey Radar Model 1397-401, 72.2 MHZ
Release times: 13 Nov 0245 GMT
14 Nov 0400 GMT
Total ozone observations with Dobson spectrophotometer No.17
Umkehr observations with the same instrument of the vertical ozone distribution, 14 November, sunrise and sunset.

Christchurch Airport (93780) 43°29'S, 172°32'E, 29.6 m AMSL
Combined Radiosonde/Radarwind flights
Radiosonde type: Plessey Radar Model 1397-401, 72.2 MHZ
Release time: 13 November 0400 GMT.

Wellington (93434) 41°17'S, 174°46'E, 126.5 m AMSL
Combined Radiosonde/ozonesonde flights
Radiosonde type: Astor 72 MHZ
Ozonesonde type: Mast Model 730-7, slightly modified to be electronically compatible with the Astor Radiosonde.
Release times: 12 November 2200 GMT
13 " 0303 "
13 " 2319 "
15 " 2029 "
16 " 0339 "
Total ozone observations with a Canterbury filter photometer.

Baring Head 41°25'S, 174°50'E, 18 m AMSL
Atmospheric CO_2 concentration measurements
URASI infrared analyser
Data are referred to a world meteorological CO_2 in nitrogen standard (C.D. Keeling, Scripps Institution of Oceanography, 1974). Data have not been corrected for pressure broadening by oxygen.

Raoul Island (93997) 29°15'S, 177°55'W, 38.4 m AMSL.
Combined Radiosonde/Radarwind flights.
Radiosonde type: Plessey Radar Model 1397-401, 72.2 MHZ
Release time: 16 November 0400 GMT

TABULATION OF RESULTS:

The first group of tables (1.1-1.10) gives vertical temperature and relative humidity distributions from significant level data for each station and ascent. Wind data are not tabulated.

Tables (2.1-2.7) giving vertical distribution of ozone partial pressures follow, listing results of both the ozone-soundings at Wellington and the Umkehr observations at Invercargill. Both types of data were processed according to standard practices adopted by WMO.

The last group of tables (3.1-3.3) gives the hourly mean CO_2 concentrations in units of parts-per-million for each day. These units can be related to the mole fraction in dry air via the WMO Standard (Communication by Dr D.C. Lowe, Institute of Nuclear Sciences, D.S.I.R.).

Table 1.1 Radiosonde Data
Campbell Island, 93944
14 November 1976, 0400 GMT

Pressure mb	Height gpm	Temperature °C	RH %
1017		8.4	88
961	495	4.0	97
949	605	5.8	60
890	1105	5.6	33
883	1185	9.0	20
854	1445	10.0	14
740	2615	0.0	19
666	3465	-3.9	15
595	4355	-10.3	44
566	4740	-10.1	13
475	6055	-19.1	15
415	7050	-26.3	15
330	8650	-40.0	20
270	10000	-52.1	
215	11440	-59.5	
133	14545	-51.7	
96.0	16625	-52.1	
82.0	17680	-48.3	
38.0	22850	-43.1	
31.0	24175	-44.5	
26.0	25350	-42.3	
20.0	27090	-44.1	
10.0	31790	-39.7	

Table 1.2 Radiosonde Data
Invercargill, 93844
13 November 1976, 0245 GMT

Pressure mb	Height gpm	Temperature °C	RH %
1022		11.0	62
1002	165	8.6	34
884	1200	- 0.9	100
876	1260	1.4	49
856	1445	3.4	38
768	2345	2.4	35
721	2825	0.0	37
675	3355	- 3.3	36
598	4310	-11.5	38
534	5170	-14.5	32
356	8085	-40.0	38
254	10300	-48.7	
234	10815	-61.9	
217	11295	-55.5	
195	11980	-55.7	
164	13100	-51.3	
153	13530	-53.1	
132	14540	-53.5	
105	15990	-49.9	
82.3	17580	-51.3	
60.8	19560	-48.3	
51.0	20695	-49.5	
42.4	21960	-46.9	
29.3	24340	-46.9	
18.2	27275	-42.7	

Table 1.3 Radiosonde Data
Invercargill, 93844
14 November 1976, 0400 GMT

Pressure mb	Height gpm	Temperature C°	RH %
1015		18.8	55
929	760	11.6	46
854	1440	7.4	18
821	1765	7.6	13
714	2905	0.0	15
421	6900	-26.9	13
347	7885	-38.9	28
255	10330	-55.7	
233	10900	-59.1	
223	11180	-58.1	
209	11585	-61.5	
194	12050	-58.9	
187	12290	-54.9	
117	15340	-54.1	
107	15895	-51.1	
86.8	17185	-52.5	
58.8	19790	-50.1	
36.3	22925	-44.1	
25.8	25250	-47.9	

Table 1.4 Radiosonde Date
Christchurch Airport, 93780
13 November 1976, 0400 GMT

Pressure mb	Height gpm	Temperature C°	RH %
1016		10.2	76
995	195	7.4	65
943	645	3.4	97
921	820	2.4	76
894	1065	0.0	100
809	1870	-4.5	100
798	1970	-2.7	36
775	2215	-2.9	25
707	2940	-7.1	41
698	3035	-7.5	82
673	3325	-9.1	22
614	4045	-12.5	43
522	5250	-21.9	17
451	6295	-29.7	34
411	6950	-33.3	26
365	7785	-40.0	34
332	8420	-46.1	
278	9600	-54.9	
252	10200	-55.3	
245	10380	-52.3	
208	11455	-49.1	
161	13160	-52.1	
134	14375	-50.5	
111	15610	-53.7	
90.0	16935	-46.9	
78.0	17880	-51.3	
59.0	19715	-49.5	
52.0	20505	-52.1	
42.0	21955	-48.1	
27.0	24825	-48.1	

Table 1.5 Radiosonde Data
Wellington, 93434
12 November 1976, 2200 GMT

Pressure mb	Height gpm	Temperature °C	RH %
1001.0		9.9	67
912	880	0.7	81
899	1000	0.0	80
808	1850	-6.5	82
777	2155	-8.4	78
768	2255	-7.2	73
745	2485	-8.0	45
729	2680	7.1	29
661	3400	-11.4	52
522	5180	-23.7	79
393	7190	-40.0	71
338	8180	-49.5	
308	8790	-54.2	
288	9240	-54.5	
279	9465	-52.5	
276	9500	-50.7	
261	9870	-50.0	
243	10305	-46.1	
211	11265	-50.0	
172	12655	-49.0	
157	13250	-46.0	
119	15095	-54.5	
111	15515	-46.1	
97.0	16350	-52.5	
86.2	17145	-50.5	
78.0	17800	-52.2	
74.1	18100	-49.2	
50.6	20595	-54.2	
40.2	22130	-53.4	
33.2	23345	-48.6	
20.5	26500	-46.6	
10.0	31304	-42.4	

Table 1.6 Radiosonde Data
Wellington, 93434
13 November 1976, 0303 GMT

Pressure mb	Height gpm	Temperature °C	RH %
1000.8		10.3	65
893	1055	0.0	84
848	1470	- 2.6	85
814	1800	- 5.9	44
785	2075	- 5.1	57
746	2480	- 7.1	76
695	3040	-11.7	79
679	3210	-11.9	49
587	4300	-17.6	32
521	5180	-24.6	27
408	6910	-40.0	32
362	7710	-46.8	
317	8600	-48.1	
308	8795	-47.1	
232	10655	-51.1	
186	12125	-43.5	
151	13495	-51.8	
142	13895	-52.3	
135	14245	-49.2	
129	14540	-49.2	
110	15565	-56.0	
106	15760	-56.0	
103	15940	-51.2	
93.2	16640	-48.3	
49.0	20840	-51.2	
40.4	22150	-53.0	
17.0	27815	-43.1	

Table 1.7 Radiosonde Data
Wellington, 93434
13 November 1976, 2319 GMT

Pressure mb	Height gpm	Temperature °C	RH %
1000.2		8.8	89
978	300	6.3	85
850	1450	- 0.9	90
837	1585	0.0	88
775	2170	- 6.6	82
753	2410	- 6.5	66
739	2560	- 8.7	54
669	3330	-13.1	30
635	3710	-14.5	45
504	5440	-26.6	30
471	5895	-30.4	29
404	6995	-40.0	32
364	7700	-45.6	
352	7915	-45.3	
247	10250	-52.2	
190	11955	-50.3	
175	12510	-45.8	
158	13200	-44.8	
133	14345	-53.2	
121	15000	-56.0	
118	15120	-55.3	
108	15675	-47.8	
103	15950	-47.0	
92.2	16695	-51.6	
84.8	17260	-52.5	
81.3	17540	-50.5	
70.0	18475	-52.0	
66.8	18800	-49.9	
21.4	26280	-49.1	
11.8	30290	-42.3	

Table 1.8 Radiosonde Data
Wellington, 93434
15 November 1976, 2029 GMT

Pressure mb	Height gpm	Temperature °C	RH %
1005.1		12.1	75
926	800	4.5	85
912	920	4.7	84
847	1520	0.0	89
804	1955	- 3.5	80
797	2000	- 3.5	40
785	2140	- 3.5	45
757	2430	- 4.9	40
743	2580	- 3.5	39
672	3355	- 8.0	27
659	3515	- 9.4	23
574	4560	-16.9	25
382	7475	-40.0	32
322	8600	-49.0	
278	9600	-48.5	
258	10065	-51.0	
238	10600	-50.4	
225	10980	-53.3	
191	12050	-51.2	
127	14705	-56.2	
120	15070	-52.0	
72.8	18265	-51.9	
62.6	19280	-54.3	
50.8	20580	-51.0	
44.2	21515	-53.3	
35.0	23050	-49.1	
22.0	26040	-51.3	
10.0	31255	-42.3	

Table 1.9 Radiosonde Data
Wellington, 93434
16 November 1976, 0339 GMT

Pressure mb	Height gpm	Temperature °C	RH %
1002.7		15.5	61
987	260	11.5	60
950	600	9.9	68
872	1290	3.6	67
843	1555	4.2	38
770	2280	0.0	21
583	4475	-14.0	25
556	4835	-17.5	26
501	5605	-21.1	26
367	7800	-40.0	32
317	8795	-48.5	
284	9505	-52.0	
266	9940	-51.0	
217	11245	-55.6	
182	12390	-54.5	
155	13400	-56.9	
114	15400	-52.9	
81.8	17530	-56.2	
78.0	17805	-53.5	
70.0	18478	-56.5	
66.4	18845	-53.0	
21.7	26070	-51.3	
17.0	27715	-45.8	

Table 1.10 Radiosonde Data
Raoul Island, 93997
16 November 1976, 0400 GMT

Pressure mb	Height gpm	Temperature °C	RH %
1012		19.0	76
983	265	15.4	55
866	1340	5.8	82
850	1497	9.0	23
742	2615	2.8	20
716	2900	2.4	20
690	3200	0.0	20
593	4400	- 7.7	22
493	5820	-14.5	25
348	8370	-31.5	30
276	9950	-45.3	
237	10950	-52.9	
186	12500	-63.5	
170	13055	-62.7	
146	14050	-63.9	
137	14425	-62.7	
127	14900	-64.7	
79.0	17790	-62.1	
68.0	18695	-61.3	
65.0	18980	-62.7	
23.0	25595	-52.7	

Table 2.1 Ozone Sounding
Wellington, 93434
12 November 1976, 2201 GMT

Total ozone:	370 matm-cm
Integrated ozone:	327 "
Residual ozone:	43 "
Correction factor:	1.345

Pressure mb	Ozone umb
1001	36.8
933	41.5
876	29.5
864	34.8
749	25.5
707	29.5
695	36.2
667	28.1
584	23.5
565	29.5
485	17.4
454	26.8
383	17.4
376	26.8
367	21.4
351	22.8
341	17.4
328	14.7
300	21.4
271	59.0
258	64.3
246	92.5
216	103.2
202	76.4
197	80.4
172	76.4
167	59.0
156	75.0
148	62.9
147	50.9
135	67.0
119	62.9
107	135.3
95	127.3
91	150.1
83	150.1

Table 2.1 continued

Pressure mb	Ozone umb
79	132.7
70	171.5
64	167.5
58	150.1
47	176.9
40	156.8
37	167.5
33	164.8
28.5	151.4
21	116.6
20	123.3
16.5	100.5
10.5	56.3

Table 2.2 Ozone Sounding
Wellington, 93434
13 November 1976, 0303 GMT

Total ozone: 375 matm-cm
Integrated ozone: 278 "
Residual ozone: 97 "
Correction factor: 1.254

Pressure mb	Ozone umb
1001	13.9
970	23.8
913	17.6
873	21.3
832	15.7
810	21.3
663	15.1
543	15.1
434	7.5
394	12.5
359	11.3
308	53.9
294	57.7
287	56.4
283	66.5
265	80.3
238	85.3
228	75.2
224	75.2
202	81.5
183	42.6
161	36.4
144	38.9
136	62.7
110	65.2
105	77.8
98	143.0
96	146.7
80	117.9
78	130.4
71	141.7
65	158.0
57	146.7
54.5	160.5
43	172.5
39	155.5

Table 2.2 continued

Pressure mb	Ozone umb
31	163.0
27.5	158.0
24	134.8
22	134.8
21	127.9
19.5	143.0
17.5	126.7

Table 2.3 Ozone Sounding
Wellington, 93434
13 November 1976, 2319 GMT

Total ozone: 380 matm-cm
Integrated ozone: 306 "
Residual ozone: 74 "
Correction factor: 1.378

Pressure mb	Ozone umb
1000	17.9
995	24.8
869	17.9
842	22.1
794	16.5
772	23.4
744	17.9
693	23.4
651	16.5
634	22.1
521	12.4
472	15.2
372	9.7
342	24.8
262	82.7
239	78.6
202	106.8
179	91.0
163	51.0
151	53.8
120	46.9
109	91.0
105	139.2
101	147.5
83	130.9
75	147.5
66	172.3
64	165.4
52	181.9
43	158.5
40	169.5
33	166.8
32	153.0
26	151.6
24	133.7
23	133.7

Table 2.3 continued

Pressure mb	Ozone umb
22	128.2
21.5	133.7
17.5	119.9
16	102.0
15	102.0

Table 2.4 Umkehr Observation
Invercargill, 93844
14 November 1976, sunrise

Total ozone: 378 matm-cm

Pressure layer No.	mb	Ozone umb
1	1000 - 250	43.7
2	250 - 125	94.8
3	125 -62.5	105.6
4	62.5 -31.25	128.0
5	31.25-15.63	117.5
6	15.63- 7.81	81.3
7	7.81- 3.91	47.1
8	3.91- 1.95	19.4
9	1.95- 0.98	6.8

Table 2.5 Umkehr Observation
Invercargill, 93844
14 November 1976, sunset

Total ozone: 378 matm-cm

Pressure layer No.	mb	Ozone umb
1	1000 - 250	43.1
2	250 - 125	88.9
3	125 -62.5	97.2
4	62.5 -31.25	128.2
5	31.25-15.63	122.0
6	15.63- 7.81	84.4
7	7.81- 3.91	44.5
8	3.91- 1.95	16.6
9	1.95- 0.98	5.4

Table 2.6 Ozone Sounding
Wellington, 93434
15 November 1976, 2029 GMT

Total ozone: 364 matm-cm
Integrated ozone: 323 "
Residual ozone: 41 "
Correction factor: 1.152

Pressure mb	Ozone umb
1005	31.1
926	30.0
907	26.5
751	21.9
707	23.0
604	18.4
489	17.3
443	19.6
400	13.8
387	11.5
370	13.8
345	8.1
273	74.9
263	73.7
254	80.6
237	71.4
215	86.4
209	87.6
185	125.6
177	127.9
173	133.6
169	124.4
139	110.6
132	129.0
129	124.4
124	132.5
123	146.3
117	155.5
110	159.0
92	118.7
90	125.6
85	123.3
81	137.1
72	134.8
68	127.9
67	134.8

Table 2.6 continued

Pressure mb	Ozone umb
61	130.2
49	157.8
47	159.0
44	141.7
34	153.2
32	129.0
31	123.8
27	130.2
22	100.2
20	104.8
17	86.4
15	85.2
11	58.8

Table 2.7 Ozone Sounding
Wellington, 93434
16 November 1976, 0339 GMT

Total ozone: 362 matm-cm
Integrated ozone: 289 "
Residual ozone: 73 "
Correction factor: 1.376

Pressure mb	Ozone umb
1005	17.9
950	26.1
906	30.3
881	22.0
842	20.6
770	30.3
706	22.0
639	20.6
597	16.5
576	26.1
446	20.6
406	9.6
373	15.1
317	8.3
300	31.6
288	31.6
269	60.5
257	50.9
251	52.3
233	72.9
226	70.2
217	55.0
167	118.3
144	110.1
141	114.2
137	110.1
133	90.8
131	96.3
130	132.1
122	125.2
118	123.8
114	103.2
97	111.5
87	125.2
86	137.6
77	144.5

Table 2.7 continued

Pressure mb	Ozone umb
71	129.3
69	118.3
60	152.7
58	144.5
52	165.1
47	152.7
44	162.4
43	168.6
41	165.1
39	167.9
35	158.2
32	147.2
30	145.9
28	133.5
25	122.5
17	94.9

Table 3.1 CO_2 Data

Baring Head
13 November 1976

Hours (NZST)	CO_2 (ppm)
0000	calibration data only
0100	324.17
0200	324.24
0300	324.24
0400	324.24
0500	324.31
0600	324.02
0700	324.24
0800	324.46
0900	324.24
1000	323.95
1100	323.80
1200	323.95
1300	323.80
1400	323.95
1500	324.09
1600	324.09
1700	324.02
1800	324.17
1900	324.02
2000	323.87
2100	323.87
2200	323.80
2300	323.87

Table 3.2 CO_2 Data

Baring Head
14 November 1976

Hours (NZST)	CO_2 (ppm)
0000	calibration data only
0100	324.01
0200	323.94
0300	323.86
0400	323.86
0500	323.86
0600	323.86
0700	323.94
0800	323.94
0900	323.94
1000	323.86
1100	323.86
1200	323.94
1300	323.94
1400	323.86
1500	324.01
1600	324.01
1700	323.86
1800	323.86
1900	323.86
2000	324.01
2100	323.86
2200	323.86
2300	323.86

Table 3.3 CO_2 Data

Baring Head
16 November 1976

Hours (NZST)	CO_2 (ppm)
0000	Calibration data only
0100	324.00
0200	324.00
0300	324.07
0400	324.15
0500	324.07
0600	324.00
0700	324.23
0800	monthly calibration data only
0900	" " " "
1000	" " " "
1100	" " " "
1200	" " " "
1300	" " " "
1400	" " " "
1500	" " " "
1600	322.47
1700	322.55
1800	322.32
1900	322.32
2000	324.07
2100	324.53
2200	324.53
2300	326.82

☆ U.S. GOVERNMENT PRINTING OFFICE: 1977— 757-070/6319